ACADÉMIE
DES SCIENCES
INSTITUT DE FRANCE

Comptes Rendus
Physique

Denis Jerome and Claude Bourbonnais

Quasi one-dimensional organic conductors: from Fröhlich conductivity and Peierls insulating state to magnetically-mediated superconductivity, a retrospective

Volume 25 (2024), p. 17-178

Online since: 20 February 2024

https://doi.org/10.5802/crphys.164

The Comptes Rendus. Physique *are a member of the Mersenne Center for open scientific publishing*
www.centre-mersenne.org — e-ISSN : 1878-1535

ACADÉMIE DES SCIENCES
INSTITUT DE FRANCE

Comptes Rendus. Physique
2024, Vol. 25, p. 17-178
https://doi.org/10.5802/crphys.164

Research article / *Article de recherche*

Quasi one-dimensional organic conductors: from Fröhlich conductivity and Peierls insulating state to magnetically-mediated superconductivity, a retrospective

Les conducteurs organiques quasi-unidimensionnels : de l'état isolant de Peierls et de la conductivité de Fröhlich à la supraconductivité à médiation magnétique, une rétrospective

Denis Jerome [*,a] **and Claude Bourbonnais** [b]

[a] Laboratoire de Physique des Solides (UMR 8502), Université Paris-Saclay 91405 Orsay, France

[b] Regroupement Québécois sur les Matériaux de Pointe et Institut Quantique, Département de Physique, Université de Sherbrooke, Sherbrooke, Québec, Canada, J1K-2R1

Abstract. It is indisputable that the search for high-temperature superconductivity has stimulated the work on low-dimensional organic conductors at its beginning. Since the discovery of true metal-like conduction in molecular compounds more than 50 years ago, it appeared that the chemical composition and the quasi one-dimensional crystalline structure of these conductors were determining factors for their physical properties; materials with incommensurate conduction band filling favoring the low-dimensional electron-phonon diverging channel and the establishment of the Peierls superstructure and more rarely superconductivity at low temperature, while those with commensurate band filling favor either magnetic insulating or superconducting states depending on the intensity of the coupling between conductive chains. In addition, the simple structures of these materials have allowed the development of theoretical models in close cooperation with almost all experimental findings.

Even though these materials have not yet given rise to true high-temperature superconductivity, the wealth of their physical properties makes them systems of choice in the field of condensed matter physics due to their original properties and their educational qualities. Research efforts continue in this field. The present retrospective, which does not attempt to be an exhaustive review of the field, provides a set of experimental findings alluding to the theoretical development while a forthcoming article will address in more details the theoretical aspect of low dimensional conductors and superconductors.

Résumé. Il est indiscutable que c'est la possibilité d'aboutir à une supraconduction de haute température qui a stimulé le démarrage des recherches sur les conducteurs organiques. Suite à la découverte il y a plus de 50 ans, d'une conduction de type métallique dans des composés moléculaires, il est apparu que la composition chimique, la structure cristalline quasi-unidimensionnelle sont des facteurs qui déterminent les propriétés physiques de ces matériaux ; un remplissage de bande incommensurable favorisant généralement

* Corresponding author.

l'apparition d'une surstructure de type Peierls avec un état fondamental à basse température généralement isolant et plus rarement supraconductrice, alors qu'un remplissage commensurable peut conduire à basse température, soit à un isolant magnétique, soit à un supraconducteur suivant la force du couplage inter chaines. Il est à noter que la simplicité structurale de ces matériaux a contribué au développement de modèles théoriques en harmonie avec pratiquement toutes les observations expérimentales. Même si ces conducteurs organiques n'ont pas encore permis de stabiliser de la supraconduction à haute température, il n'en reste pas moins que la profusion de leurs propriétés physiques originales les qualifient comme des systèmes remarquables en physique de la matière condensée ainsi que pour leur valeur pédagogique. Cette revue historique est destinée à la présentation des propriétés expérimentales tout en faisant allusion aux développements théoriques des conducteurs et supraconducteurs de basse dimension qui seront l'objet d'un article de revue ultérieur.

Keywords. Peierls–Frölich state, Physics of low dimensional systems, Phase transitions, Electron transport phenomena, Field-induced long-range order, Unconventional superconductivity, Organic conductors and superconductors, (TMTSF)2X salts.

Mots-clés. État de Peierls–Fröhlich, Physique des systèmes unidimensionnels, Transitions de phases, Transport électronique, Ordre à longue distance induit sous champ, Supraconductivité non conventionnelle, Conducteurs et supraconducteurs organiques, Sels organiques (TMTSF)2X.

Manuscript received 22 June 2023, accepted 29 October 2023.

Contents

1. Preamble

A major objective of this overview is to address the matter of competition between insulating and superconducting phases which is perfectly illustrated by the physics of low dimensional conductors.

Furthermore, the year 2023 is particularly appropriate for writing this overview because it is the occasion to celebrate the first half century of existence of a scientific domain whose development during the previous decades can be considered as a particularly successful model.

Many points will be highlighted in this article such as: the multidisciplinary character bringing together theoretical, synthetic chemistry and experimental and theoretical physics, as well as a broad intercontinental tight cooperation which has remained very productive in the long term.

It is also to be noted that the existence of new physical properties has stimulated very actively the improvement of experimental techniques such as several aspects of physics under very high pressure, the use of high magnetic fields as well as the development of physical measurements at very low temperatures, these three topics being very often coexisting in the actual research activity.

The authors wish to make clear at the outset that this overview is not intended to be an exhaustive review of the vast field of one-dimensional physics. Excellent books and journal articles have fulfilled this purpose and will be mentioned in the Supplementary Materials of the present article.

And last but not least, this overview is published in *Comptes-Rendus Physique* because Comptes Rendus are virtuous full open access journal (diamond model) which makes them accessible to everyone even not being affiliated to a university library. The authors feel that all products of research supported by public fundings should be accessed freely.

2. Introduction: the early days of organic conduction

2.1. *A long-standing need for superconductivity at high temperature*

Stabilizing superconductivity at higher and higher temperatures has always motivated the search for new materials exhibiting possible new mechanisms allowing the formation of electron-electron pairs and their Bose condensation in a state without resistivity below a critical temperature T_c [1,2].

An history of this fascinating discovery can be found among other articles in Ref. [3] and the seminal article for the so-called BCS theory in Ref. [4, 5]. An illustration for the evolution of research to make organic matter electrically conductive and ultimately superconductive has been summarized on Paul Chaikin's Web site, *see* Fig. 1.

The prerequisite for high conductivity in molecular compounds with the possibility of metal-like conduction is the existence in molecular crystals of stable open shell molecular species. Until the middle of the last century, molecular materials were not reputed for their high electronic conductivity. It is only at the beginning of the 20^{th} century that the possibility of achieving electronic conduction in molecular solids comprising open shell molecules has crossed the minds of chemists following the suggestion made by McCoy and Moore in their article of 1910 [6]. They wrote, "if the electron theory of the metallic state is as fundamental as it seems to be, there would be little reason to doubt that the aggregate of such free radicals would be a body having metallic properties; for such a hypothetical body would be made up of radicals which, analogous to metallic atoms, could easily loose electrons", and these authors to conclude, "we think that the organic radicals in our amalgams are in the metallic state and, therefore, that it is possible to prepare composite metallic substances from non-metallic constituent elements".

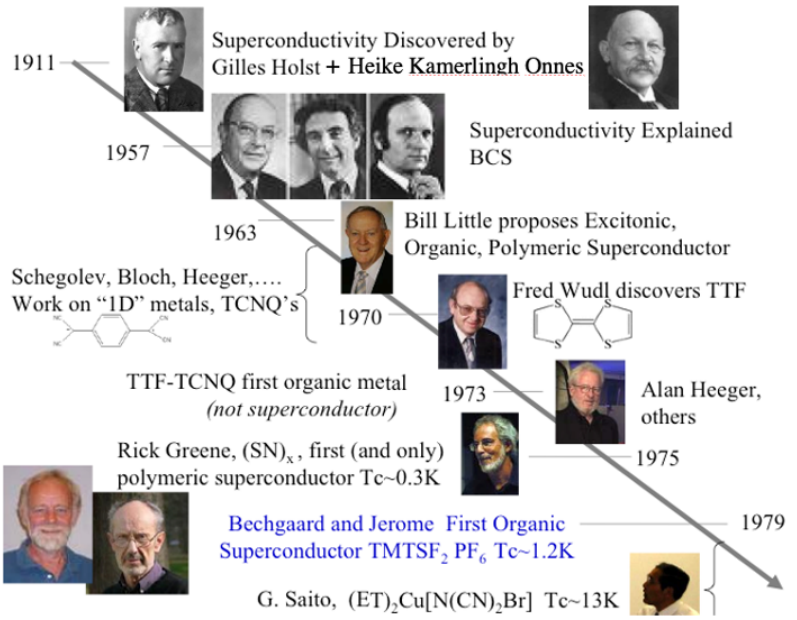

Figure 1. Timeline of the excitement around superconductivity until the beginning of the eighties. Slide provided by Paul Chaikin. Source: Paul Chaikin's personal website (not online anymore). Many thanks Paul for the slide!

The first mention of the word superconductivity in organic compounds dates back to the work of Fritz London in 1935-37 [7]. London hypothesized that the large susceptibility anisotropy of aromatic compounds such as benzene or anthracene molecules [8] could be due to superconducting currents flowing on the loops of these unsaturated molecules under magnetic field [9,10].

Even if this hypothesis does not appear to be realistic anymore after the publication of the now well established BCS theory of superconductivity [4], the idea could still have a weak connection with the persistent currents observed in mesoscopic rings [11]. However, it is interesting to note from the title of the Proceeedings of a summer school held in Germany in 1974 that the stimulus for this research in both chemistry and physics was the possibility of high-temperature superconductivity, *see* Fig. 2.

2.2. *1950, the decade of oxidized aromatic molecules*

It is only in the early fifties that the concept of electronic conduction in organic solids became reality when semiconducting properties characterized by an activated conductivity had been obtained in solids made of extended conjugated molecules containing a large number of π-electrons such as, phthalocyanine, coronene or anthracene, etc. It was suggested in turns that the current could be carried by these thermally activated π electrons [13].

In fact, research conducted in Japan by Akamatu and Inokuchi did suggest in the 1950's that semiconductivity could be attained in organic compounds via modest band gaps of the order of $10^{-1} - 10^{-2}$ eV somewhat similar to those of inorganic semiconductors [14]. Furthermore, a rather primitive application of a high pressure was able to demonstrate that the strong enhancement of conductivity observed under 8 kbar could be the result of the increase of the overlap between π orbitals of these aromatic polycyclic compounds [15]. However, the first successful

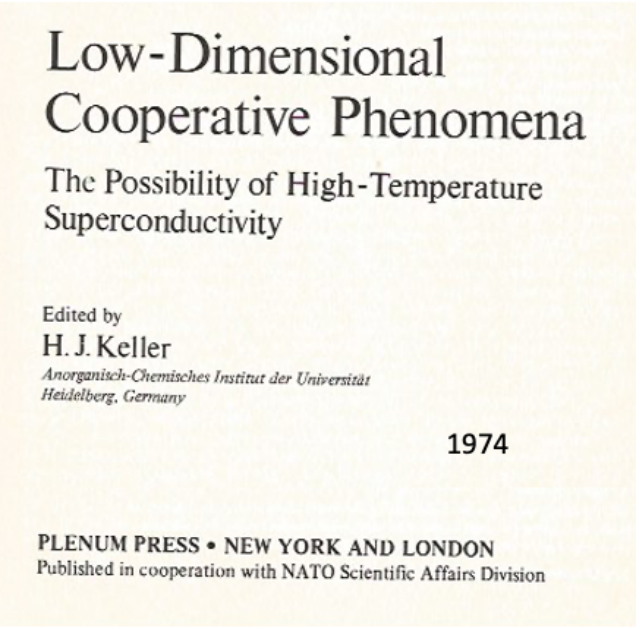
Low-Dimensional
Cooperative Phenomena

The Possibility of High-Temperature
Superconductivity

Edited by
H. J. Keller
Anorganisch-Chemisches Institut der Universität
Heidelberg, Germany

1974

PLENUM PRESS • NEW YORK AND LONDON
Published in cooperation with NATO Scientific Affairs Division

Figure 2. Front page of the *Proceedings of the Starnberg summer school (September 1974)*, edited by Heimo J. Keller, published by Plenum Press 1975 [12].

attempt to promote high conduction between open shell molecular species came out in 1954 in complexes between polycyclic aromatic compounds and halogens anions. The pressed-powder conductivity for the complex of perylene oxidized by bromine reaching 10^{-3} to 1 $(\Omega.\mathrm{cm})^{-1}$ was already considered as fairly high at that time [16]. The conduction of this oxidized perylene complex although due to the overlaping π-orbitals of these polycyclic aromatic compounds turned out to be activated with an activation energy of 0.055 eV for the perylene-bromine complex. Unfortunately, this molecular salt of perylene had the propensity to evolve over time.

2.3. *1960, the decade of* TCNQ *complexes and physicists coming into the game*

Following the above-mentioned preliminary results, it is only with the synthesis of the strong electron acceptor TCNQ (tetracyanoquinodimethane) achieved in the sixties by Acker et al. [17] that organic conduction organic conduction took off and led to the realization of what are often called "organic metals", although this term seems to be rather inappropriate since these new conductors, the subject of this review do not contain any metallic elements.

Most progresses towards organic conductivity in the years 60's have been been based on the electron acceptor TCNQ. TCNQ is a large planar molecule, consisting of a quinoid cycle. It is electrically neutral and diamagnetic with typically closed outer shells, see molecule A31 on Fig. 3. A comprehensive review of the first steps of chemistry and physics towards the synthesis of conducting organic compounds has been published in 1976 by André, Bieber and Gautier [18].

The peculiarity of the TCNQ molecule is that it is an "electron-poor" molecule which easily accepts an extra electron to become a chemically stable open shell anion (anion radical). TCNQ by itself is unable to conduct. The reason is that although the molecule will easily accept electrons from its neighbours all molecules have the same desire and finally a TCNQ crystal remains a Van der Waals solid with insulating properties. If TCNQ is in an environment where electrons can be

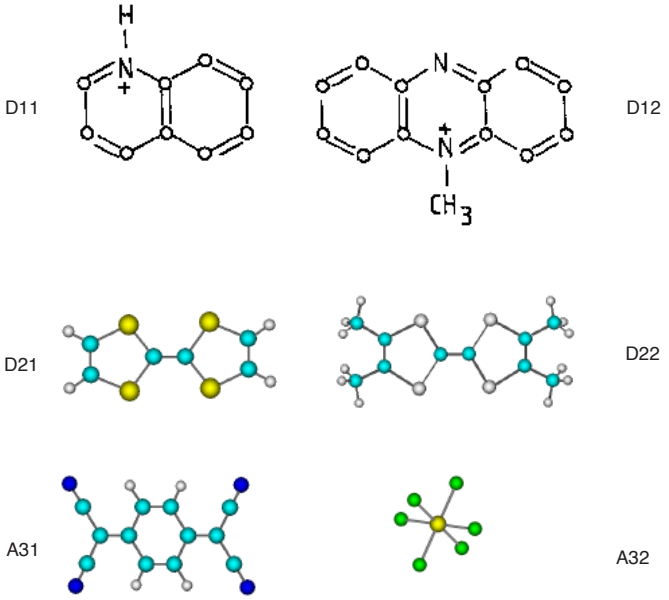

Figure 3. Some molecular components entering the synthesis of organic conductors, donors quinolinium (D11) and N-methylquinolinium (D12), TTF (D21) and TMTTF (D22) or the acceptors TCNQ (A31), and the monoanion PF_6^- (A32).

obtained from an electron donating partner, however, the situation changes [4]. To mention only a few new compounds in 1960, let us first consider simple salts involving the strong electron withdrawing TCNQ molecule forming the series of 1 : 1 complex derivatives $M^+TCNQ^{\cdot}$ with complete transfer of one electron from a metallic inorganic or organic cation M to TCNQ with the formation of the anion-radical $TCNQ^{\cdot}$ [19]. These complexes are actually very poor conductors.

There is also the possibility of forming complex salts comprising an organic cation such as quinolinium, Qn linked to two TCNQ molecules, one being formally neutral in addition to the $TCNQ^{\cdot}$ anion radical giving rise to $Qn(TCNQ)_2$. In the crystal, TCNQ molecules pile up like pancakes to form stacks. In solids such as $Qn(TCNQ)_2$, one electron is injected in each pair of TCNQ molecules. The charged counter-ion quinolinium (molecule D11 on Fig. 3) thus exhibits the structure of a closed-shell (diamagnetic) ion. For both, 1 : 1 and 1 : 2 complexes, the lowest unoccupied molecular orbital (LUMO) of the TCNQ is partially filled, being half filled for the former and one-quarter filled for the latter series. Since the highest occupied states of the TCNQ molecule are filled on average by half an electron only, the transfer of electrons between TCNQ's along a given stack is potentially possible. The 1 : 2 series exhibits a much higher and very anisotropic conductivity, reaching 10^2 $(\Omega.\mathrm{cm})^{-1}$ along the packing axis of single crystals, the largest obtained in 1960 although still behaving in temperature like a small gap semiconductor.

Regarding the series of TCNQ simple and complexes salts, much work has been accomplished over the sixties by Igor Shchegolev, Fig. 4, and his group at Chernogolovka [20] and an exhaustive review of the electrical and magnetic properties of anion radical complexes based on TCNQ has been published in 1972 [21]. Quite importantly, russian theoreticians at the Landau Institute of Moscow have played a major role in the early days of the development of non conventional superconductors, V. Ginzburg for his suggestion of exciton-mediated pairing [22] and L. Gorkov with his students who were deeply involved in the physics of low dimensional conductors in close cooperation with the Orsay laboratory.

Figure 4. Three russian pioneers in the research on organic superconductors in former Soviet Union. From left to right, Vitaly Ginzburg (1916-2009), his major achievement is the well known theory of superconductivity together with Lev Landau. Igor Schegolev (1929-1996), who developed very successfully as early as 1970, the chemistry and the physics of organic conductors with his numerous colleagues at the Institute of Chemical Physics of Chernogolovka. Lev Gorkov (1929-2016), he and the many researchers he has trained have contributed in a fundamental way to the development of the theory of organic conductors. As from 1992, L. Gorkov moved to the National High Magnetic Field Laboratory at Tallahassee of which he was one of the founders.

Pursuing his inquiry onto the cation portion of the radical anion salts of $TCNQ^{\cdot}$ and complexes, Melby [23] managed to synthesize the 1 : 1 complex N-methylphenazinium, NMP-TCNQ in short, revealing an unusually large value of 142 $(\Omega.\mathrm{cm})^{-1}$ for the conductivity measured on single crystals at 300 K.

It is with the synthesis of the 1 : 1 salt NMP-TCNQ which presents a low resistivity at 300 K decreasing like that of a metal down to a minimum at 200 K [20, 24] that the field of organic conductors started blooming and opened to the electronic aspects of solid-state physics.

From a developmental history of the organic conductors field, NMP-TCNQ is an important compound in that it bridges the gap between radical cation salts and charge transfer salts which will be discussed in the following section. NMP-TCNQ forms a chain-like structure in which donors and acceptors stack in uniform parallel chains.

There have been considerable controversies about the exact charge which is transferred from the donor molecule NMP^{+} to the acceptor TCNQ. NMP-TCNQ has first been considered as a radical cation salt similar to previously similar insulating salts. As a matter of facts, early studies assumed complete charge transfer from donor to acceptor entities [24] namely $NMP^{+}(TCNQ)^{\cdot}$ without any free electron left on NMP^{+} molecules (i.e an empty LUMO band on NMP) and a half-filled conduction band for the donor stack with an optimum π-electron interaction between TCNQ leading to conduction along the TCNQ stacks only. However, several magnetic and NMR as well as cristallographic experiments concluded to an only partial charge transfer, the exact value being very ill-defined since it was found ≥ 0.8 from NMR [25] but equal to 0.42 from TCNQ bond lengths measurements [26].

Thanks to elaborate diffuse X-ray techniques developed previously for the study of the one dimensional platinum chains [27] and successfully applied in 1975 to one dimensional organic conductors [28] the charge transfer between NMP^{+} and TCNQ stacks has been measured very accurately [29], leading to an incommensurate transfer of 0.6 electron to the TCNQ molecule making the LUMO bands of both molecules partially charged. Altogether, there is one electron per unit cell in NMP-TCNQ.

From that period on (about 1962) physicists became closely involved in this kind of research. In the mid-1960s they were very motivated by the search of new superconducting compounds with T_c higher than the current 18 K than the recently discovered (one decade earlier) intermetallic compounds of the A15 structure, namely, (V_3Si or Nb_3Sn) [30, 31] or even 22 K in Nb_3Ge, [32] which have contributed very efficiently to the manufacturing of superconducting wires until now but are still constrained by the use of liquid helium for cooling. Although B. T. Matthias had been a co-discoverer of the highest T_c in 1954 this did not stop him from expressing his doubts about high temperature superconductivity, "superconductivity at room temperature will always remain a pipedream, temperatures as high as 25-30 K are a realistic possibility and will trigger a technological revolution.compounds", as he wrote in 1971 in Physics Today [33]. To some extent, the empirical statement of Matthias about the limitations of the A15 superconducting materials turned out to be founded. But it is only the theoretical work performed by the Friedel's school which brought a firm confirmation. It is the hidden 1D nature of the A15 cubic structure which provides the enhancement of the density of states at the Fermi level lying close to the van-Hove singularity of the density of states near the band edges of the 1D d-bands. Within the BCS formalism large T_c can thus be expected. This is what is actually observed (17-23 K) but an upper limit was found to the increase of T_c since the large value of $N(E_F)$ also makes the structure unstable against a cubic to tetragonal Jahn–Teller band distortion [34, 35]. The theory [36] showed that T_c is indeed maximized in compounds such as Nb_3Sn or V_3Si. In practice, the evolution of T_c in various materials according to the year of their discovery supported the experimental findings, see Fig. 45. However, at that time, theoretical attempts to increase T_c were still based on the phonon-mediated BCS theory and its strong coupling extension [37].

In order to achieve higher T_c's than those obtained in these years, theoreticians became extremely imaginative in terms of exotic suggestions for an electron-electron pairing mechanism other than the phonon-mediated pairing proposed by Bardeen, Cooper and Schrieffer [4]. New paths were proposed. Kohn and Luttinger proposed a new mechanism for superconductivity still based on the pairing idea although the attraction is no longer phonon-mediated [38]. The attraction derives from an extension of Friedel's density oscillations around charged impurities and that are present in metals due to the sharpness of the Fermi surface [39]. It is an entirely electronic pairing mechanism process. However, the expected critical temperature should be extremely small in the milli-Kelvin range or much less depending on the symmetry of Cooper pairing, but Kohn and Luttinger emphasized that flat Fermi surfaces and van Hove singularities could greatly enhance the actual T_c.

At about the same time, the interest for improving T_c has been strongly boostered by the announcement made in 1964 by W. A. Little that the phenomenon of superconductivity for which a satisfactory microscopic theory had been proposed only seven years earlier by Bardeen Cooper and Schrieffer [4] could occur in hypothetical one-dimensional organic conductors at temperatures exceeding 300 K [40].

Little's proposal was still made within the pairing framework of the BCS model, but instead of the phonon-induced pairing, the attraction between electrons would come from an entirely electric process in long conjugated polymer such as a polyene molecule grafted by polarizable side groups [40], see Fig. 6.

Emboldened by the prospects of high T_c, Little published one year later in a mainstream magazine an article under the title "Superconductivity at Room Temperature" [42].

At about the same time, theoreticians in Soviet Union were also very active in proposing models to go beyond the well accepted phonon mechanism for superconductivity, keeping in mind the possibility of higher T_c's. This is the case for V. L. Ginzburg and his coworkers who suggested at several occasions [22, 43] that the exchange of excitons between two electrons may give rise to a net attraction and in turn to superconductivity possibly at temperatures higher

Figure 5. Walter Kohn (1923-2016), Nobel laureate in Chemistry, 1998. A picture taken during one of his numerous visits to Paris. As Walter enjoyed coming to France, he adopted the local dress.

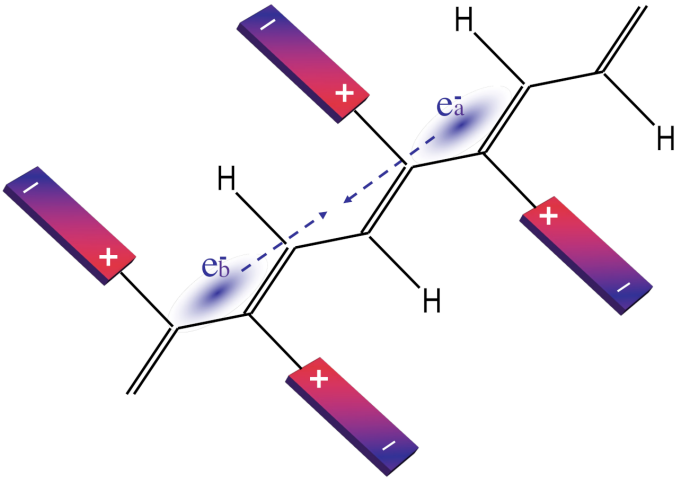

Figure 6. Schematic picture of Little's suggestion. Electron a and b belonging to a conducting spine are bound via a virtual electronic excitation of polarizable side groups. Electron a first polarizes the side groups in its vicinity creating an electric field attracting in turn a second electron b. Source: [41, Figs. 1.2, p. 5],

than the usual phonon exchange of the BCS theory since an electronic excitation energy about 100 or 1000 times larger than a typical phonon energy would enter the BCS-like formula for T_c. However, they were severe technical constraints related to Ginzburg proposal: the electrons should be contained in very thin metallic layers sandwiched between dielectrics "V. L. Ginzburg was mentioning metallic layers of thickness $0.5-1$ nm. Given the tremendous progresses made recently in thin film deposition, this idea may not be so unrealistic nowadays.", see Fig. 7.

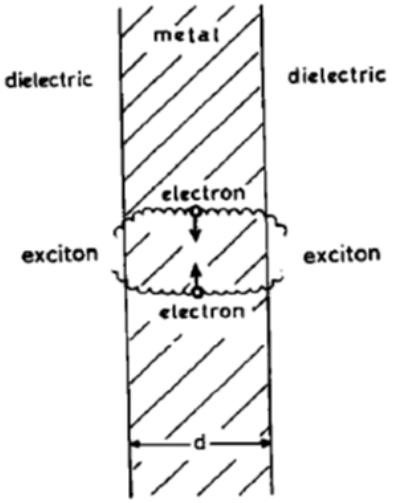

Figure 7. According to Ginzburg's proposal, the attraction between the electrons in the metal layer is enhanced by the exchange of excitons propagating mainly in the dielectric regions of the sandwich. Source: [22, Fig. 3 p. 370]. ©Taylor & Francis. All rights reserved.

Given the significant progresses made recently in metallic layers preparation, the suggestion of Ginzburg deserves to be revisited.

In relation to biological substances, Ladik and coworkers extending Little's original idea for the possibility of superconductivity in organic polymers to biological substances, have suggested the possibility of superconductivity-type enhanced conductivity in some regions of DNA polymers [44].

All these suggestions were highly speculative but the positive effect is that in 1970 they have awakened the motivation for the research of new superconducting materials.

A few years after his original article, Little succeeded organizing in Honolulu a meeting which brought together researchers from very different fields with the same objective, namely the prospects of high temperature superconductivity, and their cooperation proved to be decisive for the future [45]. Little supporting a continuous dialogue between physicists and chemists concluded his 1969 presentation by [46]: "I would like to stress that in this field there is a desperate need for an interdisciplinary approach. I think physicists on the whole understand a great deal but they know very little. On the other hand the chemist with his vast experience of reactions, compounds, conditions, etc., knows a great deal but..., well, perhaps I will not push the contrast further but will conclude by saying that we need each other."

What Little wrote in his conclusions at the 1969 conference has fortunately materialized from 1970 and led to new compounds with remarkable physical properties. Therefore in 1970 superconductivity became a challenge for organic chemistry.

But, Little's model raised subsequently multiple questions from theorists. In particular, Bychkov et al. [47] criticized this model regarding its potentiality to lead to high-temperature superconductivity. As remarked by Bychkov et al. [47], the 1D character of the model system proposed by Little makes it a unique problem in which there exists a built-in coupling between superconducting and dielectric instabilities. It follows that each of these instabilities cannot be considered separately in the mechanism proposed by Little in one dimension. This comment turned out to be crucial as future work in the field of one dimensional conductors and superconductors has shown. Last but not least, as shown by Landau [48] and Mermin [49], fluctuations should be very efficient in a 1D conductor shifting any long-range ordering toward very low temperature.

Admittedly, the formidable task in synthetic chemistry did not reached immediately the goal fixed by Little as in the sixties the chemistry of organic conductors was barely developed, but the idea to link organic metallicity and one-dimensionality was launched and turned out to be a very strong stimulant for the development of organic superconductors.

Actually, it is with the synthesis of Qn(TCNQ)$_2$ and NMP-TCNQ and the finding of a room temperature electrical conductivity of about 10^2 $(\Omega.\mathrm{cm})^{-1}$ in these charge transfer salts that the field of organic conductors started blooming and opened to the electronic aspects of solid-state physics. From that time on (about 1962) physicists became closely involved in this kind of research.

The possibility of designing and synthesizing molecules to achieve properties on the molecular scale that will lead to interesting and fundamental solid-state physics suggest an exciting future for this area of research.

One of the main pioneers of this field has been Igor Shchegolev and his group at Chernogolovka who published in 1972 a major review article, a state of the art article on the electrical and magnetic properties of anion radical complexes based on TCNQ [21].

2.4. *1970, Molecular electronics, the TTF and TTF-TCNQ decade*

A major breakthrough in chemistry arose in the 1970's when F. Wudl and his colleagues reported the synthesis of an unusually stable bis-dithiole radical cation [50]. TTF is a planar conjugated and "electron-rich" molecule, Fig. 3, which can easily give a charge to another species ready to accept it.

The group of F. Wudl also established that remarkable electronic properties could be attained when TTF is oxidized by the monoanion Cl^- giving rise to a 1 : 1 radical cation complex with a room temperature conductivity on pressed pellets of $0.3(\Omega.\mathrm{cm})^{-1}$ exhibiting semiconducting properties at low temperature with an activation gap of 0.19 eV [51].

Although the electron donor molecule TTF has become very popular for its ability to form intermolecular charge transfer complexes with the acceptor TCNQ leading to the celebrated charge transfer (CT) complex TTF-TCNQ, we may also pay attention to an other aspect of research in which TTF has been extensively used in the context of organic electronic devices (semiconductors, electrochemical switches, sensors, p/n junctions, etc.).

In this respect, TTF can be utilized as a donor in intramolecular charge transfer materials in which TTF is covalently linked to an electron acceptor moiety by a variety of linking units, sometimes giving rise to an intramolecular charge-transfer (ICT) interaction, which is most frequently manifested in the optical and electrochemical properties [52]. Aviram and Ratner [53] made a proposal to use the molecular assembly donor-spacer-acceptor based on the donor TTF to achieve molecular rectification.

The idea of Aviram and Ratner has not lived up to its promise, but it has been a source of inspiration for the synthesis of a large number intermolecular charge transfer compounds to be used for organic electronics [54].

Coming back to intermolecular charge transfer compounds, the realization of non-integral charge transfer which will be extensively discussed in the following section, has been achieved with a lattice of TTF stacks surrounded by an halide lattice, namely the non-stoichiometric salts such as TTF-halides$_x$ with $0.71 \leqslant x \leqslant 0.79$ in which the donor is partially oxidized in a mixed valence state [55]. These materials possess a room temperature conductivity on single crystals varying from 100 to 500 $(\Omega.\mathrm{cm})^{-1}$ with a small region near room temperature where the conductivity increases as temperature is lowered [56]. These TTF-(halides)$_x$ radical cation salts are interesting because the non conducting halide stack produces a Coulombic potential on the conducting TTF stacks at a wave length which is half the wave length defined by the 60%

electron filling of the band deriving form the HOMO level of TTF. The halide lattice although incommensurate with the TTF latice is thus imposing on the one dimensional electron gas a perturbation opening gaps at values of the Fermi wave vector modulo one reciprocal vector of the TTF lattice, leading to a commensurate Peierls distortion [56]. It is a situation *at variance* with the one that is observed when the Fermi wave vector is solely determined by the charge beeing transfered from donor to acceptor molecules, both contributing to the conduction as it is encountered in TTF-TCNQ to be introduced in the following.

Since TTF-TCNQ is the compound that aroused worldwide enthusiasm at the time of its discovery and which after numerous experimental and theoretical studies led in 1980 to the synthesis of the first organic superconductors, it is useful to recall how this CT complex is formed and how high quality single crystals are obtained.

The unusual stability of the TTF radical cation resulting from an oxidation of the parent molecule has led to conducting compounds with a conductivity ranging between 500 and $1000(\Omega.\mathrm{cm})^{-1}$ at room temperature [57–59] but also behaving like metals in 1973 (so-called organic metals because their resistance exhibits a positive temperature dependence down to about 60 K). Coleman et al. published data for the conductivity of TTF-TCNQ culminating at 58 K with provocative values larger than 10^6 $(\Omega.\mathrm{cm})^{-1}$, (i.e. about twice the room temperature conductivity of copper [57]), which will be commented in more details in the next Section about the physical properties of TTF-TCNQ.

As the existence of high quality single crystals is a determining element for further physical characterization, it is important to have flavour on how they are obtained. Neutral TTF and TCNQ molecules combine to form a 1:1 charge transfer complex according to a charge transfer reaction: $\mathrm{TTF} + \mathrm{TCNQ} \rightarrow \mathrm{TTF}^{+\rho}\mathrm{TCNQ}^{-\rho}$, ρ being less than unity, taking advantage of the energy gain in the charge transfer reaction which reads,

$$\Delta E_{CT} = I - A - C < 0$$

where I and A are the ionization potential of the donor and the acceptor affinity respectively, and C includes the Coulombic (Madelung), polarization and exchange energy contributions. In a complex such as TTF-TCNQ the amount of charge transfer is unknown a priori by the stoeichiometry of the complex. However, the amount of charge transferred to the anion can be determined by Raman spectroscopy [62] and even derived much more accurately from X-ray diffuse scattering experiments, see Sec. 3.1.4. In order to grow crystals, highly purified TTF and TCNQ molecules are combined in the ratio 1:1 in acetonitrile solvent and the complex precipitates from the solution [58, 63]. In forming solids, the molecules TTF and TCNQ crystallize in segregated stacks of TTF and TCNQ molecules, Fig. 8. In the individual stacks of TTF and TCNQ molecules the π-orbitals in the partially filled outer molecular shells overlap, so that the discrete levels of the individual molecules are spread out to form an energy band. The partially filled bands thus leads to metallic-like conduction, even if the intramolecular electron repulsion (the Hubbard U) is strong compared to that bandwidth, namely $U \gg W$. It would be a different situation if we had the quarter-filling for which we expect an insulator for U going to infinity. Moreover, a rather special feature of TTF-TCNQ and related compounds, as compared to ordinary metals is that the π-orbitals of the molecules are strongly directional and interact mainly along the stacks, leaving only a weak interaction in the perpendicular directions. Hence, these conductors exhibit very anisotropic conduction properties, they behave as quasi-one-dimensional conductors, although they are of course three-dimensional crystals. The electronic properties of TTF-TCNQ will described in further details in Sec. 2.

More than thousand articles on TTF and derivatives have been published since their discovery. The present article is intended to provide only the very minimum amount of chemistry needed by physicists to understand the fascinating and often unseen physical properties they have revealed.

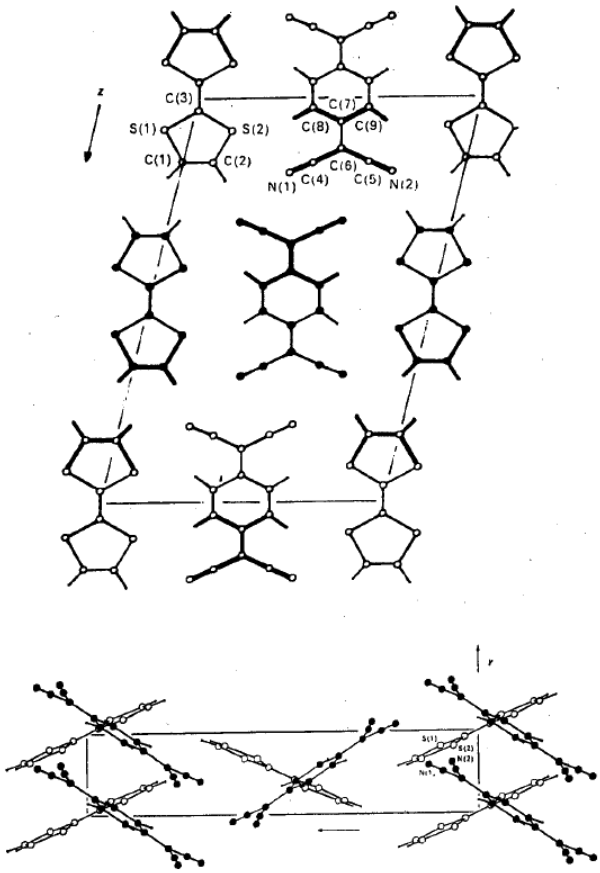

Figure 8. Crystal structure of TTF-TCNQ viewed normal to the *ac* plane of the crystal packing (top) and down the [100] axis (bottom) according to Ref. [60]. Notice the criss-cross molecular packing along the *a*-axis. Sources: [61, Figs. 3, 4 p. 766]. Reproduced with permission of the International Union of Crystallography. All rights reserved.

Lots of review papers have been published on this topic. A review has been published very early in 1976 by André and Bieber [18] and in addition we refer the interested reader to the comprehensive vol. **104**, no. 11, (2004) of *Chemical Reviews* [64]. The TTF molecule has been the starting point for the synthesis of many derivatives. For example, substituting the parent molecule with weakly donating alkyl groups, for instance methylene (CH_2) groups, has led to the molecule HMTTF [65] and methyl groups (CH_3) has led to tetramethyltetrathiofulvalene (TMTTF) [66–68]. It is interesting to note that the charge transfer compound TMTTF-TCNQ behaves from the point of view of magnetism and optics in a similar way to TTF-TCNQ [66, 69].

The TMTTF derivative turned out to be of decisive importance for the discovery of organic superconductivity since the four sulphur atoms of TMTTF substituted by selenium allowed the synthesis of TMTSF [70] (tetramethyltetraselenafulvalene), the radical cation utilized in a salt to grow the first organic superconducting radical cation salts. Furthermore, other selenium substituted molecules gave rise to new charge transfer compounds typically, TSF (tetraselenafulvalene) [70, 71] and HMTSF [72] (hexamethylene/tetraselenafulvalene) with interesting physical properties which will be discussed in the next Section.

As far as the acceptor side is concerned, following the precursor work of Wudl [73], a group of french chemists did show that simple radical cation salts such as $(TMTTF)_2X$ could be synthesized with X = SCN [74] with the possibility to extend the synthesis to an isomorphous series of simple sats with other anions such as BF_4^-, $ClO_4^-$and Br^-, with a conductivity approaching $100(\Omega.cm)^{-1}$ at room temperature but becoming semiconducting below 200 K or so [68, 75].

The following sections will show how these apparently minor modifications of the parent molecule have deeply influenced and oriented the further research of organic superconductors.

Before moving on to the next decade, let us emphasize that superconductivity has been a strong driving force for the development of this field. To underline this point E. Edelsack et al. [76] outlined during a conference in 1987 on Novel Superconductivity, one year after the discovery of high temperature superconductivity in cuprates [77] that "organics are materials which forged revolutionary paths in the quest of high T_c!".

2.5. *1980, the Bechgaard salts decade*

Towards the end of the 1970's with the study of TTF-TCNQ the main motivation of physicists was to suppress the transition to an insulating state occurring around nitrogen temperature in order to allow eventually a superconducting state to settle. There has been a close cooperation between organic chemists specializing in organic synthesis and crystal growth, physicists both experimental and theoretical, which has been materialized by the holding of numerous multidisciplinary conferences which have led to major advances.

Substitution of the four sulfur atoms with selenium leading to increased contacts between intermolecular chalcogen atoms, gave rise in charge transfer compounds to a better room temperature conductivity and a lower metal-insulator transition. Therefore, the Copenhagen chemistry group led by Klaus Bechgaard [78] has been oriented toward selenium chemistry whose properties of some compounds will be discussed in the Sec. 3.2.1. As it was established that the carriers from the donor stack are dominant according to the hole-like thermopower [79], the chemists decided to investigate single chain compounds of TMTSF by synthesizing radical cation salts of TMTSF with various mono-anions, somewhat analogous to the series of $(TSeT)_2Cl$ in which a conducting phase with $\sigma \sim 10^5$ $(\Omega.cm)^{-1}$ at helium temperature could be attained under 4.5 kbar [80].

It is worth mentioning a major step which allowed the field of organic superconductivity and all the physics surrounding it to develop. This is the success reached with the growth of high quality single crystals of radical cation salts using an electro-oxidation-crystallization method. Such a step allowed in turn the development of materials enabling very detailed physical measurements concerning most of the technical possibilities including measurements under pressure.

The electrochemical oxidation growth that enabled the fabrication of high-quality single crystals is displayed on Fig. 9. It has been extensively used by the Copenhagen chemistry school [61] and reviewed by K. Bechgaard [81] and by P. Batail and co-workers [82].

Electrocrystallization allows high-purity materials to be reproducibly obtained only if all materials and chemicals involved are properly purified beforehand. Hence, the PF_6^-anion for example enters in the electrocrystallization process as a tetrabutylammonium salt which is soluble in a solvent like tetrahydrofuran, THF. One electron is removed from every neutral TMTSF in the anode compartment being oxidized by the current passing through the cell leading in turn to the cation radical $TMTSF^{\cdot+}$. Then, two cation radicals combining with one anion of the electrolyte give rise to the simple salt $(TMTSF)_2PF_6$ which precipitates at the anode as a non soluble molecular salt, see Fig. 9. An accelerated video (×20000) shows how electrocrystallization proceeds [83], leading to centimeters long high quality single crystals, *see* Fig. 10.

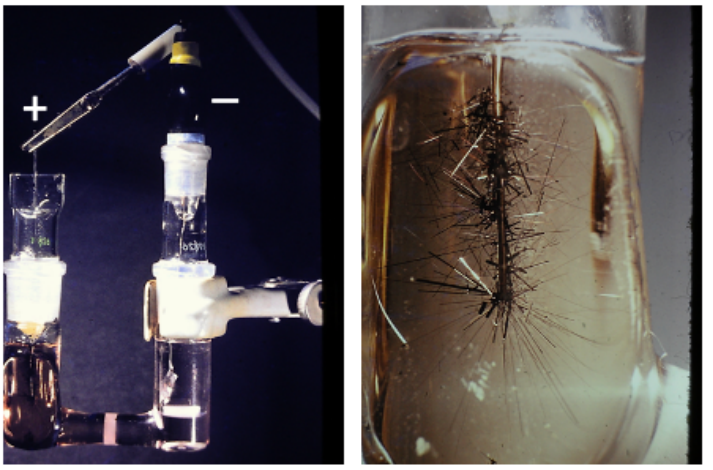

Figure 9. (Left) Electrochemical oxydation and crystal growth of $(TMTSF)_2PF_6$. A neutral TMTSF molecule dissolved in the nonaqueous tetrahydrofuran solvent is first electro-oxydized and precipitates at the anode with the PF_6^- anion provided by the tetrabutylammonium-hexafluorophosphate salt, (NBu_4PF_6). (Right) More detailed view of the anode compartment from K. Bechgaard's laboratory. The crystal growth can be seen in a video from the Orsay laboratory [83].

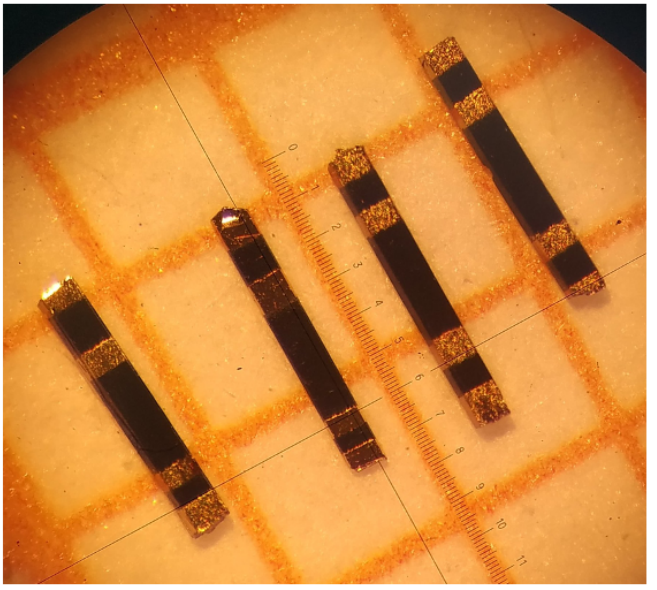

Figure 10. Crystals of $(TMTSF)_2ClO_4$ about 6 mm long viewed along their c-axis with evaporated gold pads for longitudinal conductivity measurements. We thank P. Auban-Senzier for communicating this photo.

3. First metal-like organic conductors

3.1. *Era of Peierls instability and Fröhlich conduction*

3.1.1. *Introduction to the physics of TTF-TCNQ*

It is useful to present in a little more detail the physics of the compound TTF-TCNQ which was historically the first charge transfer complex to exhibit a large conductivity evolving over a wide range of temperatures below ambient in a way similar to the conductivity of inorganic metals. In addition this organic conductor undergoes a sharp metal to insulator transition at 59 K.

TTF-TCNQ is the prototype of the charge-transfer compounds where the metallic state is achieved first by an electron transfer from the initially filled HOMO levels of TTF to the originally empty LUMO levels of TCNQ [84]. Partially filled bands thus derive from the interaction between π orbitals of HOMO and LUMO levels of open shell donors and acceptors respectively forming segregated and parallel stacks along the b direction. The overlap of molecular orbitals being largest along the stacking direction and much weaker between them makes the electron dispersion one dimensional, Fig. 8. To a first approximation, the energy depends only on the electron wave vector along the b^* direction in the reciprocal space.

The extended Hückel method has been used by Berlinsky et al. [85] to compute the conduction band parameters of TTF-TCNQ within the tight binding approximation. The lowest electron energy on the TCNQ stacks occurs when all molecular orbitals are in-phase (at $k = 0$ in reciprocal space). On the other hand, the band structure of the TTF stacks is inverted with an energy maximum at the zone center, Fig. 11.

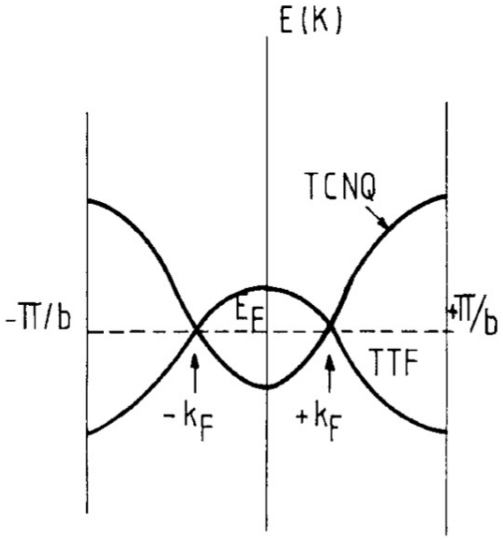

Figure 11. A very schematic picture of the HOMO-LUMO TTF-TCNQ inverted band structure. Source: [86, Fig. 19 left p. 349]. ©Taylor & Francis. All rights reserved.

The band structure calculations that have followed have confirmed that the simple tight binding approximation is relevant with bandwidths of about $0.5-0.7$ and $0.4-0.5$ eV for TCNQ and TTF bands respectively [85, 87], see also [86].

Such a band crossing picture ensures that both bands intersect at a single Fermi wave vector $\pm k_F$ in order to preserve the overall neutrality [84]. Consequently, all states between $-\pi/b$ and

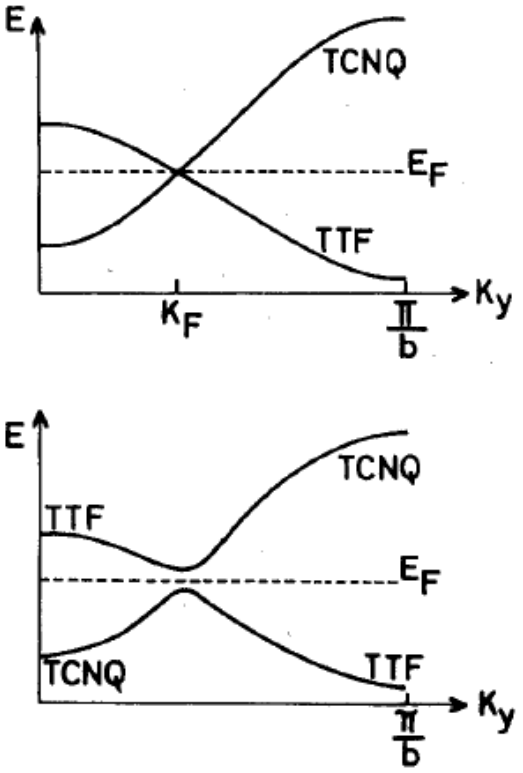

Figure 12. Energy level diagram in conducting charge-transfer compounds such as TTF-TCNQ; non-interacting 1-D chains (top), including coupling between 1-D chains of different nature (covalency gap), (bottom). Source: [88, p. 353]. ©Springer Nature. All rights reserved.

$+\pi/b$ are occupied with the restriction that between $-k_F$ and $+k_F$ occupied states belong to the TCNQ band while outside this domain they pertain to the TTF band. The mere fact that charges can delocalize in TTF-TCNQ shows that the on-site Hubbard repulsion U does not overcome the band energy $4t_\parallel$ gained in the band formation. However, Coulomb repulsions still play some role as experiments will reveal especially for magnetic and structural properties of the TTF stacks.

A second crucial requirement to preserve the conducting state is the need for a uniform structure as one dimensional conducting structures are predicted to be unstable to lattice distortions due to the Peierls instability characterized by a divergent dielectric response to an external perturbation with the wave vector $2k_F$ [90].

The simple band picture in terms of non interacting neighbouring stacks is actually strongly oversimplified. Some small although non negligible transverse coupling exists between neighbouring stacks of different molecules. The bands derived from the TTF and TCNQ molecular orbitals must cross the Fermi level where states $\psi_Q(k_F)$ and $\psi_F(k_F)$ are degenerate [88], Fig. 11.

However the existence of any finite interchain coupling between F and Q chains mixes the states of same k_F vector which become non-degenerate. They form a bonding state $(\psi_Q+\psi_F)/\sqrt{2}$ and an antibonding state $(\psi_Q-\psi_F)/\sqrt{2}$ which are $2t_\perp$ apart in energy, the so-called covalency effect, Fig. 12. However, in case of a coupling between like chains, the interchain coupling (Q-F) leads to a replacement of the Q1D warped Fermi surface by small pockets semi-metallic like [86, 88] as displayed on Fig. 13. The density of states at Fermi level is strongly depressed by

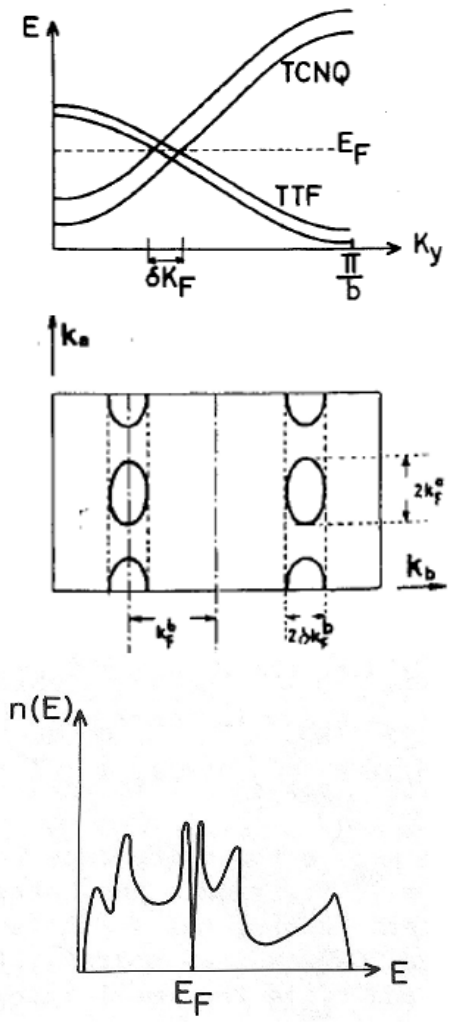

Figure 13. A very schematic picture of the semi-metallic Fermi surface in the low temperature three-dimensional regime. Sources: [88, p. 353] and [89, Fig. 4b, p. 110]. The depression of the density of states at Fermi level (bottom) is the result of the coupling between unlike chains.

the addition of a coupling between unlike chains (bottom). More realistic shapes of semi-metallic Fermi surfaces at low temperature have been derived by Shitzkovsky and Weger [87]. As the Fermi energy of these electron or hole pockets is small, of the order of $t_\perp$ or so, there is no hope of observing a three-dimensional Fermi surface in a quasi-one-dimensional conductor unless the temperature is low enough $k_B T < t_\perp$. In TTF-TCNQ, the onset of a Peierls transition around 55 K precludes the observation of a 1D to 3D cross-over of the Fermi surface since $t_\perp \approx 5$ meV.

As we shall see later in Sec. 3.2.2, among charge transfer compounds undergoing a Peierls transition, the condition $k_B T_p < t_\perp$ required for the observation of a 1D to 3D cross-over, seems to be fulfilled only for HMTSF-TCNQ (and possibly also in TMTSF-TCNQ under pressure) when covalency effects due to strong Se–N bonds are especially large compared to the interchain coupling of TTF-TCNQ.

The band formation of a compound such as TTF-TCNQ is thus *at variance* with what has been encountered previously for radical cation salts which are single-chain conductors where the band filling of a single band can be predicted by the stoichiometry.

TTF-TCNQ has been remarkable as a model compound for the development of both theoretical one dimensional physics and several aspects of experiments, that we intend to discuss briefly in the following [86]. We think it is the right place in this overview to recall the central role played by Heinz J. Schulz (1954-1998), see Fig. 14, member of the theory group in the Orsay Solid State Physics Laboratory. Heinz was a specialist of Fermions at low dimension. He brought a very valuable collaboration to many experimentalists, in particular to one of the authors of the present article.

Figure 14. Heinz J. Schulz at Orsay in 1998 when he was awarded the CNRS silver medal. We thank Anuradha Jagannathan for providing this photo.

3.1.2. *The conductivity of TTF-TCNQ*

The year 1973 saw the announcement by two american groups, a chemistry group led by D. O. Cowan at Baltimore and the other a physics one led by A. J. Heeger[1] at Philadelphia of both the synthesis and the measurement of remarkable conducting properties in TTF-TCNQ [57, 58]. Both publications announced a conductivity at room temperature of about 400 $(\Omega.\mathrm{cm})^{-1}$ along the stacking axis significantly higher than found for any other TCNQ salt such as quinolinium and a metal-like behavior for the conductivity of TTF-TCNQ down to a maximum around 58 K ($\sigma_{max} \approx 10^4$ $(\Omega.\mathrm{cm})^{-1}$) followed by a sharp transition toward an insulating ground state.

This report was the subject of a post deadline invited paper at the March 1973 meeting of the American Physical Society in San Diego. According to G. Lubkin in *Physics Today*, the Penn report has excited great interest, but the theoretical explanation met with considerable skepticism [91].

Furthermore, the authors of Ref. [57] reported in the same article that three out of seventy measured samples revealed a conductivity exceeding $\sigma > 10^6 (\Omega.\mathrm{cm})^{-1}$ at 60 K with a slope appearing

[1] Alan Heeger is a co-laureate of the 2000 Nobel Prize in Chemistry together with Alan Mac Diarmid and Hideki Shirakawa for the discovery organic conductive polymers.

to be divergent. These same authors have suggested that this extraordinary conduction could come from superconducting fluctuations just above a Peierls-type metal-insulator transition at 58 K following a one-dimensional power law divergence with the 3/2 exponent [92]. Moreover, this publication hypothesized that superconducting fluctuations could be at the origin of this remarkable increase in conductivity above a possibly Peierls transition occurring at 58 K by basing this argument on a phonon soft mode $\omega(2k_F)$ tending towards zero and responsible for a strong increase in the BCS-type phonons mediated electron-electron coupling.

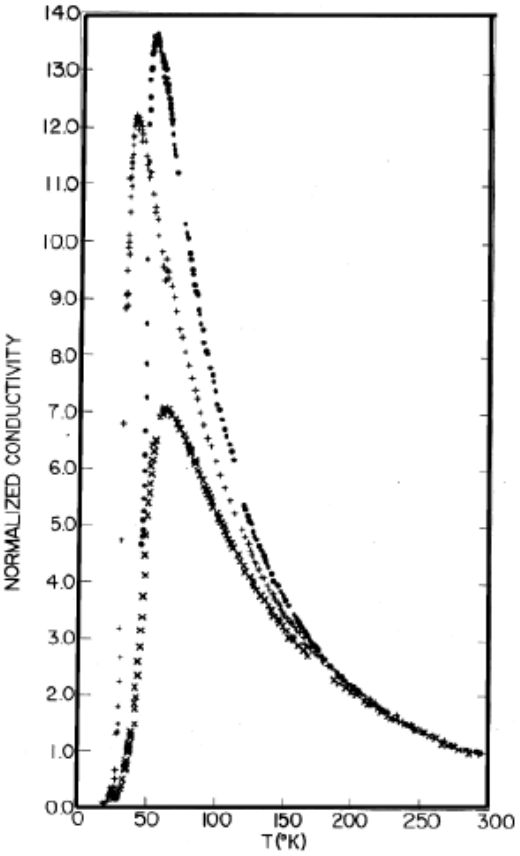

Figure 15. Normalized conductivity $\sigma(T)/\sigma(295\ K)$ of (•) TTF-TCNQ (+) TSF − TCNQ and (×) DSDTF − TCNQ. Source: [93, Fig. 2, p. 742]. ©American Physical Society and the authors. All rights reserved.

The conclusion of the latter paper indicated unambiguously that regarding the superconductivity mechanism their authors had in mind a standard BCS phonon type mechanism probably inspired by the physics of A15 superconductors in which van-Hove singularities were responsible for the high values of their T_c [94]. They proposed an increase of the interchain coupling in order to limit the one-dimensional Peierls divergence and thus to favor superconductivity at a temperature above the Peierls transition temperature. The enormous conductivity peak claimed in Ref. [57] triggered a worldwide interest and led to numerous verifications in various laboratories.

Even if the claim for the observation of superconducting fluctuations at high temperature has been considered as very controversial at the time. It is clear 50 years later that it was a decisive event that contributed to strengthen a common activity between chemical synthesis, experimental and theoretical physics.

The most elaborate verification came from the Bell Telephone and Baltimore groups [95]. Without going into the details of this latter report, it turned out that the extraordinary conductivity maximum is an experimental artefact likely due to the points at which electrical contacts are made on the samples. This article even suggests recipes to guarantee meaningfull conductivity measurement namely, the so-called unnested voltage check which should give a voltage as close as possible to zero when the current is injected through adjacent voltage and current leads and the voltage detected on the two others leads or equivalently, a large unnested ratio.

The controversy about a reliable value of the peak conductivity in TTF-TCNQ led G. A. Thomas et al. to gather and compare experimental data from 18 different laboratories in a single article comprising 30 co-authors [96], Fig. 15.

It is interesting to note that until 1974 the results of transport in molecular conductors were generally published in the form of conductivity versus temperature, when it was not the log of conduction versus inverse temperature. This habit probably originated from the history of molecular conductors, which until that time were semiconductors. It was only later, when these conductors showed a metallic conductivity, that the results were presented the way metal physicists do, in resistivity as a function of temperature.

This controversy over the interpretation of TTF-TCNQ conductivity measurements has shown that conductivity measurements on materials with very anisotropic transport properties require single crystals not only of excellent chemical purity but also of very high crystalline quality. As isotopically substituted materials often lead to crystals of better quality, the investigation of the metal-insulator transition around 53 K has shown that the ^{15}N substitution of TCNQ molecules lead to single crystals with a remarkably sharp transition and a peak conductivity 15 times the room temperature value [97]. Crystals of the same origin used for pressure conductivity studies to be presented in the next section have confirmed values of $\sigma(\text{peak})/\sigma(300\ \text{K})$ of between 10 and 25 with unnested ratios exceeding 20 at $\sigma(\text{peak})$ [98]. These results are also in agreement with earlier measurements [93] and with an estimate based on the statistical average over the data of 18 laboratories [96]. Finally, we can be confident that the longitudinal DC conductivity of TTF-TCNQ amounts to 400±100 $(\Omega.\text{cm})^{-1}$ at 300 K and rises up to a maximum of $\approx 10^4 (\Omega.\text{cm})^{-1}$ at 60 K, Fig. 15. Although reference [96] suggested that the observed magnitude of the conductivity can be described by single particle scattering with reasonable values of mean free paths, they had left the door open to the possibility that the conduction may be enhanced by collective effects. It is this latter scenario that high pressure studies turned out to confirm a few years later.

3.1.3. *The dilemma of transport in TTF-TCNQ*

The understanding of the conduction of TTF-TCNQ in its metallic state has generated multiple controversies over several years. Even if a consensus about the enhancement of the longitudinal conductivity peaking at 60 K has been quickly reached with a ratio $\sigma(\text{peak})/\sigma(300\ \text{K})$ being at most 25, there were still remaining problems regarding the behavior of the transport anisotropy both in temperature and pressure.

It is accepted that the conduction process in TTF-TCNQ is coherent and diffusive along and perpendicular to the chains respectively [99, 100]. Therefore, according to the Einstein's relation applied along the transverse a direction the transverse conductivity reads [99]:

$$\sigma_\perp = n_0 D_\perp e^2 / k_B T \tag{1}$$

where $D_\perp = a^2 \tau_\perp^{-1}$ is the diffusion constant along the a direction, $\tau_\perp^{-1}$ being the hopping rate between neighboring chains and n_0 the number of carriers within the Fermi volume ($n_0 = n(E_F) k_B T$) with a degenerate Fermi statistics, $k_B T \ll E_F$) leading to:

$$\sigma_\perp = n(E_F) a^2 e^2 \tau_\perp^{-1} \tag{2}$$

On the other hand the longitudinal transport follows a Drude formulation namely,

$$\sigma_{\parallel} = n_0 e^2 \tau_{\parallel} / m^* \tag{3}$$

where m^* is the effective mass of carriers along the conducting direction. The conductivity anisotropy thus reads:

$$\sigma_{\parallel}/\sigma_{\perp} = \left(t_{\perp}/t_{\parallel}\right)^2 (a/b)^2 \tag{4}$$

provided the transverse hopping rate $\tau_{\perp}^{-1}$ is related to $\tau_{\parallel}$, namely [99],

$$\tau_{\perp}^{-1} = (2\pi/\hbar)\, t_{\perp}^2 \left(\tau_{\parallel}/h\right). \tag{5}$$

There is access to this three dimensional escape rate via NMR experiments according to the field dependence of the nuclear relaxation rate [99].

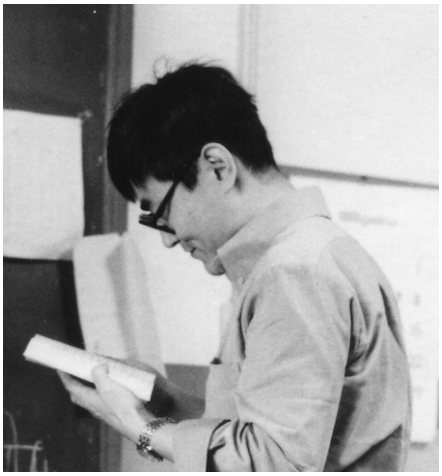

Figure 16. Gen Soda was one of the lead experimentalists for the early NMR studies of one-dimensional charge transfer conductors during his stay at Orsay 1974-1976. Sadly, he died accidentally at Okazaki in 1987.

There exists a cross-over value of the electronic resonance frequency ω_e at $\omega_e \tau_{\perp} \approx 1$ between a high field 1D regime ($1/T_1 \propto H^{-1/2}$) and a low-field 3D regime ($1/T_1 = \text{const}$). Consequently, the field dependence of the relaxation rate allows a remarkably direct derivation of $\tau_{\perp}$ provided this time is in the limits of the NMR experiments, i.e. $10^{-12}\text{s} \leqslant \tau_{\perp} \leqslant 10^{-10}\text{s}$. This is the case for TTF-TCNQ where $\tau_{\perp} > \tau_{\parallel}$ with $\tau_{\perp} \approx 8 \times 10^{-12}$s and $\tau_{\parallel} \approx 3 \times 10^{-15}$s from optical data [101] or the NMR derivation [99]. However, the condition $\tau_{\parallel} \gtrsim \hbar/t_{\parallel}$ is actually not fulfilled strictly speaking in TTF-TCNQ at room temperature since $\hbar/\tau_{\parallel}$ is likely to be in-between 0.075eV and 0.2eV, with $t_{\parallel}$ being of the order of 0.1 eV. In short, the conduction regime which is relevant for TTF-TCNQ in its conducting regime is coherent along the conducting axis although incoherent along the transverse directions, namely $\hbar/t_{\parallel} < \tau_{\parallel} < \hbar/t_{\perp}$. Around and certainly above room temperature the situation $\tau_{\parallel} < \hbar/t_{\parallel}$ is encountered, leading in turn to a diffusive longitudinal conduction.

Eq. (4) giving the anisotropy implies that the motion of the carriers is coherent along the chains but diffusive along transverse directions [99, 102].

According to the experimental data [100] such a picture is still valid under pressure at room temperature but *a serious problem remains* since the measurements [95, 103] have shown that the b/a conductivity anisotropy being in the range from 60 [95] to 1300 [103] at room temperature is strongly temperature dependent, see for instance the conductivity data in reference [104].

Actually, for the parallel component, $\sigma_{\parallel}$, the conductivity peak ratio (CPR) $\sigma_{\parallel}(\text{peak})/\sigma_{\parallel}(300\text{ K})$, lies in-between 10 and 25 depending on the measured samples in the vast majority of laboratories, whereas for the transverse conductivity $\sigma_{\perp}$, $\sigma_{\perp}(\text{peak})/\sigma_{\perp}(300\text{ K})$ is no more than a factor 3 and usually sample independent. Therefore the b/a conductivity anisotropy ends up being multiplied by a factor ~ 7 on cooling from room temperature down to about 70 K. Therefore, Eq. (4) cannot apply to the transport properties of TTF-TCNQ in the conducting temperature regime.

Understanding the DC metallic conductivity has thus remained the great puzzle in the study of TTF-TCNQ and of its derivatives. It has even generated numerous controversies in the years 1974-75.

Bardeen [105] and co-workers [106] suggested that long living fluctuating charge density waves (CDW) of the Fröhlich type [107, 108] could reasonably contribute to the DC longitudinal conductivity of TTF-TCNQ. But the model in question was left without any clearcut experimental verification until the year 1979. This is the issue which will be addressed in the next section.

3.1.4. *The TTF-TCNQ phase diagram*

The dilemma about the nature of the conduction in TTF-TCNQ could not be solved until an extensive use of transport, magnetism, X-rays and neutrons diffraction techniques very often performed under high pressure. This activity has been widely presented in numerous journal articles or contributions to book chapters. In this article we will limit ourselves to develop only a few highlights that have led to the understanding of the physics of TTF-TCNQ.

We thus begin with an overview of the rich $T-P$ phase diagram before addressing the question about the conduction.

3.1.5. *The TTF-TCNQ phase diagram in temperature*

The phase diagram reveals the existence in temperature of several resistive transitions namely, two major transitions which can be seen in transport: one at $T_H = 54$ K, where the conductivity drops by a factor of 2, and another at $T_L = 38$ K [98] which is the signature of a sharp first-order transition toward an insulating ground state, according to the data 1 bar data on Fig. 17. Furthermore, at a temperature T_M between T_H and T_L the transport data reveal a sluggish and hysteretic regime related to the onset of a CDW on the TTF chain.

The transport behavior is the consequence of a Peierls transition (a periodic lattice distortion, PLD) which has been extensively studied by X-ray diffuse scattering experiments [28, 109] and elastic neutron scattering [110]. To summarize, between T_H and T_M there is $2a, 3.4b$ superstructure, and between T_M and T_L the period in the a direction evolves continuously and jumps discontinuously to $4a$ at T_L. These are the experiments which have provided the clear-cut signature for a Peierls instability in a 1D conductor. They have also given the first accurate determination of the charge transferred between TTF and TCNQ molecules. With a periodicity along the stack axis of $\lambda = 3.4b = 2b/\rho$, the charge transfer amounts to 0.59 at low temperature. Notice that the charge transfer measured at higher temperatures from diffuse X-ray experiments leads to a smaller value for the charge transfer namely, $\rho = 0.54$ at K [28]. Such a difference between low and high temperature values can be understood by the thermal contraction at constant pressure acting on the bandwidths. A temperature decrease from 300 to 77 K is essentially equivalent as far as the structure is concerned to the effect of a 5 kbar hydrostatic pressure [86].

Furthermore, transport has shown that the Peierls transition of TTF-TCNQ occuring at T_H is only partial and suggests that the insulator-metal transition involves only one of the chains at 54 K leaving the other conducting.

This question has been settled by ^{13}C Knight shift experiments in selectively enriched samples of TTF-TCNQ [111] improving previous NMR [112] and EPR [113] studies which have shown that the loss of the spin degrees of freedom of the TCNQ stacks is already complete below T_H with no

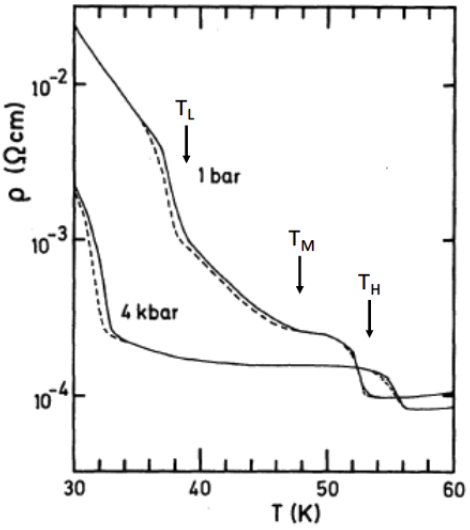

Figure 17. TTF-TCNQ resistivity data at 1 bar and 4 kbar on cooling (dashed) and warming (solid) for a sample with CPR 25 at 1 bar. Source: [98, Fig. 1, p. 1048]. The temperatures of phase transitions are those related to the run at 1 bar.

marked spin gap on the TTF stack between T_H and T_L (although a noticeable dependence of the conductivity is observed in the same temperature domain according to Fig. 17. It is only below T_L that the spin gap in the TTF stack becomes fully open. However, there is still no common agreement in the conducting regime above T_H between the three previously mentioned studies regarding the respective contributions of the two chains to the total susceptibility. Following the experimental results a theory for these structural phase transformations has been proposed by Bak and Emery in 1976 in terms of a Ginzburg–Landau type expansion of the free energy [114].

An other way to visualize the Peierls distortion has been achieved via scanning tunneling microscopy. These studies have confirmed in a very elegant way the structural results obtained by diffraction studies [115] and even solved some of the pending questions [116].

Fig. 18 displays an ultrahigh vacuum image of the $a-b$ plane of a cleaved TTF-TCNQ single crystal taken at 63 K [116]. The 1D structure of parallel chains is clearly visible on this figure. Those containing a triplet of balls are the TCNQ molecules, The TTF molecule appears usually as a single ball feature in STM imaging, although reports of doublet structures have also been made in the literature [117]. The distances between chains or between units within each chain in Fig. 18 compare fairly well with the a = 1.23 nm and b = 0.38 nm lattice constants of TTF-TCNQ [60]. A salient result of this STM work is shown on Fig. 19 where the CDW is seen in direct space superimposed to the underlying TCNQ lattice at 36.5 K, i.e, below the transverse lock-in occurring at $T_L = 38$ K.

These STM experiments have settled open questions related to the phase below T_M when, because of the onset of a CDW on TTF chains, the transverse wave vector departs from $2a$ and increases smoothly at lower temperature. Below T_M the CDW's of the 2D superlattice can be described equally well either by plane waves with the wave vectors $q_+ = [q_a(T), 2k_F]$ or $q_- = [-q_a(T), 2k_F]$ leading to energetically equivalent configurations [118, 119] with CDWs of fixed amplitude and a phase varying like $q_a a$ along the a direction. Consequently, the diffraction pattern of the CDW state should display domains characterized by the vectors q_+ or q_-. This is

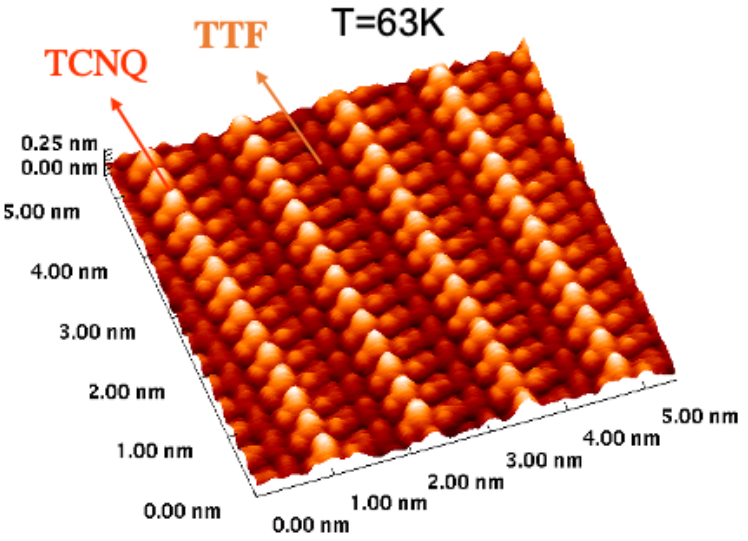

Figure 18. STM image of the $a-b$ plane of TTF-TCNQ taken at 63 K. The image area is 5.3×5.3 nm^2. Source: [116, Fig. 1 p. 1].

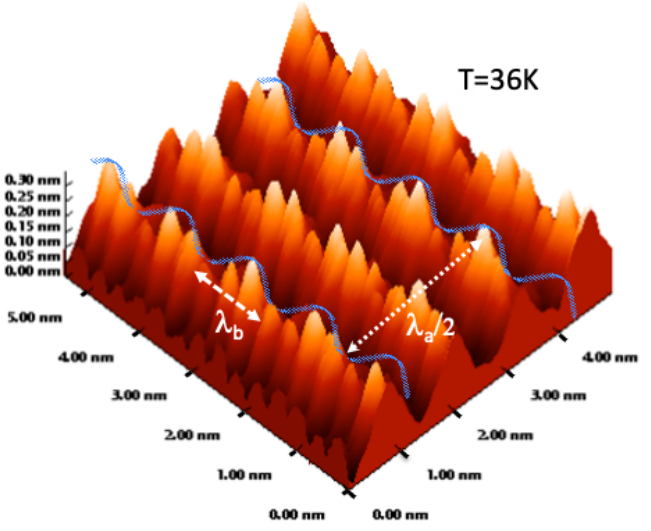

Figure 19. The STM image of the same $a-b$ plane of TTF-TCNQ as Fig. 18 but taken at 36 K according to Ref. [116], revealing the periodic lattice distortion in blue with wave length $\lambda_b = 3.4b(1.15\text{ nm})$ along b and the transverse ordering $\lambda_a = 4a$ along a. The TTF chains are not visible by STM on this figure unlike higher temperatures, Fig. 18. This figure is adapted from the work of J. C. Girard and Zhao. Z. Wang. Source: [116, Fig. 5.4 p. 156].

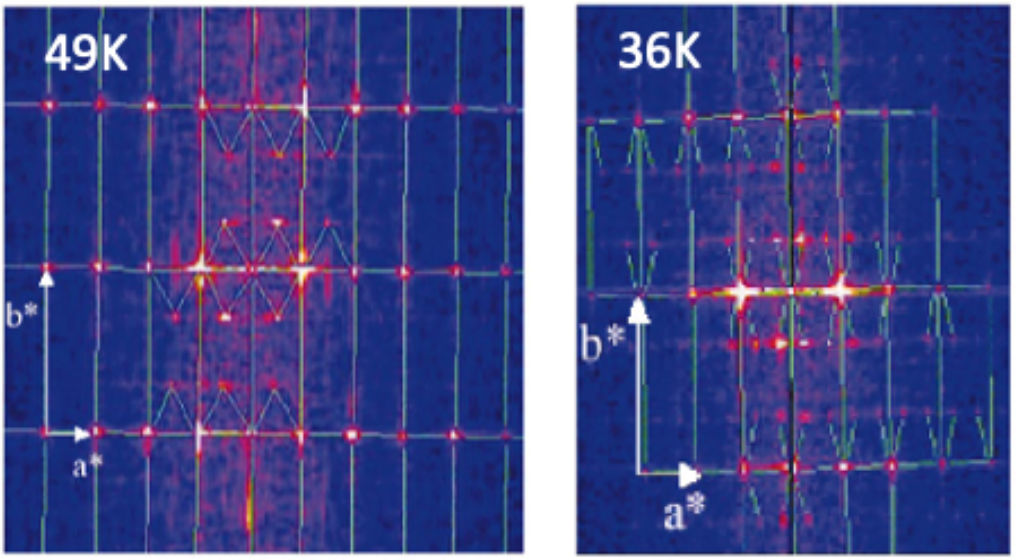

Figure 20. Fourier transformed pattern of TTF-TCNQ showing the single-q CDW in the sliding temperature domain (left) at 49 K and the pattern showing the double-q ($4a \times 3.3b$) CDW in the commensurate phase at 36 K (right). Sources: [116, Figs. 2, 3d p. 2].

the situation which has been validated by the STM analysis between T_M and T_L. There also exists another possibility, namely: the superposition of the two plane waves q_+ and q_-, which leads to a CDW with constant phase but a modulated amplitude along the a direction [118,119]: a double-q configuration.

The only solution which can take advantage of the commensurability energy related to the transverse commensurate periodicity $4a$ through the fourth order Umklapp term in a Landau–Ginzburg expansion is the double-q configuration. Fig. 20 showing the 2D Fourier transformation of the real space data of Fig. 19 reveals even more clearly the transverse period $4a$ and with the existence of four satellite spots around every Bragg spot, i.e, the coexistence of the two wave vectors in the same region of the real space that prevail below T_L. This configuration is quite different from the Fourier transform, Fig. 20 where the wave vector activated in the same area is the signature of a phase modulation existing in the incommensurate transverse regime between T_L and T_M.

3.1.6. *Towards strong coupling*

As mentioned earlier, the metal-insulator transition occurring at 54 K as a result of a new lattice periodicity π/k_F opening a gap at the Fermi level in the electronic band at $\pm k_F$ is the manifestation of the Peierls instability in a one-dimensional chain. In the non-ordered phase above 54 K, the Peierls instability is announced, by joint PLD/CDW fluctuations being uncorrelated between neighboring chains (one-dimensionality) and whose finite-length correlation is strongly dependent on the temperature. It is only in the very vicinity of the actual Peierls transition (a few degrees above) that 1D fluctuations on neighbouring chains become correlated with a short range lateral order which ends up in a 3D phase transition. The physics of these lattice fluctuations is well documented by the early studies in one dimensional platinum chains $K_2Pt(CN)_4Br_{0.33}H_2O$

where they give rise to both a giant Kohn anomaly of the acoustic phonon branch at $2k_F$ observed in inelastic neutron diffraction [120] and to diffuse sheets centered at the $\pm 2k_F$ wave vectors in reciprocal space on each side of the Bragg spots, see Fig. 21 [27]. R. Comes, see Fig. 22, played a major role in the first experimental evidence of the Peierls transition predicted in 1955 [90] but only demonstrated by diffuse X-ray scattering in the inorganic 1D conductor, $K_2Pt(CN)_4Br_{0.33}H_2O$, at Orsay in 1973. This result has marked the beginning of the study of one-dimensional conductors, which was rapidly extended to organic conductors.

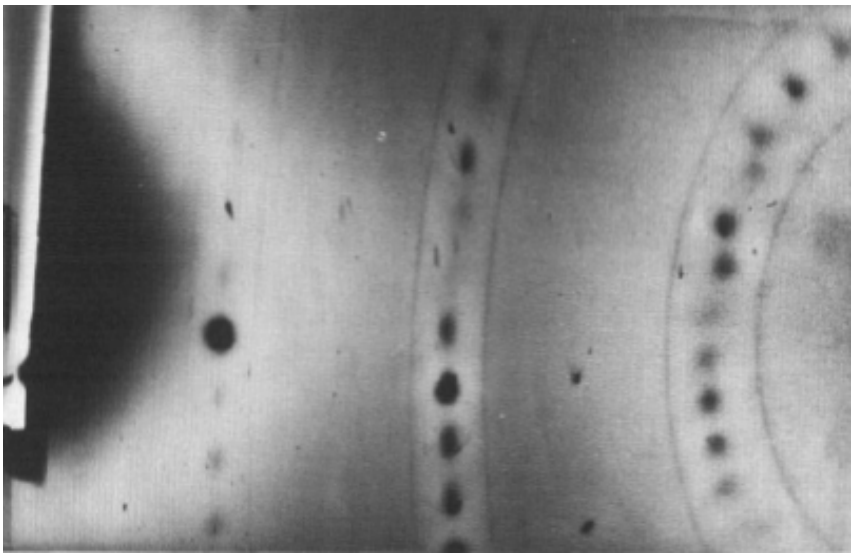

Figure 21. Typical diffuse X-ray scattering pattern from the 1D conductor $K_2Pt(CN)_4$ $Br_{0.33}H_2O$ showing the diffuse streaks on both sides of the Bragg spots. Source: [27, Fig. 6 p. 573].

Figure 22. R. Comes in 2007 at the LPS Orsay. Source: Patrick Batail.

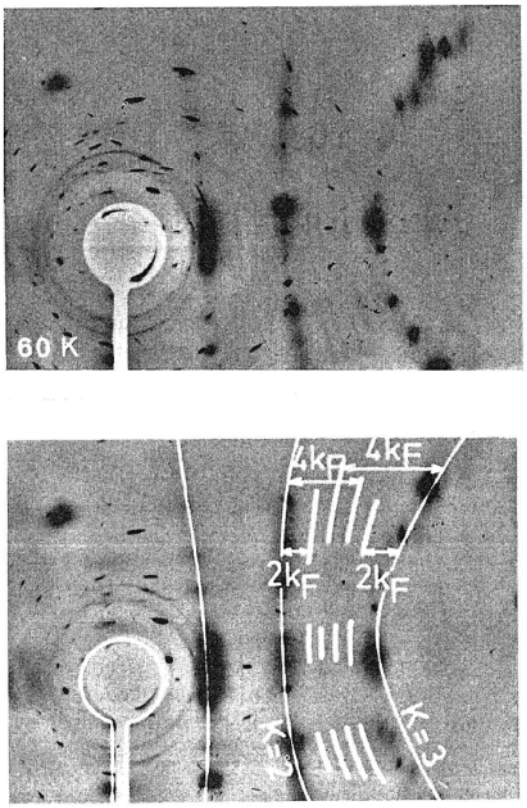

Figure 23. X-ray pattern of TTF-TCNQ at 60 K. Diffuse lines at $2k_F$ and at $4k_F$ are observed on each sides of the layers of main Bragg reflections. The sample is oriented with the $b^\star$ axis horizontal. Source: [121, Fig. 1 p. 437].

Similar experimental findings have been obtained in 1D organics conductors although with a much milder intensity. They are well documented by numerous publications of the Orsay X-ray group [122]. However, somewhat unexpected has been the finding in diffuse X-ray patterns of a structural instability at twice the $2k_F$ wave vector in TTF-TCNQ, a 1D conductors which presents an incommensurate band filling [121, 123]. This $4k_F$ scattering is already visible below 250 K and becomes predominant below 100 K over the regular $2k_F$ Peierls scattering occurring at 150 K, Fig. 23. This scattering at wave vector $4k_F$ has been viewed as the fingerprint on the lattice of a Wigner charge localization with a periodicity $\pi/2k_F$ developing into a lattice distortion at the same $4k_F$ vector because of the electron-phonon coupling [124]. This $4k_F$ scattering has been attributed to the TTF chain better described by a 1-D electron gas with repulsive interactions in which charge and spin fluctuations are both gapless [125, 126] unlike the $2k_F$ related to the smaller $e-e$ coupling TCNQ chains [127].

Without going into much details, this phenomenon can be understood as the precursor of a Peierls transition in a spinless fermion gas, where, because of the loss of the spin degree of freedom a given k state cannot be occupied by more than one fermion. This has been considered as the strong coupling limit of the Peierls transition of a Hubbard chain when $U \to \infty$ [128]. This $4k_F$ scattering will become far more dominant for compounds in which the charge transfer amounts to 0.5, i.e., the quarter-filled band situation, see Sec. 3.2.3.

3.1.7. *The TTF-TCNQ phase diagram under pressure "fluctuat nec mergitur"*

Thanks to the development of helium gas high pressure techniques up to 15 kbar [129] and teflon cell techniques for pressures above 15 kbar [130], reliable conductivity measurements on TTF-TCNQ single crystals could be obtained. They have contributed to understanding both the phase diagram and the conduction process of TTF-TCNQ. The transport properties of TTF-TCNQ have revealed a remarkably rich $T-P$ phase diagram, confirmed by magnetic, calorimetric and diffraction experiments. It is actually the high pressure studies that have enabled us to understand transport properties of TTF-TCNQ.

Somewhat surprising was the existence above 15 kbar of a single transition peaking at 74 K under 19 kbar, Fig. 24 [98]. The width of the peaked region in the phase diagram amounts to a domain of ~4 kbar in pressure units. In that pressure domain, the phase transition also exhibits a first-order character as shown by the one Kelvin hysteresis observed at the transition [131, 132].

The peaking of the single-phase transition temperature around 19 kbar and its first-order character have suggested the occurrence of a (×3) commensurability ($2k_F = b^*/3$) at this pressure [98] which turned out to have been confirmed subsequently by elastic neutron scattering under pressure leading to a $(a \times 3b \times c)$ superstructure [133], see Fig. 24. Such an increase in the charge transfer under pressure should not be a great surprise since it is in line with the increase already noticed upon cooling under ambient pressure and due to the effect on the band structure of the significant thermal contraction [86].

When the longitudinal conductivity of TTF-TCNQ is studied under high pressure there occurs an important drop of this quantity in the pressure regime corresponding to the peak of the first order transition ($P = 19 \pm 2$ kbar) [131, 132], Fig. 25. The drop of conduction in the vicinity of 19 kbar is becoming less pronounced as the temperature is increased and even practically unobservable above 250 K.

These data imply that the longitudinal conduction contains more than one channel, actually two different channels acting in parallel though responding differently to pressure. Since the transverse component of the conductivity failed to show such a similar anomaly in the vicinity of 19 kbar, Fig. 25, it was suggestive that one channel for $\sigma_\parallel$ is a single particle scattering channel which follows the transverse conduction since from the previous section we know that as long as the electron scattering is a single particle process, longitudinal and transverse conductivities should exhibit similar behavior in temperature and pressure as long as $\tau_\perp$ is much larger than $\tau_\parallel$, a condition easily satisfied in TTF-TCNQ as we shall see below, the other channel being of a collective nature. Hence, both conduction channels acting in parallel add in order to give the total parallel conductivity [86],

$$\sigma_\parallel = \sigma_{coll} + \sigma_{\parallel,sp} \tag{6}$$

The problem now at hands was to determine what fraction of the total conductivity could be attributed to Fröhlich fluctuating channel in the vicinity of the Peierls transition. Actually, high-pressure optical reflectance studies [135] allow us to discard the possibility of drastic (non-monotonous) changes in the band structure evolving slowly under pressure in particular at commensurability.

In addition we can reject the existence of the dip as being due to an increase of the single particle scattering mechanism and/or a decrease in the density of states at the Fermi level in the commensurability domain because of the data of transverse conductivity. Whenever the transverse conduction is diffusive, which is verified since as long as the 1D escape time $\tau_\perp$ is larger than $\tau_\parallel^{sp}$, a condition easily fulfilled in TTF-TCNQ according to the NMR results [99], $\tau_\perp/\tau_\parallel^{sp} \approx 10^3$, $\sigma_{\parallel,sp}$ is sensitive to both the density of states at the Fermi level and to the smearing of the one-dimensional Fermi surface by the single particle scattering time $\tau_\parallel^{sp}$.

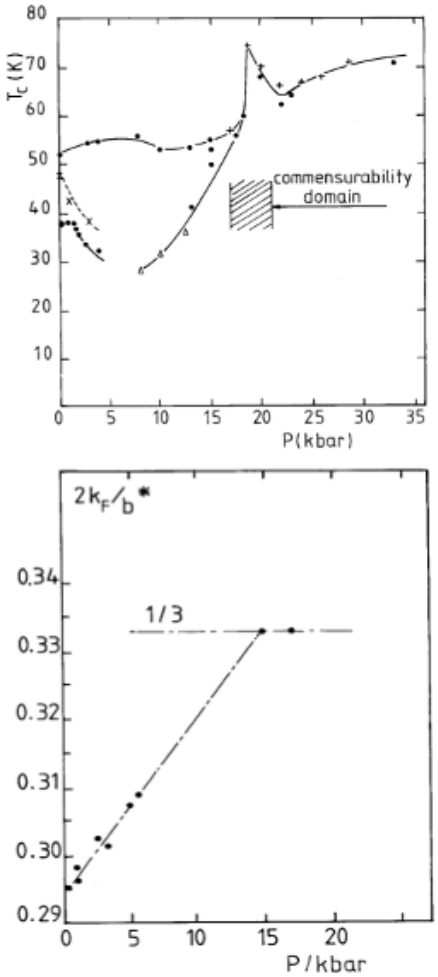

Figure 24. (Top) Pressure dependence of the phase transitions in TTF-TCNQ as defined by maxima in $dlnR/dT$. Sources: [98, Fig. 2 p. 1049]. (Bottom) Pressure dependence of the $2k_F$ measured by neutron elastic scattering experiments. Between 14.5 and 17.5 kbar, the superstructure at 35 K has the periodicity $a \times 3 \times c$. Source: Ref. [133, Fig. 3 p. 876].

According to the experimental data of Fig. 25 displaying the pressure dependence of the transverse conductivity no dip in the commensurability regime is observed. Therefore, Fig. 25 leads to the conclusion that neither $N(E_F)$ nor $\tau_{\parallel}^{sp}$ are significantly affected by commensurability. Hence, we may conclude that the dip of longitudinal conductivity around 19 kbar in TTF-TCNQ can be taken as a serious indication for the existence of a significant part of a conduction channel originating in the collective (fluctuating Fröhlich conduction) becoming pinned in this pressure range by a low order commensurability effect.

Given the data of parallel and transverse conductivities against temperature obtained at various pressures, see Fig. 26 including the commensurability range we can analyze in more details how Fröhlich fluctuations behave in temperature at various pressures.

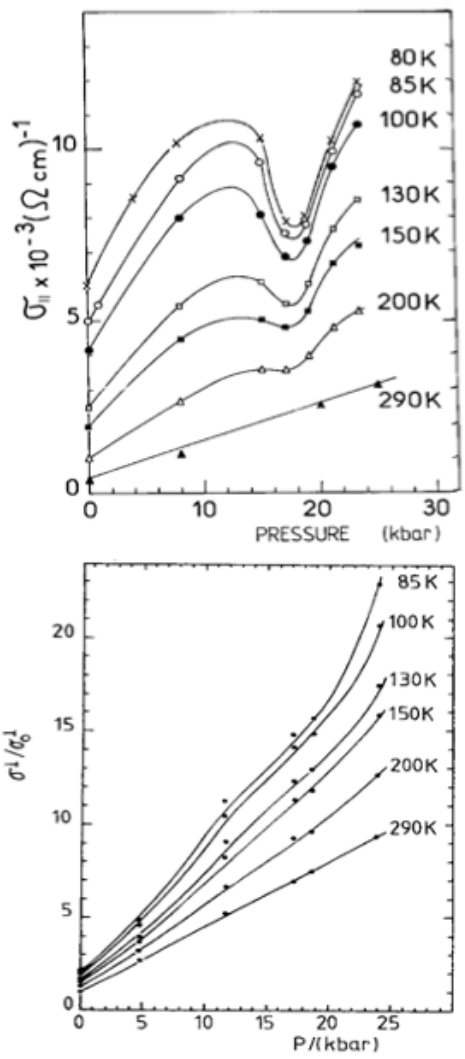

Figure 25. (Top) Pressure dependence of the longitudinal conductivity of TTF-TCNQ at various temperatures. The ratio CPR is 25 under ambient pressure. ©American Physical Society and the authors. All rights reserved. (Bottom) Pressure dependence of the transverse conductivity of TTF-TCNQ at various temperatures. Sources: [131, Fig. 2a p. 229] (top), Ref. [134, Fig. 14 p. 191] (bottom). ©Taylor & Francis. All rights reserved.

Assuming both conductivity channels to be additive according to Eq. (6), we can extract the fluctuating contribution from the measured total conductivity. To accomplish this decomposition two assumptions are required.

The first one is that at 300 K, σ_{coll} is negligibly small compared to $\sigma_{\parallel,sp}$. This assumption is justified by the monotonous increase of $\sigma_{\parallel}$ through the commensurability regime around room temperature. The accuracy of the data on Fig. 25 shows that $\sigma_{coll}(300\ \mathrm{K})$ is smaller than, say, $\sigma_{\parallel,sp}/10$ at (19 kbar, 300 K) thus leading to $\sigma_{coll}(300\ \mathrm{K}) \ll 250(\Omega.\mathrm{cm})^{-1}$.

The second assumption of the derivation is based on the fact that in the one-dimensional regime $\sigma_{\perp}$ and $\sigma_{\parallel,sp}$ exhibit the same temperature dependence as already discussed above the model decomposition of the conductivity [134]. This is illustrated by the experimental

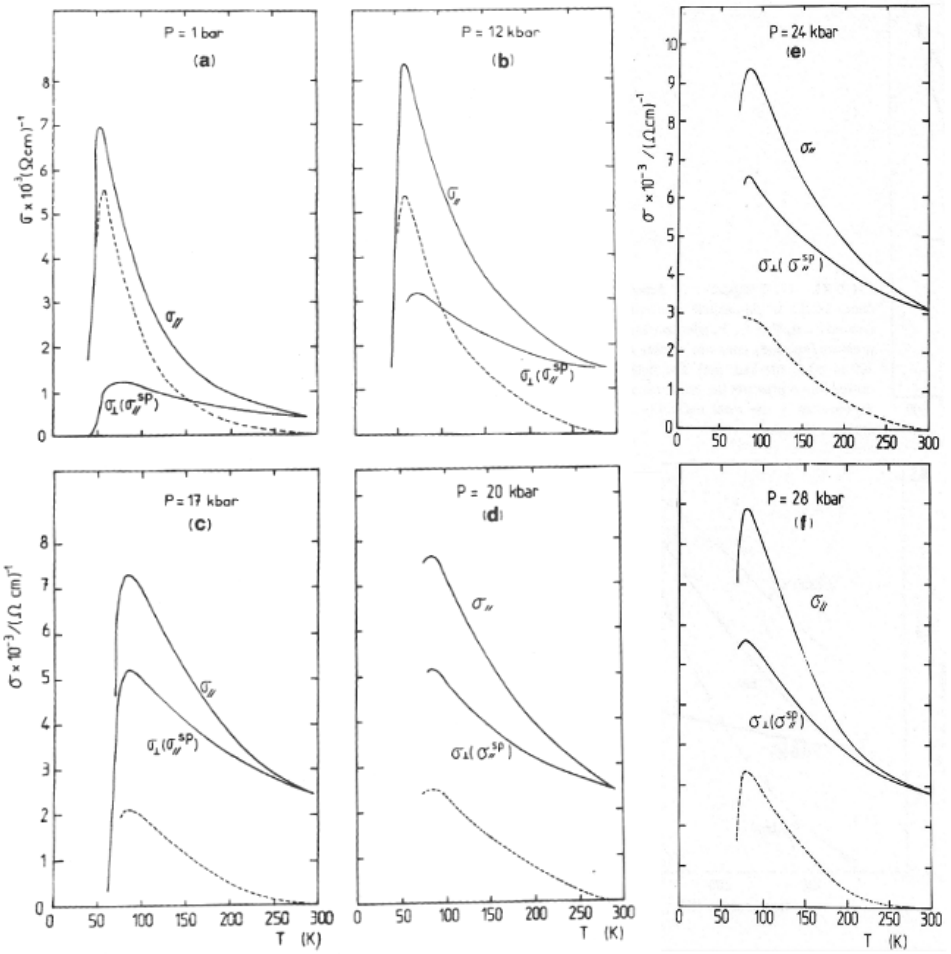

Figure 26. Temperature dependence of the total conductivity $\sigma_{\parallel}$ and of the $\sigma_{\perp}$ normalized to $\sigma_{\parallel}$. The dashed line corresponds to the fluctuating contribution. The room temperature value of $\sigma_{\parallel}$ is $400(\Omega.\mathrm{cm})^{-1}$. Notice, the strong depression of σ_{coll} in the commensurability range. Source: [134, Fig. 16 p. 196-197].

situations of Fig. 26 where at every pressure we have plotted the temperature dependence of σ_{coll} normalized to the value of $\sigma_{\perp}$ at room temperature with the assumption of zero σ_{coll} under ambient conditions.

We may notice that except for the commensurability regime, the fluctuating conductivity is only mildly pressure dependent and consequently the strong pressure dependence of the total conduction which is observed especially at high temperature must be ascribed to the single-particle contribution enhanced by strongly pressure dependent correlation effects.

Given the data on Fig. 26 we are thus able to derive σ_{coll} versus temperature, see Fig. 27 at 1 bar and 12 kbar and also at selected temperatures versus pressure, Fig. 28.

Let us make a few remarks.

First, from the temperature dependence of σ_{coll} on Fig. 27 we notice that the fluctuating contribution agrees fairly well with the divergence of a 1D law $\alpha\ T^{-3/2}$ above 60 K at variance with a 3D behaviour $\alpha\ T^{-1/2}$ expected below 60 K in the very vicinity of the Peierls transition

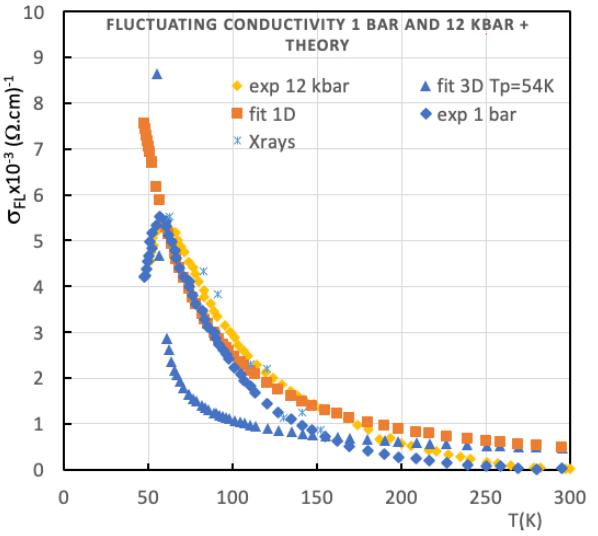

Figure 27. Temperature dependence of the experimental σ_{coll} at 1 bar and 12 kbar together with the peak intensity of the $4k_F$) scattering divided by T. Source: [123] compared to the expected dependences for 1D and 3D (T_p = 54 K) theories. Obviously the 1D fit is much better than the 3D one above 60 K.

which would not agree with the data above 60 K. Both transport and the intensity of X-ray diffuse scattering data [123] point to one dimensional physics in TTF-TCNQ above 60 K. Regarding the 3D Peierls fluctuations domain, diffuse X-ray scattering locate it in the range from 54 K to 60 K [28]. As far as the coherence length is concerned, X-ray studies give a value along the chains of 20 nm at 55 K [28] decreasing to 6 nm at 100 K [123] with a transverse coherence length less than the interchain distance which is consistent with the one-dimensionality.

Second, as shown on Fig. 28, the fluctuating contribution to the total longitudinal conduction is much less pressure dependent (if any) at all temperatures than the single particle part.

Third, the appreciable drop of σ_{coll} shown on Fig. 28 around 19 kbar without any effect on the transverse component as shown on Fig. 25, has been interpreted in terms of the pinning by the commensurability potential of sufficiently long-lived CDW fluctuations. We may notice that the drop of conduction in the commensurability regime is somewhat moderate, about only half the total fluctuating contribution at 80 K, the signature of a modest pinning potential. Hence, the temperature dependence of the relative drop of conduction enables us to estimate the strength of the pinning potential Δ as $\sigma_{min}(T)/\sigma_{max} \propto \exp(-\Delta/T)$.

The inset of Fig. 28 shows that such an activation law is followed with $\Delta \approx 55$ K.

Additional evidence for an important contribution of CDW fluctuations to the longitudinal conductivity comes from experiments on irradiated samples [136] showing a suppression of the 19 kbar conduction dip, as shown in Fig. 29. Defects, introduced by irradiation should very effectively pin the free motion of CDW fluctuations, thus suppressing the CDW-fluctuation conductivity even in the incommensurate situation. Correspondingly, the drop of conductivity observed for irradiated samples near commensurability is much smaller that the one observed in pristine samples. Were the drop of conductivity due to changes in the single-particle scattering, one would expect (from Mathiessen's rule) a similar drop to appear in the irradiated samples. This is not observed. Irradiation has shown that an important part of the metallic conductivity of (incommensurate, non-irradiated) TTF-TCNQ is due to the CDW-fluctuation mechanism.

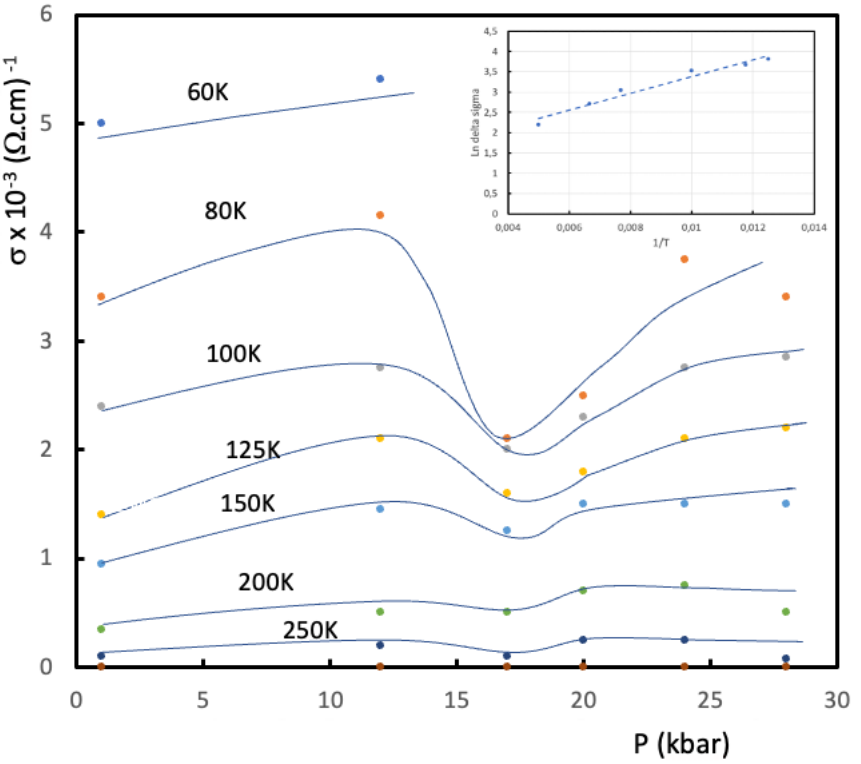

Figure 28. The Fröhlich fluctuating contribution versus pressure at various temperatures for a TTF-TCNQ sample with a CPR = 17 at 1 bar. The 60 K contribution cannot be measured above 12 kbar since the critical temperature becomes larger than 60 K in the commensurability range. The dependence of this collective contribution in pressure is small compared to its temperature dependence. (inset) Activation of the CDW pinned by commensurability with the activation gap of 55 K.

Detailed far-infrared measurements on TTF-TCNQ from 25 K to 300 K have also provided a strong support for a charge density wave mechanism contributing to the dc conductivity in TTF-TCNQ [137].

Fig. 30 shows the b-axis frequency-dependent conductivity of TTF-TCNQ derived from the reflectance data by a Kramers–Krönig analysis following the procedure described by Tanner et al. [137]. The strong peak of the conductivity around 40 cm^{-1} at 25 K has been taken as the signature of the phase-mode of the pinned CDW in the Peierls state. At 60 K, the peak of conductivity has shifted to zero frequency. This phenomenon can be considered as the existence of a collective mode at zero frequency: the collective mode giving rise to the sliding of finite lifetime CDW's.

These FIR studies have also led to a better knowledge of this conduction mode with an effective mass about $20m^*$ and a fluctuation lifetime at 60 K of $\tau_c = 1.6 \times 10^{-12}$ s in contrast with the much shorter single particle lifetime of $\tau_{\parallel,sp} \approx 4.6 \times 10^{-15}$ s derived at 300 K from the NMR measurements [99] or 3.1×10^{-15} s from optical reflectance at room temperature increasing up to 6×10^{-15} s at 70 K [66]. Let us notice that already in 1974, the authors of Ref. [66] concluded that the dc conductivity should be carried in a collective manner.

Now it is interesting to comment on the pressure dependence of the TTF-TCNQ resistivity reported at various temperatures in the conducting regime, Fig. 31. According to the data in

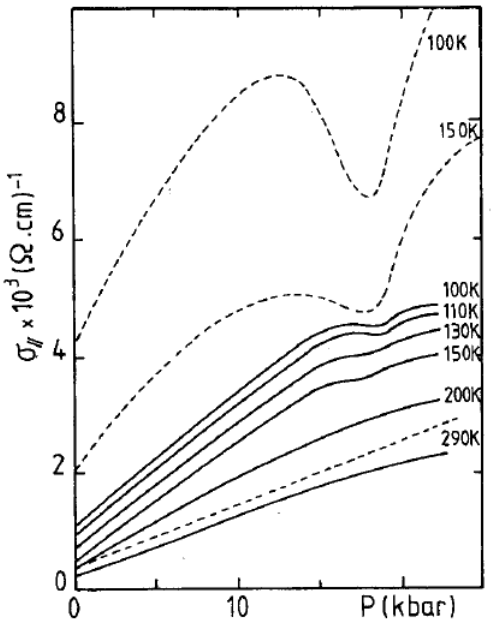

Figure 29. Pressure dependence of the longitudinal conductivity at constant temperature for irradiated TTF-TCNQ (continuous line). Source: [136, Fig. 2 p. 406]. The dashed lines indicate the behaviour of pristine samples according to the data on Fig. 24.

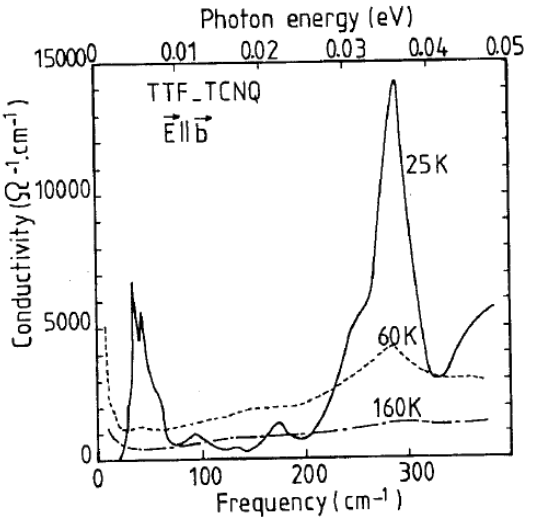

Figure 30. Frequency-dependent *b*-axis conductivity of TTF-TCNQ at four temperatures: 25, 60, and 160 K. Source: [137, Fig. 2 p. 598]. The low frequency conductivity at 60 K is in very good agreement with the DC data of Fig. 26.

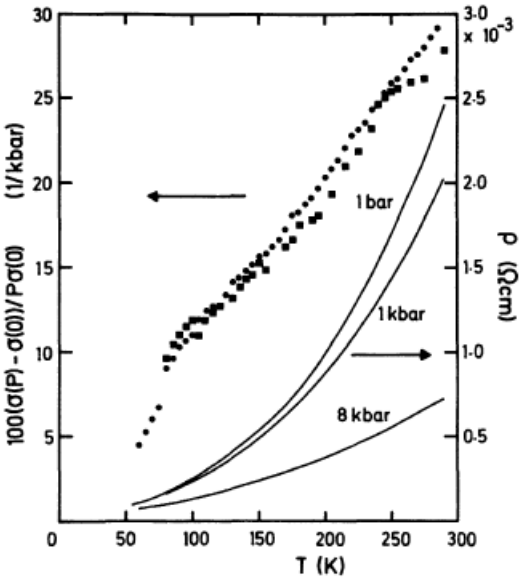

Figure 31. Temperature dependence of the pressure dependence of the conductivity of TTF-TCNQ. Source: [138, Fig. 3 p. 136].

Ref. [138], the pressure dependence of the resistivity dropping from 28 to 5% between room temperature and 60 K. Such a temperature dependence is in very good agreement with a collective conduction very weakly pressure dependent as shown above, becoming dominant at low temperature. Taking the collective contribution into account, we are left with a pressure coefficient for the single particle conductivity of about 25%kbar^{-1} showing hardly any temperature dependence. This is still a very large volume dependence which cannot be understood solely by the modest volume dependence of the bare band theoretical parameters [139, 140] of the order of 2%kbar^{-1}. High pressure measurements concluded that the large volume dependence of the conductivity can be interpreted as a result of a large electron-electron interaction [135]. However, given the predominance of a collective contribution to the conductivity below 100 K, identified more recently, a new visit to the question of the single particle conduction would be valuable.

In short, since we can be confident that the longitudinal conduction data of pristine TTF-TCNQ carry the signature for the existence of a large conductive Fröhlich fluctuating component present anywhere but in the commensurability domain up to about 250 K, the variety of CPR reported in the literature over the past 1974-1975 years is thus likely to be attributed (besides incorrect measurements of the conductivity) to differences in the amount of impurities contributing to an efficient pinning of Fröhlich fluctuations in different samples of TTF-TCNQ. This can be as inferred from the study on irradiated samples [136] with much milder effects on the single particle contribution.

The decomposition of the conduction into two components has shown that the fluctuating part is hardly sensitive to pressure [134] see, Fig. 28, (besides the suppression which is related to the commensurability domain).

We have seen above that thanks to the one dimensional character of the electronic structure of TTF-TCNQ, the fluctuating Fröhlich mode provides a major contribution to the longitudinal conduction whenever there exists no correlation between CDW fluctuations of adjacent stacks.

In addition, TTF-TCNQ provides a brilliant and instructive illustration of the non-linear conduction mechanism observed in several inorganic reduced dimensionally trichalcogenides extensively studied in the eighties [141]. As far as TTF-TCNQ is concerned there exists the

possibility to put the 3D-ordered CDW condensate into motion and thus observe an additional conduction of collective origin. However this collective channel becomes active only when the applied electric field exceeds a certain threshold field, Fig. 32, making in turns the conduction non-linear in terms of the electric field.

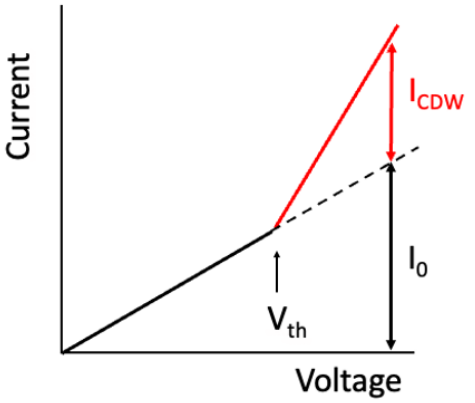

Figure 32. Schematic I-V characteristics in the presence of a collective extra contribution from the CDW condensate active above a threshold voltage (field). The conductance I/V become non-linear at V^{th}.

The existence of nonlinear conduction is well-known from quasi 1D inorganic materials such as $NbSe_3$ below the Peierls transition, where the nonlinear conduction has been interpreted as resulting from CDW depinning [141].

The mechanisms which can pin a CDW are impurity pinning, commensurability pinning, and Coulomb interaction between oppositely charged chains in two-chain systems such as TTF-TCNQ.

The collective conduction channel is observed in TTF-TCNQ below T_H with E_T reaching a minimum of 0.25 V/cm at 51.2 K in the narrow temperature interval between T_H and T_M in which TTF-TCNQ behaves as a single chain CDW [142], see also Fig. 17.

A fast increase of E_T is observed on cooling below TM when a CDW arises on the TTF chains, with E_T becoming of the order of 1-10V/cm [143], see Fig. 33. This rise of E_T has been understood in terms of the sliding of joint CDW's on TTF and TCNQ stacks moving together in the same direction with a pinning mechanism governed by impurities [143]. According to a Landau type theory of the CDW formation [114], the enhancement of the impurity pinning mechanism is linked to the growth of a CDW on TTF chains below T_M and the existence of a Coulomb attraction between oppositely charged chains [143]. In the absence of any coupling between TTF and TCNQ chains, an electric field would lead to CDW motion in opposite directions in the two-chain systems because of the electron (TCNQ) and hole (TTF) character of the electronic bands.

However, the motion of the TTF and TCNQ CDW's in opposite directions, which provides the maximum CDW current would require a threshold field of $E_T \approx 5 \times 10^4$ V/cm [143]. This cannot be responsible for the nonlinear effects found here with $E_T \approx 1-10$ V/cm, Fig. 33. The whole picture is confirmed by the behaviour of the threshold field in TTF-TCNQ under 4 kbar, Fig. 34, when the range of one-chain CDW is more extended towards low temperatures than at ambient pressure, Fig. 17, with a concomitant smaller increase of E_T at low temperature.

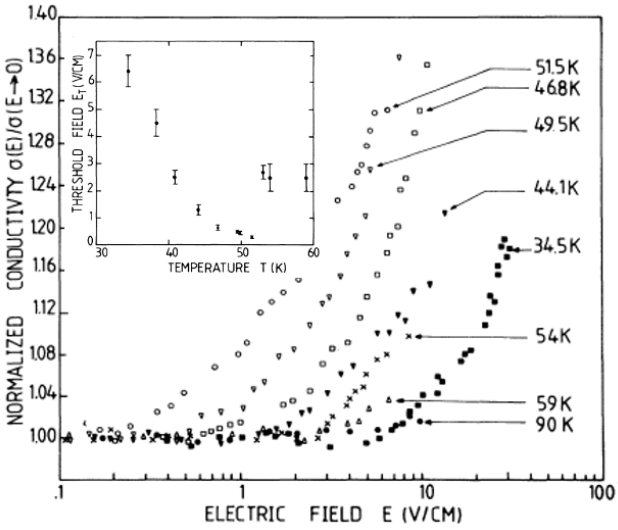

Figure 33. Normalized conductivity $\sigma(E)/\sigma(E \to 0)$ vs logE of TTF-TCNQ at 1 bar. The inset shows the temperature dependence of the threshold field. Source: [143, Figs. 1, 2 p. 2552]. ©American Physical Society and the authors. All rights reserved.

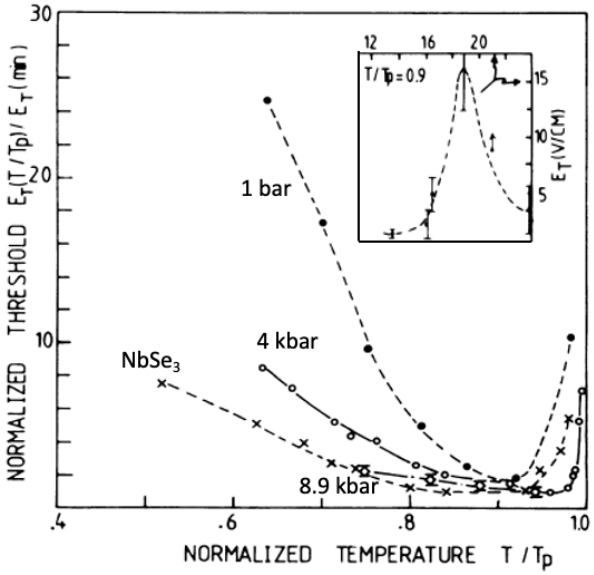

Figure 34. Normalized threshold field $E_T/E_T(min)$ versus the normalized Peierls temperature at different pressures. Source: [144, Fig. 1 p. 263], including the data for $NbSe_3$ at 1 kbar. Source: inset [145, p. 137]. ©American Physical Society and the authors. All rights reserved.

3.1.8. *TTF-TCNQ under higher pressure*

An investigation of the phase diagram of TTF-TCNQ at much higher pressures than what the Orsay had published has been performed using the cubic anvil technique up to 80 kbar [146], Fig. 35.

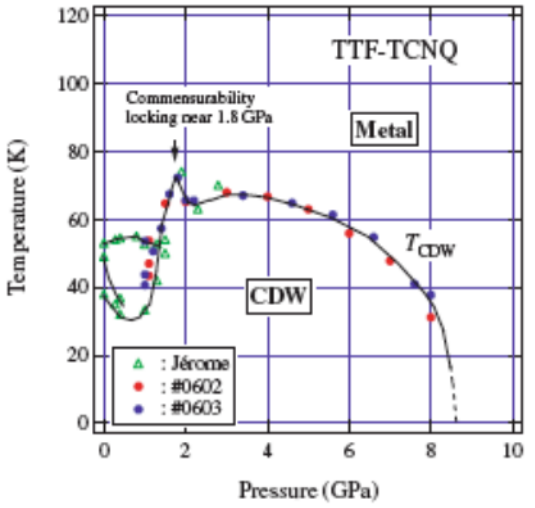

Figure 35. T-P phase diagram of TTF-TCNQ . Source: [146, Fig. 4 p. 2]. The previous data of Ref. [98] are also displayed with green triangles. The authors of Ref. [146] expect the suppression of the Peierls transition near 9 GPa.

The motivation for such a study was the suppression of the Peierls instability as a result of the enhancement of the interchain coupling leaving an open possibility for the stabilization of superconductivity due to the $2k_F$ phonon softening [147]. This experiment although confirming the results of the Orsay group for commensurability at 19 kbar [98], has revealed that the Peierls instability is gradually depressed under higher pressure with a concomitant decrease of the activation energy. Under 80 kbar, the resistivity shows a metallic behaviour down to a CDW transition at 25 K. At lower temperatures a semimetallic behaviour is observed without any sign of superconductivity at least above 2.5 K. Such a failure to stabilize a superconducting state might be due to an increased gap at the Fermi level coming from the hybridization coming from the molecular orbitals on neighbouring chains. We are not aware of any study on TTF-TCNQ performed at pressures beyond 80 kbar.

3.2. *Other charge transfer salts, selenide molecules*

3.2.1. *TSF-TCNQ*

In the seventies the leading ideas governing the search for new materials likely to exhibit good metallicity and possibly superconductivity were driven by the possibility to minimize the role of electron-electron repulsions and at the same time to increase the electron-phonon interaction while keeping the overlap between stacks as large as possible [147]. This suggestion not having kept its promises with the TTF-TCNQ family led to other attempts and the synthesis of new series of charge transfer compounds, for example changing the molecular properties while retaining the same crystal structure. It was recognized that electron polarizability was important to reduce the screened on-site e-e repulsion and that the redox potential $(\Delta E)_{1/2}$ should be minimized [84]. Hence, new charge transfer compounds with TCNQ have been synthesized using other heteroatoms for the donor molecule, i.e. substituting sulfur for selenium in the TTF skeleton thus leading to the TSF molecule ($(\Delta E)_{1/2}$=0.37 eV for TTF [84] but only 0.32 eV for TSF [148]) and the synthesis of the charge transfer compound TSF – TCNQ. This compound

has the same monoclinic structure as TTF-TCNQ and the slight increase of the unit cell by 0.057Å does not compensate for the significant increase of 0.15Å for the van der Waals radius going from sulfur to selenium. Consequently, the cationic bandwidth of TSF – TCNQ is increased by 28% as shown by the tight binding calculation, while the TCNQ band is hardly affected [139]. It is probably the increase in the donor bandwidth with a concomitant decrease of the e-e repulsion on the TSFstacks which suppresses $4k_F$ fluctuations *at variance* with TTF-TCNQ where $4k_F$ scattering is observed from 300 K [149].

Measurements of the conductivity [93], Fig. 15 and thermopower [150] show a single transition into a semiconducting Peierls distorted state at $T_p = 29$ K. Below this transition an incommensurate $2a \times 3.15b \times c$ superstructure is observed [151]. In contrast to the behaviour of TTF-TCNQ no further phase changes occur down to the lowest observed temperatures, and the electronic gap is obtained consistently from resistivity [152], susceptibility [153] and infrared [154]measurements as $E_g = 250$ K, showing that both TSF and TCNQ stacks order at the same Peierls transition.

Furthermore, the observation of $2k_F$ scattering in TSF – TCNQ already below 230 K [149, 155] prior to the Peierls transition at 29 K has led to an accurate determination of the incommensurate charge transfer, namely $\rho = 0.63$.

As inferred from a detailed study of the conductivity, the sliding CDW's are also contributing to the total conduction although in a proportion much smaller than it is for TTF-TCNQ [156].

As far as structural precursor effects are concerned there are significant differences between TTF-TCNQ and TSF – TCNQ. While precursor effects are one-dimensional in TTF-TCNQ over almost the entire temperature domain where they are observed, the picture is different in TSF – TCNQ since a short range 3D coupling is observed between 29 and 50 K and only a limited 2D coupling is noticed up to 100 K [155, 157].

Commensurability between CDW and the underlying lattice (×3) has been detected at 6.2 kbar through a small peaking of the Peierls transition and a small concomitant drop of the longitudinal conductivity [158]. The modest amplitude of the conductivity drop accompanying the commensurability suggests that the CDW's in the non-ordered phase above 29 K are already partially pinned by transverse coupling and therefore cannot contribute dominantly to the fluctuating conduction of the metallic domain as it is the case for TTF-TCNQ [156]. Altogether TSF-TCNQ evolves under pressure [158] in a way quite similar to TTF-TCNQ with the single phase transition at T_p increasing steadily up to 45 K under 25 kbar with no sign of any suppression in this pressure range. Unfortunately, unlike TTF-TCNQ no higher pressure studies have been undertaken with TSF – TCNQ.

3.2.2. *HMTSF-TCNQ-like compounds*

The goal of the effort to develop new organic metals was to find systems which remain metallic down to low temperature a requirement to give rise to superconductivity.

The main idea guiding the work of researchers in the 1970's for a stabilization of superconductivity in organic conductors was to increase the two-dimensional character of the electronic structure in order to suppress the Peierls instability favored by the one-dimensionality [147, 159].

The attempt to increase the transverse overlap and in turn stabilize a metallic phase at low temperature has been partly successful with the synthesis of new TCNQ charge transfer compounds in which the structure exhibits a chessboard-like pattern, Fig. 36. This is the case for hexamethylene-donor molecules with sulfur or selenium heteroatoms, HMTTF or HMTSF respectively [65, 160] where metallicity is nearly achieved at low temperature. In HMTTF – TCNQ, an incommensurate CDW system with $\rho = 0.72$ [157], a semimetallic character can be maintained at low temperature under pressure above 19 kbar with $\delta\rho/\delta T > 0$ although a weak transition is still observed in resistivity at 30 kbar [161]. It was anticipated that the complete suppression of the distortion would require a pressure between 35 and 40 kbar.

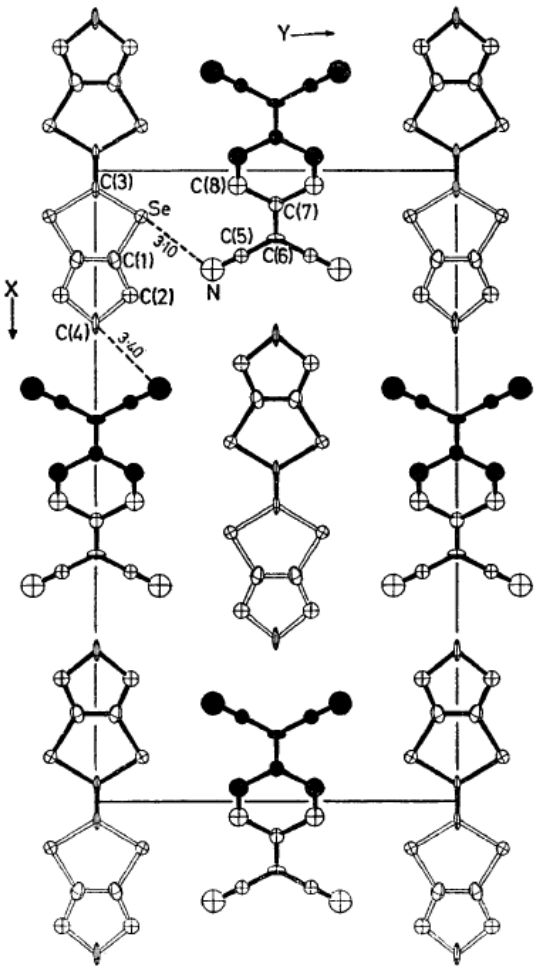

Figure 36. A projection of the structure of HMTSF-TCNQ onto the plane perpendicular to the stacking axis. The chessboard pattern *at variance* with the packing of TTF-TCNQ is clearly visible. The planes of the molecules in the Figure are tilted relative to the projection plane by 22° (HMTSF) and 34° (TCNQ). The transverse contact Se…N of 3.10 Å is particularly strong, much shorter than the S…N contacts in TTF-TCNQ with a criss-cross molecular packing along the *a*-axis, see Fig. 8. Source: [162, Fig. p. 335]. ©Royal Society of chemistry.

The selenide related compound, HMTSF-TCNQ, Fig. 36, exhibits a resistance minimum prior to a phase transition at $T_c = 24$ K [163] which although decreasing under pressure, never vanishes in good quality samples [86]. This 24 K anomaly arises from the formation of a 3D superstructure $a \times 2.7b \times c$ corresponding to a charge transfer $\rho = 0.74$ [127].

One of the first studies of this compound suggested that the three-dimensional order state of 24 K could be suppressed under pressure allowing the establishment above 4 kbar of a conducting state up to 100 mK [164]. This study aroused a lot of interest since for the first time a metallic-like conductivity exceeding $10^4(\Omega.\text{cm})^{-1}$ could be stabilized at helium temperature in a charge transfer conductor member of the TTF-TCNQ family. A model of semi-metallic Fermi surface for the undistorted three-dimensional Fermi surface of HMTSF-TCNQ, i.e. at T> 24 K has been

proposed by Weger [165], leading to a 3D semi-metallic Fermi surface consisting of small section cylinders or elongated ellipsoids in the c-direction. However, subsequent experiments suggested that the stabilization of the semi-metallic state previously claimed [164] could have been the result of defective samples. But the suggestion that the coupling between neighboring donor and acceptor chains is important in determining the shape of the Fermi surface at low temperature ($k_B T < t_\perp$) proved to be important for the future.

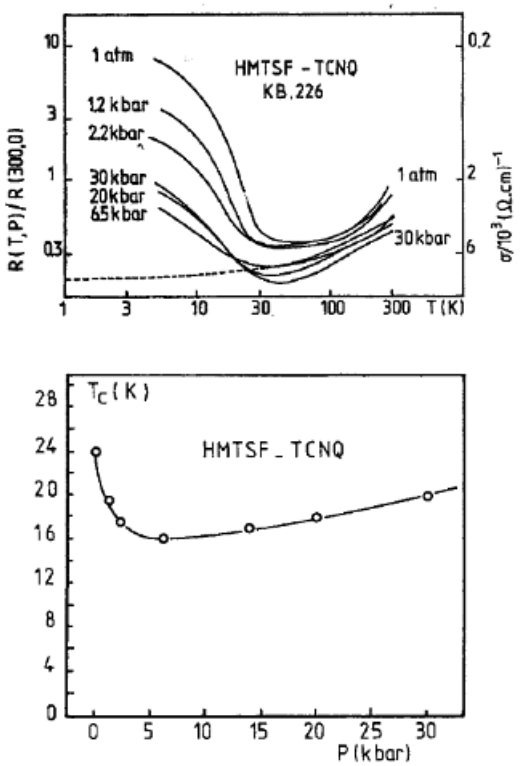

Figure 37. (Top) HMTSF-TCNQ crystal showing no stabilization of a semi-metallic state above 4 kbar as reported in Ref. [86]. The dotted line corresponds to the stabilization of a semi-metallic state observed in a poor quality crystal. (Bottom) Pressure dependence of the Peierls phase transition of HMTSF-TCNQ. Unpublished data from M. Miljak at Orsay.

Actually, in good quality samples, the initial drop of T_p below 24 K observed up to 5 kbar is followed by a re-increase up to 20 K under 30 kbar as displayed on Fig. 37, (bottom). In this picture a possible explanation for the decrease of T_p with pressure in Fig. 37 is a pressure-induced increase of the interchain transfer integrals, which increases the non-planarity of the Fermi surface so that the Peierls instability can only affect a smaller portion of the Fermi surface and therefore occurs at lower temperature.

It was concluded that in HMTSF – TCNQ, due to the important deviation from planarity of the Fermi surface, the Peierls transition can only partly destroy it. There are plenty of experimental results supporting the picture of a semi-metallic Fermi surface at low temperature in HMTSF-TCNQ [88]. A striking confirmation was provided by the measurement of the Hall effect [166] providing a very large Hall constant at low temperature related to the semi-metallic behaviour with approximately 1/500-1/1000 large mobility ($\mu \approx 4 \times 10^4$ cm^2/Vs) carrier per

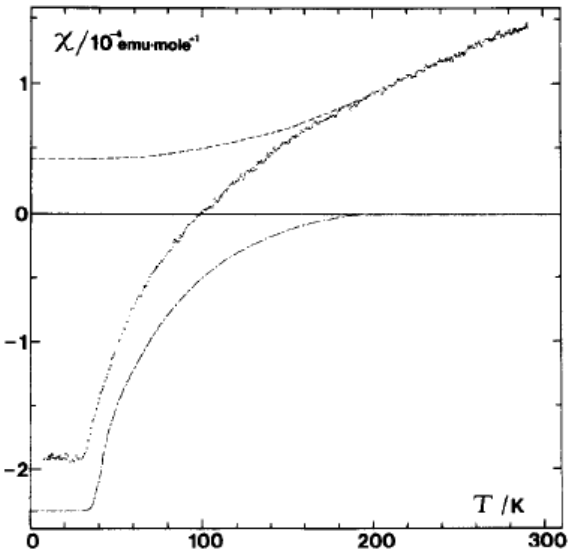

Figure 38. Temperature dependence of the HMTSF-TCNQ susceptibility measured by NMR. The Pauli contribution is the dashed line and Landau–Peierls, the dashed dotted line. Source: [89, Fig. 3 p. 108]. ©(1976) Elsevier. All rights reserved.

formula unit compared to the small Hall constant measured at room temperature, signature of the 1D metallic nature. Another confirmation was provided by the measurement of the magnetic susceptibility found to become diamagnetic below 100 K [89] and attributed to a large Landau–Peierls orbital diamagnetism associated with very small cross-sectional areas of the Fermi surface. The LP diamagnetic susceptibility being proportional to m_0/m^* becomes appreciable at low temperature because of the small effective masses of the carriers in the semi-metallic pockets as measured by Shubnikov–de Haas oscillations describing adequately the semi-metallic band structure [167].

It is usually agreed that a cross-over from the 1D (planar) to a 3D (ellipsoidal semi-metallic) Fermi surface occurs around 100 K in this compound [89]. In addition, the conductivity does not vary significantly through the cross-over regime since both the density of carriers and the Fermi wave-vector are changing in about the same proportion [167].

If the transition is to be suppressed by pressure, this would require much higher pressures as Murata et al. recent results [168] imply that if it occurs, this would arise above 8 Gpa or so, *see* Fig. 39. The resistivity data displayed on Fig. 39 reveal a ratio between 5 and 24 K under ambient pressure much larger than the one reported in the early studies in the 1976's. Resistivity data would thus lead to an activation energy of the order of 35 K, in line with transition temperature around 24 K. This is likely the result of an improved sample purity minimizing the role of impurity conduction in the low temperature phase. In addition, the possibility of a field-induced charge density wave state (topic not covered in the present article, *see* Ref. [169] for instance), have been claimed when the component of the magnetic field along the least conducting direction exceeds 10T (under 1.1 GPa) accompanied by the observation of a quantized Hall effect and angular magnetoresistance oscillations [168, 170]. These remain interesting possibilities which will require further confirmations.

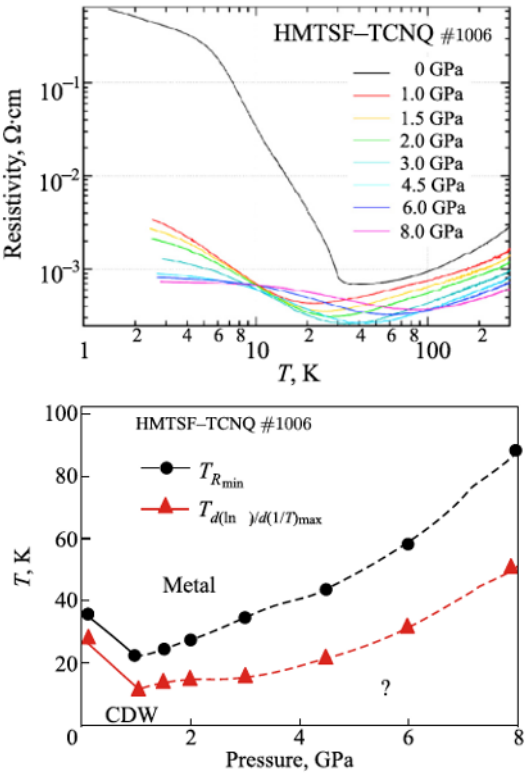

Figure 39. (Top) Recent temperature dependence of the resistivity under pressure in cubic anvil pressure device. According to the zero pressure data, the activation energy of the resistivity amounts to ≈ 35 K. (Bottom) temperature-pressure phase diagram according to Ref. [168]. Source: [168, Figs. 3 and 4 p. 372]. ©2014 AIP Publishing. It is in fair agreement with the data on Fig. 37 bottom.

3.2.3. *TMTSF-DMTCNQ*

The study of the two-chain charge transfer compounds went on with a system where both donor and acceptor molecules had been methylated namely, TMTSF – DMTCNQ, so-called (TM-DM), where the donor is the tetramethyl selenide derivative of TTF and the acceptor. The outcome of this study has been truly decisive for the quest of organic superconductivity. This 1-D conductor undergoes a Peierls transition at 42 K detected by conductivity [79] and magnetic [171] measurements where unlike TTF – TCNQ a distortion occurs simultaneously on both chains [172]. Several other results have triggered the attention. X-ray experiments had shown that the charge transfer is only $\rho = 0.5$ namely, a quarter-filled band situation [172] for both acceptor and donor bands. Such a band filling leads in turn to a high order commensurate CDW with a periodicity of $4a$. a is the direction of best conductivity. Transport and thermopower data have emphasized the dominant role played by the TMTSF chain in the mechanism driving the Peierls transition and also in its contribution to the conduction at high temperature [171].

In addition, according to the pressure study displayed on Fig. 40, the commensurate state is remarkably stable under pressure since the Peierls transition stays at practically the same temperature of 42 K up to 8 kbar [173].

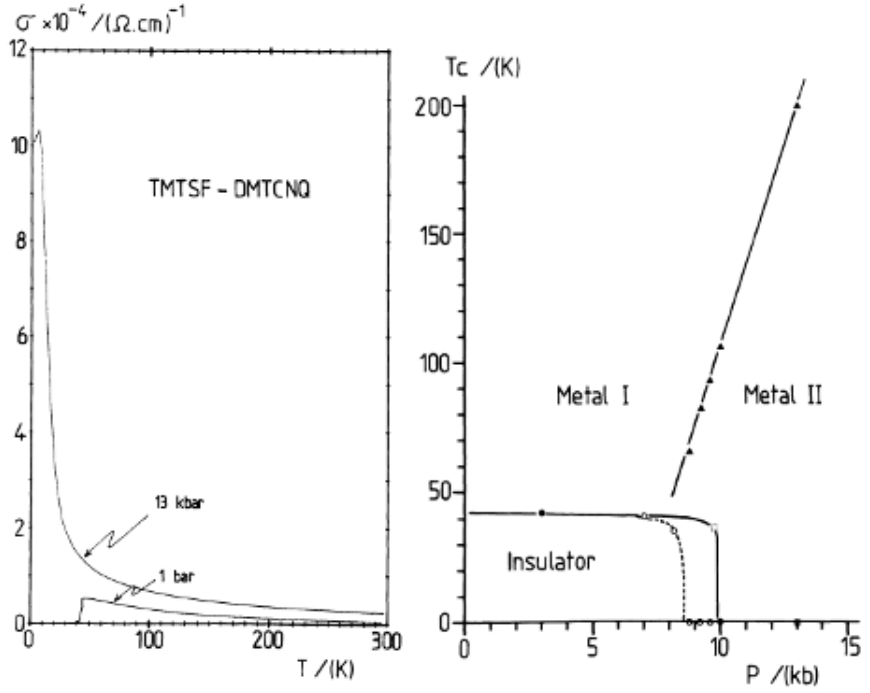

Figure 40. Temperature dependence of $\sigma_{\|}$ in TMTSF-DMTCNQ, at atmospheric pressure and under 13 kbar (left). Phase diagram of TMTSF-DMTCNQ, under pressure (right). Sources: [173, Figs. 2, 3 p. 1200].

The really new and unexpected finding has been the sharp suppression of the Peierls transition under a pressure of about 9 kbar and the conductivity remaining metal-like down to low temperature, reaching $10^5(\Omega.\mathrm{cm})^{-1}$ under 10 kbar at liquid helium temperature [173], Fig. 40.

The stabilization in TM-DM of the conducting state at low temperature under pressure, see Fig. 40, is apparently related to a pressure-driven S-shape anomaly which is visible on the temperature dependence of the resistivity.

The very high value of the low temperature conductivity above 10 kbar has stimulated more investigations under high magnetic field in order to better characterize this high conduction state.

Magnetoresistivity experiments performed on high purity TMTSF-DMTCNQ single crystals reveal well formed Shubnikov de Haas oscillations below 3 K for the longitudinal resistance in fields up to 7T aligned along both transverse directions [174], Fig. 41. When these magnetoresistance oscillations are analyzed in terms of the celebrated Shubnikov–de Haas theory [175], the characteristics of the Fermi surface at low temperature can be derived, leading to ellipsoidal Fermi surfaces with cross sections 1.16×10^{17} m^{-2} and 2.6×10^{17} m^{-2} in the $(a-b)$ and $(a-c)$ planes respectively. Furthermore, the cyclotron mass and the Dingle temperature derived from the temperature dependence of the amplitude at fixed field and the field dependence at constant temperatures respectively amount to $m_c = 0.56m_0$ and $T_d \approx 0.8$ K. If we assume parabolic bands and use the above mentionned ShdH parameters and Figure 41 we obtain the Fermi energy of a pocket namely, $E_F \approx 50$ K. Moreover, the volume enclosed within such small pockets is about 3×10^{-4} times smaller than the volume enclosed by the original high temperature 1-D Fermi surface. Thus, the density of carriers measured by SdH effects in the highly conducting phase at low temperature is about 10^{-4} per formula-unit, i.e. 3×10^{18} cm^{-3} (assuming two pock-

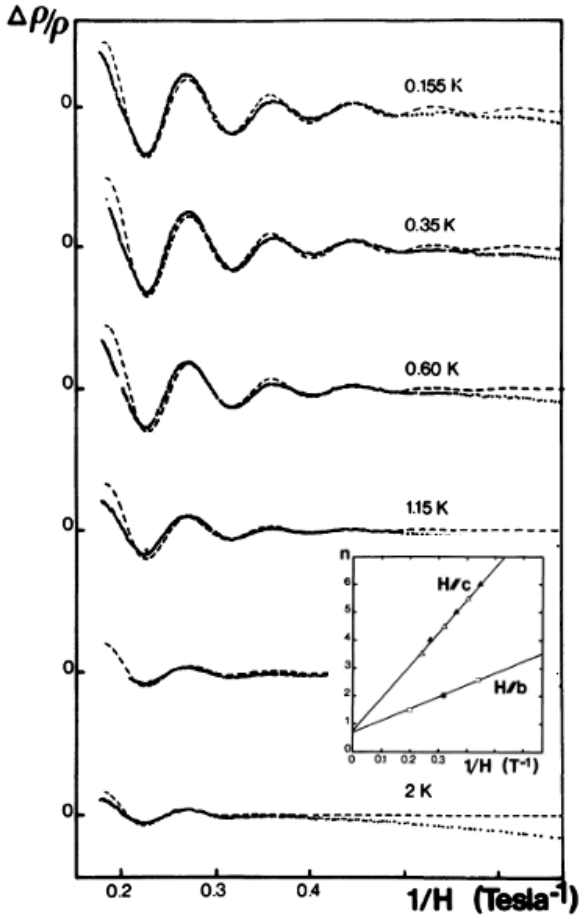

Figure 41. Oscillatory magnetoresistivity of TMTSF-DMTCNQ under 12 kbar (H//c) versus 1/H for different temperatures. Sources: [174, Figs. 2, 4 p. 288-289], the inset shows successive integers and half-integers corresponding to maxima and minima of the oscillations versus 1/H for both transverse directions. In TM-DM, the stacking axis is usually called a while b and c are the transverse axes.

ets of such carriers per Brillouin zone, a semi-metallic situation). Given the data from quantum oscillations, an upper limit value for the single particle low temperature conductivity should be around $2\text{-}3\times10^3(\Omega.\text{cm})^{-1}$.

The semi-metallic structure under pressure has also been confirmed by a Landau–Peierls contribution to the susceptibility occurring below 30 K [176], contrasting with the 1D to 3D cross-over of HMTSF-TCNQ developing below ≈200 K, see Fig. 38. A conclusion from the susceptibility study was that the TM-DM transverse coupling between unlike chains should be smaller than that of HMTSF-TCNQ under ambient pressure with a consequent lowering of the 1D to 3D cross-over temperature.

As discussed in more details in Ref. [174], the semi-metallic picture of TMTSF-DMTCNQ at low temperature under pressure cannot explain the remarkably high value of the conductivity under pressure which amounts to more than $\approx 10^5(\Omega.\text{cm})^{-1}$ as shown on Fig. 40.

The semi-metallic picture which can explain the low temperature state, quantum oscillations, Landau–Peierls diamagnetism of HMTSF-TCNQ [89] and $\sigma \approx 10^3 - 10^4(\Omega.\text{cm})^{-1}$ thus fails to

provide a reasonable interpretation for the extraordinary large value of the conductivity of TMTSF-DMTCNQ which is ten times larger at helium temperature.

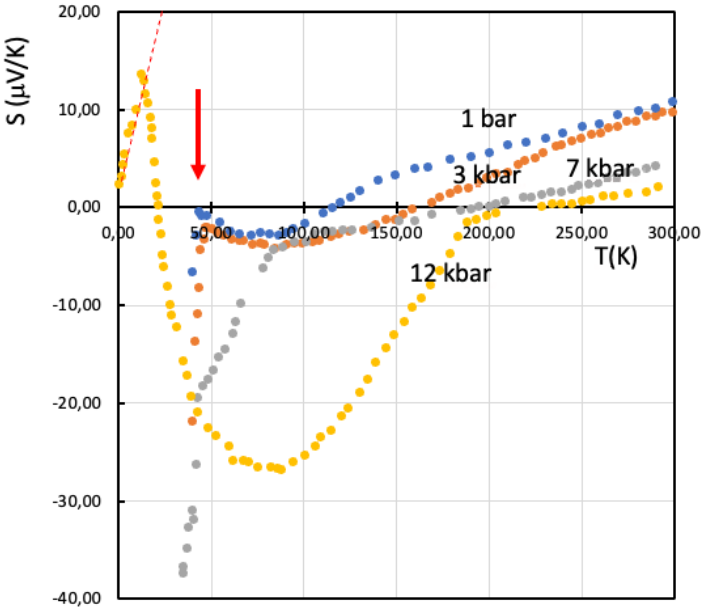

Figure 42. Temperature dependence of the absolute thermoelectric power of TM-DM at 1 bar (data from [79]) and under pressure. Source: [173, Fig. 5 p. 1202]. Notice the semi-metallic behaviour below 25 K characterized by the large slope of S(T). The arrow marks the temperature of the Peierls transition which is nearly unchanged between 1 bar and 8 kbar.

It is now quite instructive to look how the thermopower of TM-DM behaves in temperature and pressure, see Fig. 42. These data displayed on this figure show together ambient [79] and high pressure [173] measurements. At low temperature ($T < 10$ K), the inset of Fig. 42 the TEP is positive and quite linear in temperature, extrapolating close to the origin. This behaviour is indicative of a 3D semi-metallic ground state dominated by small hole pockets. Assuming 3-D semi-metallic pockets, the Seebeck coefficient reads [56],

$$S = \frac{\pi^2}{2}\frac{k}{e}\frac{kT}{E_F}. \tag{7}$$

Therefore, the low temperature experimental data of TEP in Fig. 42 would lead to the estimate $E_F \approx 300$ K according to Eq. (7). This value is admittedly much larger than what can be derived from the data of the dHSh measurements [174], with a crude estimate of parabolic bands [174] namely, $E_F \approx 30$ K. However, we can reconcile both values, as it has been proposed in Ref. [174], assuming the existence of a channel of collective conduction acting in parallel with the single particle channel leading to a total conduction of $\sigma = \sigma_{coll} + \sigma_{sp}$. Thus, with a two-fluid model the thermopower becomes,

$$S = \frac{\sigma_{coll} S_{coll} + \sigma_{sp} S_{sp}}{\sigma_{coll} + \sigma_{sp}} \tag{8}$$

Since no heat can be carried by a current of collective origin, $\sigma_{coll}S$ is expected to be negligible and the measured thermopower becomes,

$$S = \frac{\sigma_{sp}S_{sp}}{\sigma_{coll}} \tag{9}$$

Consequently, the Seebeck coefficient related to the small semi-metallic pockets would thus becomes $(\sigma_{coll}/\sigma_{sp})$ × the measured value of S, leading in turn to a reduction for the value of the actual Fermi energy of the pockets, in better agreement with the estimate of $E_F \approx 30$ K from dHSh data since $\sigma_{coll}/\sigma_{sp}$ is > 1 at 50 K.

In order to explain the intriguing question of extra conduction in TMTSF-DMTCNQ, an other conduction mechanism should necessarily be active in parallel with the single particle channel. Since the existence of a collective conductivity seems to be the only way to reconcile fermiology and thermopower data in TM-DM under 12 kbar, the salient question is about the actual nature of this collective contribution.

At the beginning of the eighties a suggestion has been made for the huge conductivity of order $10^5(\Omega.\text{cm})^{-1}$ in TM-DM which is observed at low temperature under pressure. The interpretation of this conductivity in terms of a single-particle conduction mechanism would lead to a huge mean free path of about 3000 Å at helium temperature. This possibility seemed to be rather hard to accept at that time. Instead, an interpretation based on superconducting fluctuations induced paraconductivity was proposed [177]. We shall see in the following Sections that very large mean free paths have been measured in materials such as $(TMTSF)_2PF_6$ and they are even required to explain the stability of the 3D superconducting state which is very sensitive to the presence of non-magnetic defects. Therefore, the suggestion of a superconducting origin for the collective conductivity of TM-DM should be nowaday taken with a grain of salt.

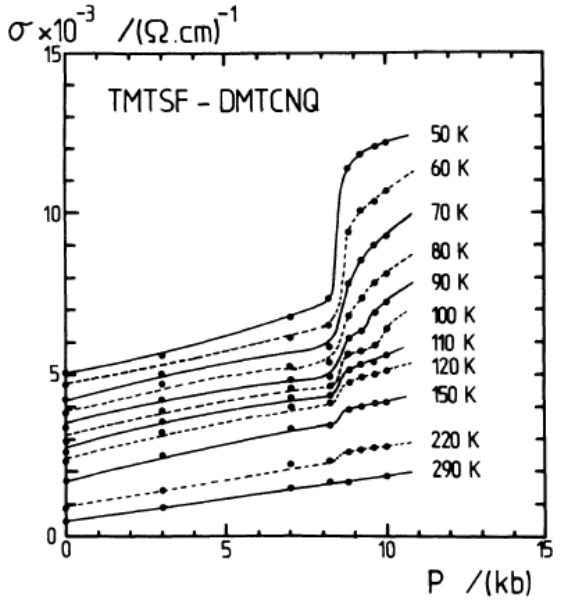

Figure 43. Pressure dependence of $\sigma_\parallel$ in TMTSF-DMTCNQ above 42 K. $\sigma_\parallel(300\text{ K}) = 500(\Omega.\text{cm})^{-1}$. Source: [173, Fig. 1 p. 1200]. ©EDP sciences. All rights reserved.

An other possibility can also be considered. According to the behaviour of the pressure dependence of the conductivity for different temperatures performed in a helium gas pressure

apparatus, see Fig. 43, the suppression of the Peierls insulating state is accompanied by a clear increase of the conductivity bearing some resemblance with TTF-TCNQ where a dip in the $\sigma(P)$ curves is observed in the commensurability regime, (Fig. 25). Consequently, the way the conductivity of TM-DM behaves is strongly suggestive for the existence of a Fröhlich conducting channel becoming active outside a broad commensurability domain, i.e. above 8 kbar.

Following the data analysis used for TTF-TCNQ, we have displayed on Fig. 44 the fit for one-dimensional Fröhlich fluctuations contributing to the longitudinal conduction normalized to the experimental value of the conductivity under 13 kbar at 10 K according to Ref. [173]. In addition, subtracting the theory from the measured conductivity, we can derive the single particle contribution plotted in the inset of this figure. As we can see in the inset of Fig. 44, $\sigma_{\parallel,sp}$ is dominant over the Fröhlich contribution at 300 K and reaches $\approx 5\times10^3$ $(\Omega.\mathrm{cm})^{-1}$ at low temperature, both channels contributing about equally around 100 K. Such a behaviour is indeed reminiscent of TTF-TCNQ, see Fig. 26.

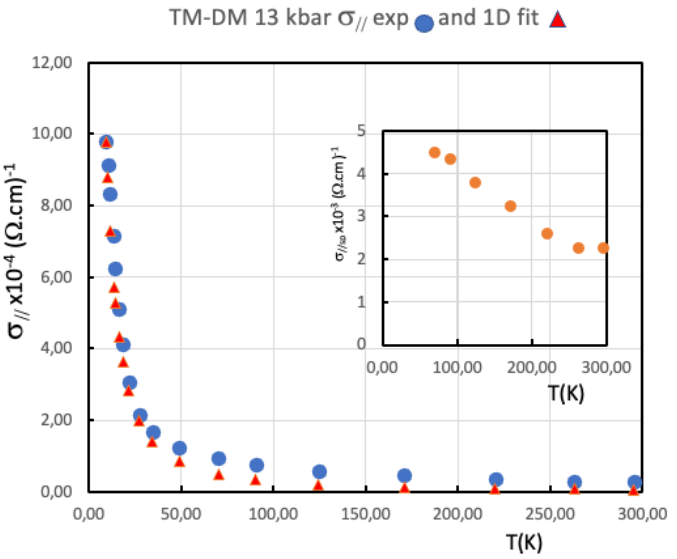

Figure 44. One-dimensional fit in $T^{-3/2}$ for the experimental conductivity of TM-DM at 13 kbar taken from Ref. [173] normalized at 10 K, dots are experimental data while triangles are the theoretical 1D fit. The inset shows the single particle contribution derived by subtracting the 1D collective contribution from the experiment.

It is worth paying more attention to the very broad width of the commensurability regime in pressure as displayed on Fig. 43 which is at least of 9 kbar. While at $P > 9$kbar, we have seen previously that the conduction is dominated by the Fröhlich mode of incommensurate fluctuations, we may suggest that below 9 kbar we are in presence of a state which is not commensurate strictly speaking. Instead, in the conducting state above the metal-insulator transition at 42 K commensurate and incommensurate regions (discommensurations) could coexist. It is plausible that the proportion of incommensurate volume is evolving under pressure, reaching 100% for incommensurate volume only above 9 kbar. Thus, the observed S-shape anomaly in resistivity occurring at an increasing temperature with pressure, see Fig. 40, would mark the limit in pressure between a low pressure regime with a mixture of commensurate and in commensurate domains and a high pressure regime regime in which the CDW is uniformly incommensurate. The steep slope of this transition, with a 5 kbar difference between ambient

temperature and 50 K, is in a good agreement with the change in bandwidth due to the large thermal contraction for TTF-TCNQ already mentioned above.

To be noted that doubts had been expressed about the possibility of Fröhlich conduction in this material under pressure [178] arguing that long coherence lengths at low temperature should lead to a three-dimensional ordering of the one-dimensional fluctuations and consequently to an insulating ground state. The argument expressed in the reference [178] is understandable although the increase of conductivity noticed out of the commensurability domain on Fig. 43 and subsequent dHSh results [174] seem to support the existence of a collective contribution to the conduction at least down 30-20 K where a cross-over between 1D and semi-metallic electronic structure could take place.

In conclusion for TM-DM, a transition 1D-3D is observed around 30 K in the incommensurate state of this compound above 9 kbar, suppressing the Peierls ground state. In this two-chain material, the closed FS is thus a result of interstack hybridization with a value for the transverse overlap lying in-between that of TTF-TCNQ and HMTSF-TCNQ. Such an hybridization being responsible for a significant lowering of the density of states at Fermi level [87] may in turn prevent the establishment of superconductivity although the Peierls transition is suppressed under pressure.

3.2.4. *Beyond TMTSF-DMTCNQ*

TM-DM is a very interesting system which should have deserved more work but since all these phenomena were new and unexpected the effort was quickly put on a simpler structure built on a single organic stack comprising the novel and lucky TMTSF molecule together with an inorganic monoanion which was able to achieve the situation of a quarter-filled band which prevails in TMTSF-DMTCNQ, at low pressure. Such a structure was already known from the early and extensive work of the Montpellier chemistry group who synthesized and studied the series of isostructural $(TMTTF)_2X$ organic salts [68, 179] where TMTTF is the sulfur analog of TMTSF and X is a monoanion such as ClO_4^-, BF_4^- or SCN^- etc. All these compounds turned into strong insulators at low temperature under atmospheric pressure. It is the reason why they did not attract much attention until the day when they have been revisited by Klaus Bechgaard who, taking advantage of the results obtained in TM-DM, had the intuition to synthesize similar radical cation salts but with the TMTSF molecule. It is the synthesis of this $(TMTSF)_2X$ series which has marked the beginning of a new era in the physics and the chemistry of one dimensional conductors.

3.3. *Concluding the charge transfer era*

Proposals of theorists in the 1960's, in search of new materials and new mechanisms likely to lead to the stabilization of superconductivity at temperatures higher than the 20-23 K range of the time gave rise to a remarkably productive effort to synthesize new molecular crystals possessing electronic conduction properties unknown at the time.

In 1973, the first molecular crystals with electronic properties similar to those of metals in a wide range of temperatures appeared. These organic conductors whose protoptype is the TTF-TCNQ charge transfer complex, have led to numerous physical studies (crystallography, electrical and magnetic measurements, NMR, calorimetry, etc.) often under extreme temperature and pressure conditions which have stimulated numerous theories in the six years that followed.

What made this area of research so popular was on the one hand the hope that these systems could eventually lead to high T_c superconductors and on the other hand the possibility to synthesize and grow single crystals of large size and very high purity to perform sharp physical investigations contributing to a better understanding of the one-dimensional world.

- The main property of the TTF-TCNQ family materials is a crystal structure formed by parallel segregated columns of donors and acceptors along the b stacking axis.

  Consequently, the metal-like conduction is made possible by the overlap along the b axis of the π orbitals from HOMO and LUMO levels of the open shell donors and acceptors respectively. The lowest electron energy on the TCNQ stacks occurs when all molecular orbitals are in-phase (at $k = 0$ in reciprocal space) while the situation is inverted for TTF stacks, leading for this stack to an energy maximum at the zone center. Such a band crossing picture ensures that both bands intersect at a single Fermi wave vector $\pm k_F$ in order to preserve the overall neutrality. Consequently, all states between $-\pi/b$ and $+\pi/b$ are occupied with the restriction that between $-k_F$ and $+k_F$ occupied states belong to the TCNQ band while outside this domain they pertain to the TTF band. In addition, the fact that the charges can delocalize in TTF-TCNQ shows that the on-site Hubbard repulsion U does not overcome the band energy $4t_\parallel$ gained in the band formation.

  The feature of inverted bands opens many possibilities such as an incommensurate charge transfer becoming commensurate under pressure as it is the case for TTF-TCNQ in a narrow pressure window around 19 kbar.
- Although the one dimensional crystal structure and intermolecular interactions within each stacks priviledge a band formation with planar Fermi surfaces at $\pm k_F$, non negligible although much smaller couplings exist as well along lateral directions. Molecular overlaps between like-chains give rise to a warping of the 1D Fermi surface but overlaps between unlike-chains are destructive for the density of states at Fermi level and tend affect the shape of the surface leading at low temperature to electrons and holes semimetallic pockets, namely a 1D to 3D cross-over for the Fermi surface.
- Whenever the temperature is larger than the transverse couplings, the Fermi surface looks 1D and as such is likely to undergo a transition which lowers the energy of the electrons by a lattice modulation of such a wave length that it produces energy gaps at the Fermi level with a $2k_F$ periodic lattice modulation and charge density wave, the so-called Peierls ground state which is the leading divergence in these compounds. Such a phenomenon has been thoroughly studied in several members of the TTF-TCNQ series including the charge transfer complexes including conductors comprising various selenide fulvalene donors, TSF-TCNQ, TMTSF-DMTCNQ or HMTSF-TCNQ.
- In addition, the chain structure has enabled to reveal a major feature of one-dimensional physics which is the existence at high temperature of PLD-CDW fluctuations, those which condense into the long-ranged Peierls ground state when the 3D character becomes dominant at lower temperature. These precursors known as Fröhlich precursors are well established through their manifestation on X-ray scattering and on the conductivity with a collective contribution. The latter contribution could be evidenced in TTF-TCNQ thanks to the possibility of making under pressure the charge transfer commensurate with the lattice, thus pinning the conductivity of collective origin. We believe a similar collective mechanism is at work in TMTSF-DMTCNQ under pressure.
- Electron-electron repulsions though less important in this charge transfer series than in the radical cation series of organic superconductors are visible through the tendency to prevent two electrons with opposite spins with a lattice modulation to occupy the same k state ending up to fluctuating lattice modulations with a wave vector $4k_F$. The situation is thus a superimposition of lattice distortion and strong electronic correlations (namely, the observability of $2k_F$ and $4k_F$ X-ray diffuse scattering which is the signature 1D physics).

- Finally, the stabilization of superconductivity turned out to be hopeless in these charge transfer conductors, possibly because of the negative role played by the interactions between unlike chains on the density of states at Fermi level.
- However, the turning point to superconductivity may have been guided by the commensurate quarter-filled conductor TMTSF-DMTCNQ in which the conduction band becomes actually half-filled with spinless Fermions once the manifestations of strong electron repulsions observed experimentally are taken into account.

4. Organic conductors becoming superconductors: The Bechgaard salts

4.1. *Experimental evidences for organic superconductivity*

4.1.1. *Introduction*

Based on metallurgical considerations, some authors at the end of the 1970's were considering 25-30 K as an upper limit for the superconducting T_c [33] but for others the saturation of superconducting critical temperatures slightly above 20 K was certainly a strong stimulus for the search of both new superconducting materials and new pairing mechanisms in the framework of the BCS theory.

As can be seen in Fig. 45, the period starting in the mid-1970's has been very fruitful in terms of progress in the field of superconductivity. The figure presents some superconducting materials and their critical temperature according to the year of their discovery. Obviously, they don't represent at a given time, materials with the maximum T_c. It is interesting to note that most published figures displaying the T_c's of the various superconducting materials fail to mention organic Q1D's compounds, which are nevertheless of major educational interest.

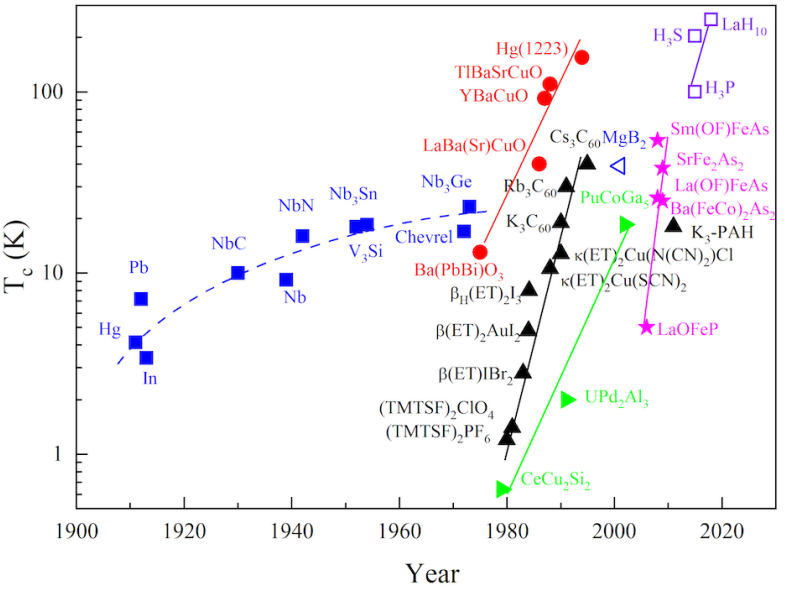

Figure 45. Evolution of T_c in various families of superconductors over the years. Notice that superconductivity in hydrides requires pressures in the megabar regime.

In addition to the development of new materials, extreme conditions have often been required to stabilize superconductivity, as illustrated with the recent discovery of superconductivity near

PHYSICAL REVIEW VOLUME 134, NUMBER 6A 15 JUNE 1964

Possibility of Synthesizing an Organic Superconductor*

W. A. LITTLE
Department of Physics, Stanford University, Stanford, California
(Received 13 November 1963; revised manuscript received 27 January 1964)

London's idea that superconductivity might occur in organic macromolecules is examined in the light of the BCS theory of superconductivity. It is shown that the criterion for the occurrance of such a state can be met in certain organic polymers. A particular example is considered in detail. From a realistic estimation of the matrix elements and density of states in this polymer it is concluded that superconductivity should occur even at temperatures well above room temperature. The physical reason for this remarkable high transition temperature is discussed. It is shown further that the superconducting state of these polymers should be distinguished by certain unique chemical properties which could have considerable biological significance.

Figure 46. Abstract of the seminal article published by W. A. Little in 1964. ©American Physical Society and the authors. All rights reserved.

room temperature in hydrides requiring extremely high pressure conditions in the megabar domain [180].

Such is also the case for the superconductivity in organic matter, which is the *raison d'être* of this overview, since its discovery has required besides the skill of a talented chemical engineering, the joint use of hydrostatic pressures of the order of 10 kbar together with low temperatures ^{3}He $-^4$ He dilution refrigerators below the boiling temperature of helium not so developed in the 1970's. Fortunately, chemical synthesis has rapidly made new organic superconductors stable under ambient pressure. The growth of very good quality single crystals has also allowed the achievement of delicate experiments whose results could be confronted with the theory of quasi 1D conductors.

Designing new materials for superconductivity at high temperature is the proposal of the seminal paper of Bill Little in 1964 (*see* Fig. 46) in which the author suggested the possibility to use a virtual electronic excitation of polarizable molecules grafted on a one-dimensional polymer such as polyacetylene for electron-mediated pairing instead of the electron-phonon mechanism of the celebrated BCS theory [4]. The idea of Little was indeed deeply rooted in the extension of the isotope effect proposed by BCS since we could expect an enhancement for T_c of the order of $(M/m_e)^{1/2}$ where m_e is the small electron mass compared to a much larger ionic mass M. It is also a virtual excitonic excitation of electronic origin which was suggested in the same years by Ginzburg in layered structures [22].

The conference held in Hawaii in 1969 brought together a large number of top scientists in physics and chemistry, both theoreticians and experimentalists, and was certainly the trigger for a worldwide research effort with the goal of synthesizing organic conductors undergoing a transition towards superconductivity, *see* Fig. 47. It took another decade to stabilize superconductivity in an organic molecular conductor.

This has been an essential decade (from 1965 to 1974) for the development of organic synthesis and the growth of new materials marked in particular by the discovery of the first conductors belonging to the class of inverted band charge transfer compounds, the so-called TTF-TCNQ series. It was also the decade during which physicists managed to develop with much profit new cristallographic X-ray and neutron diffraction techniques and extend transport, magnetic and NMR measurements at high pressures and down to very low temperatures. Last but not least, the development of this field has only been possible thanks to a remarkable and close cooperation between synthetic chemists, experimental and theoretical physicists enabling the discovery of long predicted behaviours in one-dimensional conductors. An ultimate goal was to avoid the appearance of a metal to insulator transition so characteristic of one-dimensional conductors, as we have seen previously for compounds undergoing a Peierls instability.

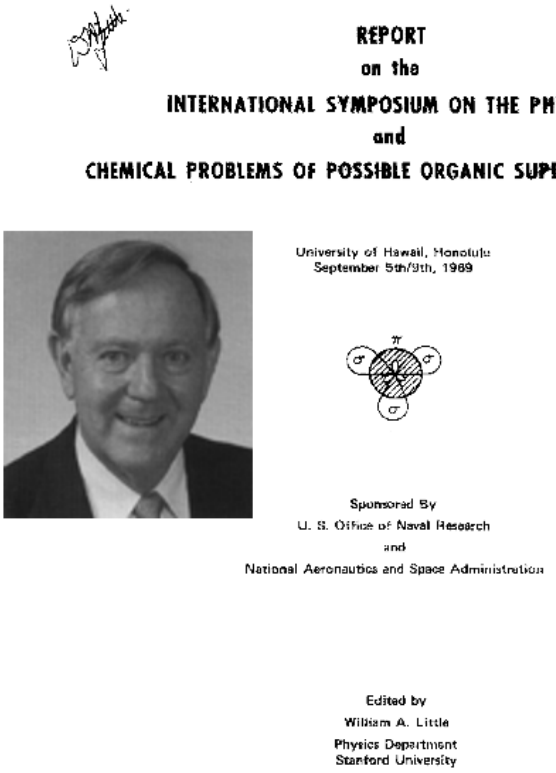

Figure 47. Masthead of the *Proceedings of the Conference on Organic Superconductors* organized by W. A. Little and held at Hawaii in 1969 with the signature of the organizer.

Hoping to be able to stabilize superconductivity, the research was directed towards the increase of the interchain coupling either by the application of a large hydrostatic pressure or by short S – N or Se – N contacts between donor and acceptor pairs. As shown in Sec. 3.1.8, high pressure although responsible for the discovery of numerous basic phenomena related to 1D physics, has failed to stabilize superconductivity in the TTF-TCNQ family of charge transfer conductors.

However an important step has been accomplished at the end of the 70's by the Copenhagen group led by Klaus Bechgaard, as highlighted in Sec. 2.5, with the development of the synthesis of tetraselenafulvalene molecules together with the electrochemical growth of very high quality radical cations single crystals.

First, the selenide charge transfer compound TM-DM, (TMTSF-DMTCNQ) [182] enabled the suppression of the metal-insulator under a pressure in excess of 9 kbar keeping a conductivity of the order of 10^5 $(\Omega.\mathrm{cm})^{-1}$ at helium temperature even if the reason for the existence of this low temperature metallic (or semi-metallic) state is still not fully clarified [183].

Second, emphasis has been put on the molecule TMTSF since for the first time in the experimental investigation of the TTF-TCNQ series the band filling of a charge transfer conductor, TM-DM, was found commensurate with 1/4 band filling under ambient pressure.

The new and exciting properties of TM-DM have provided a strong motivation to synthesize stoichiometric one chain radical cations compounds with TMTSF emphasizing the role of the donor molecule in a commensurate band filling environment.

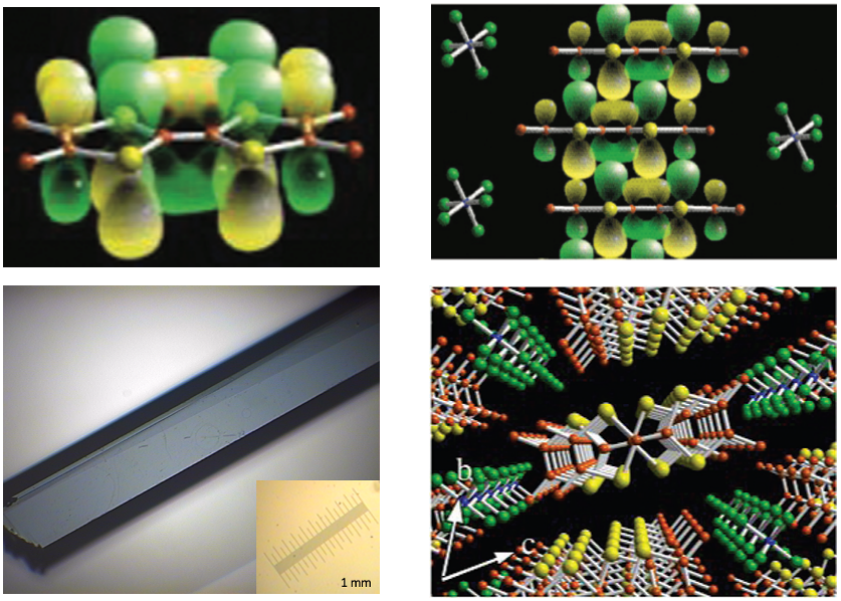

Figure 48. (Top left), The TMTSF molecule. (Top right) Side view of $(TMTSF)_2ClO_4$ along the b axis showing ordered ClO_4^- anions. (Bottom left) A $(TMTSF)_2ClO_4$ single crystal viewed along the $c^\star$ axis. (Bottom right) Stacking of TMTSF molecules along the a axis. Sources: [181, Fig. 5.7, 5.8, 5.9 p. 160]. ©2011 Elsevier. All rights reserved. We thank P. Auban-Senzier from the Orsay lab for the photograph of the crystal and P. Batail, B. Domercq and J.-C. Ricquier for the views of molecules and crystal structure.

Figure 49. Jacques Friedel (1921-2014). An enthusiastic supporter of low dimensional physics which he used to teach in his graduate course at the University of Orsay. We thank Jean-François Dars who kindly agreed to give us one of his pictures of Professor Friedel.

Such radical cations salts were already known in 1979 with the $(TSeT)_2Cl$ conducting salt known to retain a metallic state down to 24 K [184] and remaining metallic under pressure down to helium temperature [185].

Fortunately, the Montpellier chemistry group [179] had synthesized in 1978 a series of isomorphous radical cationic conductors based on TMTTF (the sulfur analog of the TMTSF molecule) with an inorganic mono-anion, namely, $(TMTSF)_2X$, with structures even simpler than those of the two stacks charge transfer compounds. These materials were all poor conductors under ambient conditions becoming semiconductors at low temperature [75] but they provided the motivation for the synthesis of a similar series based on the TMTSF molecule and they were inspiring for the Copenhagen group expert in selenium chemistry.

This group succeeded in 1979 the synthesis of a new series of radical cationic conducting salts all based on the TMTSF molecule [61] namely, $(TMTSF)_2X$ where X are inorganic mono-anions with various symmetries such as centrosymetrical PF_6^-, AsF_6^-, tetrahedral BF_4^- or triangular NO_3^- anions with a uniform cationic stacking.

The success of the Orsay group is largely due to the open-mindedness of Professor J. Friedel, Fig. 49, one of the founders of the solid state physics laboratory, who despite his commitment to the defense of physics at the national and international level has always been a strong supporter for the field of low-dimensional conductors.

4.1.2. *Basic evidences for superconductivity*

Figure 50. Klaus Bechgaard (1945-2017) used to ship his samples to Orsay in these famous tobacco boxes. It is interesting to read on one side of the tube KS 284 *runs at 12 kbar or below* and on the other *keep results confidential*. Great premonition!

The compound with $X = PF_6^-$ caught much attention since the conductivity reaches the value of about $10^5(\Omega.cm)^{-1}$ at 12 K before the onset of an insulating ground state at this temperature with still a strong temperature dependence. In addition, very large and nice-looking crystals good for transport properties measurements could be grown via the electrochemical route cited in Sec. 2.5.

For historical reasons, Fig. 50 shows the tube sent by K. Bechgaard which contained the samples from batch KS 284 that were synthesized in Copenhagen. It is instructive to read K. Bechgaard's comment on the tube, *runs at 12 kbar or below* on one side and *please keep result confidential* on the back side. The authors of Refs. [61, 186] also noticed that the temperature of the metal to insulator transition is apparently not enhanced by commensurability since the period of the presumably Peierls distortion amounts to two crystallographic units according to the stoichiometry. All these reasons were strong motivations for further investigations of this compounds.

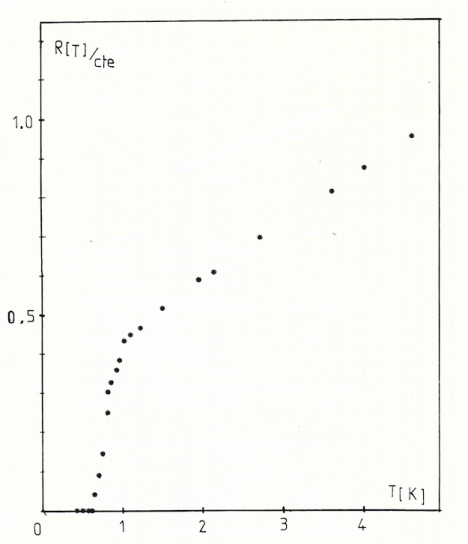

Figure 51. First observation of organic superconductivity from the resistance of $(TMTSF)_2PF_6$ under 9 kbar normalized to the temperature of 4.6 K (November 1979) a figure reproduced from the doctoral thesis of Alain Mazaud with his permission. Data can also be found in the initial publications [187, 188]. It was clear from the outset that the large temperature dependence was unusual for a conventional metallic conductor.

The behaviour of transport properties together with the absence of any static lattice distortion [172, 189] concomitant with the metal-insulator transition, were new features in a field still dominated until then by the Peierls phenomelogy and this stimulated further investigations under pressure suppressing the insulating state at liquid helium temperature under a pressure of about 9 kbar. The finding in a first step of a very small and *still non-saturating* resistivity at 1.3 K. The strong temperature dependence of the resistance below 4.2 K observed in Fig. 51 was by no means an experimental artefact. It has been explained by a strong single particle scattering against spin fluctuations, see Sec. 4.5. Since a finite and temperature independent resistivity is usually observed in conventional metals at very low temperature, such an experimental finding was a strong enough motivation for the Orsay low temperature group with our colleague Michel Ribault to trigger further studies and develop a new equipment adapted to measurements under hydrostatic pressure in a specially designed dilution refrigerator down to much lower temperatures.

Rather quickly by the end of November 1979 a narrow transition of the $(TMTSF)_2PF_6$ longitudinal resistance to a non-measurable value was observed at 0.9 K under 9 kbar as shown on Fig. 51. As this zero resistance state was reproducible with different samples and easily suppressed by a moderate magnetic field transverse to the most conducting direction, superconductivity was announced in an article published in February 1980 [187].

This result has aroused much interest in the scientific world, as evidenced by numerous reactions, the first being from our colleague Bill Little who since 1964 has been supporting this field enthusiastically, *see* Fig. 52.

FAC ORS G92136F
Q30 Q612
25Q374 Z ORSAY F
ZCZC SJA297 UFF1Q6 T254 FCM16Q SXA242 Q29Q1QQ8Q123
FRXX CO UTFL Q43
MIAMIFLO TLX FM STANFORDCA Q43/Q39 29 1748

D. JEROME
LABORATOIRE DE PHYSIQUE DES SOLIDES
UNIVERSITE-PARIS SUD, 914Q5
ORSAY

CONGRATULATIONS ON YOUR BEAUTIFUL WORK ON TMTSF. I WAS
DELIGHTED TO SEE YOUR REPRINT. YOUR INTUITION ON THE EFFECTS
OF PRESSURE PAID OFF HANDSOMELY. BEST WISHES,
BILL LITTLE

COL UNIVERSITE-PARIS 914Q5

Figure 52. Telex received by D. Jerome from W. A. Little, early 1980.

The first international event after the publication of these results took place in August 1980 at Helsingör, Denmark, with the International Conference on Low Dimensional Synthetic Metals, which which brought together 135 active researchers in this field. In this regard, it is interesting to mention the Conference summary given by W. A. Little published in the conference Proceedings. It is illuminating to have a look at the words of Bill Little in the foreword of these Proceedings. "This announcement generated a certain euphoria, a sense of relief and represents to many a psychological barrier successfully surmounted. It is a great encouragement to the synthetic chemist and experimentalists in the field. One should note that this was not the first Conference on organic superconductors. Some eleven years ago an International Conference on possible Organic Superconductors was held in Hawaii for which I was responsible. In the publication of the proceedings of that meeting a farsighted journal editor truncated the title simply to the 'Conference on Organic Superconductors' and it was thus with a sense of relief that I received the news of the properties of $(TMTSF)_2PF_6$".

The finding of superconductivity was also reinforced by the observation of a large diamagnetic contribution below 0.9 K [190] disappearing under a transverse magnetic field of about 1 kOe at 0.1 K applied along the $c^\star$ axis. The results of AC susceptibility suggested a strong expulsion of the magnetic flux from the sample and type II superconductivity but it is the DC Meissner experiment which brought the proof of a bulk superconductivity [191].

What is so special with $(TMTSF)_2PF_6$, the prototype of the so-called Bechgaard salts, unlike previously investigated TTF-TCNQ, is the magnetic origin of the ambient pressure insulating state which contrasts with the Peierls-like ground states discovered until then in TTF-TCNQ.

Magnetic susceptibility measurements [192] indicate that the metal-insulator transition is remarkably low in view of the commensurate Fermi wave vector provided data showing that the low temperature semiconducting phase is not simply Peierls in nature. The Bell Telephone research group made the suggestion that a SDW modulation could be responsible for the disappearance of the metallic state below 12 K in order to explain the non-linear electronic properties of the insulating state [193].

However, it is the ^{77}Se NMR study that subsequently validated this hypothesis on a microscopic scale [194], *see* Fig. 53. The ground state of $(TMTSF)_2PF_6$ turned out to be a spin-density-wave state [195], similar to the predictions of Slater Hartree-Fock theory when applied in lower dimensions [196], and akin to the approaches by Lomer [197] and Overhauser [198] for metals.

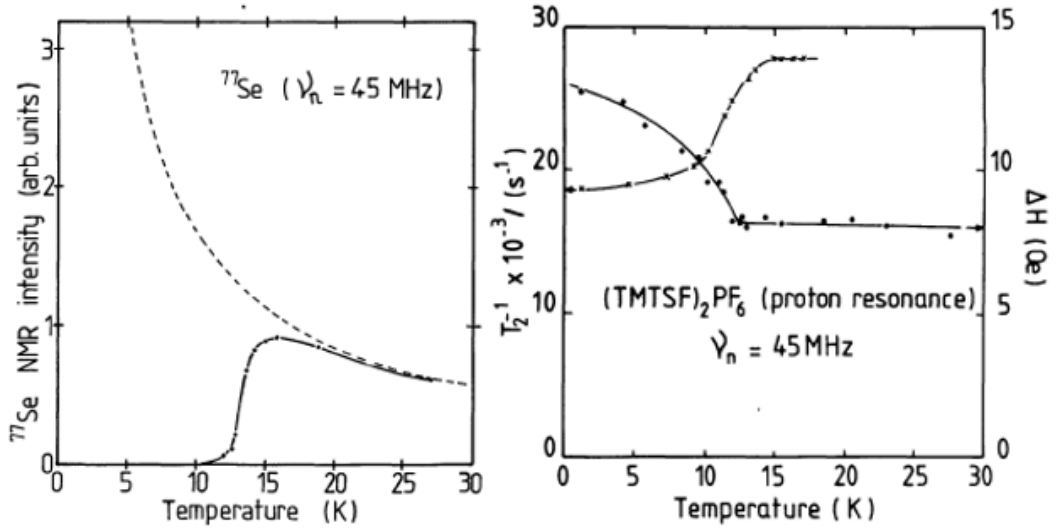

Figure 53. (Left) The ^{77}Se (I=l/2) NMR signal versus temperature in $(TMTSF)_2PF_6$.The signal vanishing observed below 12 K, instead of a Curie law temperature dependence (dashed curve), is due to the inhomogeneous broadening by internal magnetic fields in the state. (Right) The proton NMR signal in $(TMTSF)_2PF_6$ revealing an inhomogeneous line broadening and a concomitant decrease of the homogeneous line width ($1/T_2$) below 12 K. Source: [194, Figs. 1, 3, p. 88]. ©EDP sciences. All rights reserved.

The onset of itinerant antiferromagnetism opens a gap at Fermi level, and since the Fermi surface is nearly planar, the gap develops over the entire surface leading in turn to a semimetallic ground state. These experimental findings had a decisive influence on the theoretical development of the superconducting pairing in these quasi 1D organic materials.

The magnetic origin of the insulating ground state of $(TMTSF)_2PF_6$ was thus the first experimental hint for the prominent role played by correlations as induced by repulsive interactions and that the electron-phonon interaction is relatively weak in these organic conductors [194].

The competition between a charge density-wave superstructure and superconductivity had already been observed, for instance, in the transition metal dichalcogenides layer crystals under pressure such as 2H-$NbSe_2$ [199, 200]. However, in the latter situation superconductivity preexisted in the low-pressure metallic phase with a Peierls distortion due to the nesting of some regions of the Fermi surface [201], decreasing the density of states at the Fermi level. As noticed by Friedel [202], the effect of pressure on the T_c of $2H-NbSe_2$ compounds is likely to result in an

increase of $N(E_F)$ by reducing the gaps on some parts on the Fermi surface leading to a concomitant enhancement of T_c. It is a situation at variance with what is encountered in $(TMTSF)_2PF_6$ since the whole single component Fermi surface is involved in the transition and the SDW phase is truly insulating. However, the analogy with dichalcogenides may make sense close to the border between SDW and superconducting phases when T_{SDW} is already strongly depressed. The reasons why superconductivity is optimized at the border with the SDW state are likely to be quite different from what has been suggested for layer compounds, as it will be further discussed in Sect. 4.2.

Because of its past experience in the physics of dichalcogenides the Orsay high pressure group was not discouraged by the finding of an insulating ground state of $(TMTSF)_2PF_6$ stable under ambient pressure and quickly undertook an investigation of this compound under pressure which gave rise to the discovery of the first organic supertconductor [187].

Shortly after the announcement of superconductivity, the IBM group performed a high pressure experiment revealing a pressure dependence for T_c of about 0.1 K per kbar and also a coexistence of superconductivity with SDW in the low pressure regime [203]. Subsequently, the pressure dependence of the superconducting phase of $(TMTSF)_2PF_6$ has been extended up to 24kbar where T_c amounts to 0.2 K [177] and a $T-P$ phase diagram could be proposed for $(TMTSF)_2PF_6$ [86], *see* Fig. 54. The phase diagram thus obtained under pressure figured as the first clear example of a superconducting dome emerging on the brink of a parent SDW state.

Thanks to developments of chemistry, a generic diagram for one-dimensional conductors mixing high pressure and chemistry including both $(TMTSF)_2X$ and the isostructural series $(TMTTF)_2X$ was proposed [204].

This is how different ordered states coming from one-dimensional quantum liquids evolve towards superconductivity and ultimately to a Fermi liquid behavior could be established on solid experimental grounds through the whole generic diagram. This is to be covered by the following section.

4.2. *A generic* $(TM)_2X$ *phase diagram*

In the mid-1980's first, the isostructural family comprising the sulfur molecule TMTTF with the same series of monoanions was synthesized and second, high pressure techniques enabling access to pressures above 30 kbar under quasi-hydrostatic conditions at low temperature have been developed [208].

It was realized that $(TMTTF)_2X$ and $(TMTSF)_2X$ salts both belong to a unique class of materials with the possibility of evolving from one to the other by means of pressure forming in turn a generic $(TM)_2X$ phase diagram [204] sketched on Fig. 57. The investigation of this series as a whole under pressure has thus been extended to centro-symmetrical anions such as AsF_6^- [206, 209], SbF_6^- [210], TaF_6^- [211], or Br^- [212, 213] in the case radical cation TMTTF, and also with non-symmetrical anions ReO_4^- [214] and ClO_4^- [211]. $(TMTTF)_2PF_6$, although one of the most insulating compound of the phase diagram on Fig. 57, is of particular interest not only because it can be made superconducting at low temperatures under a pressure of 45 kbar, [215, 216] but also because its position in the diagram allows, thanks to the adequate adjustment of pressure, to explore not only all the ordered phases at low temperature but the also to provide experimental evidences for the existence of 1D quantum liquids as precursors of the phase transitions. These govern essentially the non ordered state in the left hand side of the phase diagram and evolve on the right towards a 3D, though anomalous, metal above superconductivity under pressure.

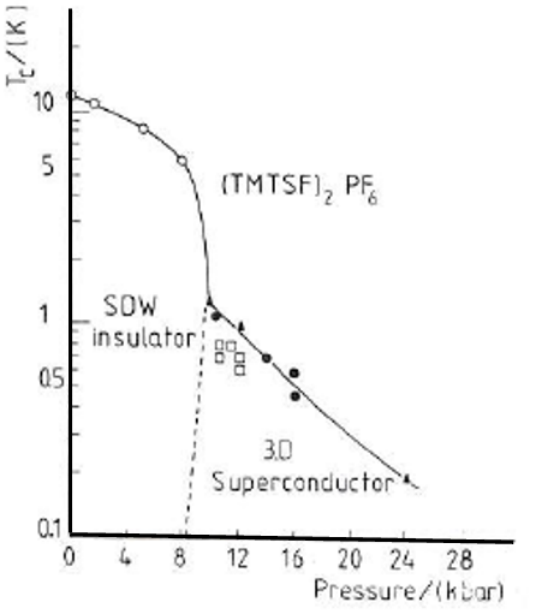

Figure 54. The initial version of the low temperature phase diagram of $(TMTSF)_2PF_6$. The various experimental points on the superconducting transition line have been compiled in the literature, (triangles, Orsay [86, 205], …, Bell Labs [191] and open squares, IBM [203]). A closer investigation of the phase diagram for $(TMTSF)_2AsF_6$ [206] reveals a reentrance phenomenon near the triple point at $P_c \approx 8.5$ kbar, $T_c \approx 1.2$ K. Source: [207, Fig. 78 p. 166].©1982 Gordon and Breach.

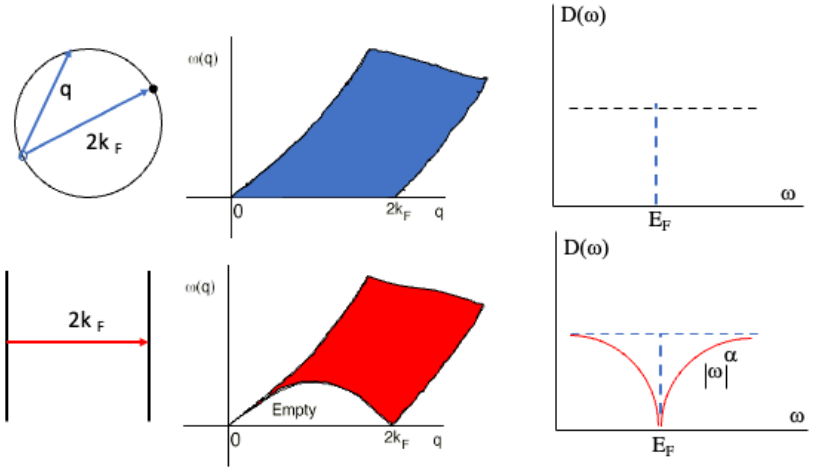

Figure 55. Basic differences between Fermi and Luttinger liquids. (Top) Electrons-holes excitations are possible in a FL for all vectors from 0 to $2k_F$ leading to a constant density of states at Fermi level. (Bottom) In a LL liquid the only excitations are those with wave vector 0 or $2k_F$ and the density of quasi particle states follows a power law around the Fermi energy.

4.2.1. *1D quantum liquid physics in a nutshell*

Given the place that one-dimensional physics holds in the non ordered states on the left of the $(TM)_2X$ phase diagram of Fig. 57, it is helpful to recall some basic features of quantum physics of the interacting electron gas in 1D [217–221]. To do this different approaches has been extensively developed over the years, like the fermion many-body technique, the boson representation and of course numerical techniques. In this brief overview, we will focus on the boson representation. First, at low enough energy the electron spectrum ϵ_k can be considered as essentially linear with respect to the 1D Fermi points $\pm k_F$, namely $\epsilon_k \approx v_F(|k| - k_F)$, where v_F is the Fermi velocity. In these conditions the hamiltonian of electrons with spin can be rigorously transposed into a bosonic one associated to long wavelength spin (σ) and charge (ρ) density excitations, each with a linear acoustic dispersion relation, $\omega_{\sigma,\rho} = u_{\sigma,\rho}|q|$, where $u_{\sigma,\rho}$ is the velocity for each sound mode.

In the model, interactions are given by the set of different scattering processes of electrons that can be projected on the two Fermi points. The above bosonic representation remains valid so that the low energy properties of the electron system become entirely governed by collective sound like excitations that can be described as vibrating strings for spin and charge degrees of freedom. Both strings are decoupled, a feature known as spin-charge separation, and each of them is characterized solely by two parameters, a velocity $u_\sigma(u_\rho)$ and a stiffness constant $K_\sigma(K_\rho)$, both being in general non universal, that is, dependent on interactions. These excitations are the true eigenstates of the system and have actually no available phase space to decay. Therefore in contrast to the situation found in a Fermi liquid in higher dimension, fermion quasi-particles are absent at the Fermi level for a 1D system of interacting electrons at zero temperature (*see* Fig. 55). This is illustrated by the power law decay in energy predicted of the fermion density of states at the Fermi level,

$$N(\omega) \propto |\omega|^\alpha \tag{10}$$

with α related to K_ρ,

$$\alpha = \frac{1}{4}\left(K_\rho + 1/K_\rho - 2\right). \tag{11}$$

The electron gas model for 1D conductors with repulsive Coulomb scattering matrix elements with only small momentum transfer, noted as g_2 and g_4 couplings in the g-ology jargon of the model, corresponds to the exactly solvable Tomonaga–Luttinger (TL) model with purely harmonic string excitations in both spin and charge sectors, with $1 > K_\rho > 0$ and $K_\sigma = 1$ (due to rotational symmetry of the spins). The TL model is generic of the so-called Luttinger liquid phenomenology where in addition to the Fermi level density of states (10), the $2k_F$ density-wave and superconducting susceptibilities develop power law behaviors in temperature with exponents that are non universal namely, dependent on interactions. This is the case of the antiferromagnetic or SDW susceptibility which, aside from logarithmic corrections, reads

$$\chi_{\rm SDW}(2k_F, T) \propto T^{-\gamma_{SDW}} \tag{12}$$

with the exponent

$$\gamma_{\rm SDW} = 1 - K_\rho, \tag{13}$$

which is congruent with a singular growth of SDW correlations at $T \to 0$ for repulsive interactions.

One can go beyond the TL model by including other possibilities of scattering process. The backward scattering, noted g_1, is one of these. For this process, particles near the Fermi points exchange momentum of the order of $2k_F$ introducing non linearity in the string excitations in the spin sector. For repulsive $g_1 > 0$, however, this non linearity turns out to be irrelevant, in the sense that as the energy distance from the Fermi level goes to zero this process becomes vanishingly small in amplitude. One then recovers an effective TL model in the low energy fixed point limit. Although less pertinent to $(TM)_2X$ materials for which interactions are expected to be dominantly

repulsive, it is worth mentioning that the outcome would have been completely different in the attractive case ($g_1 < 0$), where g_1 then becomes relevant and evolves toward strong attractive coupling at low energy with the formation of a gap for spin excitations alone. The presence of a gap in one of the two sectors defines a different quantum liquid known as a Luther–Emery liquid [217].

Another important extension to the TL model applies for systems like $(TM)_2X$. These materials actually consist of weakly dimerized stacks that introduces a small dimerization gap Δ_D in the middle of the three-quarter filled band in terms of holes (or quarter-filled in terms of electrons) which is fixed by the 2:1 stoichiometry (*see* Table 59) [222–224]. The spectrum then splits into an empty upper band and a half-filled lower band having one hole per unit cell with one dimer of TM molecules [225]. This underlying lattice effect leads to half-filling umklapp scattering processes, noted as g_3, which can transfer two holes from one Fermi point to the other. This is made possible *via* the inclusion of the reciprocal lattice vector G in the momentum conservation of electrons at the Fermi points the latter taking the special value $G = 4k_F(= 2\pi)$ at half-filling. Following the example of backward scattering, the presence of g_3 introduces non linearity in the string excitations but this time for the charge whose impact is of major importance. As a relevant coupling, its amplitude grows at lower energy or temperature favoring the formation of a gap Δ_ρ in the charge excitations known as a Mott gap. The spin part, as we have seen, remains gapless. The 1D electron system then becomes at low energy a Mott insulating Luther–Emery liquid with the concomitant downward renormalization of $K_\rho^* \to 0$ to its minimum value in the low energy or temperature limit. According to (13) this yields a maximum power law singularity for the rotationally invariant SDW susceptibility ($\chi_{\rm SDW} \sim T^{-1}$). For weakly dimerized systems, $\Delta_D \ll E_F$, the bare amplitude $g_3 \approx g_1\Delta_D/E_F$ is weak and as a result the Mott insulating gap regime is pushed back at lower energy values ($\Delta_\rho \ll E_F$).

The observation of an insulating charge localised state in the intermediate temperature range on the left hand side of the diagram of Fig. 57 for more dimerized sulfur based compounds [226] has been early interpreted as the consequence of one-dimensional physics coming from electron-electron umklapp scattering at half-filling [222, 227, 228] (*see* Sec. 4.2.2 for more experimental consequences).

The actual electronic state preceding the charge gaped one in $(TM)_2X$ materials shows a metallic resistivity at high temperature with $d\rho/dT > 0$ [226], rather than $d\rho/dT < 0$ predicted for umklapp momentum dissipation in the weakly dimerized case at half-filling [229, 230] – neglecting here all other sources of inelastic scattering such as phonons. This has stimulated another route of interpretation for the origin of the charge gap [231]. Neglecting dimerization, the band of the TM organic stack is actually 1/4-filled in terms of electrons. The corresponding lattice commensurability then yields a different kind of Umklapp scattering noted $g_{\frac{1}{4}}$, which is also responsible for non linearity in the excitations of the charge string alone. In terms of the on-site Hubbard repulsion parameter U alone, for instance, one finds a bare amplitude of the form $g_{\frac{1}{4}} \approx U(U/E_F)^2$. This corresponds to a three-particle interaction linked to the higher order fourfold commensurability with the undimerized lattice. As such, it is an irrelevant coupling. However, the strength of interactions as a whole can reverse the situation and make $g_{\frac{1}{4}}$ a relevant coupling. This indeed occurs with the proviso that K_ρ falls below the critical value $K_{\rho,c} = 1/4$, a condition that can be reached when the long-range part of the Coulomb interaction becomes sufficiently strong. In such a case an insulating charge gap Δ_ρ is present and is usually referred to as a charge ordered or a Wigner state [232], whereas the spin degrees of freedom remain gapless.

Since the stacks are weakly dimerized in practice one may expect that both Umklapp terms are present and interfering with one another [233]. This may reflect in electrical transport. In the gapless 1D regime for $T > \Delta_\rho$, the resistivity coming from electronic Umklapp dissipation considered above has been shown to vary according to the power law [229, 234]

$$\rho(T) \sim T^{\theta} \tag{14}$$

with the exponent

$$\theta = 4n^2 K_\rho - 3, \tag{15}$$

where $1/n$ is the filling of the band. At quarter filling $n = 2$ and one gets a metallic regime when K_ρ is not too small, with $\rho(T) \sim T^{16K_\rho - 3}$, while at half-filling, $n = 1$ and $\rho(T) \sim T^{4K_\rho - 3}$, which is most likely showing non metallic resistivity in lowering the temperature. Therefore if one restricts the mechanisms of momentum dissipation in transport to electronic Umklapp alone, the metallic behavior seen in sulfur based $(TM)_2X$ compounds above the charge localisation in Fig. 57 is most likely attributable to quarter-filling Umklapp scattering (See Fig. 56). [231] A crossover to the second Mott precursor regime at half-filling then appears as an interesting possibility for these weakly dimerized materials [233].

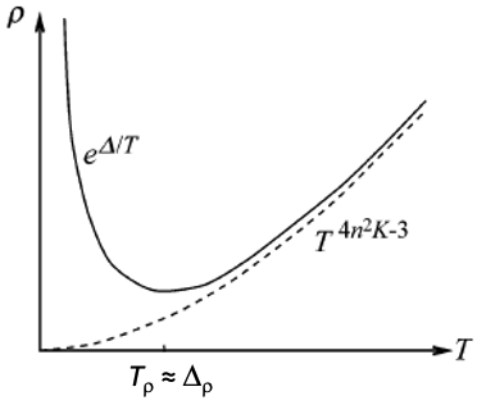

Figure 56. The expected behaviour for the dc transport of a charged gap insulator. At high temperature the power law dependence provides access to the Luttinger parameter K_ρ. Source: [234, Fig. 16 p. 5047]. ©2004, American Chemical Society. All rights reserved.

The generic phase diagram for the $(TM)_2X$ family displayed on Fig. 57 is actually based on the sulfur compound $(TMTTF)_2SbF_6$ taken for the origin of the pressure scale although $(TMTTF)_2PF_6$, $(TMTSF)_2PF_6$ and $(TMTSF)_2ClO_4$ have been the subject of most high pressure measurements because they are the samples that have focused the efforts of chemists and also because these samples can be grown as high quality single crystals of fairly large size for physical measurements. Notice that $(TMTSF)_2ClO_4$ is the only compound in this family to exhibit superconductivity under ambient pressure which explain why some very delicate experimental investigations reported in this article have only been performed on this latter compound so far. In order to to appreciate the wealth of this generic diagram and establish a link with the theory of quasi one dimensional conductors we shall base the presentation mainly on two compounds, $(TMTTF)_2PF_6$ and $(TMTSF)_2PF_6$ which have been thoroughly investigated using various experimental approaches. Thanks to the high pressure work they are able to exhibit practically properties of low dimensional physics.

4.2.2. $(TMTTF)_2PF_6$ *: A model Quasi-1D conductor*

Because of their particular crystal structures, such $(TM)_2X$ materials can be considered at first glance as protoptypes for 1D physics [236].

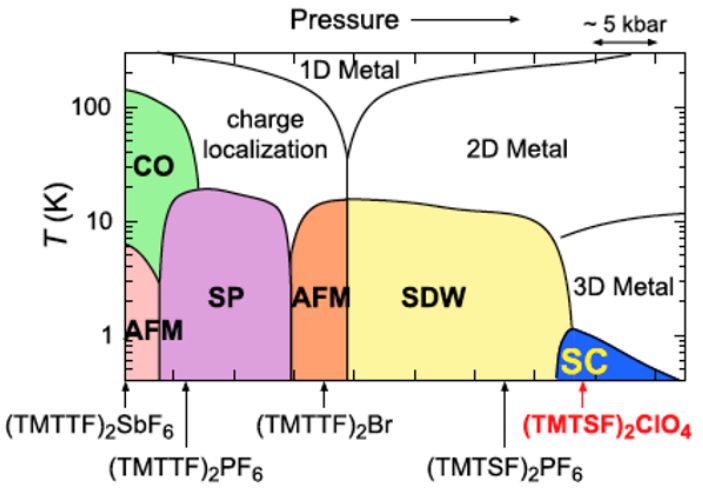

Figure 57. A generic diagram for the $(TM)_2X$ family. The horizontal tics correspond to a 5 kbar interval. All colored phases are long-range ordered. The origin of the pressure scale is set for the compound $(TMTTF)_2SbF_6$ according to its ordered state at ambient pressure. Notice that all compounds marked on this figure but $(TMTSF)_2ClO_4$ exhibit superconductivity provided a high enough pressure is applied, $(TMTTF)_2PF_6$ [208], $(TMTTF)_2Br$ [212] and $(TMTSeF)_2PF_6$ [187]. The highest pressure investigated for superconductivity in this series of organic salts is for the compound $(TMTTF)_2BF_4$ which requires a pressure of 33 kbar for a maximum T_c at 1.5 K [235]. We thank Shingo Yonezawa for the communication of this figure.

The development of this field has aroused enthusiasm in the 80's and its progress is due to the close and efficient collaboration between various scientific fields ranging from synthetic chemistry to the elaborate theory of electrons in low-dimensional solids, through numerous experimental techniques. Fig. 58 allows us to recall some of the actors in the 1990's.

However, an important peculiarity of $(TM)_2X$ materials makes them different from the usual picture of TL conductors. Unlike incommensurate two-stacks TTF-TCNQ materials, $(TM)_2X$ conductors exhibit a band filing which is commensurate with the underlying 1D lattice due to the 2:1 stoichiometry imposing half a carrier (hole) per TM molecule. Consequently, assuming a uniform spacing of the molecules along the stacking axis, the unit cell contains 1/2 carrier, i.e. the conduction band becomes quarter-filled in terms of electrons. However, non-uniformity of the intermolecular spacing had been noticed in the early structural studies of $(TMTTF)_2X$ crystals [237]. It is due to the periodicity of the anion packing being twice the periodicity of the molecular packing. This non-uniformity is at the origin of a dimerization of the intrastack overlap between molecules which is important in the sulfur series but still present although less developed in some members of the $(TMTSF)_2X$ series as shown on Tab. 59.

Hence, taking into account the symmetry imposed by the anion lattice, the conduction band may also be considered as effectively half-filled at sufficiently low energy.

As discussed in Sec. 4.2.1, a dramatic consequence of this commensurate situation for $(TM)_2X$ materials is the existence of two localization channels due to electron-electron Umklapp scatterings. The first at half-filling with momentum transfer $G = 4k_F$ to the lattice and to which the two particles scattering coupling constant $g_3 \approx U(\Delta_D/E_F)$ is associated. The second at quarter filling where $G = 8k_F$ and the umklapp coupling $g_{1/4} \approx U(U/E_F)^2$ corresponding to three-particle coupling [222, 231]. This localization is a typical outcome of 1D physics in the presence of repulsive

Figure 58. A large part of the Low Dimensional Organic Conductors family at the Gordon Conference (also first International Symposium on Crystalline Organic Metals, ISCOM meeting) organized in Germany at Irsee in 1991 by P. M. Chaikin and D. Jerome. Participants may recognize themselves 32 years ago. Unfortunately some of them have already left us.

	$(TMTTF)_2PF_6$	$(TMTSF)_2PF_6$	$(TMTSF)_2ClO_4$
t_1	137	252	258
t_2	93	209	221
$\bar{t}$	115	230	239
$\frac{\Delta t}{\bar{t}}$	0.38	0.187	0.155
$t_\perp$	13	58	44

Figure 59. Calculated band parameters for three representative members of the $(TM)_2X$ series according to the room temperature crystallographic data in reference [237]. The bond dimerization is shown in the line $\Delta\bar{t}/\bar{t}$. Energies are in meV.

interactions and leads to a charge gap Δ_ρ in the charge excitation spectrum although no ordering is expected at any finite temperature for a purely 1D system. The spin sector remains gapless on account of the separation between spin and charge degrees of freedom in 1D conductors. Fortunately, most features of the 1D localization and the physical properties of this electron gas can be studied by transport, optical and NMR experiments on the materials.

The system $(TMTTF)_2PF_6$ also known under the name of a Fabre salt since it has been first synthesized in the Montpellier chemistry laboratory [238], can be considered as the workhorse of Q1D conductors as far as 1D physics is concerned because of the existence of high quality single crystals enabling in-depth studies under very high pressure either with the piston-cylinder or with diamond anvils techniques.

Nuclear magnetic resonance and 1D nature of spin correlations. It is instructive at this point to discuss the nature of correlations in the low pressure domain of Fig. 57 for a model system like $(TMTTF)_2PF_6$. An extensively used tool to this end was NMR. In Fig. 60, we show the results of Creuzet et al. [239] for the temperature dependent ^{13}C nuclear spin-lattice relaxation rate T_1^{-1} of $(TMTTF)_2PF_6$ at $P = 1$bar and 13 kbar. For both pressures an activated resistivity temperature profile confirms the existence of a charge localization gap Δ_ρ over a large temperature domain, as indicated in Fig. 57. For the single crystals used in these NMR experiments, each ^{13}C of enriched TMTTF molecules has a nuclear spin $I = 1/2$ that is locally coupled to the spins of conduction electrons *via* an hyperfine coupling $\bar{A}$. The coupling is responsible of the nuclear spin-lattice relaxation governed by the Moriya expression

$$T_1^{-1} = \left|\bar{A}\right|^2 T \int d^d q \, \frac{\chi''(\boldsymbol{q},\omega)}{\omega}, \tag{16}$$

which is sensitive to the contribution of low frequency spin correlations coming from all wave vectors $\boldsymbol{q}$ through the imaginary part of the dynamic magnetic susceptibility $\chi''(\boldsymbol{q},\omega)$.

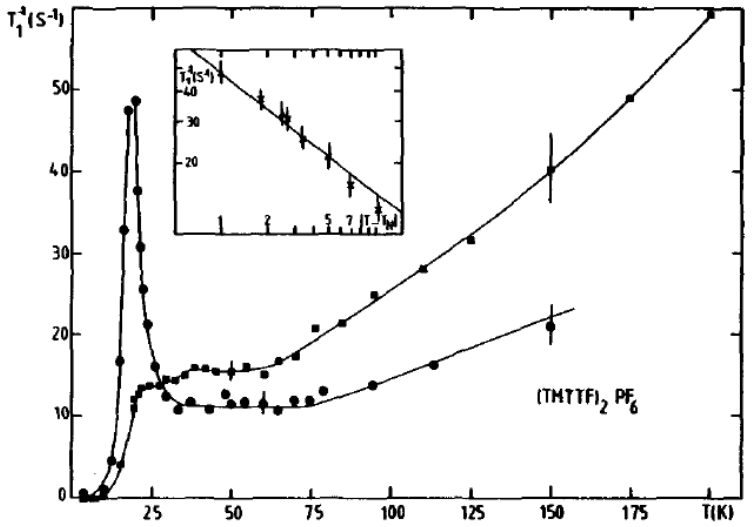

Figure 60. ^{13}C NMR spin-lattice relaxation rate T_1^{-1}, as a function of temperature for $(TMTTF)_2PF_6$ at $P = 1$bar (full squares) and $P = 13$ kbar (full circles). Inset: antiferromagnetic critical behavior of T_1^{-1} near T_N at $P = 13$ kbar. Source: [239, Fig. 1 p. 291]. ©(1987) Elsevier. All rights reserved.

For an interacting electron system in $d = 1$ spatial dimension, T_1^{-1} takes the form

$$T_1^{-1} \simeq C_{q\sim 2k_F} T^{1-\gamma_{SDW}} + C_{q\sim 0} T \chi_\sigma^2(T), \tag{17}$$

which superimposes as a function of temperature the power law singularity of $2k_F$ SDW correlations Eq. (12) and the long-wavelength spin correlations of the uniform static spin susceptibility $\chi_\sigma(T)$. In the presence of Δ_ρ, e.g., for a Mott–Luther–Emery liquid, the charge stiffness evolves at low energy or temperature towards its minimum value $K_\rho^* \to 0$. This leads to the power law exponent $\gamma_{\rm SDW} = 1$, which according to Eq. (17), is responsible for a constant, temperature independent, SDW contribution to the relaxation rate. As for the uniform part, the regular enhancement of susceptibility $\chi_\sigma(T)$ by interactions will give rise to a superlinear temperature dependent contribution to T_1^{-1}, which grows in importance as temperature is raised to ultimately become the

dominant part of the relaxation rate [240]. This temperature sequence for T_1^{-1} is clearly visible in the data of Fig. 60 at both pressures where Δ_ρ is present. This constitutes an experimental confirmation of the 1D character of spin correlations and the actual vanishing value of K_ρ^* in a sizable part of the non ordered phase of the Fabre salts [241].

Figure 61. François Creuzet (1957-2020) made major contributions to the understanding of the physics of Fabre and Bechgaard salts for his PhD at Orsay in the eighties using NMR in close cooperation with the Sherbrooke group. He became Deputy Director, Scientific director at the Saint Gobain Company in 2016.

It is worth concluding this paragraph by noting that the NMR results of Fig. 60 also give precise information about the nature of long-range ordering in $(TMTTF)_2PF_6$ in the low pressure range of the phase diagram. At ambient pressure for instance, T_1^{-1} undergoes an exponential fall below $T_{SP} \simeq 20$ K of the form $T_1^{-1} \sim e^{-\Delta_s/T}$ due to the coupling of spins to phonons and the onset of a spin gap Δ_s compatible with 3D spin-Peierls order [239, 242](SP in Fig. 57). One also notes in Fig. 60 the presence of 1D precursors to the SP transition, in the form of a gradual decrease or a spin pseudogap occuring well above T_{SP}. Finally at $P = 13$ kbar, T_1^{-1} presents a singularity at $T_N \simeq 19$ K, signaling the crossover from 1D to 3D magnetic long-range order. The critical temperature profile $T_1^{-1} \sim |T - T_N|^{-1/2}$ shown in the inset of Fig. 60 near the transition is the signature of an antiferromagnetic 3D Néel state promoted by superexchange coupling between spins of neighboring chains [239] (AFM in Fig. 57).

Transport. The investigation of $(TMTTF)_2PF_6$ transport properties under several pressures covering the whole phase displayed on Fig. 57 has offered a remarkable illustration for the evolution from a 1D quantum liquid of different form (Luther–Emery–Mott, charge or Wigner ordered insulators, LL) to a higher dimensional metallic state thanks to the control under pressure of the strength of both the electron-electron Coulombic repulsion and the interchain kinetic coupling.

What makes the data displayed on Fig. 62 particularly interesting is the difference noticed between the temperature dependences of longitudinal and transverse transport along the least conducting c direction [243].

At ambient pressure longitudinal and transverse components of the $(TMTTF)_2PF_6$ transport exhibit a strong insulating character. However, at increasing pressure, the longitudinal resistivity $\rho_a(T)$ begins to show a weak metallic temperature dependence below room temperature down to T_ρ where according to Fig. 62 a broad minimum takes place ($T_\rho = 180$ K under 13.8 kbar), and below which the resistance becomes activated. T_ρ is strongly depressed by pressure and tends to vanish around 15 kbar giving way to the appearance of a sharp metal-insulator transition around 20 K.

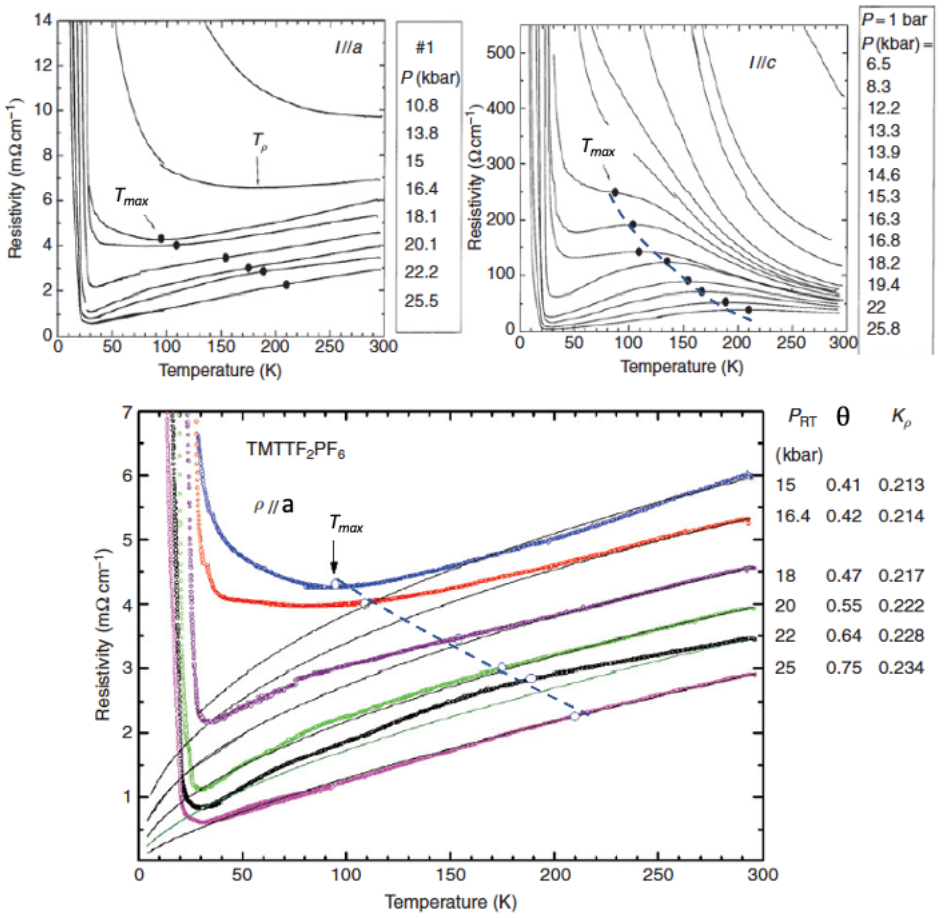

Figure 62. $(TMTTF)_2PF_6$, longitudinal (left) and transverse (right) resistances versus temperature at different pressures. The data for ρ_a shown in the bottom figure provide the pressure dependence of the Luttinger coefficient K_ρ derived from fitting the experimental data to T^θ with $\theta = 16K_\rho - 3$, i.e, $(n = 2)$ *vide infra.* Notice that the decrease in compressibility under pressure makes the constant volume correction less significant for the temperatures dependences measured at high pressures which are *at variance* with the case of $(TMTSF)_2PF_6$ presented on Fig. 63. Sources: [243, Fig. 1 p. 42] (top), [181, Fig. 5.14 p. 166] (bottom). ©EDP sciences. All rights reserved.

On the other hand, $\rho_c(T)$ remaining insulating $(d\rho_c/dT < 0)$ below room temperature from 1 bar up to about 13 kbar, develops a maximum at higher pressures at the temperature T_{max} (= 100 K at 15 kbar) which keeps increasing at higher pressures. The upper right part of Fig. 62 shows how T_{max} moves up to room temperature under 25 kbar. Under that latter pressure, both ρ_c and ρ_a undergo the sharp metal-insulator transition in the temperature regime of 20 K. Furthermore, it is important to realize that the phase diagram of $(TMTTF)_2PF_6$ above 25 kbar becomes quite similar to the $T - P$ diagram of $(TMTSF)_2PF_6$ above ambient pressure. Notice that the ground state of $(TMTTF)_2PF_6$ becomes superconducting around 45 kbar [208], but this is not shown on this figure. Consequently, one may consider that there exists a pressure shift of about 35 kbar between the phase diagrams of $(TMTTF)_2PF_6$ and $(TMTSF)_2PF_6$. The different

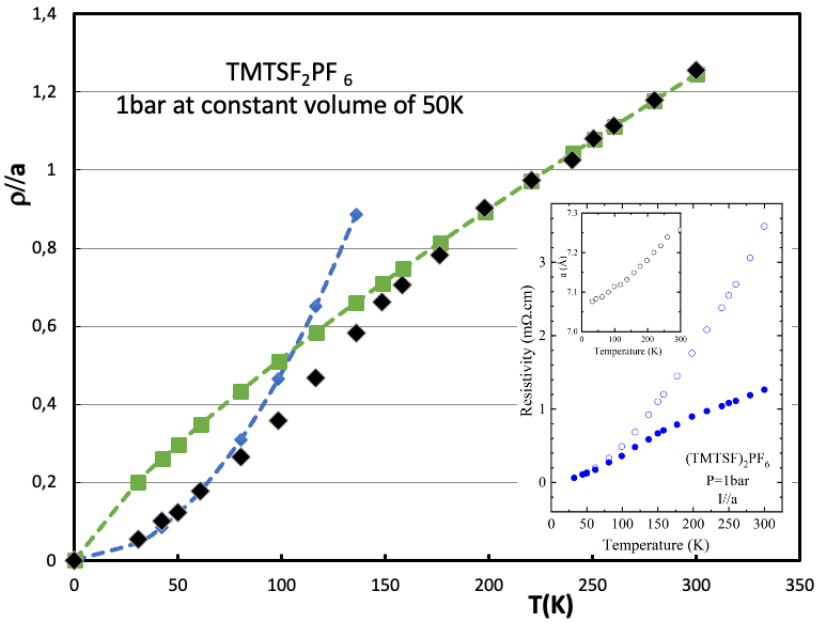

Figure 63. Temperature of the $(TMTSF)_2PF_6$ longitudinal resistance after making the constant volume transformation (black losanges). The fit to $T^{0.8}$ are the green squares while blue losanges are the T^2 low T behaviour. The inset shows the strong volume dilatation of a lattice parameter and the actual temperature dependence of ρ_a as measured under 1 bar (open circles) plus the conversion to the constant volume T-dependence (full blue dots).

behaviours of transport are made crystal-clear with the example of $(TMTSF)_2PF_6$ under ambient pressure on Fig. 64.

All experimental results relating to $(TMTTF)_2PF_6$ and $(TMTSF)_2PF_6$ are gathered on Fig. 65 which can be considered as the model diagram for a commensurate quasi one dimensional conductor which constitute the basic experimental facts to be compared with the theory proposed for the deconfinement of a one-dimensional Mott insulator in the presence of interchain kinetic coupling [234, 244]. In the Mott-insulator phase of $(TMTTF)_2PF_6$, the finite interchain coupling $t_\perp \approx 200$ K [86, 237, 245] is small compared to a Mott gap of ≈ 500 K [246], a value which is such that the interchain hopping is suppressed by the insulating nature of the 1D phase.

Consequently, the interchain coupling becomes no longer relevant in these sulfur compounds at ambient pressure [247]. The situation evolves quickly under pressure as both the Mott gap is sharply depressed while the interchain coupling increases driving the compound toward a situation where the two quantities are interplaying. From the experimental view point, Fig. 65 provides a good illustration for this evolution from the 1D Mott insulator to a higher dimensionality metal at a pressure overpassing 15 kbar. A measure of the gap extracted from the optical conductivity shows that at this pressure the gap is roughly of the order of magnitude of the interchain coupling [248, 249]. These observations are supporting the existence of a deconfinement transition which has been treated theoretically very satisfactorily using a generalization of the dynamic mean field theory [250]. The $T_{\max}$ line shown on the $(TMTSF)_2PF_6$ panel of the general diagram, Fig. 65 marks the temperature where motion along c becomes coherent [251]. This temperature coincides also with the recovery of a T_1^{-1} Korringa, though strongly renormalized, behaviour for spin fluctuations observed either in $Se-ClO_4$ or in $Se-PF_6$ under 8 kbar, *see* Ref. [252] and Sec. 4.5.1.

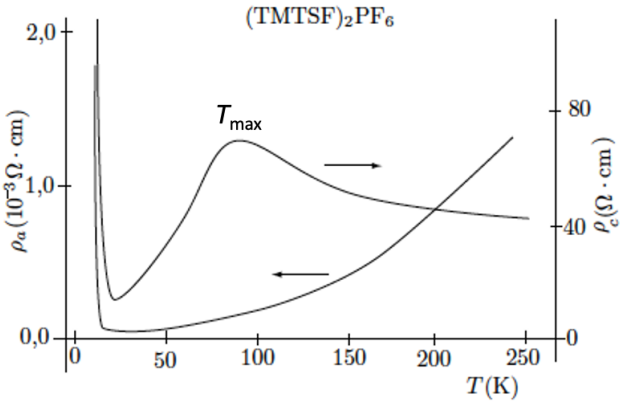

Figure 64. Temperature dependence of transport along a and c for $(TMTSF)_2PF_6$ providing a simple illustration of the non-metallic behaviour of ρ_c above T_{max}. Source: [246, Fig. 31 p. 5584]. ©2004, American Chemical Society.

In spite of the charge gap Δ_ρ a metal-like behaviour of the longitudinal resistance can still be obtained at T larger than Δ_ρ. According to Eqs. (14) and (15) the resistance is displaying a power law $\rho_a(T) \approx T^{4n^2K_\rho-3}$ for 1D interacting electrons in the presence of umklapp scattering.

Experimental studies have revealed such a metallic-like behaviour for the resistance either in $(TMTSF)_2PF_6$ at ambient pressure [86] and also in $(TMTTF)_2PF_6$ under pressure above 15 kbar [243, 249].

Since transport properties of these molecular crystals are known to be strongly volume dependent [86], before any comparison between experimental data and a theoretical model it is required to derive the proper experimental temperature dependence of the resistivity (to be compared with the theory) under a constant volume, taking into account both the thermal dilatation at constant pressure (inset of Fig. 63 and the volume dependence of transport at constant temperature, *see* Ref. [253]. Then we derive the equivalent pressure $P_i(T)$ which is needed at each temperature to recover the reference volume of 50 K. The procedure for the derivation of the constant volume temperature dependence is detailed in the following note[2].

Although the constant volume transformation is crucial for $(TMTSF)_2PF_6$ under ambient pressure as discussed above and on Fig. 63 it becomes of less importance for $(TMTTF)_2PF_6$ since for this latter compound a pressure of 15 kbar is already requested for the observation of a metallic behavior for ρ_a and the lattice expansion in temperature is known to be much depressed under pressure [253].

What has been found for $\rho_a(T)$ in $(TMTTF)_2PF_6$ above 15 kbar is a sublinear exponent of the order of $\theta = 0.7$ (*see* Fig. 62) whereas in $(TMTSF)_2PF_6$ the fit of $\rho_a(T)$ above 100 K at the constant volume of 50 K on Fig .63 [243, 249] would rather provide the result $\theta = 0.8$.

Taking into account the power law for longitudinal transport found in the metallic regime of Fig. 65 namely $\theta \approx 0.7-0.8$, the assumption of a relevant a half-filling of the band (commensurability unity) would lead to the Luttinger parameter K_ρ very close to unity (corresponding to very weak repulsive interactions) since $\theta = 4n^2K_\rho - 3$, n being the order of commensurabilility ($n = 1$ for a half filled band. This weak coupling ($K_\rho \approx 1$) can be discarded since it would be hard to reconcile with the exchange enhancement of the spin susceptibility [254].

[2]Using the helium gas pressure technique it has been established that the pressure coefficient of the longitudinal conductivity σ_a is temperature independent between 80 and 300 K, namely, $(\sigma_a(P) - \sigma_a(0)/\sigma_a(0) = +25\%/\text{kbar}^{-1}$.

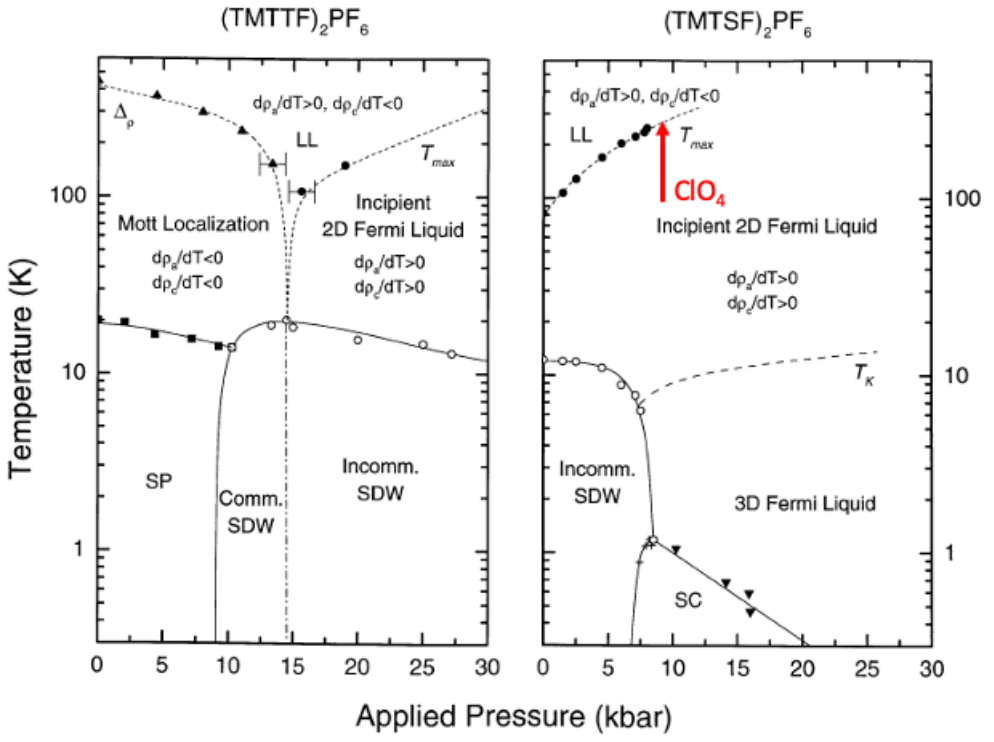

Figure 65. $(T-P)$ phase diagram of $(TMTTF)_2PF_6$ (left panel) and $(TMTSF)_2PF_6$ (right panel). The T_{max} versus P line (full circles) setting a border between a Luttinger regime (LL) and a transient phase towards a Fermi liquid is shown for both compounds. The T_K line (right panel) marks the restoration of a 3D Fermi liquid at low temperature with ρ_c becoming coherent. SP stands for the Spin–Peierls phase. Commensurate (Comm) and Incommensurate (Incomm) SDW states have been singled out. Also displayed in red, the location of $(TMTSF)_2ClO_4$ at ambient pressure for which the cross-over between Luttinger-like and Fermi-like physics occurs around 300 K. Source: [251, Fig. 2 p. 42]. ©Springer Nature. All rights reserved.

On the other hand, when quarter-filled Umklapp scattering is dominant at high temperature $\theta = 16K_\rho - 3$ and consequently $K_\rho = 0.23$ according to the data of $(TMTSF)_2PF_6$ from Fig. 63. This is also a reasonable value for the Luttinger parameter of $(TMTTF)_2PF_6$ at very high pressures of 25 kbar or so, Fig. 62. Additional arguments have been given in Ref. [255] in favour of the 1D quarter-filled band scenario in the high temperature metallic region in both series of $(TM)_2X$ compounds.

Regarding the ordered phases at low temperature in the phase diagram Fig. 57, what happens for $(TMTTF)_2PF_6$ below the 1D Mott localization line is a phase transition towards a long range ordered insulating phase observed in the charge localized temperature domain, *see* the left part of Fig. 57. The phase at low temperature has been ascribed, according to NMR data, to the onset of a charge disproportionation between molecules of each dimer on the molecular chains [256] or charge ordered (CO) state. Since the charge of this low temperature phase is no longer uniform, manifestations of ferroelectricity can be expected as shown by a signature in dielectric measurements [257, 258]. The stability of this CO state (often called a Wigner state) is a direct consequence of the long range nature of the Coulomb repulsion which, in terms of

the extended Hubbard model, amounts to finite on-site U repulsion along with first and second nearest-neighbors Coulomb V terms. Another example of the charge ordering in 1D conductors will be given in Sec. 4.2.5.

We turn now to the study of transport along the least conducting direction which has contributed significantly to better understand the diagram in Fig. 65 and in particular the evolution from Luttinger to higher dimensional metallic physics under pressure. Let us notice that measurements along the c axis, *see* Fig. 66, are also very reliable as no cracks develop on cooling unlike those along the a direction (at least at ambient pressure).

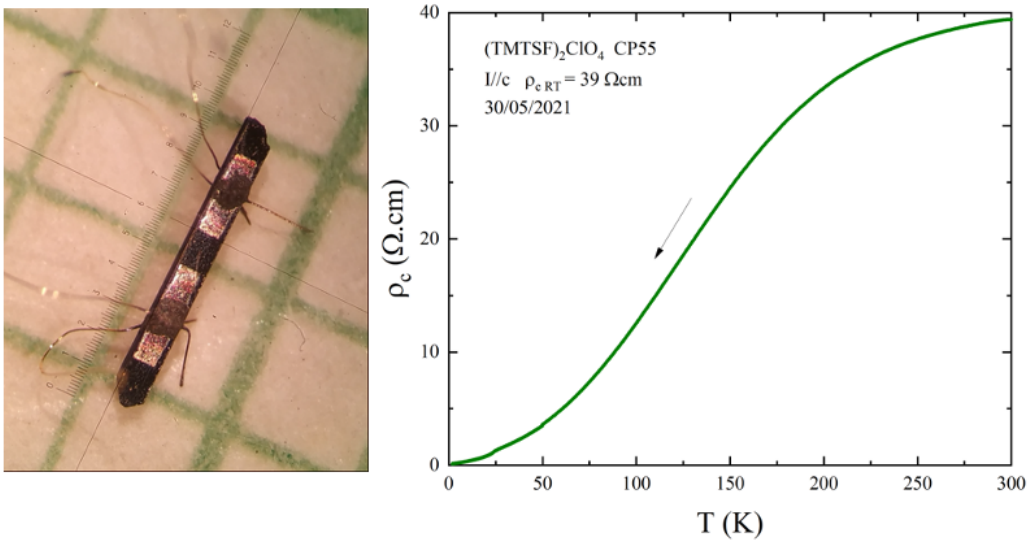

Figure 66. This picture shows how samples with c axis perpendicular to the figure are prepared for the measurement of ρ_c. Gold pads are evaporated on both equipotential ($a-b$) planes for current and voltage leads along c. Usually measurements along c are free from any cracks during cooling unlike a axis data for which severe cracks are often observed under ambient pressure. The tiny kink on $\rho_c(T)$ at 24 K is due to the ClO_4^- anion ordering transition. We thank P. Auban-Senzier for the communication of this picture.

Transverse transport requires the tunneling of Fermions between neighbouring chains (*at variance* with the longitudinal transport which is related to 1D collective modes) and therefore transverse transport along the least conducting direction probes the physics of the $a-b$ planes namely, the amount of quasi-particles (QP) weight existing close to Fermi level of the weakly interacting Luttinger chains. In the case of a Landau–Fermi state, these QP are characterized by an in-chain (or in-plane) lifetime τ, there exists a proportionality relation between single particle contribution to conduction of $\sigma_\perp$ and $\sigma_\parallel$ which has been well established for TTF-TCNQ using the Fermi Golden rule for incoherent transverse transport, as discussed above in Sec. 3.1.3.

$(TM)_2X$ compounds behave quite differently with very often opposite T-dependence for the a and c components of transport, an activated character for the transverse transport at high temperature and a metal like behaviour for ρ_a (*see* Figs. 62 and 67). These features can be interpreted as the signature of a remnant in-chain non Fermi–Landau behaviour [251].

Below a temperature $T_{\max}(P)$ the c-axis transport switches from an insulating at high temperature to a metal-like temperature dependence which has been attributed to the manifestation of a cross-over between two regimes; a high temperature 1D regime with reduced QP weight at

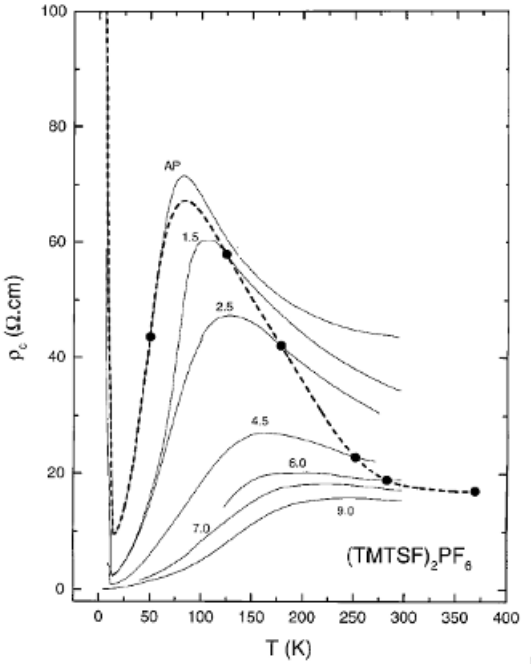

Figure 67. c-axis resistivity of $(TMTSF)_2PF_6$ under various hydrostatic pressures up to 9 kbar showing the procedure followed to extract the temperature dependence at the volume of 50 K under ambient pressure. The bold points and the dashed curve represent the T-dependence under constant lattice parameters and in-turn ρ_c amounts to 17 instead of 42(Ω.cm) at 300 K. Source: [251, Fig. 4 p. 45].

Fermi energy (possibly a LL liquid) and another regime in which the weight acquires higher dimensional metallic (HDM) features with decreasing temperature. The strong pressure dependence of $T_{\max}$ on Fig. 62 rules out a simple relation $T_{\max}(P) \propto t_b$ since the pressure coefficient of the bare transverse coupling should be the order of what is expected for the rather weak volume dependence of the kinetic couplings namely, 2%/kbar. The crossover is also quite visible comparing the pressure dependence of σ_a and σ_c at constant temperature, *see* Fig. 68 for the case of $(TMTSF)_2PF_6$. Following the data on Fig. 67 the cross-over temperature is thus increased by a factor of order 3 under 10 kbar which is definitely inconsistent with a non-interacting electrons model.

Consequently, the strong pressure dependence of $T_{\max}(P)$ is very suggestive of some kind of renormalization of the transverse coupling $t_\perp$, as pointed out in Ref. [259] based on the NMR data, with intrachain interactions renormalizing downward the interchain hopping between the weakly coupled Luttinger chains as a result of the decay of the density of states (10), which reduces the probability for coherent interchain quasi-particle tunneling. The renormalized cross-over thus becomes,

$$t_b^\star \sim W\left(\frac{t_\perp}{W}\right)^{1/(1-\alpha)}, \tag{18}$$

where α is given by the exponent (Eq. (10)) entering in the QP density of states. It has been argued following the optical data of $(TM)_2X$ salts [247], that given a value for K_ρ of the order of 0.23, which means $\alpha = 0.64$. The renormalization of the transverse coupling according to Eq. (18) would lead to a cross over temperature between the 1D regime and a higher dimensional

coherent regime for single particle motion [247] much too severe, below 10 K or so, *at variance* with transport data which locate it around 100 K or higher. However, the above expression for $t_b^\star$ assumes that the exponent α is fixed at all temperature up to the high-energy cutoff W, which is of the order of the bandwidth along the chains. The actual α is likely to evolve as a function of energy in the presence of Umklapp scattering, its averaged – lower – value over the whole energy interval would give a more realistic scale for the crossover.

According to the transport data of $(TMTSF)_2PF_6$ displayed on Fig. 67, the renormalisation which cannot exceed a factor about 3 at ambient pressure in $(TMTSF)_2PF_6$ is practically suppressed under a pressure of 10 kbar.

Hence, we may conclude that Eq. (18) is exaggerating the renormalisation of the transverse coupling due to intrachain Coulombic interactions as well as its pressure dependence. A reexamination of this question would be useful in regard to the value of α extracted from ρ_c.

Below the deconfinement temperature $T_{\max}$, charge excitations lose their 1D character and resemble in certains respects to what is expected in a Fermi liquid with a quadratic temperature dependence for the longitudinal resistivity observed in $(TMTTF)_2X$ compounds under very high pressure [235] or even at ambient pressure in $(TMTSF)_2PF_6$ [260] although electron excitations of this apparent "Fermi liquid" retain a low energy gap in the far infra-red spectrum in which most of the oscillator strength is carried by states above the gap coexisting with a very narrow and intense zero frequency peak in the conductivity, [247, 261] as we shall detail in Sec. 4.2.3.

Such a picture does not necessarily imply that the transport along the c-direction must become coherent below the cross-over as the c-axis transport may remain incoherent with a progressive establishment of a Fermi liquid like state in $a-b$ planes at temperatures much below $T_{\max}$ and the emergence of a weak Drude peak with an edge along $c^\star$ [262]. As a result, the coupling t_c along c is of the order of 1 meV.

The question of the evolution between 1D physics and the higher dimensionality conductor has stimulated numerous theoretical treatments. A first attempt has been made following the treatment of the the c axis conductivity between adjacent confined Luttinger liquids in underdoped cuprate superconductors [263], with the conclusion "it would be of great interest to examine the conductivity along the weakest hopping direction in the quasi 1D and 2D organic conductors".

The interplane transport can only proceed via the hopping of quasi-particles. For such a situation to occur a *real* particle has to escape the Luttinger liquid by recombining its charge and spin components.

The *real* particle can then hop onto a neighboring stack, contributing to σ_c and then decay into the Luttinger liquid again. The transverse interplane conductivity has been derived theoretically when the physics of electrons in chains is governed solely by a 1-D Luttinger regime and when conduction can be approximated in the tunneling approximation by [251]:

$$\sigma_c(T) \propto t_c^2 \left(\frac{T}{\nu_c}\right)^{2\alpha} \tag{19}$$

where the exponent α enters the density of states near the Fermi energy according to Eq. (10).

Following this model, ρ_c should behave like,

$$\rho_c(T) \propto T^{-2\alpha} \tag{20}$$

in the Luttinger liquid domain with α positive and ranging from infinity in a Mott insulator to zero in a non-interacting Fermi liquid. However, fitting the high temperature regime of the constant volume transverse transport on Fig. 67 by Eq. (20) would lead to $\alpha = 0.7$ [251] and in turn to $K_\rho \simeq 0.22$, from solving the second order equation for K_ρ. Such a value would be too large to agree with the findings of longitudinal transport and optical conductivity at high frequency to be presented below. This mismatch between transport data calls for an improvement of the

theory for transverse resistivity, *see* Sec. 4.2.4. In the case of a Landau–Fermi liquid in which electron states are characterized by an in-chain (or in-plane) life time τ, Eq. (19) recovers the proportionality between $\sigma_{\parallel}$ and $\sigma_{\perp}$ has mentioned above and which is fairly well followed for $(TMTSF)_2ClO_4$ at room temperature, *see* Fig. 68. However, these conditions are not fulfilled for $(TMTSF)_2PF_6$ which according to the diagram of Fig. 65 is located in the "Luttinger liquid" domain.

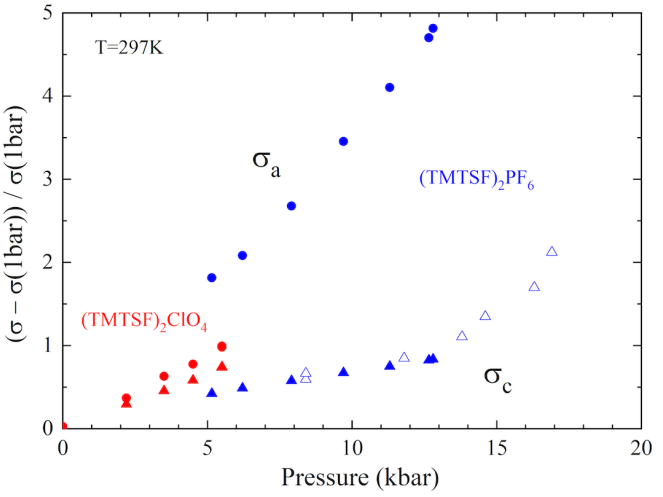

Figure 68. Pressure dependence of conductivities at 300 K along a and c for $(TMTSF)_2PF_6$ in blue and $(TMTSF)_2ClO_4$ in red. According to Fig. 65, the pressure regime for these $(TMTSF)_2PF_6$ data is almost entirely located in the "Luttinger" regime since P_{max} corresponding to the cross-over is about 10 kbar. On the other hand $(TMTSF)_2ClO_4$ is already at ambient pressure in the incipient 2D Fermi liquid phase in which the concept of single particle relaxation time develops. The upturn of σ_c in PF_6 around 14 kbar might be attributed to the passing through the cross-over under pressure with σ_c evolving from an activated mode to a metal-like behaviour at high pressure. It is noticeable that transport is much more volume dependent in the "Luttinger" domain than it is in the 2D incipient Fermi liquid phase. We thank P. Auban-Senzier for the communication of these unpublished data.

Fig. 68 shows that in this phase the pressure dependence of the conductivity is at least 25 %/kbar for the longitudinal component while it is only ≈ 10-15%/kbar along the least conducting direction that still shows an activated temperature profile.

We are now facing a problem dealing with the constant volume dependences of longitudinal and transverse transport since the consensus on $K_\rho = 0.23$ giving $\alpha = 0.64$ cannot afford for the amplitude of the temperature dependence of ρ_c between 300 and 100 K. Notice that a $K_\rho = 0.20$ would raise α up to 0.8.

What is learned from longitudinal transport and the attempt to explain the transverse transport starting from the 1D Luttinger model is that the behaviour of the electronic transport of $(TM)_2X$ at low temperature although at first sight looking perfectly classical, Fermi liquid type with T^2 law components in these strongly anisotropic conductors may be nothing more than a "Canada Dry" effect. The physics of the conducting phase is actually far more complex and subtle as we shall see, looking at crucial data brought by the examination of the frequency dependence of the metallic conductivity regime in the far infrared range.

Concluding this section, Fig. 65 provides quite a general experimental picture based on transport for the generic diagram of $(TM)_2X$ for the physics going on at high temperature. Next, we intend to see how these data can be connected to the studies of the optical conductivity and will force us to reconsider some of the conclusions reached from longitudinal transport.

4.2.3. *Optical response in the* $(TM)_2X$ *series*

Measurements of optical properties of $(TMTSF)_2PF_6$ began very early after the discovery of superconductivity in this compound, first with reflectance studies for light polarized along the stacking axis [61] providing a plasma edge around 10.000 cm^{-1} and a bandwidth of approximately 1 eV, significantly larger than for TTF-TCNQ.

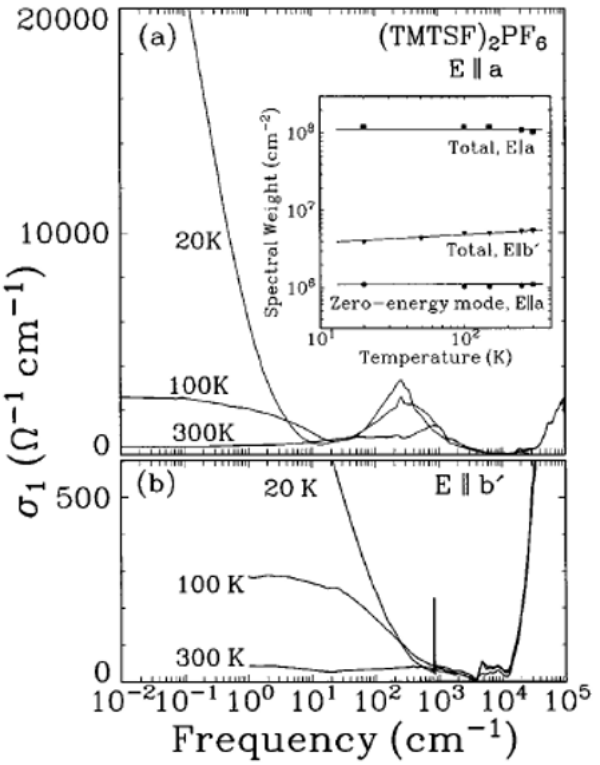

Figure 69. Optical conductivity of $(TMTSF)_2PF_6$ obtained after a Kramers Krönig analysis of the reflectance in both ∥ (a) and ⊥ (b) polarization directions. The inset shows the spectral weight of both modes with the zero energy mode carrying about 1% of the total spectral weight. Source: [264, Fig. 2 p. 399].

Subsequent measurements performed by the danish group [265] from far infrared to visible pointed out the growth below 100 K of an infrared reflectance edge for electric field perpendicular (∥ (b')) to the stacking axis resembling the plasma edge of a Drude metal. It was thus suggested that the $(TMTSF)_2PF_6$ compound evolves from a 1D conductor at high temperature to a 2D conductor at low temperature (≈ 100 K). A few years later, a new investigation of the $(TMTSF)_2PF_6$ reflectance covering an extremely broad frequency range led after a Kramers–Krönig analysis to the determination of the optical conductivity for parallel and perpendicular polarizations [264].

Optical studies have been finalized in an article covering the electrodynamic response of several members of the $(TM)_2X$ series all showing a similar behaviour [247], all compounds exhibiting a behaviour departing drastically from the response of a simple Drude metal. An overview of the electrodynamics of Fabre and Bechgaard salts can be found in Ref. [266].

From these optical studies it turned out that the metallic state of $(TMTSF)_2PF_6$ or $(TMTSF)_2ClO_4$ above the establishment of long-range order (SDW or SC) is of great interest since it exhibits characteristic features of both the correlations-gapped Mott insulator around $E_{gap} = 200$ cm^{-1}, (~ 275 K) together with the high energy excitations of a 1D Luttinger liquid [248] with a conductivity revealing a power law in frequency $\sigma(\omega) \propto \omega^{-1.3}$, *see* Fig. 70. This is the power law expected for the AC conductivity of a Luttinger liquid [231] taking into account the quarter-filled band Umklapp scattering namely,

$$\sigma_{\parallel}(\omega) \propto \omega^{16K_\rho - 5} \tag{21}$$

at $\omega > E_{gap}$, leading in turn to $K_\rho = 0.23$ and $\alpha = 0.64$ according to the experimental data on Fig. 70.

4.2.4. *Back to the transverse transport*

The optical conductivity data let believe that the assumption of the high temperature phase as a set of 1D Luttinger chains is likely too naive. As a result, the question of the transverse transport has been reconsidered including precursor effects revealed by high frequency optical investigations [247,248] which provide remnants of the Mott localization. Using a DMFT approach treatment of the transverse coupling establishing the link with the low temperature Fermi liquid state, a derivation for $\rho_c(T)$ valid all the way from the Luttinger liquid to the Fermi regime has been obtained namely,

$$\rho_c(T) \approx T^{1-2\alpha} \tag{22}$$

Unfortunately, Eq .(22) does not represent much improvement as compared to the treatment leading to Eq. (20) since a value $\alpha = 0.64$ in agreement with $K_\rho = 0.23$, would lead to a constant volume temperature dependence of the resistivity too small compared to the experiments, *see* Fig. 67. Hence, the authors of Ref. [267] have made the remark that the underlying Mott physics cannot be neglected and propose that this effect is the one responsible for the significant increase of ρ_c on cooling. The phenomenological fit by an activated behaviour,

$$\rho_c(T) \propto T^{(1-2\alpha)} \exp(\Delta/T) \tag{23}$$

provides the activated behaviour in Fig. 67 using the values of the optical Mott gap for Δ.

The authors of Ref. [267] concluded that "incoherent tunneling between LL chains in a purely metallic regime is insufficient and that the physics of Mott localization plays an important role in the temperature range $150\text{K} < T < 300\text{K}$".

4.2.5. *Chemistry coming to rescue the quarter-filled scenario*

So far, the details of the T/P phase diagram for the TMTTF compounds described previously clearly involve a competition between half and quarter-filled Umklapp scatterings. The dimerization in the g-ology approach to the physics of 1D conductors [222] results in a localization of charges on the bonds between adjacent molecules due to half-filled Umklapp scattering [234]. The ground state is referred to as a dimer-Mott insulator. In actual $(TM)_2X$ materials, spin-Peierls (SP) or antiferromagnetic (AF) orderings occur at low temperature [239,241,269]. On the other hand, the next near neighbor Coulomb interaction competing with the on-site interaction is known to lead to charge ordering [232] which tends to favor an AF ground state, but here the exchange integrals, and consequently the AF wave vector, are controlled by the CO (charge order) order parameter. Although there already exists a strong suspicion as discussed in Sec. 4.2.2

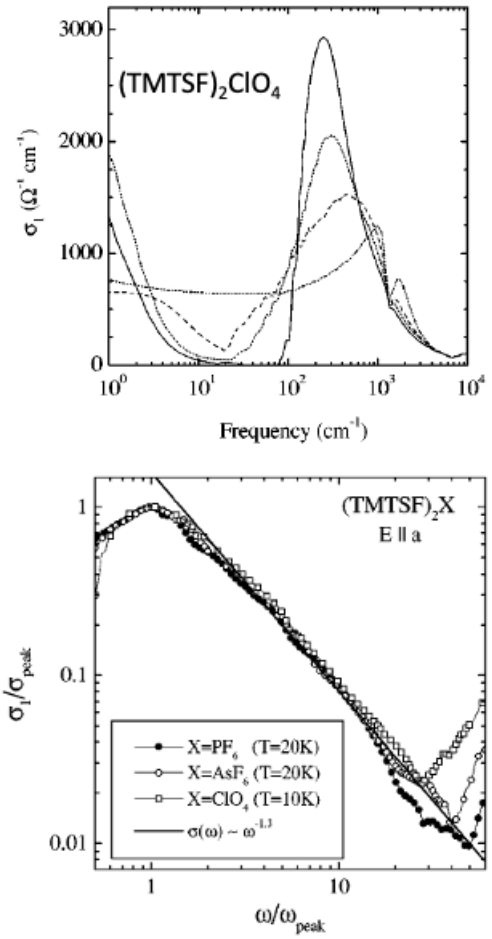

Figure 70. The conductivity of $(TMTSF)_2ClO_4$ for E|| a at 300, 200, 100, and 10 K. The lower part displays the power law frequency dependence of the conductivities for several members of the $(TM)_2X$ series in the low temperature metallic regime such as $\sigma_{\parallel}(\omega)^{-1.3}$, after Eq. (21). Sources: [247, Figures 3, 4 p. 1264, 1266]. ©American Physical Society and the authors. All rights reserved.

in favour of the dominant role played by the quarter-filled Umklapp scattering in the generic diagram of the $(TM)_2X$ series, it is clear that a system in which the competition between half and quarter filled Umklapp is no longer relevant is most welcomed.

The opportunity to study the progression from insulator-metal in a structurally quarter-filled quasi-1D compound (i.e., without dimerization) has been given by chemistry with the crystallization of 2 : 1 salts from the-non symmetrical molecule, $(EDT-TTF-CONMe_2)_2X$ [268] for which there is no center of symmetry between the molecules along the stack, (*at variance* with the $(TM)_2X$ series and their inherent dimers) as a result of a glide plane symmetry and where extensive refinement of X-ray synchrotron data indicate a uniform distribution of the molecular units, *see* Fig. 71, yielding a band quarter-filled with holes [270].

The T/P phase diagram shown in Fig. 72, drawn from a combination of transport and NMR measurements on two members of this family, is simpler than for the TMTTF series because of the absence of dimerized stacks [181]. At ambient pressure and T = 300 K, both compounds

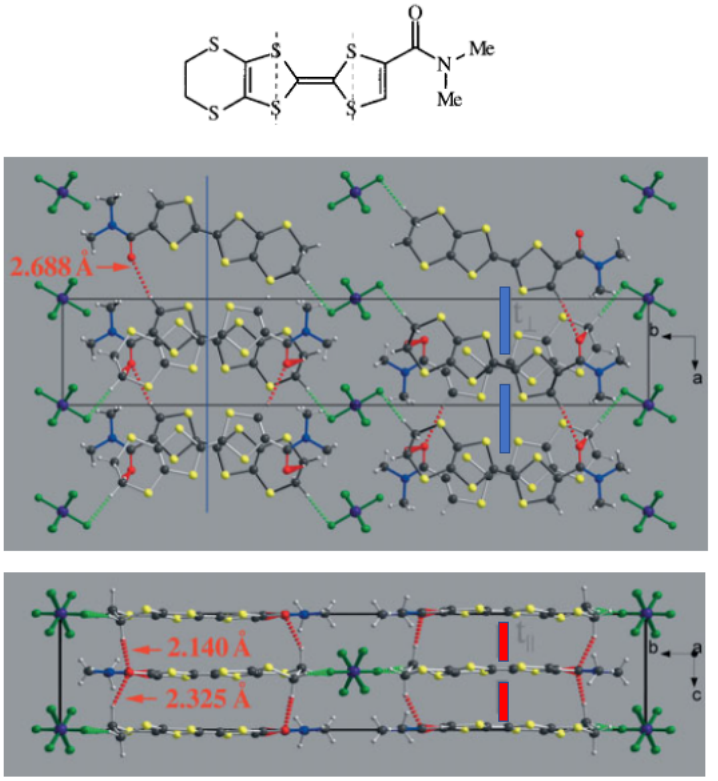

Figure 71. (Top) The non-symmetrical radical cation molecule EDT – TTF – $CONMe_2$. (Middle) Projection onto (110) of the low temperature monoclinic form of $(EDT-TTF-CONMe_2)_2AsF_6$. The vertical thin line is the trace of the glide plane at $3b/4$. Notice the criss-cross stacking along the c axis. (Bottom) Parallel uniform stacks in the low temperature monoclinic form. The red bars show the uniform kinetic coupling along the c direction. Source: [268, Fig. 1, 2 p. 1252].

in the EDT series are in a CO (Wigner) insulating state and cooling results below about 12 K in antiferromagnetically ordered ground states. The application of pressure suppresses the CO phase in favour of a quasi-1D conductor that, upon cooling, undergoes a transition toward which is likely to be a Peierls state since no sign of magnetic ordering could be detected in NMR experiments. Still higher pressures suppress the Peierls transition, presumably as the nesting condition responsible for this Peierls transition is weakened. Similar properties were observed for both compounds provided the pressure is shifted for the $(EDT)_2AsF_6$ material by 7 kbar relative to $(EDT)_2Br$ and for this reason the phase diagram as presented in Fig. 72 applies to both compounds, $(EDT)_2Br$ and $(EDT)_2AsF_6$, *albeit* with the appropriate shift in pressure. The lesson to be draw from these compounds born intrinsically quarter-filled 1D organic conductors is the relevance of 1/4 Umklapp processes to induce electronic localization in highly correlated 1D conductors.

In addition, one should not forget that in spite of serious attempts [271], no sign of superconductivity could be detected above 70 mK under high pressure in the generic diagram of Fig. 72. This let us suggest that *the existence of a SDW ground state may be a prerequisite for the stabilization of superconductivity in its proximity.*

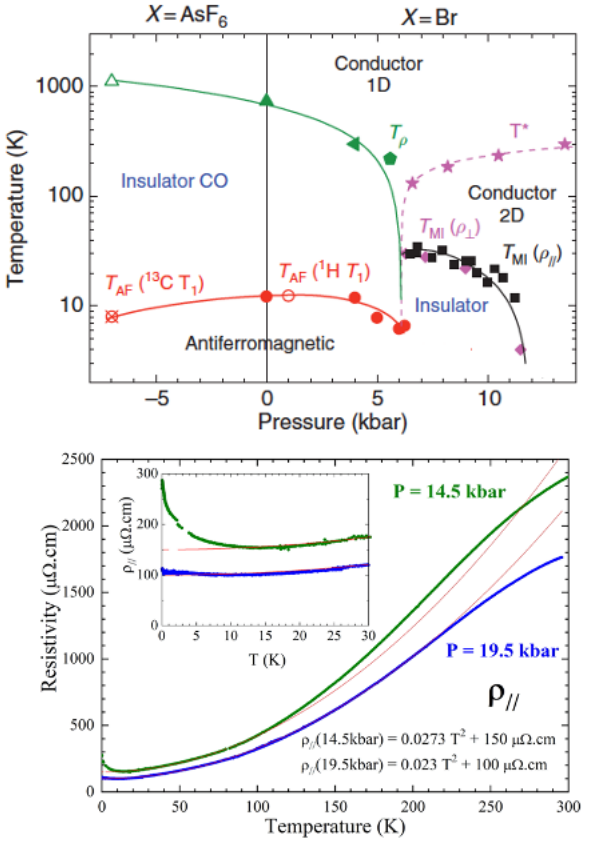

Figure 72. Generic (P/T) phase diagram for the quarter-filled compounds $(EDT-TTF-CONMe_2)_2X$. Source: [271, Fig. 1 p. 2]. Open and close symbols refer to $(EDT)_2AsF_6$ and $(EDT)_2Br$, respectively. The origin of pressure is taken for $(EDT)_2Br$. High-temperature triangles provide a determination of T_{CO} from the P-dependence of the longitudinal conductivity at room temperature assuming a BCS relation between the gap and the transition temperature. T_{CO} is also deduced from the kink on the P-dependence of the conductivity at room temperature (triangle at 4 kbar). The minimum of the longitudinal resistivity (T_ρ) in the 1D regime is reported when it is observed below room temperature (triangle at 4 kbar, losange at 5.6 kbar)). Circles (crossed (×)) indicate the antiferromagnetic ground state observed by H and ^{13}C NMR [270, 271]. In all respects, the high temperature 1D regime of this diagram is similar to the generic diagram of the $(TM)_2X$ series displayed in Fig. 65. The insulating phase suppressed around 12 kbar is non-magnetically ordered unlike the SDW phase of the $(TM)_2X$ diagram. The lower part shows the T dependence of ρ_a without any sign of superconductivity above 70 mK. Notice the absence of the T-linear contribution to the resistivity at low temperature next to superconductivity due to AF fluctuations and commonly observed in the $(TM)_2X$ series, *see* Sec. 4.5.1.

So, can this help answer the question raised by T.Giamarchi in his review [234]: "... the fact that these compounds, $(EDT)_2X$, are indeed insulators and with a structure similar to the Bechgaard salts strongly confirms the interpretation that the dominant mechanism is also in these systems the quarter-filling of the band. It would be of course very interesting to investigate

the phase diagram and the physical properties under pressure of these compounds. Since they share the same basis microscopic $(EDT)_2AsF_6$ features, it is crucial to assert whether these quarter filled systems also exhibit superconductivity under pressure as in the Bechgaard salts".

We feel that, although there is now little doubt about the predominance of the quarter-filled picture on the physics of high temperature phases, the respective role of half-filling versus quarter-filling for the existence of superconductivity in these Q1D compounds remains an important open question. Why the metallic phase of $(EDT)_2X$ compounds under pressure does not exhibit superconductivity is a challenge, which is probably waiting for additional investigations from physicists and possibly new materials from chemists. Let us suggest that the dimerization which is present in the $(TM)_2X$ series may be a hidden prerequisite for the existence of superconductivity in these 2:1 conducting salts.

4.3. *Superconductivity and symmetrical versus non-symmetrical anions*

By the end of 1980, the Copenhagen group in the attempt to stabilize the superconducting state under ambient pressure succeeded with the evidence from resistance measurements of a superconducting transition in $(TMTSF)_2ClO_4$ beginning around temperatures between 1.2 K and 1.4 K depending on the samples [272, 273]. The rationale behind changing the anion X from octahedral PF_6^- to tetrahedral ClO_4^- is that the latter is smaller, which might have the same effect on the conducting TMTSF stacks as pressure has in $(TMTSF)_2PF_6$. The idea of a synthesis using ClO_4^- anions turned out to be justified since structural analysis shows that the two compounds $(TMTSF)_2PF_6$ and $(TMTSF)_2ClO_4$ are isostructural with a unit cell volume for $(TMTSF)_2ClO_4$ smaller by 2.8% compared to $(TMTSF)_2PF_6$. "We wish to recall that it is important to be aware that the preparation of salts with ClO_4^- anions requires the handling of unstable and possibly explosive perchlorates. This has led to the death of a chemical engineer, Mrs Maldy, at the Orsay laboratory. We should not forget her". In the triclinic structure of $(TMTSF)_2PF_6$, PF_6^- resides in a center of inversion [274]. In the case of non-centrosymmetrical anions such as ClO_4^- or ReO_4^-, the tetrahedral anion located at inversion center of the structure but lacking the inversion symmetry will introduce an ordering expected at low temperature for the entropy minimization and consequently change the periodicity of the lattice. It can also, by preventing perfect ordering after fast cooling, introduce non-magnetic disorder in an otherwise superconducting compound. This possibility will be a determining factor in characterizing the nature of the mechanism of organic superconductivity as we shall *see* in Sec. 4.4.5.

The investigation of superconductivity in the entire $(TM)_2X$ family [211] has shown that there exists a critical pressure, above which the superconducting phase is stabilized with respect to the insulating phase stable at low pressures and temperatures. For all compounds belonging to the $(TM)_2X$ series but $(TMTSF)_2ClO_4$, the critical pressure ranges between ≈ 8 kbar and 12 kbar. Furthermore, as implied by the extensive high pressure work [211], the critical pressure correlates with the separation between the stacks of TMTSF molecules at ambient pressure and room temperature, this separation being related crystallographically to the size of the different anions, Fig. 74.

The possibility of observing superconductivity in $(TMTSF)_2ClO_4$ under ambient pressure with a T_c around 1.2 K [272] has made sophisticated experiments much more accessible than for the case of centrosymetrical anions.

In addition, as far as $(TMTSF)_2ClO_4$ is concerned, ambient pressure may even be slightly above the critical pressure since it has been shown that a SDW phase can be stabilized under an uniaxial tension [275].

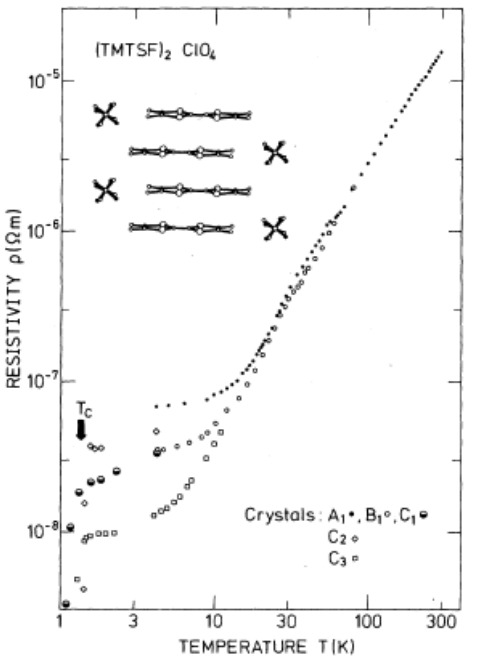

Figure 73. Temperature dependence of the resitivity for $(TMTSF)_2ClO_4$. Results for different samples are normalized to the same room temperature value of $1.45 \times 10^{-3}\Omega$.cm. Source: [272, Fig. 1 p. 853]. Notice that from the log plot, the resistivity is still temperature dependent at liquid helium temperature, very much like $(TMTSF)_2PF_6$ using a T-linear plot on Fig. 51. ©American Physical Society and the authors. All rights reserved.

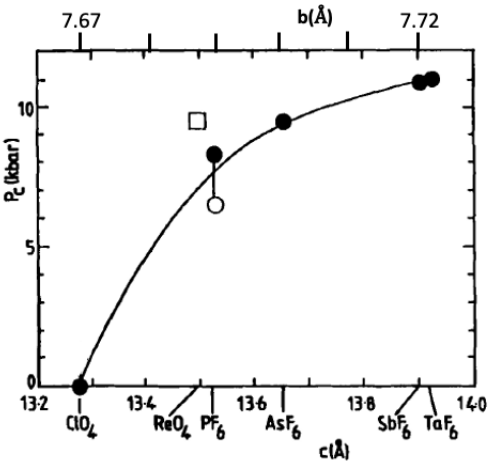

Figure 74. A correlation between the critical pressure for the stabilization of a SC ground state and transverse lattice parameters of several superconducting members of the $(TM)_2X$ series. Source: [211, Fig. 9 p. 5316]. The critical pressure correlates better with the c rather than the b parameters as shown on this diagram, since by $b = 7.71$Å for $(TMTSF)_2PF_6$ [274] is actually similar to $b = 7.72$Å in $(TMTTF)_2SbF_6$ [276]. ©IOP Publishing. Reproduced with permission. All rights reserved.

These experimental findings have had a major influence on the development of the theory of superconductivity of these quasi 1D conductors to be discussed later for which the transverse coupling is the major parameter for determining the stability of the SC state.

Although most of the physics of organic conductors is governed by the organic molecules, the anions, the presence of which is essential for electric neutrality, may in some case suppress the stability of the conducting phase. As a matter of fact, the possibility for $(TM)_2X$ compounds having non-centrosymmetrical anions to undergo a structural phase transition can modify the band structure and the topology of the Fermi surface.

The role of anions is particularly manifest when it is compared to compounds with spherical anions such as PF_6^-, AsF_6^-, and so forth, for which the absence of alteration of the Fermi surface via anion ordering entails, for example, the stabilization of spin density-wave long-range order in zero magnetic field at ambient pressure. The anion potential produced by spherical anions leads to a modulation of the charge along the organic stack with the same periodicity as the dimerization. It may independently contribute to the half-filled character of the band and then enhance the strength of the electron-electron interaction at low temperature [277, 278].

On the other hand, anions such as ClO_4^-, ReO_4^-, NO_3^-, SCN^-, and FSO_3^- have two equivalent orientations corresponding to short and long contacts between the Se atoms of the TMTSF molecule and a peripheral electronegative atom of the anion.

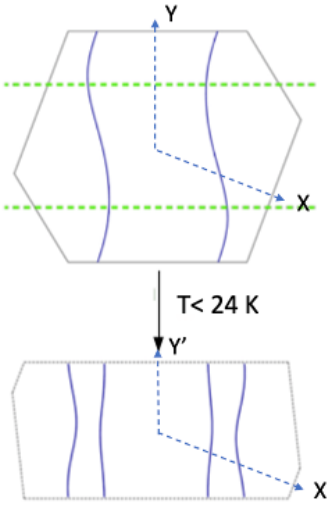

Figure 75. At the ClO_4^- ordering temperature of 24 K, new Brillouin zone boundaries are formed at $\pm\pi/2b$ (top) leading to a folding of the Fermi surface (bottom).

Consider the case of $(TMTSF)_2ClO_4$, a compound from which most of the characteristics of the organic superconducting state have been obtained due to the stability of this phase under ambient pressure. The anion lattice orders at 24 K, leading to a superstructure of the Se-O contacts with a wave vector $q = (0, 1/2, 0)$ [279], *see* Fig. 75. The periodic potential thus created, connects two Fermi points along the transverse b direction and opens a gap with a new zone boundary which doubles the unit cell along that direction. The folding of the Fermi surface that results introduces two warped Fermi surfaces near $\pm k_F$ providing an only limited disturbance to the conductivity with a slight drop of the resistivity at 24 K related to the decrease of the elastic scattering.

Anion lattice superstructure has thus important consequences on the one-particle spectrum and in particular the nesting properties of the Fermi surface. This plays an important role in the

efficiency of electron-electron interactions at low temperature and in the nature of the ground states as remarked by Bruinsma and Emery [277]. Anion ordering also controls the stability of the superconducting phase in $(TMTSF)_2ClO_4$ below 1.2 K at ambient pressure when the long range orientation is defective as already mentioned. The proper ordering of the ClO_4^- anions at wave vector $q = (0, 1/2, 0)$ in $(TMTSF)_2ClO_4$ requires much care during the sample cooling procedure. As it has been reported in the early study of this compound [280], too rapid cooling leads to an anion disorder and a SDW ground state (notice that this discovery has been made by chance by T. Takahashi). The influence of the anion ordering on the nature of the $(TMTSF)_2ClO_4$ ground state is a good illustration for the famous talk pronounced by Louis Pasteur at the University at Lille in 1854 [281] *"In the fields of observation, chance only favors the prepared mind"*. The issue of the ordering of non-centrosymmetric anions challenged Toshihiro Takahashi who one day as he was trying at Orsay to confirm the magnetic nature of the strange phase observed at high fields above 6T or so (now known as the field induced SDW phase, *see* Sec. 4.9). When he saw the disappearance of ^{77}Se-NMR signal, he thought he had got the evidence for the field induced phase. However, next morning, cooling the sample again (probably too fast) to check its reproducibility, he failed to observe the same behavior and observed a magnetic ordering below $\approx$3.5 K nearly field-independent between 1 and 6.5 T. This observation has been subsequently related to the anion ordering with a wave vector $q = (0, 1/2, 0)$ occurring at 24 K by X-ray diffuse scattering experiments and providing the clue for understanding the dependence of the nature of the electronic ground state on the cooling rate dependence [279].

This effect called the "quenched" state of $(TMTSF)_2ClO_4$ has been extensively used for the characterization of the superconducting phase as it enables a proper control of the electron elastic scattering in the superconducting phase to be discussed below, see Sec. 4.4.5.

For other compounds with a non-centrosymetrical anion like ReO_4^-, the structural ordering is different and takes place at $q = (1/2, 1/2, 1/2)$; its impact on the electronic structure turns out to be more marked, since the anion potential at this wave vector creates a gap over the whole Fermi surface which is so large in amplitude (of the order of the Fermi energy) that it leads *at variance* with $(TMTSF)_2ClO_4$ to an insulating state at 200 K in which electron-electron interactions probably play little role. The application of an hydrostatic pressure is then required to establish a less damaging anion ordering configuration [282] and restore the metallic state with the possibility of long range ordering for the electronic degrees of freedom [214, 283].

The case of $(TMTSF)_2ReO_4$ is particularly instructive since thanks to the possibility to change the helium gas pressure at low temperature (although above the freezing point of helium gas) it is possible to bypass the phase (1/2,1/2,1/2) anion ordered and release the pressure at low temperature, *see* Fig. 76. This experiment has shown that the (0,1/2,1/2) anion ordering does have a bad impact on the stability of SDW and SC phases at low temperature.

For $(TMTSF)_2BF_4$, having a tetrahedral anion as in $(TMTSF)_2ReO_4$, no structural analysis has been carried out so far; however, the very sharp transition at relatively high temperature (39 K) compared with hexafluoro-compounds suggests a transition similar to that of $(TMTSF)_2ReO_4$. Also, the observation of an ESR line below the transition clearly shows that the insulating state is not magnetic. Although this anion ordered insulating phase can be removed by pressure no superconductivity could be evidenced above 1.2 K in $(TMTSF)_2BF_4$ [211].

4.4. *A detailed investigation of the ambient pressure superconductor* $(TMTSF)_2ClO_4$

4.4.1. *Superconductivity under magnetic field, very anisotropic type II superconductors*

The application of a magnetic field has led to important and unexpected results for the characterization of these anisotropic superconductors.

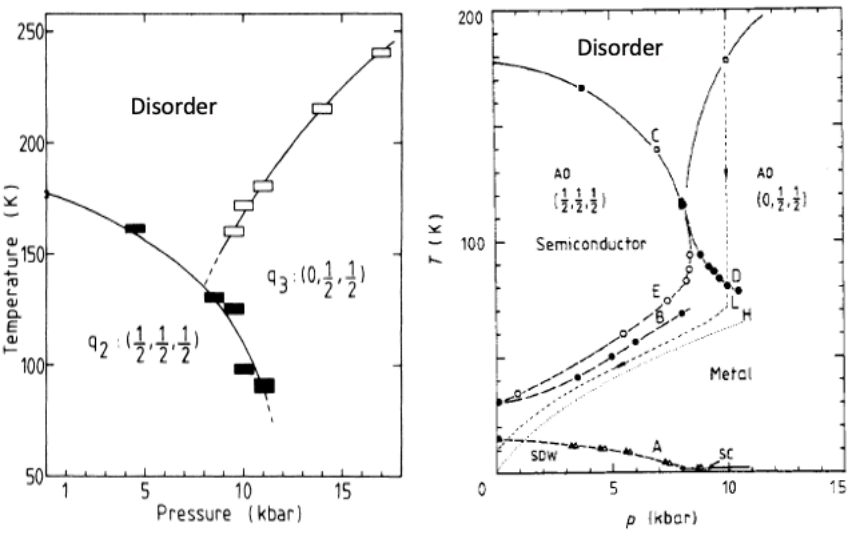

Figure 76. (Left) T-P phase diagram of $(TMTSF)_2ReO_4$ showing the various phases with their anion ordering according to Ref [282]. Sources: [282, Fig. 1 p. 1916]. ©American Physical Society and the authors. All rights reserved. (Right) Applying pressure above 200 K, entering the conducting (0,1/2,1/2) phase, cooling down to 72 K and then releasing pressure and temperature above the melting line of helium (the small dotted line) allows to bypass the semiconducting (1/2,1/2,1/2) phase and keep the (0,1/2,1/2) ordering in a metastable state to explore the electronic instabilities (SDW and SC) in the low temperature region. Source: [214, Fig. 1 p. 4453]. ©IOP Publishing. All rights reserved.

The bulk nature of superconductivity could be inferred from diamagnetic shielding (AC susceptibility) measurements observed in the early days of this research, pointing to a type II superconductivity in $(TMTSF)_2PF_6$ [190], but it has been confirmed by more detailed Meissner effect experiments (i.e., a flux expulsion on cooling in a field) [191] and subsequently in $(TMTSF)_2ClO_4$ [284–287].

Regarding evidences for the Meissner expulsion, the lower critical field H_{c1} is obtained from the magnetization curves of $(TMTSF)_2ClO_4$ at 50 mK [289]. According to Fig. 77 the obtained values are 0.2, 1, and 10 Oe along the a, b, and $c^\star$ axes, respectively.

Following the values for the upper critical fields H_{c2} derived either from the Meissner experiments and the knowledge of the thermodynamical field $H_c = 44$ Oe [288] or from a direct measurements of transport [290], it is found that superconductivity is in the extreme type-II limit. The Ginzburg–Landau parameter κ can even overcome 1000 when the field is along the a axis due to the weak interchain coupling, making field penetration very easy for this external-field configuration. An interpretation of the critical fields assuming the clean limit has been suggested in 1985 [291]. The clean limit theory could be questionable nowadays with the current knowledge of the evolution of T_c in the presence of controlled non magnetic impurities [292], but based on the microscopic expressions for the effective mass tensor in the Ginzburg-Landau equations for anisotropic superconductors near T_c lead, using the experimental slopes of the transport H_{c2} [290, 291] (*see* Fig. 78), $dH_{c2a}/dT = -67$ kOe/K, $dH_{c2b'}/dT = -36$ kOe/K, $dH_{c2c^\star}/dT = -1.5$ kOe/K, to $t_a : t_{b'} : t_{c^\star} = 1200 - 818$, 310-220 and 7-4.6 K, which are of the order of the tight binding band parameters [225, 237, 276, 293]. From the experimental slope dH_{c2}/dT in the vicinity of T_c, a derivation of the coherence length is possible for $(TMTSF)_2ClO_4$ and leads to 700, 330 and 20Å along a, b and $c^\star$ directions respectively [294].

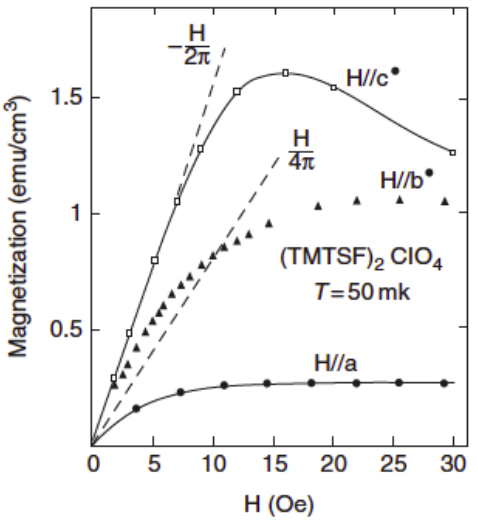

Figure 77. Magnetization of $(TMTSF)_2ClO_4$ at $T = 0.05$ K for magnetic fields along the three axes. Source: [288, Fig. 3 p. 714]. ©EDP sciences. All rights reserved.

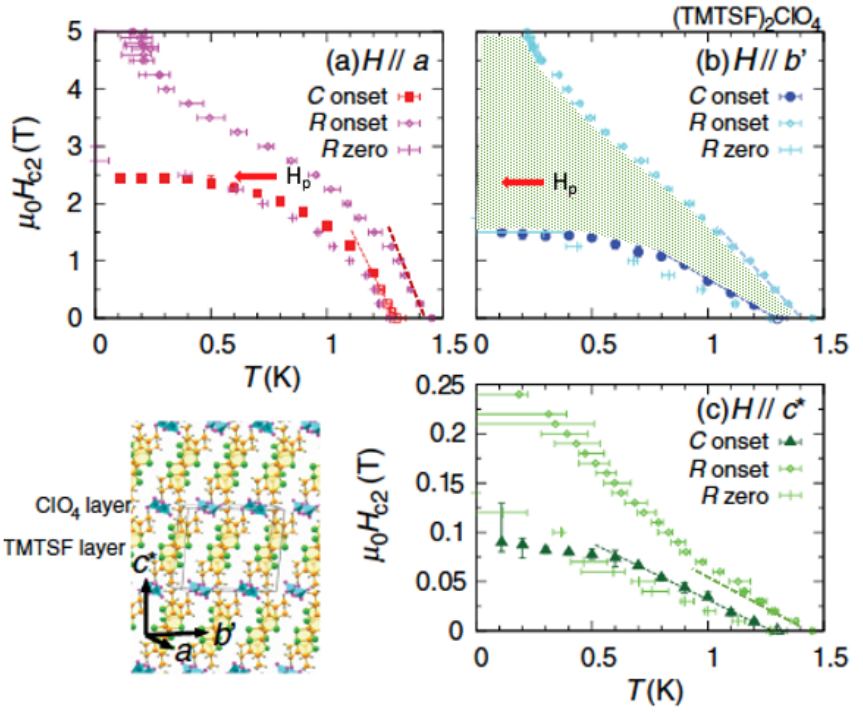

Figure 78. $H_{c2} - T$ phase diagram of $(TMTSF)_2ClO_4$ obtained from specific heat and the $c^\star$ resistivity measurements with the magnetic field aligned along the three crystal axes. The Clogston limit for spin-singlet pairing at $T = 0$ is shown as the red arrow. The orbital limitation in field applies to $H \parallel b'$ and $H \parallel c$. The shaded region for $H \parallel b'$ corresponds to the HSC domain of superconductivity. Source: [290, Fig. 5 p. 3]. ©American Physical Society and the authors. All rights reserved.

Fig. 78 reveals several important features. First, paying attention to the behaviour of the transport H_{c2} we notice a divergence decreasing temperature, in particular below 0.2 K for both a and b' directions. Such a divergence had already been noticed in 1997 in the superconducting state of $(TMTSF)_2PF_6$ [295,296] with peculiarity that the $H_{c2}^{b'}$ becomes even larger than H_{c2}^{a} above the field of order 2 T. A few years later a similar situation has been encountered in $(TMTSF)_2ClO_4$ [297] and from resistivity and torque measurements [287], confirmed subsequently by the extensive measurements performed by the Kyoto group [298, 299] showing that transport critical fields along a and b' largely exceed the orbital critical field of about 2.4 T given by the Clogston limit [300] $H_p(T=0) = 1.84\ T_c$ for singlet superconductors.

Second, most papers following experiments until 2004 were pointing toward triplet paring in the $(TM)_2X$ series but following recent specific heat field-angle resolved measurements in the superconducting phase of $(TMTSF)_2ClO_4$ [290] a new $H_{c2} - T$ phase diagram has been drawn as also displayed on Fig. 78, opening other possibilities. The salient difference between resistivity and thermodynamic phase diagrams is most clearly seen on Fig. 78. The field at which the specific heat recovers its normal state value is much smaller than the field related to the onset of the resistivity drop in temperature and above this field superconductivity has a density of states nearly equal to that in the normal state [290] (see Fig. 80 and also the forthcoming discussion in Sec. 4.4.3).

4.4.2. *Thermodynamics and NMR in the superconducting phase of* $(TMTSF)_2ClO_4$

The existence of superconductivity is also evidenced via the measurement of the thermodynamic properties. But equally important is the behaviour of the specific heat in superconducting phase which provides crucial informations about the nature of single particle excitations in the presence of a superconducting gap. Whereas in the usual BCS case, excitations are created over the finite gap with a probability $e^{-\Delta/k_BT}$, the specific heat of superconductors with nodes in their gap function exhibits a power law behaviour in the limit of $T \to 0$ [301].

Although thermodynamic evidences for superconductivity in $(TMTSF)_2ClO_4$ have appeared as early as 1982 [288], we will focus this presentation on more recent data [302] and will explain the reasons for this approach.

Fig. 79 displays the specific heat of a $(TMTSF)_2ClO_4$ single crystal weighing 0.3 mg versus temperature behaving like $C/T = \gamma + \beta T^2$ in the low temperature regime with $\gamma = 10.6$ mJ/K^{2}mol and β =10 mJ/K^{4}mol. These values are in fairly good agreement with the previous data, [288] but there are some notable differences which need serious comments. The two major differences between the data displayed on Fig. 79 and those of 1982 are on the one hand the dependence of C/T in temperature below T_c which reveals a striking difference with the usual BCS behaviour and on the other hand the jump of specific heat occurring at the transition even though P. Lee wrote in his article PRL 71, 1887, 1993 that "according to conventional wisdom, a single experiment showing activated behavior is sufficient to invalidate the d-wave hypothesis", we think that in the particular case of Q1D organic superconductivity there exists a considerable amount of recent experimental observations in favour of singlet d-wave which allows to take the conventional wisdom with a grain of salt!. While $\Delta C/\gamma\ T_c$ amounts to 1.67 in the data of Ref. [288], Fig. 79 leads to a ratio smaller than unity, actually $\Delta C/\gamma\ T_c = 0.73$ (which is quite reproducible between different samples) fitting these data with the theory of polar superconductors [301]. Using the fit for the data on Fig. 79, the residual density of states at $T = 0$ amounts to 35% of the normal state value.

The thermodynamic data suggest the existence of a finite residual density of states at Fermi level in the very low temperature regime even for a pristine sample. This experimental result is corroborated by the temperature dependence of the spin-lattice relaxation of ^{77}Se nuclei performed in the superconducting phase of $(TMTSF)_2ClO_4$ [303] as single particle excitations are probed by $1/T_1T \propto \chi^2(q=0,T)$ according to the celebrated Korringa law. Fig. 80 shows that the

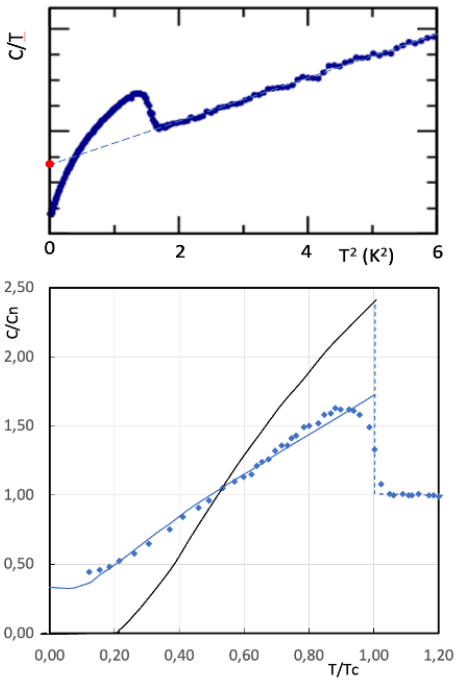

Figure 79. (Top) Total specific heat for a $(TMTSF)_2ClO_4$ single crystal of 0.1mg in the relaxed (R) state showing a law $C/T = \gamma + \beta T^2$ at $T > 1.3$ K for the electrons and phonons contributions with the anomaly at the mid-transition $T_c = 1.22$ K due to the superconducting transition. The red dot at $T = 0$ is the value of the normal state electronic specific heat, $\gamma = 10.6$ mJ/K^{2}mol for $(TMTSF)_2ClO_4$. (Bottom) Electronic contribution normalized to the normal state value (blue dots) plotted as C/C_n against T/T_c. The black continuous line is the behaviour expected for a weak coupling fully gapped BCS superconductor while the blue continuous line is the behaviour expected for a polar superconducting state with a ratio $\Delta C/C_n \approx 0.73$ for $\Gamma/T_c = 0.1$ from Ref. [301]. This value of the scattering rate for a pristine sample agrees with the measurements of a slowly cooled $(TMTSF)_2ClO_4$ crystal [292]. We thank Shingo Yonezawa for communicating the data used for this figure, also published in Ref. [302].

Korringa law is fairly well obeyed above T_c (which amounts in the field of 0.96T $\| b'$ to 0.8 K and also below 0.3 K with a T-linear dependence of the relaxation rate with a prefactor in the field of 0.96T $\| b'$ decreased by about 3.3 between high and low temperature regimes. The prefactor being proportional to the square of the density of states, this result shows that the density of states at Fermi level has decreased by a factor 1.8 from just above T_c and low temperature in the SC state.

In addition, since electronic specific heat measurements at low temperature have shown that the density of states measured by C/T is H-field dependent, (*see* bottom of Fig. 80) the density of states drops by another factor two from 0.96T down to zero field leading to a final residual density of states at zero magnetic field which amounts to 28% the normal state value. It is a value although different, which compares favourably with the residual density of states given by the specific heat fit (35%) displayed on Fig. 79.

The behaviour of the specific heat below T_c as shown on the latter figure is very reminiscent of the numerous experimental studies performed on Uranium-based heavy fermions materials over the years 80 to 90's, systems in which non conventional pairing in the superconducting phase, in

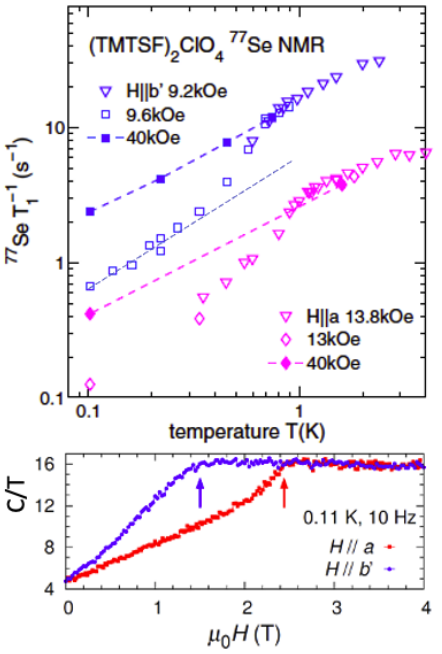

Figure 80. (Top) $1/T_1$ versus T for the ^{77}Se spins of $(TMTSF)_2ClO_4$ for $H\|b'$ and $H\|a$ according to Ref. The dotted blue line at low temperature for the field $H\|b' = 0.96T$ has a slope unity and suggests that the relaxation at low temperature is due to a residual density of states provided by unpaired single particles at the nodes of the SC gap. (Bottom) Field dependence of C/T at $T = 0.3$ K. Sources: [303, Fig. 2 p. 3] (top), (top) [290, Fig. 1 p. 2] (bottom).

particular polar or axial gap functions must be considered [301, 304]. We intend to return to the comparison with heavy fermions when we look at the field-angular dependence of the specific heat.

One feature that the ^{77}Se NMR experiments [303] have provided is the existence of a residual density of states at $T = 0$ in the superconducting state of $(TMTSF)_2ClO_4$ but it is equally important to remark that between T_c and the the low temperature regime $1/T_1$ follows a T^3 law, the signature for lines of superconducting gap nodes. Actually, this possibility had been considered long ago by Takigawa et al., who reported a spin lattice relaxation for the protons of $(TMTSF)_2ClO_4$ behaving like $1/T_1 \propto T^3$ which goes with the absence of the common enhancement of relaxation rate just below T_c in usual BCS superconductors [305]. This led Hasegawa and Fukuyama [306] to propose that superconductors in the $(TMTSF)_2X$ family belong to a novel class with the order parameter exhibiting lines of nodes on the Fermi surface. However, both spin lattice relaxation and specific heat measurements suggesting nodal superconductivity were unable to discriminate between (p)-triplet and (d)-singlet pairing.

In the early days of these experimental studies, the option of spin-triplet superconductivity has been claimed following a Knight shift experiment [307] performed on $(TMTSF)_2PF_6$ showing no change of the resonance shift through T_c. However, this conclusion could have been reached by a still poor understanding of the superconducting $H-T$ phase diagram at that time. It can be noticed that the 2002 experiment in $(TMTSF)_2PF_6$ had been conducted under a relatively high magnetic field of 1.43 T aligned along the most conducting a axis. Given NMR studies performed five years later on the superconducting state of the sister compound $(TMTSF)_2ClO_4$, it

was therefore quite likely taking into account the possible different $H-T$ superconducting phase diagrams between $(TMTSF)_2PF_6$ and $(TMTSF)_2ClO_4$, that the field of 1.43 T used in Ref. [307] locates the data of the $(TMTSF)_2PF_6$ sample in the high-field SC phase (so-called HSC, *see* Fig. 78 for the case of $(TMTSF)_2ClO_4$) in which the spin susceptibility does not reveal any noticeable change through the resistive SC transition [303] *at variance* with the low field state behaviour.

Different thermodynamic and resistive SC transitions are also evidenced from NMR relaxation and resistive measurements, *see* Fig. 82.

Therefore, it is the NMR result of 2007 which has really contributed to answer important questions regarding the nature of the spin pairing in the superconducting phase. As shown on Fig. 81, in a field of 0.96 T parallel to b' or a axes the drop of selenium Knight shift below T_c is now providing a solid evidence in favour of spin-singlet pairing. It is unfortunate that the study of the superconducting state as it was conducted on $(TMTSF)_2ClO_4$ and to be presented in the following section, could not be performed on $(TMTSF)_2PF_6$. It does not seem that this crucial measurement should meet major technical challenges in the future.

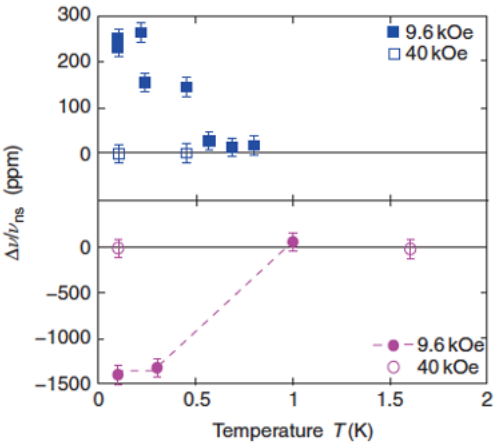

Figure 81. $(TMTSF)_2ClO_4$ ^{77}Se line shift versus temperature for $H\|b'$ (top) and a (bottom) with the zero shift value arbitrarily set to the normal state first moment position. Source: [303, Fig. 1 (bottom) p. 2]. ©American Physical Society and the authors. All rights reserved.

In conclusion, although different symmetries for the order parameter in $(TMTSF)_2ClO_4$ and $(TMTSF)_2PF_6$ cannot be totally ruled out as long as an NMR investigation of the latter compound is conducted at fields below 1T, we consider such a scenario as quite unlikely. In order to show evidences for spin-singlet pairing, we have reported on the $H_{c2}-T$ phase diagram of $(TMTSF)_2ClO_4$, Fig. 83, the locations of the various NMR findings from Ref. [303], (recovery of the normal state $1/T_1T$, onset of the $1/T_1T \propto \chi^2(T)$ SC transition and the $R_{zz}(H\|a)=0$ point) showing that these data have been taken in the low field superconducting phase (LSC). As we can see, all these points are in good agreement with the diagram derived from the zeroes of the resistivity or from the onset of the specific heat anomaly. Bulk superconductivity becomes Pauli limited when $H\|a$. Consequently, it is now hard to dispute the experimental fact that the superconducting pairing in the $(TMTSF)_2X$ family is spin-singlet.

4.4.3. *The high magnetic field phase*

The low field domain of superconductivity of $(TM)_2X$ salts is fairly well understood in terms of a GL model for a 3D anisotropic type II superconductor as developed in Sec. 4.4.1. However, as already mentioned in Sec. 4.4.2, $(TM)_2X$ salts are characterized by a divergent behavior above

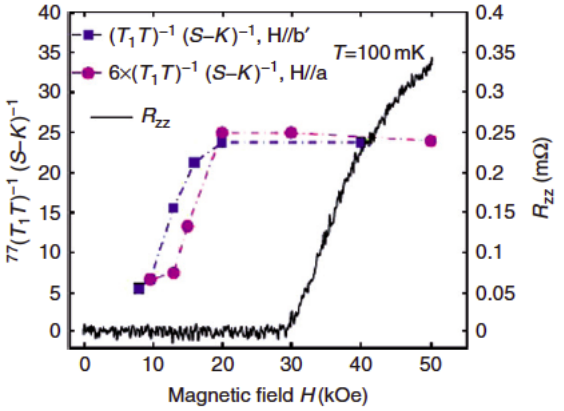

Figure 82. $(TMTSF)_2ClO_4$ ^{77}Se spin lattice relaxation for two orientation of the magnetic field showing the large difference in temperatures between the onset of the SC transition from relaxation and the zero of the resistive transition. Source: [303, Fig. 3 p. 3]. ©American Physical Society and the authors. All rights reserved.

the Pauli critical field at decreasing temperatures for the critical field $H_{c2}(T)$ determined from transport measurements. This feature is particularly clear on Fig. 83 for $(TMTSF)_2ClO_4$ with the shaded areas, but a similar behaviour had first been reported in 2000 for $(TMTSF)_2PF_6$ under pressure in which the onset of superconductivity persists up to four times the Pauli limit when $H_{c2} \parallel b$ [296]. These latter authors have considered the possibility of overcoming the Pauli effect thanks to the stabilization of an inhomogeneous Larkin–Ovchinnikov–Fulde–Ferrell (LOFF) superconducting state [308, 309], although they discarded such a scenario because of no evidence of first order transition between homogeneous and inhomogeneous states, instead, they privileged the scenario of a triplet pairing in order to exceed the pair-breaking limit, a scenario that has been made obsolete after new NMR experiments [303].

Before looking at the SC in high magnetic field, let us concentrate on the normal state above T_c but in the 3D coherent regime, i.e. $T < t_c$, ($T < 5$ K or so). The role of the magnetic field perpendicular to the c axis, suppressing the coherent hopping between adjacent $a-b$ planes thus resulting in a 2D confinement has been considered by Strong et al. [310] and its effect on the conductivity along c has been treated formally by the Kubo formula [311] but a simple semiclassical treatment gives rise, in real space, to a linear trajectory along the a direction modulated by periodic oscillations along the c axis with an amplitude $\delta z = 4ct_c/ev_F H$ which decreases as the magnetic field increases, making the electrons confined in the $(a-b)$ plane [312]. For a field strength of the order of t_c, the electrons get confined in a single plane perpendicular to c. Finding $d\rho_c(T)/dT < 0$ at fields above $H \parallel b' \approx 1$T is consistent with an inter-plane coupling of order of a few degrees [311].

In this semi-classical picture, we do not expect a strong effect of the field on the conductivity along the a direction. On the contrary, the electron confinement in the $(a-b)$ planes should correspond to a field induced dimensional cross-over (FIDCO) in the c direction accompanied by a metal to insulator transition, as observed experimentally in $(TMTSF)_2PF_6$ under pressure [295] and also in $(TMTSF)_2ClO_4$ at ambient pressure [297].

Lebed has shown that the FIDCO should suppress the orbital pair-breaking limitation leading in turn to the stabilization of superconductivity at fields higher than H_{c2}^{orb}.

A major breakthrough arose when the Kyoto group managed to perform a study of the high field SC phase under accurately aligned fields using a vector magnet [298, 299]. For the sake of brevity, let us mention only the results for H perfectly aligned with the $a-b$ plane.

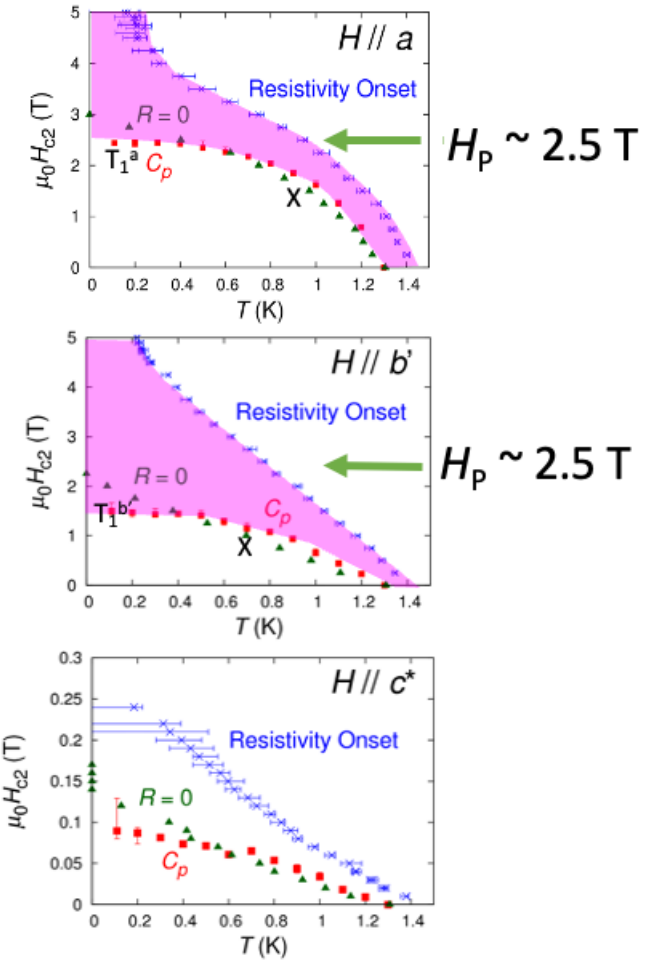

Figure 83. $H_{c2}-T$ phase diagram for $(TMTSF)_2ClO_4$, similar to Fig. 78 on which the location of NMR data points from Ref. [303] have been added. The high field phase is shown as the shaded area. X is related to the onset of the $1/T_1$ transition on cooling and T_1 marks the field location where the normal state value of $1/T_1T$ is recovered at increasing field. Therefore, according to this diagram, 0.96 T$\|b'$ and 1.43 T$\|b'$ are in the LSC and HSC domains respectively. b' is perpendicular to the $a-c^\star$ plane.

In 2008, Yonezawa et al. [298, 299] investigated the in-plane field-angle dependence of the onset temperature of superconductivity, T_{co}, based on the c-axis resistance measurements of $(TMTSF)_2ClO_4$ single crystals [298, 299].

What was found is that for $H\|$ either to b'or to a, T_{co} remains finite up to 5T at least, *see* Fig. 83. The behaviour for $H\|a$ resembles the theoretical treatment of a FFLO scenario [313,314] but the peculiar feature was found with the maxima of the $T_{co}(\phi)$ curve, located at ϕ=0 deg for $H\|a$ and ϕ=90 deg for $H\|b'$ at fields lower than 2.5T shifting away from the crystalline b' and a axes at high fields, *see* Fig. 84. A new principal axis related to the SC phase is emerging above 3T (red line) and progressively moves back to b at higher fields, after [298, 299].

Although the existence of high field SC phases have been suggested in heavy fermions superconductors ($CeCoIn_5$ in particular, although in this compound antiferromagnetism may inter-

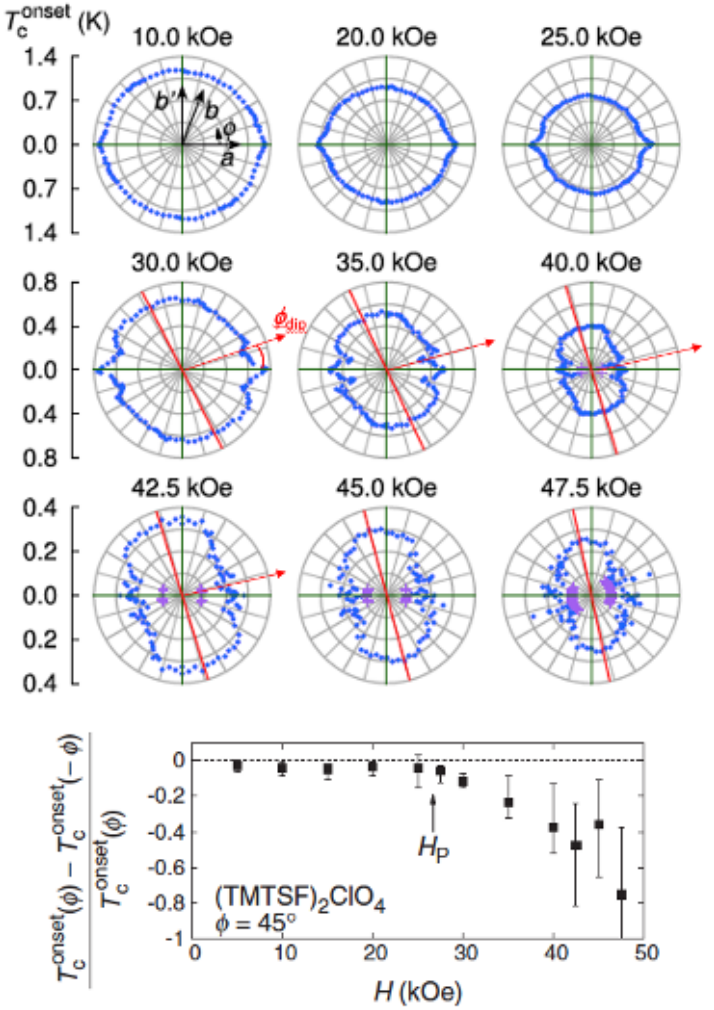

Figure 84. (Top) Polar plot of the ϕ dependence of T_{co} at several magnetic fields below and above the Pauli limit of 2.5T. $\phi_{dip} = 17°$ under 30 kOe corresponds to the angle above which the 2D confinement begins when the field is rotated in the $a-b$ plane. The new principal axis X is observed above 30 kOe. (Bottom) Field dependence of the relative angular difference between positive and negative $\pm\phi = 45°$ showing that the stability of the high field phase is linked to the Pauli limiting field at 2.5 kOe. Sources: [299, Fig. 3 p. 3].

fere with a text-book FFLO state) [315] and in several 2D organic superconductors according to magnetic, thermodynamic and NMR studies, *see* Ref. [302] for more details, we choose to focus in the present article on the possible FFLO state of $(TMTSF)_2ClO_4$ because it can be considered as a textbook-like FFLO state supported by the numerous experimental studies performed on $(TMTSF)_2ClO_4$ in the Kyoto laboratory [299].

What is remarkable in Fig. 84 is first the sharp peaking of T_{co} observed above 30 kOe at $\phi = 0°$ together with dips at $\phi = 17° \pm 1°$. As shown by transport data under aligned fields [311], the angle of 17° corresponds also to the onset of the FIDCO. Since this angle shows a tendency to decrease

at higher fields it has been inferred that these dips are related to an interplay between the FIDCO and the 3D GL theory.

However, the most significant finding is that in magnetic fields above 30 kOe, the b' axis is no longer a symmetry axis of $T_{co}(\phi)$ as it is under low fields, *see* Fig. 84. The appearance of the asymmetry in the rotation pattern is related to the field corresponding to the Pauli pair-breaking effect as shown on Fig. 84.

As seen on the rotation pattern, $T_{co}(\phi)$ is enhanced around X *at variance* with low fields where $T_{co}(\phi)$ exhibits a broad minimum around the b' axis. In addition this X axis shows a clear field dependence tendency as its deviation from the b' axis is reduced by 10° at 47.5 kOe.

The FFLO state can be realized when spin-singlet Cooper pairs are formed between Zeeman-split Fermi surfaces in high magnetic fields. As a result of the Zeeman splitting, the Fermi wave number for the up-spin electron $\mathbf{k_F}\uparrow$ and that for the down-spin electron $\mathbf{k_F}\downarrow$ are non centro-symmetrical as shown on Fig. 85 for Q1D superconductors.

Thus, when a Cooper pair is formed between $\mathbf{k_F}\uparrow$ and $\mathbf{k_F}\downarrow$ electrons, the pair acquires the non-zero center-of-mass momentum $\mathbf{q_{FFLO}} = \mathbf{k_F}\uparrow - \mathbf{k_F}\downarrow$. This momentum results in the spatial oscillation of the SC order parameter. Consequently, this non-zero center-of-mass momentum breaks the original translational symmetry.

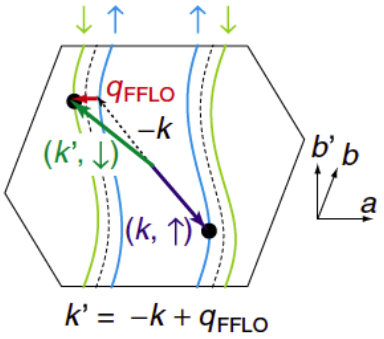

Figure 85. Pair formation in a Q1D superconductor under magnetic field. Partners in a Cooper pair are the black dots. Source: [302, Fig. 10 p. 9]. ©(2008) The Physical Society of Japan. All right reserved.

For Q1D systems, $\mathbf{q_{FFLO}}$ should be nearly parallel to the a axis, since the number of pairs can thus be maximized and the energy minimized if $\mathbf{q_{FFLO}}$ matches the nesting vector between the spin-up and spin-down Fermi surfaces, which is nearly parallel to the a axis, as schematically shown in Fig. 85 providing the highest T_c under magnetic field [314]. The evolution under magnetic field noticed in Fig. 84 might be related to the influence of the magnetic field on the Q1D surface given the tight connexion existing between $\mathbf{q_{FFLO}}$ and the warping of these surfaces.

The situation of a field parallel to the conducting axis ($H \parallel a$) may be somewhat similar to spin-ladders [316] where superconductivity was found experimentally to overcome the Pauli limit [317, 318] with the possibility of a FFLO state, as proposed by Roux [319].

Another support to the existence of a FFLO phase for $H \parallel b'$ is provided by the experimental data showing that the stability of the high field regime may be affected by impurities far more than the superconductivity of the low field regime as predicted by theories [313, 320]. While the critical field $H_{c2} \parallel b$ data reveal a clear up-turn going to low temperature in $(TMTSF)_2PF_6$ [296], the situation is more confused in $(TMTSF)_2ClO_4$. First, the distinct upturn of $H_{c2} \parallel b$ noticed in the first cool down of a sample is no longer observed in subsequent cool downs [287] and second, study of different $(TMTSF)_2ClO_4$ samples, Fig. 86, shows that the high-field phase may not be present in certain samples, suggesting that its stability is linked to sample purity [299].

The existence of the high field SC state is actually of significant importance for the theory of these superconductors, as it as been ascribed to the signature of the interplay between magnetism and d-wave superconductivity in these Q1D conductors under magnetic field [313, 321].

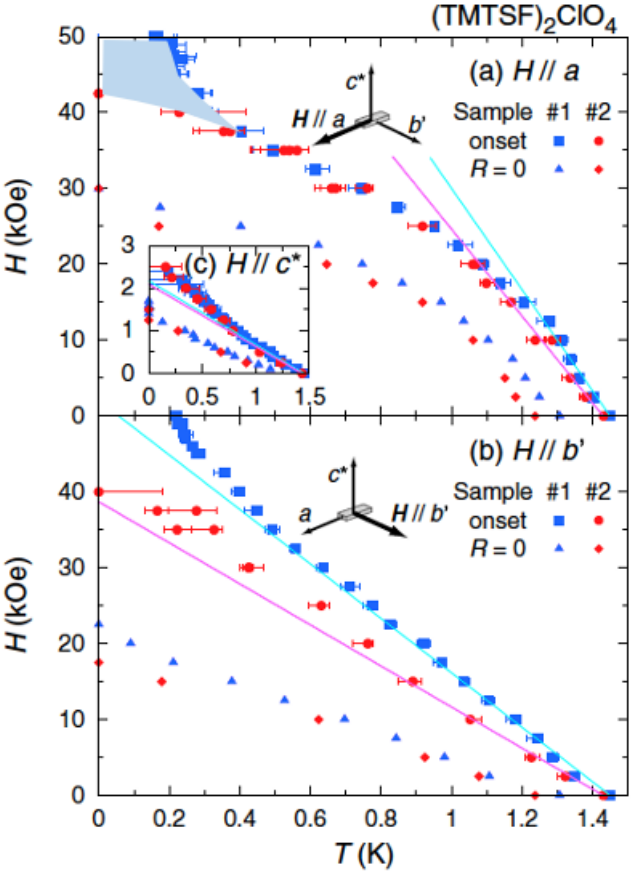

Figure 86. Critical fields H_{c2} from the onset of the resistive transition derived from two aligned $(TMTSF)_2ClO_4$ samples. The light blue shaded domain at low temperature and high fields illustrates the strong sensitivity of the FFLO state to impurities although T_c at H=0 is only weakly affected. Source: [299, Fig. 4 p. 5]. ©(2008) The Physical Society of Japan. All right reserved.

Thermodynamics performed under oriented fields in $(TMTSF)_2ClO_4$ is also of great interest in the context of possible FFLO phases. The recovery of the normal state density of states occurs at H_{c2}^{therm} around 2.5T (the Pauli limit) for $H \parallel a$ [290], *see* Fig. 80, i.e at a field much smaller than than the orbital critical field of about 7.7T. Consequently, there exists a broad SC phase at low temperature above H_{c2}^{therm} without any noticeable change for the density of states compared to the normal state in which transport exhibits a zero resistance. The nature of this state remains to be clarified. A fluctuating order parameter might be a possibility [313], as well as an inhomogeneous FFLO-like static order.

With the physics of the superconducting phase of $(TMTSF)_2ClO_4$ at high fields we are facing quite interesting questions; interplay between orbital pair-breaking effect, the Pauli pair-breaking effect, the dimensionality of the electronic system (FIDCO), and the possible emergence

of FFLO states and their response to impurity scatterings or to the tilt of the magnetic field away from the $a-b$ plane. Further investigations should be highly valuable using for instance in case of $(TMTSF)_2ClO_4$ the cooling rate to monitor the amount of non-magnetic scatterers.

4.4.4. *Response of superconductivity to non-magnetic defects*

A basic property of the s-wave superconductivity proposed in the BCS theory is the isotropic (k-independent) gapping on the Fermi surface. Hence, no pair breaking is expected from the scattering of electrons against spinless impurities [322], since such scatterings essentially just mix and average gaps at different k positions. Experimentally, this property has been verified in non-magnetic dilute alloys of s-wave superconductors and provided a strong support to the BCS model of conventional s-wave superconductors. However, the condition for an isotropic gap is no longer fulfilled for the case of non-s-wave pairing, in which the average of the gap $\Delta(\boldsymbol{k})$ over the Fermi surface vanishes due to sign changes in $\Delta(\boldsymbol{k})$, i.e. $\sum_{FS}\Delta(\boldsymbol{k})\sim 0$. Consequently, T_c for these superconductors should be strongly affected by any non-magnetic scattering, cancelling out positive and negative parts of the gap. Theories on effects of non-magnetic impurities on T_c in such superconductors have been deduced by generalizing conventional pair-breaking theory of Abrikosov and Gorkov (A-G) for magnetic impurities in s-wave superconductors [323].

Then the famous relation,

$$\ln\left(\frac{T_c^0}{T_c}\right)=\psi\left(\frac{1}{2}+\frac{\alpha T_c^0}{2\pi T_c}\right)-\psi\left(\frac{1}{2}\right), \tag{24}$$

is obtained [309,324], with $\psi(x)$ being the Digamma function and $\alpha=\hbar/2\,\tau k_B\,T_c^0$, the depairing parameter related to the elastic scattering time τ.

Experimentally, it has been found that this relation holds for non-s-wave superconductors such as Sr_2RuO_4 ($T_c=1.5$ K; most likely a p-wave spin-triplet superconductor) [325,326].

It is also the remarkable sensitivity of organic superconductivity to irradiation detected in the early years [327,328] that led Abrikosov to suggest the possibility of triplet pairing in these materials [329].

A more recent investigation of the influence of non magnetic defects on organic superconductivity has been conducted following a procedure which rules out the addition of possible magnetic impurities, which is the case for X-ray irradiated samples [330]. Attempts to synthesize non-stoichiometric compounds have not been successful for these organic salts. However, what turned out to be feasible is an iso-electronic anion solid solution keeping the charge transfer constant. One attempt has been to create non-magnetic disorder through the synthesis of solid solutions with centrosymetrical anions such as AsF_6^- and SbF_6^-. This attempt turned out to be unsuccessful as the effect of disorder happened to be very limited with only a minute effect on T_c [331]. Another scheme with which non-magnetic defects can be introduced in a controlled way for non-centro-symetrical anions in the $(TMTSF)_2X$ series is either by fast cooling preventing the complete ordering of the tetrahedral ClO_4^- anions or by introducing ReO_4^- anions to the ClO_4^- site by making the solid solution $(TMTSF)_2(ClO_4)_{(1-x)}(ReO_4)_x$. We will start with the study of the solids solutions $(TMTSF)_2(ClO_4)_{(1-x)}(ReO_4)_x$ and consider the effect of quenching in a subsequent paragraph.

As displayed on Fig. 87, superconductivity in the solid solution is suppressed and the reduction in T_c is clearly related to the residual resistivity namely, the enhancement of the elastic scattering in the normal state. The data on Fig. 87 show that the relation T_c versus ρ_0 follows Eq. (24) with a good accuracy using $T_c^0=1.23$ K.

At this stage, it is worth pointing out that the determination of the residual resistivity is not a trivial matter. Various procedures have been used in the literature. First, the resistivity displays an usual quadratic temperature dependence both above the anion ordering temperature T_{AO} =24 K

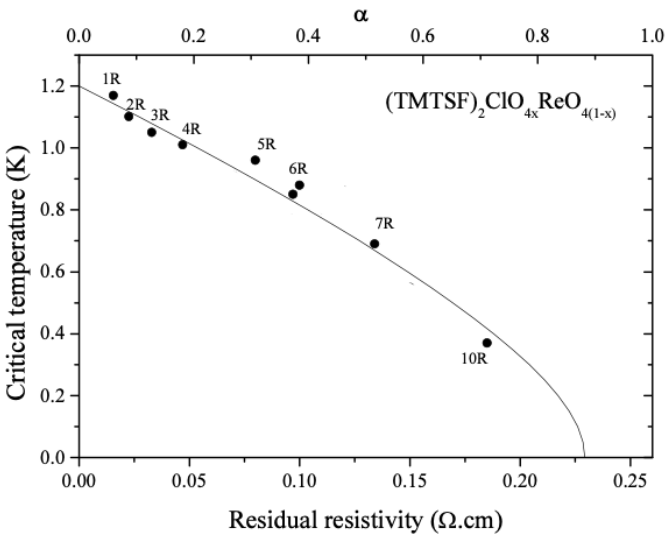

Figure 87. Phase diagram of $(TMTSF)_2(ClO_4)_{(1-x)}(ReO_4)_x$, governed by non magnetic dilute disorder. The data are obtained by newly analysing the temperature dependence of resistivity reported in Ref. [332] (*see* text). Data points with labels R refer to very slowly cooled samples in the R-state (the so-called relaxed state) with different ReO_4^- contents (% ReO_4^-).

and below down to approximately 10 K. Consequently, a first attempt to determine ρ_0 was to extrapolate $\rho(T)$ down to zero temperature the $T+T^2$ behaviour observed between T_{AO} and 10 K. It turned out that ρ_0 is rather ill defined with this procedure (*see* Ref. [332]). Second, another procedure was to use a linear extrapolation of the temperature dependence below 10 K down to T_c, leading to lower values of ρ_0 [333].

Furthermore, several recent re-analysis of the temperature dependence of the resistivity in the neighborhood of T_c in pure $(TMTSF)_2ClO_4$ [334] and in the alloy series [335] have emphasized the existence of two different regimes: a regime between 10 and 2 K where the single particle scattering is dominated by antiferromagnetic fluctuations leading in turn to a linear dependence, and another regime between 2 K and T_c where the downturn of the resistivity can be ascribed to a collective sliding of SDW waves in the vicinity of an antiferromagnetic order. This latter ordering is not accessible in $(TMTSF)_2ClO_4$ since it would require a negative hydrostatic pressure. However as shown by uniaxial elongation experiments along the b axis [275] decreasing the interchain coupling, such a SDW state can be recovered below 6 K. The temperature domain between 2 K and T_c will be more thoroughly presented in Sec. 4.5.

The procedure used to derive ρ_0 in Fig. 87 was a linear extrapolation to zero temperature of the linear regime between 2 and 10 K where the scattering is dominated by AF fluctuations (to be described in Sec. 4.5). This procedure should be rather accurate, in particular, in $(TMTSF)_2ClO_4$. Beware that it is the quadratic fitting procedure which has been used for the cooling rate dependence of T_c, *see* also below.

Notice that it has been checked that the additional scattering cannot be ascribed to some magnetic scattering with the electron paramagnetic resonance (EPR) technique, which shows no additional traces of localized spins in the solid solution. Thus, the data in Fig. 87 cannot be reconciled with the picture of a SC gap keeping a constant sign over the whole ($\pm k_F$) Fermi surface. They require a picture of pair breaking in a superconductor with an anisotropic gap symmetry.

It is interesting to compare the residual density of states predicted by theories with experimental data. Fig. 87 shows that the depairing parameter of the pristine sample amounts to about 6.25% the critical value for the suppression of superconductivity. Given the ratio $\Gamma/\Gamma_0 = 0.0625$ for the pristine sample where Γ is the scattering rate, the calculation of Sun and Maki [336] performed for the unitarity scattering limit leads in turn to a residual density of states $N(0) = 0.26N_0$ which is fairly close to the residual density of states derived from specific heat experiments and from the NMR data, [303] *see* Sec. 4.4.2.

4.4.5. *Cooling rate-controlled superconductivity*

A very peculiar property of the $(TMTSF)_2ClO_4$ superconductor is the possibility to control T_c without introducing any extrinsic impurities as achieved in the previous Section. This property made it possible to examine the mechanism of superconductivity in $(TMTSF)_2ClO_4$ and likely the same for all members of the $(TM)_2X$ series.

It has long been known that the ground state of $(TMTSF)_2ClO_4$ clearly depends on the rate at which the ClO_4 anion ordering transition is crossed. The significant feature of $(TMTSF)_2ClO_4$ is actually related to the non-centrosymmetric nature of the tetrahedral ClO_4 anion located on the inversion centers of the full structure. At high temperature, the thermal motion of the ClO_4 orientation makes it possible to preserve inversion symmetry on average since ClO_4 occupy randomly one or the other inversion-symmetry-related orientations. The structural disorder between two possible orientations no longer persists at low temperatures below $T_{AO} = 24$ K, because an entropy gain due to the reduction of degrees of freedom triggers the anion ordering below this temperature.

Diffuse X-ray work has shown that, while ClO_4 anions adopt a uniform orientation along a and c axes, they alternate along b [279]. Furthermore, the ordering of these anions involves a slow dynamics. Unless the compound is cooled slowly enough through the ordering transition, some anion disorder remains at low temperature ($T < 24$ K). The two extreme situations, namely the relaxed state (slowly cooling) and the quenched state (fast cooling $\approx dT/dt > 17$ K/mn) with SC and SDW ground states respectively, have been recognized from the beginning and are fairly well documented. However, only limited studies have been published for the intermediate cooling-rate regime, where superconductivity is moderately suppressed [285,288,332,337]. High-resolution X-ray investigations [338–340] have shown that samples in an intermediate cooling rate regime exhibit a peculiar anion ordering, in which domains with ordered anions of finite size are embedded in a disordered background. In addition for the regime up to 5 K/min, high-resolution X-ray-diffraction measurements have determined both the volume fraction of ordered anions and the average size of ordered domains leading for the relaxed state to more than 90% ClO_4 ordered becoming only 50% at 5 K/mn with domains of size $(150 \times 150 \times 235)$ nm^3 and $(30 \times 60 \times 50)$ nm^3 along (a-b-c) respectively [340].

The influence of the cooling rate on the stability of the SC phase of $(TMTSF)_2ClO_4$ has been recently revisited using transport along $c^\star$ and AC susceptibility measurements [292] with a very careful control of the cooling speed from 0.02K/mn to 18K/mn through the anion ordering transition. The importance of this study is the control of the elastic electron mean free path in otherwise identical samples.

The salient result is the finding of two regimes for the effect of the cooling rate as evidenced by a significant evolution of the elastic mean free path dependence on T_c, *see* Fig. 90. As far as the effects of scattering centers on SC are concerned, the fast-cooled states cannot be described by an average distance between disordered centers as it is the case for ClO_4^- -ReO_4^- alloys presented previously in Fig. 87, evolving smoothly as a function of the cooling speed, but instead as a state comprising a cooling-rate-dependent volume fraction of well-ordered domains with the rest of the volume occupied by disordered anions. There exists a crossover around 1-2 K/mn where

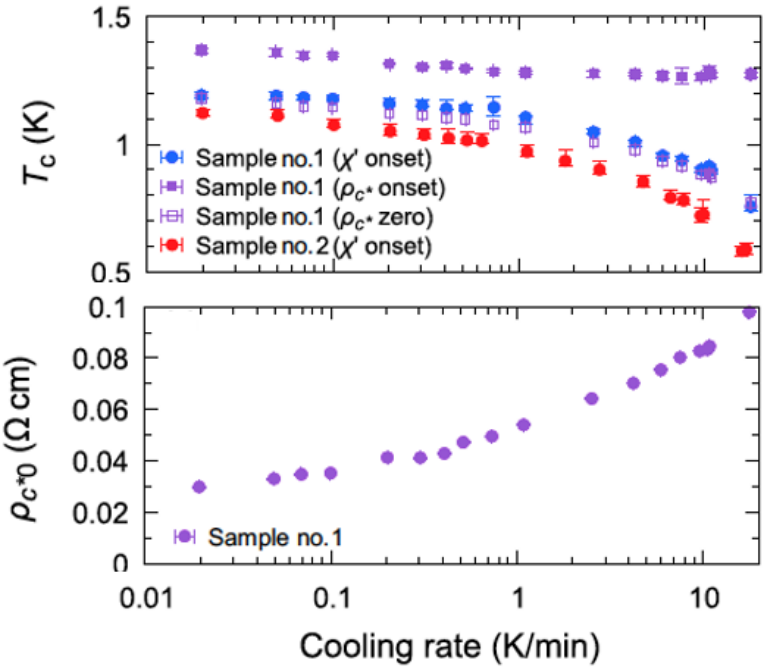

Figure 88. (Top) Cooling rate dependence of T_c in $(TMTSF)_2ClO_4$. Black dots are the onset of the resistive transition. Lower blue and red marks are the temperature for zero resistivity, onset of diamagnetic shielding and mid-transition for specific heat. (Bottom) Cooling-rate dependence of the residual resistivity $\rho_{c_{\star 0}}$ derived from the polynomial fitting procedure explained in the text. Sources: [292, Fig. 2bc p. 4].

below this cooling rate the electron mean free path is given by the size of well ClO_4^- ordered SC puddles and superconductivity propagating through the narrow disordered medium between puddles via a proximity effect [341, 342], while above 1 K/mn and up to 18 K/mn the system enters a regime of granular superconducting medium. In order to get the residual elastic mean free path following the procedure developed in Ref. [292] in which the residual resistivity is given by the zero temperature value of the second order polynomial fit for the normal state resistivity between 12 and 6 K.

As shown on Fig. 91, the fit of T_c data for the specific heat transition by the A-G theory extended to non-magnetic impurities in nodal superconductors [323] provides a very good agreement with the theory over the whole range of cooling rates. It is worth comparing mean free paths obtained from the A-G fit of the fast cooled data with the determination of the domain sizes by high resolution X-ray scattering [340]. These features provide additional supports in favour of a nodal d-wave superconducting coupling. The scattering rate Γ_0 of the slow cooled sample amounts to $\Gamma_c/5$ according to Fig. 91. Since $\Gamma_c = 0.88\ T_{c0}$ [343], a value of $\Gamma_0 = 3.4 \times 10^{10}$ s^{-1} (or $\tau_0 = 3 \times 10^{-11}$s) is derived for the residual electronic life time of a slowly-cooled pristine crystal. This would lead in turn to a mean free path of about 5400 nm, given $v_F = 1.8 \times 10^5$m/s [298], a value which is at least of the order of magnitude of ordered domains size for pristine crystals [340].

However, from the plot on Fig. 91 one cannot tell whether the scattering is in the limit of strong scattering (unitarity) [336] or weak scattering (Born approximation) [344], *see* also Ref. [345] for impurity-scattering effects in unconventional superconductors.

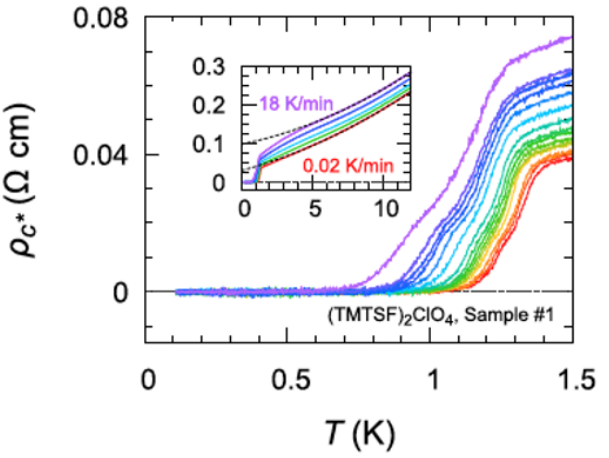

Figure 89. SC transition from $\rho_{c_{\star 0}}(T)$ after various cooling rates from 0.020 K/mn up to 18 K/mn. The inset presents $\rho_{c_\star}(T)$ on a broader temperature range for 0.020, 0.52, 2.5, 7.6, and 18 K/min. For the 0.020 and 18 K/min data, the results of the fitting performed using the procedure explained in the text are presented with broken curves. The down turn of the resistivity mentioned in Sec. 4.5.2 in $(TMTSF)_2ClO_4$ alloys and due to fluctuating SDW's is clearly observed for the run 18 K/mn. Source: [292, Fig. 1d p. 3]. ©American Physical Society and the authors. All rights reserved.

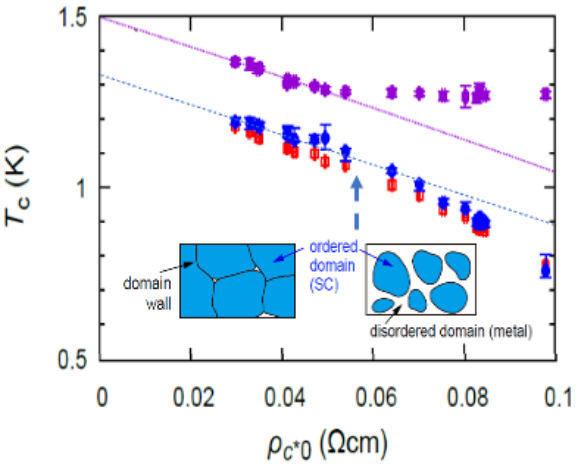

Figure 90. Cooling rate dependence of T_c in $(TMTSF)_2ClO_4$. Black dots are the onset of the resistive transition. Lower blue and red marks are the temperature for zero resistivity, onset of diamagnetic shielding and middle of specific heat transition. The dashed blue arrow shows the cross-over between homogeneous SC below ≈ 1K/mn (at $\rho_{co} = 0.055$ (Ω.cm) and granular SC above. Source: [292, Fig. 6 p. 8]. ©American Physical Society and the authors. All rights reserved.

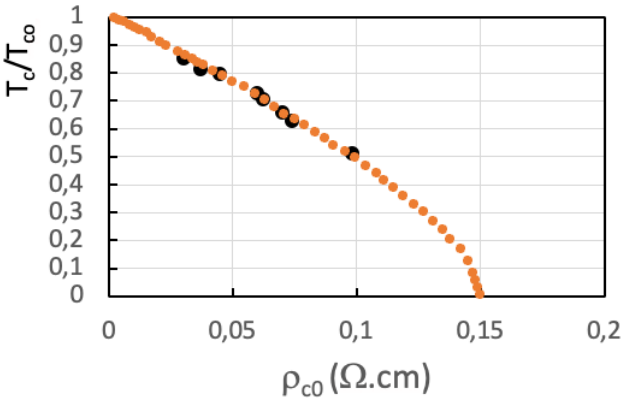

Figure 91. Dependence of the normalized T_c for the half-height C_v transition ($T_{c0} = 1.32$ K) versus residual resistivity displaying a very good agreement with the Abrikosov–Gorkov behaviour (yellow dots). Such a good agreement cannot tell the difference between weak and strong scattering limit, namely Born or unitarity limits. Actually, the strength of the electron scattering when the mean free path is governed by the size of the superconducting puddles may be different from what it is when only residual chemical impurities are at work. In order to have access to the nature of the scattering leading to a decrease of T_c in fast cooled samples, the relevant measurement is the evolution of the residual density of states as the mean free path of the electrons becomes controlled by the size of anion-ordered superconducting domains in fast cooled samples. This on-going experimental study will be the subject of a forthcoming publication.

To conclude on the role of non-magnetic impurities, we can anticipate that the influence of non-magnetic impurities on the SC phase implies the existence of positive as well as negative values for the SC order parameter on the Fermi surface. The singlet nature is implied from the NMR data as shown in Sec. 4.4.2 but NMR conclusions were still unable to discriminate between the two possible options namely, singlet-d or g [346].

The main questions still at hands now are to locate the d-wave nodes on the Fermi surface and be able to determine the strength of the electron scattering in the superconducting state for rapidely cooled samples affecting the ordering of ClO_4 anions below 24 K. As far as the latter question is concerned, a recent investigation of the superconducting phase of $(TMTSF)_2ClO_4$ under various cooling rates, has inferred that when the size of the anion-ordered domains is governing the electron mean free path, the residual density of states at zero temperature stays constant at a finite value of about 25% its normal state value, although T_c can be suppressed down to $T_c/T_{c0} = 0.5$. This residual DOS is actually due to preexisting chemical impurities in the pristine sample. This experiment suggests that the borders of anion-ordered domains act as weak scatterers for the electrons (Born limit scattering) [343] with a limited consequence on the residual density of states unlike preexisting dilute chemical defects which suppress T_c and also strongly increase the residual density of states (unitarity limit scattering) [336]. It would be very interesting to look at the residual DOS of slowly cooled alloyed samples since the behaviour which is displayed on Fig. 87 is unable to provide information regarding the strength of the scattering.

4.4.6. *$(TMTSF)_2ClO_4$, low field nodal and high field modulated superconductor*

As shown in the previous section, nodal superconductivity with spin singlet pairing is suspected from the NMR results but these experiments were still unable to locate the nodes on the Fermi surface.

To reveal more precisely the gap structures and the location of nodes, one of the common technique is to look at the field-angle-dependent quasiparticle excitations through either specific heat or thermal conductivity measurements while rotating the magnetic field within a certain plane. These studies have been developed at the turn of 2000's in relation with quasi 2D heavy fermions [347, 348], quasi-2D organic [349], borocarbide [350]and ruthenate [351] superconductors.

These experiments have made an extensive use of a property of type II superconductors with gap nodes where supercurrents surrounding vortices induce field-induced excitations of the quasi particles. Volovik made the remark that these quasi-particles acquire in turn an energy shift δE (usually called Doppler shift) which is proportional to the scalar product of the Fermi velocity $\mathbf{v_F}$ at the node and the superfluid velocity $\mathbf{v_s}$.

Such field-induced excitations are now called the Volovik effect, [352, 353]. These quasiparticle excitations become therefore field-direction dependent [354] since $\mathbf{v_s}$ is perpendicular to the applied field. Whenever regions on the Fermi surface exist where quasi particle excitations are larger than the superconducting gap, they will contribute to the density of states.

Thus, if one rotates the magnetic field within a certain plane, it is expected that the quasiparticle density of states will oscillate as a function of the field angle. This effect becomes important at such angles where the local energy gap becomes smaller than the Doppler shift, a situtation which can be achieved in the case of superconductors with nodes [354].

Hence, the density of states in the vortex state becomes angular-dependent, as found for instance in the compound Sr_2Ru0_4, where the rotation pattern displays a fourfold symmetry. Because the superfluid velocity $\mathbf{v_s}(\mathbf{r})$ is perpendicular to $\vec{H}$, when the field becomes parallel to $\mathbf{v_F}(\mathbf{k_n})$ at a node $\mathbf{k_n}$ a minimum contribution of the QP's to the specific heat can in turn be expected in such conditions, *see* Fig. 92.

For 2D conductors, $\mathbf{v_F}(\mathbf{k})$ is usually collinear with $\mathbf{k}$. Therefore, the angular resolved specific heat (or thermal conductivity) enables us to reveal the positions of the gap nodes according to the angles corresponding to minima of specific heat (thermal conductivity), as depicted in Fig. 92. However the situation is *at variance* with the case of a Q1D Fermi surface. More specifically, $\mathbf{v_F}(\mathbf{k})$, which is parallel to the gradient of the quasiparticle energy $\nabla\epsilon(\mathbf{k})$ in the reciprocal space and consequently perpendicular to the Fermi surface, is not always parallel to $\mathbf{k_F}$. There, anomalies in the rotation pattern of C_v/T are expected at angles ϕ_n between $\vec{H}$ and $\mathbf{v_F}(\mathbf{k_n})$, where $\mathbf{k_n}$corresponds to a nodal position on the Fermi surface, *see* Fig. 93.

For such a situation the interpretation of the angular dependence of the specific heat requires a model for the Fermi surface and also for the superconducting gap function. This research has been performed very successfully by the Kyoto group over the past fifteen years and reported in several publications [290, 355].

The extensive study of the angular dependence of the specific heat in the low temperature and low field domain of the superconducting phase of $(TMTSF)_2ClO_4$, rotating the field in the basal plane $a-b'$. Detailed experimental results have been published in several articles [290, 355] and reviewed in [302].

We will not present here on Fig. 94 the full treatment but only the most relevant results to characterize the nature of the superconducting coupling of these Q1D superconductors. As far as Q1D superconductors are concerned, the angular dependence of C_v/T can give only access to the direction of the Fermi velocity at nodes. To reveal the gap structure in k-space, one should

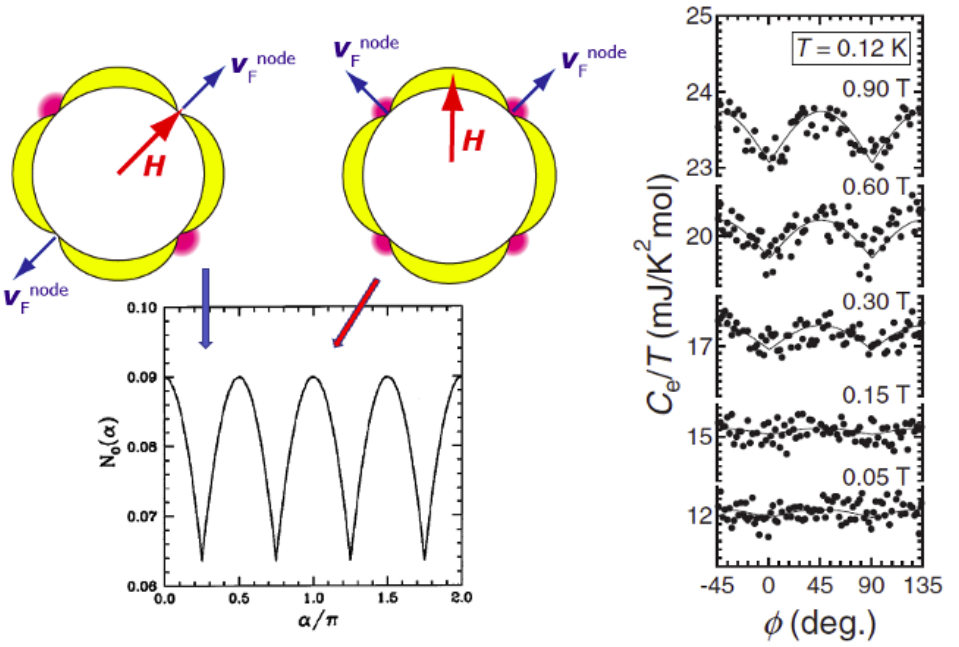

Figure 92. Angular dependence under magnetic field of the electronic specific heat in a 2D superconductor with a tetragonal symmetry.(Left) Theory for the gap function showing minima (maxima) of the density of states for $\vec{H}$ parallel and (non parallel) to $\mathbf{v}_\mathbf{F}^\mathbf{node}$ respectively. (Right) Experimental data for Sr_2Ru0_4 with the field rotated in the basal plane, Adapted from [354, Figs. 1, 2 p. 9024-9025] and [351, Fig. 3 left p. 2]. ©American Physical Society and the authors. All rights reserved.

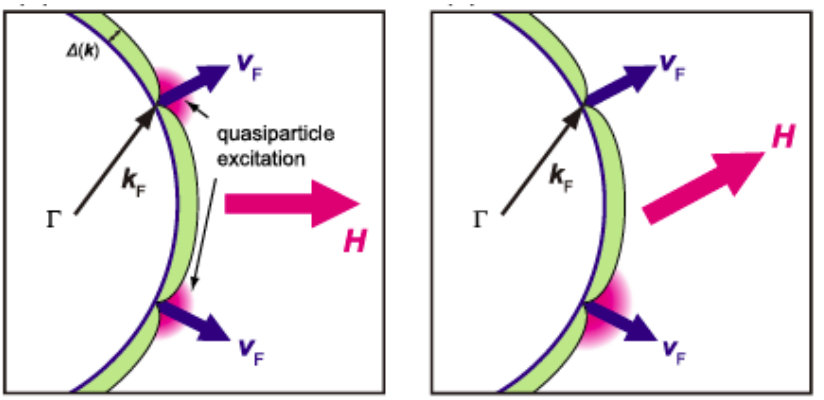

Figure 93. A schematic representation of 1D Fermi surface showing the quasi particle excitations due to the Doppler shift shown in pink. Whenever the field is parallel to $\mathbf{v}_\mathbf{F}$ at a node (right), the contribution of the excitations to the density of states is reduced. Source: [302, Fig. 9bc p. 365].

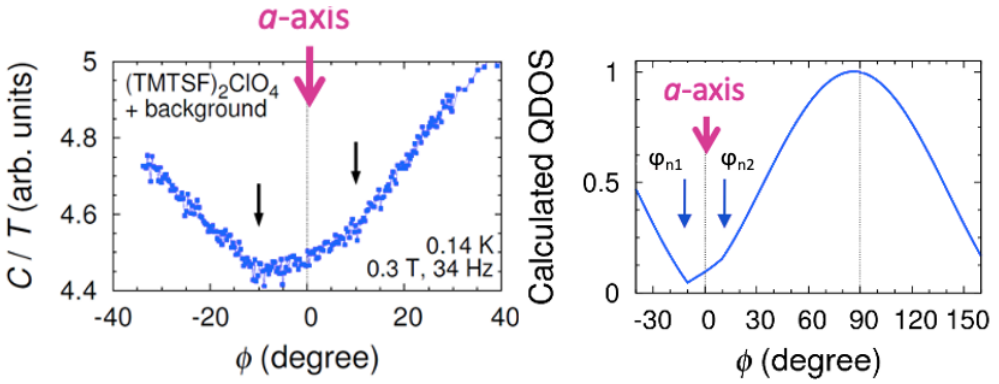

Figure 94. (Left) Observed in-plane field-angle dependence of the heat capacity of $(TMTSF)_2ClO_4$. What is remarkable is (i) the absence of symmetry of C_v/T with respect to inversion around the a axis and (ii) the presence of two kinks in the rotation pattern at $\phi = \pm\ 10°$.(Right) Simulated results by calculating the density of states based on a simple Doppler-shift model with nodes at $\phi = \pm\ 10°$. Sources: [290, Fig. 3a p. 3] (left), [290, Fig. 2g p. 2] (right). ©American Physical Society and the authors. All rights reserved.

know the band structure of the material. For these reasons, the gap-structure investigation of Q1D superconductors by the field-angle-induced quasiparticle excitation method had not been explored.

A simple model has been used to understand the data of angular-resolved C_v of $(TMTSF)_2ClO_4$ of Fig. 94. The rotation pattern has been modeled by,

$$N(\phi) \propto \left(\Gamma^2 \sin^2\phi + \cos^2\phi\right)^{1/4} \sqrt{\frac{H}{H_{c2}(0)}} \times \sum_{n,nodes} A_n \left|\sin(\phi - \phi_n)\right| \tag{25}$$

where the first factor reproduces the anisotropic character of the critical field in the basal plane, while the weighted space summation over angles accounts for the existence of nodes at angles ϕ_n between the magnetic field and the special $\mathbf{k_n}$ points where the Fermi velocity is parallel to $\vec{H}$.

The experimental observation of a rotation pattern at low field and low temperature which is non-symmetric with respect to the inversion of C_v around a and the existence of kinks for C_v/T at $\pm\ 10°$ in Fig. 94 have been taken as the signature of line nodes along the $c^\star$ direction [290]. In Eq. (25), Γ takes into account the in-plane anisotropy of the upper critical field H_{c2} whereas the coefficients A_n represent the contribution of every node to the field-angle dependent specific heat. Because of the triclinicity of the $(TMTSF)_2ClO_4$ structure, A_n depends on the details of the band structure and of the SC gap structure near the gap nodes. Regarding the overall anisotropy of the specific heat, a good fit of the data on Fig. 94 is obtained with the H_{c2} anisotropy ratio $\Gamma = 3.5$ which compares favourably with a ratio of 5 announced in Ref. [291]. Furthermore, the A_n parameters responsible for the $N(\phi)$ asymmetry around the a axis are such that $A_{n1}/A_{n2} = 3$ on Fig. 94.

In order to conclude about the nodal nature of the superconducting gap, a comparison with a model calculation turned out to be indispensable [357]. The observation of nodes at $\phi_{ni} = \pm 10°$ and the asymmetry around the a axis are strong constraints on the theory and consequently allow to discriminate between several possibilities of nodal superconductivity [355]. The net result of this confrontation between experimental results and theory [357] is that among the many possible configurations of the gap, the most plausible is the one which locates the nodes of a d-wave pairing at $\mathbf{k_y} \sim \pm\mathbf{0.25b}^\star$ as shown on Fig. 94 at the angles $\pm 10°$. Two other nodes are

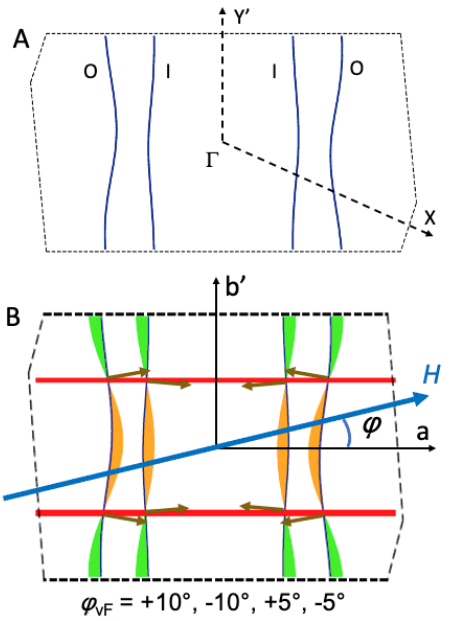

Figure 95. (A) Doubling of the $(TMTSF)_2ClO_4$ Fermi surface due to the anion-ordering, according to band structure calculations. The anion gap for this figure amounts to Δ = 100 meV. Source: [356, Fig. 8 p. 361]. ©Springer Nature. All rights reserved. (B) The arrows indicate the k points where the magnetic field is parallel to $\mathbf{v_F}(\mathbf{k})$ leading to particular angles ϕ at ± 10 and 5 degrees away from the a axis which are located on the outer surfaces. Different colors indicate positive and negative signs for the superconducting gap function. We thank Shingo Yonezawa for communicating this figure.

also expected at $\pm 5°$ but they contribute less to the rotation pattern of the specific heat [355] and only a much improved sensitivity could make their detection possible.

4.5. *The conducting state above T_c: antiferromagnetic fluctuations and their relation to transport and superconducting properties*

4.5.1. *Precursor regime from NMR data*

Interestingly, the metallic phase of $(TMTSF)_2X$ in the 3D coherent hopping regime when pressure is located in the neighborhood of the critical pressure P_c, typically $(TMTSF)_2PF_6$ around 8 kbar or $(TMTSF)_2ClO_4$ under ambient pressure or slightly higher behave in a way far from what is expected for a Fermi liquid. This behavior indicates the dominance of quantum critical fluctuations emerging from the onset of superconductivity at the brink of antiferromagnetism near P_c. Moreover, the close relation between the non-Fermi-liquid behavior and superconductivity has also been supported by recent theoretical developments as described shortly below.

The existence of antiferromagnetic fluctuations below about 25 K have been discovered originally by the NMR measurements of $1/T_1$ [252, 358]. Its behaviour is such that the temperature dependent Korringa law, $1/T_1T \propto \chi^2(q = 0, T)$, is well obeyed at high temperatures [240, 241], say, above 25 K, but at the low-temperature its deviates strongly from the standard relaxation in paramagnetic metals.

As shown in Figs. 96 and 97 an additional contribution to the relaxation rate emerges on top of the usual Korringa relaxation.

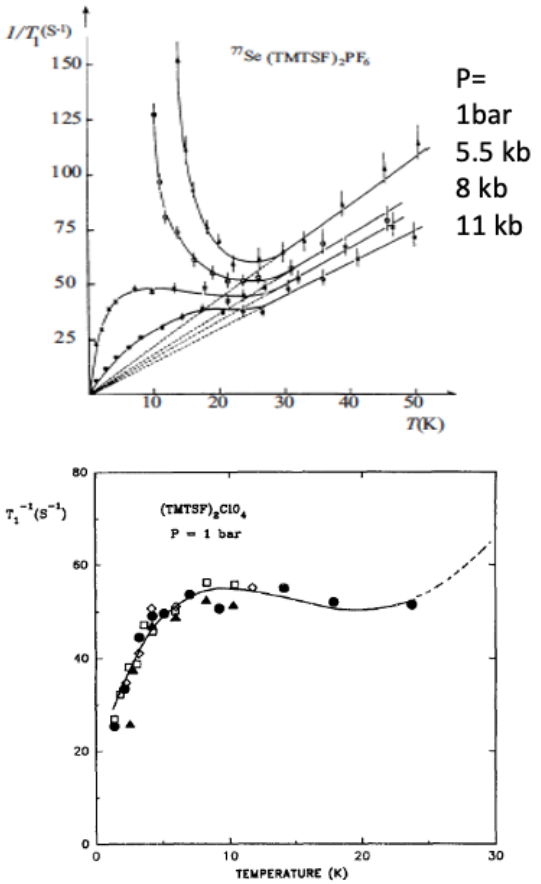

Figure 96. ^{77}Se$(1/T_1)$ versus T in $(TMTSF)_2PF_6$ at 1 bar and 5.5 kbar (ground state SDW) 8 and 11 kbar (ground state SC). The lower part shows a similar behaviour for $(TMTSF)_2ClO_4$ at ambient pressure showing how AF fluctuations are visible up to about 25 K. Sources: [252, Fig. 1 p. 278] (top), [241, Fig. 11 p. 184] (bottom).

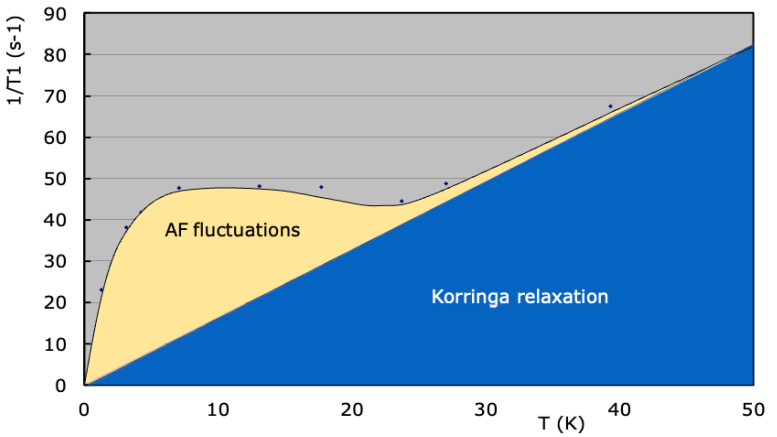

Figure 97. The two different contributions to the spin lattice relaxation from the data on $(TMTSF)_2PF_6$ under 8 kbar [241].

This additional contribution rising at low temperatures, *see* Fig. 97, has been attributed to the onset of antiferromagnetic fluctuations in the vicinity of P_c [259, 359]. In the lower-temperature regime, the relaxation rate follows a law such that $T_1T = C(T+\theta)$, as shown in Fig. 98. This is the Curie–Weiss behavior for the relaxation which is to be observed in a 2D fluctuating antiferromagnet [303, 360–363]. Similar behavior is also found in a ^{13}C NMR study [364]. The positive Curie–Weiss temperature θ, which provides the energy scale of the fluctuations, becomes zero when pressure is equal to P_c (the quantum critical conditions). When θ becomes large comparable to T, the standard relaxation mechanism is expected to recover down to low temperatures, in agreement with the observation at very high pressures [241].

These fluctuations manifest themselves also as an anomalous (non Fermi liquid) behaviour in transport at low temperature. At $P = P_c$, the inelastic scattering in transport reveals at once a strong linear term at low temperatures, most clearly seen in a log-log plot of the resistivity versus T, Fig. 99. This strongly linear behaviour, more recently dubbed as a strange metal or Planckian dissipative behavior in other unconventional superconductors, evolves to a quadratic behavior in the high-temperature regime. As pressure is increased away from P_c, the resistivity exhibits a general tendency to become quadratic at all temperatures, (*see* Fig. 99). The existence of a linear temperature dependence of the resistivity is *at variance* with the T^2 dependence expected from the ordinary electron-electron scattering in a conventional Fermi liquid, indicating that the dominant scattering would involve spin fluctuations seen by NMR in the same temperature range.

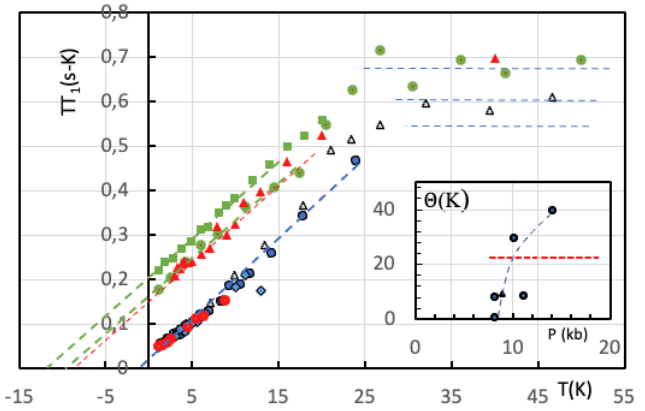

Figure 98. Temperature dependence of the nuclear relaxation time multiplied by temperature versus temperature according to the data of Ref. [252]. A Korringa regime, T_1T= const is observed down to 25 K. The 2D AF regime is observed below 15 K and the small Curie–Weiss temperature of the 9 kbar run is the signature of the contribution of quantum critical fluctuations to the nuclear relaxation. The Curie–Weiss temperature becomes zero at the QCP (around 8 kbar for the present pressure scale). The dashed line in the inset sets the upper limit for the 2D AF regime. This figure is an other presentation for the data on Fig. 97.

Notice that an early study [177] on $(TMTSF)_2PF_6$ also claimed a non-Fermi-liquid temperature dependence such as shown on Fig. 99. However, in the 1980's the research on organic superconductors has been over-influenced by the observation of a downward curvature of $\rho_a(T)$ close to T_c as shown on Fig. 51. Moreover, the theory in these years was very much influenced by the Landau–Ginzburg models of low-dimensional superconductors suggesting the possibility of non-Fermi-liquid behaviour with superconducting fluctuations at temperatures well above the three-dimensional order [205].

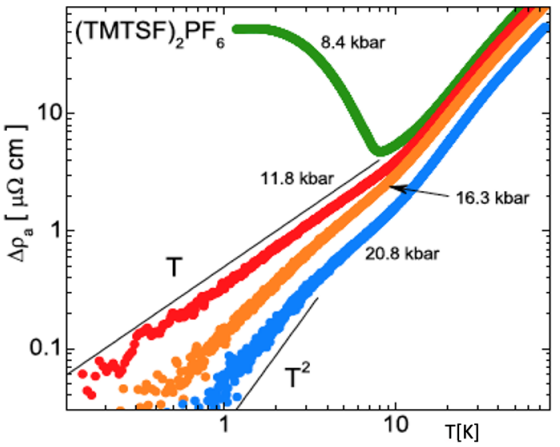

Figure 99. Inelastic part $\Delta\rho_a(T) = \rho_a(T) - \rho_0$ of the normal-state a-axis electrical resistivity of $(TMTSF)_2PF_6$ at 8.4, 11.8, 16.3, and 20.8 kbar. The lines represent $\Delta\rho(T) \propto T$ and $\Delta\rho(T) \propto T^2$. Notice that for the 8.4 kbar run a sharp transition to the zero resistance state (not shown on the figure) is observed around 0.9 K. Source: [365, Fig. 4 (Top) p. 3].

It is the extensive reinvestigation of $(TMTSF)_2PF_6$ and $(TMTSF)_2ClO_4$ under pressure performed in an experimental cooperation between Sherbrooke and Orsay from 2009 which allowed to eliminate the interpretation of the low temperature transport in terms of paraconductivity of superconducting origin with the reservation as we will see below that some paraconducting contribution is present in the very vicinity of the superconducting transition, although from the different – SDW – origin.

In the previous paragraph, we mentioned the non-Fermi-liquid behaviour which is manifested by the linear component of the $\rho(T)$ resistivity measured along the a axis. However, comparing resistivity data of the Q1D superconductors $(TMTSF)_2PF_6$ and $(TMTSF)_2ClO_4$ along the least conducting c-axis and along the high conductivity a-axis as a function of temperature and pressure, a low temperature 3D coherent regime of the generic $(TM)_2X$ phase diagram is observed in which a unique scattering time governs the transport along both directions of these anisotropic conductors [366].

In this low temperature regime, both materials exhibit for ρ_c an inelastic temperature dependence $\rho_c(T) \sim AT + BT^2$. The T-linear ρ_c was also found to correlate with T_c in close analogy with the ρ_a data displayed on Fig. 100.

4.5.2. *Precursor regime from DC transport data*

The data for $\rho(T)$ in $(TMTSF)_2X$ reveal a particular sublinear behaviour observed up to about two of three time T_c when the pressure is located in the vicinity of the critical pressure suppressing the insulating SDW phase, *see* Fig. 101, such a behaviour being particularly visible on the ρ_c component.

It is instructive to analyze the sub-linear temperature regime in the vicinity of T_c in terms of an additional conducting contribution, $\Delta\sigma$, as performed on Fig. 101 for $(TMTSF)_2PF_6$ under 10 kbar. Then $\Delta\sigma$ is derived from the resistivity by,

$$\Delta\sigma = \frac{\rho_n - \rho_{ex}}{\rho_n \rho_{ex}} \tag{26}$$

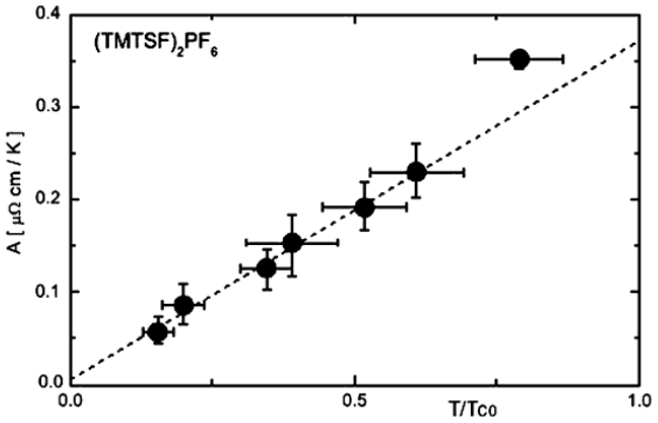

Figure 100. Coefficient A of linear resistivity as a function of normalized T_c (the maximum $T_{co} = 1.23$ K occurs in the SDW/SC coexistence regime) for $(TMTSF)_2PF_6$, from a second order polynomial fit over the range $0.1 - 4.0$ K to all resistivity curves at different pressure runs displayed on Fig. 99 between 11.8 and 20.8 kbar. The vertical error bars show the variation of A when the upper limit of the fit is changed by 1.0 K. T_c is defined as the midpoint of the transition and the error bars come from the 10% and 90% points. The dashed line is a linear fit to all the data points except that at $T_c = 0.87$ K. Source: [365, Fig. 5 (Top) p. 3]. ©American Physical Society and the authors. All rights reserved.

where ρ_{ex} is the measured resistivity while ρ_n is the behaviour of resistivity derived from the fit to a polynomial law of the measured transport to a polynomial law between 6 and 12 K.

This figure reveals that the onset of superconductivity can be characterized by two regimes, first the SC transition *per se* with a width in temperature of about $\Delta t \approx 0.1 - 0.2$ K and second, a much broader temperature regime above T_c in which the sublinear resistivity is observed.

The striking feature of Fig. 101 is the kink marking a cross over between the SC transition regime and the precursor regime where the resistivity is sublinear. For the vicinity of the SC transition the plot such as $(\Delta\sigma)^{-2} = \alpha\epsilon, (\epsilon = \frac{T-T_c}{T_c})$, could be related to a 3D Azlamazov–Larkin regime [205, 367] for 3D superconducting fluctuations with $T_c = 1.06$ K. Although we may have some reservation about the actual existence of this AL regime, T_c of organics are known to be crucially affected by crystal defects.Therefore, the apparent AL law followed by the excess conductivity on the figure should be taken with a grain of salt as possibly not related to any sign of intrinsic paraconductivity. A support for this interpretation is provided by the extensive investigation undertaken in $(TMTSF)_2ClO_4$ controlling the amount of ClO_4^- anions ordering the broad temperature regime may reveal a different kind of contribution, namely a fluctuating AF contribution provided by the SDW channel [368].

Such a contribution extending over a broad temperature regime has also been observed in $(TMTSF)_2ClO_4$ [292]. The collective magnetic channel can act in parallel with the single particle transport and leads to a experimentally measured resistivity given by, $1/\rho_{ex} = \sigma_n + \Delta\sigma_{coll}$, where the collective contribution to the conductivity $\Delta\sigma_{coll}$ according to Eq. (26) displayed on Fig. 102.

We can estimate the SDW paraconductive contribution using the value of $\Delta\sigma_{coll}$ at $\epsilon = 0.2$ ($T = 1.27$ K) *see* Fig. 101 leading in turn to $\Delta\sigma_{coll} \approx 4$ or $12.5(\Omega.cm)^{-1}$ for the linear or quadratic single particle contribution respectively [335].

The compound $(TMTSF)_2ClO_4$ is quite interesting since the collective contribution is not only easily visible but it also can be controlled different ways, either through the cooling rate dependence of the elastic free path or by the addition of local impurities in alloys.

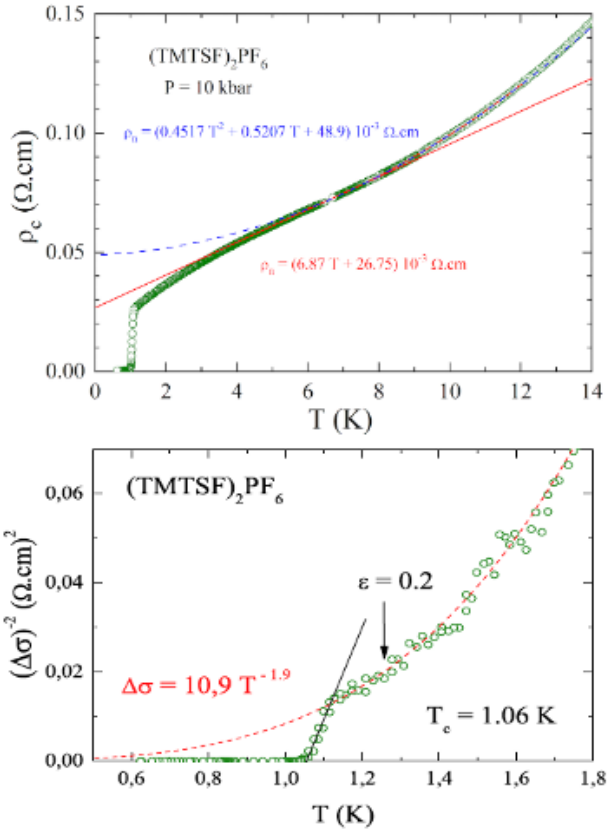

Figure 101. (Top) Temperature dependence of ρ_c for $(TMTSF)_2PF_6$ at a pressure of 10 kbar. The dotted blue line is the second order polynomial fit between 6 and 12 K, while the continuous red line is a linear fit between 4 and 8 K. These fits are supposed to be related to the single particle scattering. (Bottom) Plot of the temperature dependence of the additional conducting contribution for $(TMTSF)_2PF_6$ as $(\Delta\sigma)^{-2}$ versus T using the linear fit for the single particle contribution. The dotted line is the power law fit of the collective paraconduction after suppression of superconductivity under a magnetic field of 0.0875T. It is suggestive of a contribution diverging like $1/T^2$ at very low temperature. Source: [335, Fig. 1ab p. 2].

The study of transport properties under various cooling conditions [292] has revealed a very strong down turn of the resistivity under fast-cooling as already displayed in the inset of Fig. 89. Interestingly, the SDW paraconductive contribution is easily visible when the sample is mostly anion-disordered, i.e. cooling rate of 18 K/mn, *see* Fig. 89 because of the large value of the normal state resistivity which enhances the contrast of resistivity. When the paraconductivity is extracted according to the procedure of Eq. (26) a power law divergence is observed, Fig. 103 with an exponent 1.5-2 similar to what has been obtained with $(TMTSF)_2PF_6$.

Although the incommensurate character allowing free sliding of the SDW is established by the observation of a double-horn shape of the ^{13}C-NMR spectrum and the shape of the ^1H resonance line in $(TMTSF)_2PF_6$ [369], this excess of conduction can still be severely suppressed when the density of defects is increased. It is the situation which is encountered in ClO_4^--ReO_4^- alloys [335] where ReO_4^- anions play the role of active pinning centers, see Fig. 104.

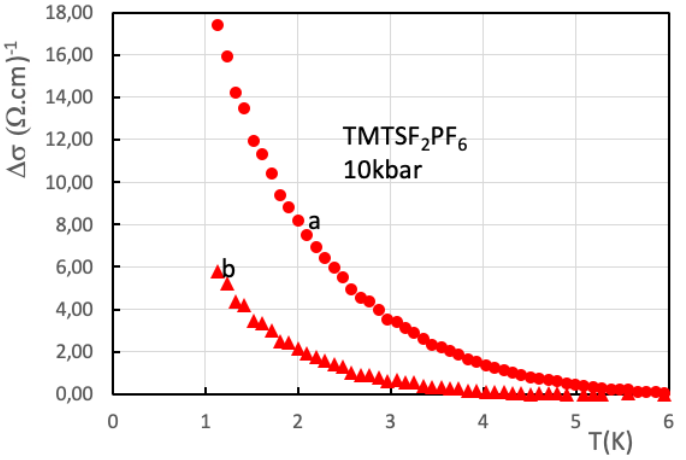

Figure 102. Derivation of the fluctuating SDW collective conduction in $(TMTSF)_2PF_6$ under 10 kbar according to two different hypothesis for the single particle contribution, quadratic plot (a), linear plot (b). It is difficult to say which of the two hypotheses is the best, but given the predominance of the linear term in the single particle resistivity of $(TMTSF)_2PF_6$, *see* Fig. 99 and Ref. [335], case (b) leading to a residual resistivity quite close to what is obtained in $(TMTSF)_2ClO_4$ (*vide infra*) may be more appropriate. We thank P. Auban for the communication of the raw data of $(TMTSF)_2PF_6$.

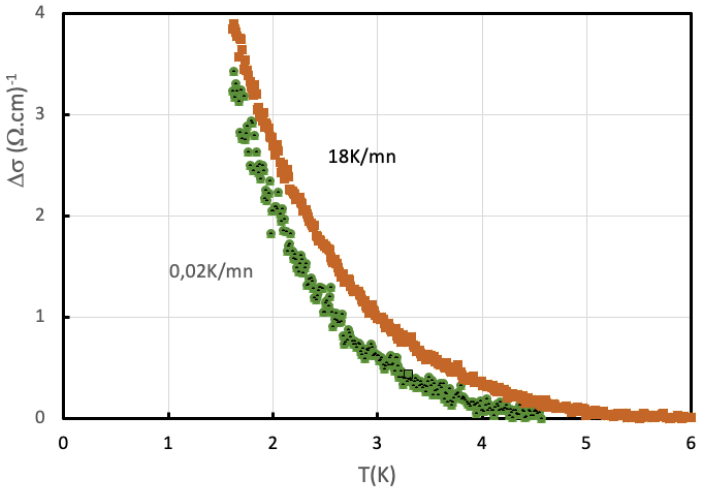

Figure 103. SDW paraconductive contribution to the conduction of $(TMTSF)_2ClO_4$ cooled at 18 K/mn and 0.02 K/mn extracted from the original data of resistivity displayed on Fig. 89. We thank S. Yonezawa for communicating the full data sheets. The paraconductive contribution is quite similar for both cooling rates. Notice the order of magnitude which is also similar to what is observed in $(TMTSF)_2PF_6$ under 10 kbar in the same temperature range, *see* Fig. 101. This paraconductivity follows a power law $T^{-\alpha}$ with $T_c = 0$ in this narrow temperature range and an exponent α in-between 3/2 and 2.

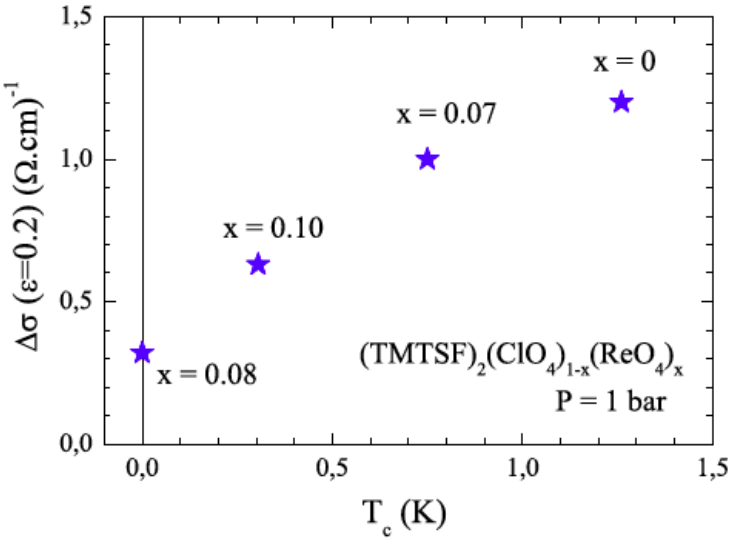

Figure 104. Paraconductive contribution characterised by $\Delta\sigma$ at $1.2T_c$ in the precursor regime, *vs.* T_c in the alloy series of ClO_4^--ReO_4^- alloys at 1 bar. For the sample not showing any finite T_c, the fluctuation contribution has been derived from a linear extrapolation of $\Delta\sigma$ to 0 K. Source: [335, Fig. 4 p. 4].

Contribution between $(TMTSF)_2PF_6$ and $(TMTSF)_2ClO_4$. When the mean distance between pinning centers becomes smaller than the SDW coherence length, the impurity pinning suppresses $\Delta\sigma$ heavily [86].

Data for the SDW coherence length support this interpretation as the zero-temperature longitudinal length ξ_{oa} is of order 32nm in $(TMTSF)_2PF_6$ [370]. Consequently, it makes sense that the SDW can be strongly pinned by defects when the mean distance between pinning centers, ($\approx$ 7.3nm at 10% ReO_4^- doping) is four times smaller than the coherence length leading in turn to a decrease of the fluctuation conduction independent of the current direction.

Given the size of the collective contribution, the sublinear behaviour for the resistivity requires a single particle conductivity small as compared to the collective part. This is actually the case for the *c*-axis component. Regarding the longitudinal component, the excess conduction should be more difficult to observe since the normal resistivity along this axis is several orders of magnitude smaller than along ρ_c. The first data for superconductivity in $(TMTSF)_2PF_6$ shown on Fig. 51 revealed a large temperature dependence of the resistivity in the helium temperature range which turned out to be confirmed by subsequent investigations but the claim of a downward curvature below 2 K should be taken with caution since the resistivity was supposedly measured along the *a*-axis.

4.5.3. *A brief incursion into theory*

To summarize, the investigation of both transport and superconductivity under pressure in $(TMTSF)_2PF_6$ has established a tight correlation between the amplitude of the linear temperature dependence of the resistivity and the value of T_c, as displayed in Fig. 100. This is very suggestive of a common origin for the inelastic scattering of the metallic phase and pairing in the SC phase $(TMTSF)_2PF_6$ both rooted in the low frequency antiferromagnetic fluctuations, as detected by NMR experiments [241,361,363,371] which we intend to summarize very briefly in the following.

Such a correlation is not limited to 1D organics. It has also been observed in the pnictides $Ba(Fe_{1-x}Co_x)_2As_2$ [365] and electron-doped cuprates with similar phase diagrams [372,373] where a detailed temperature dependence of the resistivity and the correlation with T_c strongly suggest that antiferromagnetic fluctuations play also a fundamental role in pnictide superconductors and electron-doped cuprates, although their temperature scales T_{SDW} and T_c is twenty times higher.

Within the framework of a weak-coupling limit, the problem of the interplay between antiferromagnetism and superconductivity in the Bechgaard salts has been theoretically worked out using the renormalization group (RG) approach [363,374,375] as summarized very briefly below.

The theory developed extensively by the Sherbrooke's school over several decades takes into account a two dimensional situation.

The RG integration of high-energy electronic degrees of freedom was carried out down to the Fermi level, and leads to a renormalization of the couplings at the temperature T. The RG flow superposes the $2k_F$ electron-hole (density wave) and the electron-electron Cooper pairing many-body processes, which become entangled and interfere quantum mechanically at every order of perturbation. As a function of pressure which is represented by the parameter t_b' i.e. the antinesting interchain coupling in a 2D tight binding spectrum

$$E(k) = v_F(|k| - k_F) - 2t_b \cos k_b - 2t_b' \cos 2k_b, \tag{27}$$

a singularity in the course of renormalization for the scattering amplitudes signals an instability of the metallic state toward the formation of an ordered state at some characteristic temperature scale.

For typical input bare interactions and band parameters, the calculations show that at low t_b' (small pressure) nesting is still sufficiently good to induce a SDW instability in the temperature range of experimentally observed $T_{SDW} \approx$ 10-20 K as displayed, in Fig. 105.

When the antinesting parameter approaches the threshold coupling $t_b'^{\star}$ from below ($t_b'^{\star}$ ~25.4 K using the above parameters), T_{SDW} sharply decreases as a result of an interference between the Cooper and the Peierls channel (or SDW correlations). This situation leads in turn to an attractive pairing in the SC d-wave (SCd) channel. This gives rise to an instability of the normal state against SCd order at the temperature T_c with pairing coming from the exchange of antiferromagnetic spin fluctuations between carriers of neighboring chains [227,244]. Such a pairing model actually supports the conjecture of interchain pairing made by V. J. Emery in 1983 and 1986 [278,376] and taken up by others [377,378], a mechanism for electrons to avoid the Coulomb repulsion.

The calculated phase diagram shown in Fig. 105 is obtained with a reasonable set of parameters for a g-ology electron gas model introduced in Sec. 4.2.1, namely $g_1 = g_2/2 \approx 0.32\pi v_F$ for the backward and forward scattering amplitudes, respectively and $g_3 = 0.02\pi v_F$ for the longitudinal half-filling Umklapp scattering term for weakly dimerized chains like for $(TMTSF)_2X$ [359,363]. The model captures the essential features of the experimentally-determined phase diagram of $(TMTSF)_2PF_6$ presented in Fig. 57.

Regarding the non-ordered quantum critical phase, Sedeki et al. [363,379,380] have shown the existence of Curie–Weiss (C-W) regime of SDW fluctuations above the critical $t_b'^{\star}$, where $\chi_{SDW} \sim 1/(T+\theta)$ is still enhanced according to Fig. 105, consistently with the above NMR results. They also proceeded to an evaluation of the imaginary part of the one-particle self-energy. In addition to the regular Fermi-liquid component whose scattering rate goes as T^2, low-frequency spin fluctuations yield $\tau^{-1} = aT\xi$, where a is a constant and the antiferromagnetic correlation length $\xi(T)$ increases according to $\xi = c(T+\theta)^{-1/2}$ as $T \to T_c$, where θ is the Curie–Weiss temperature scale for spin fluctuations [363,380]. It is then natural to expect the Umklapp resistivity to contain (in the limit $T \ll \theta$) a linear term AT, whose magnitude would presumably

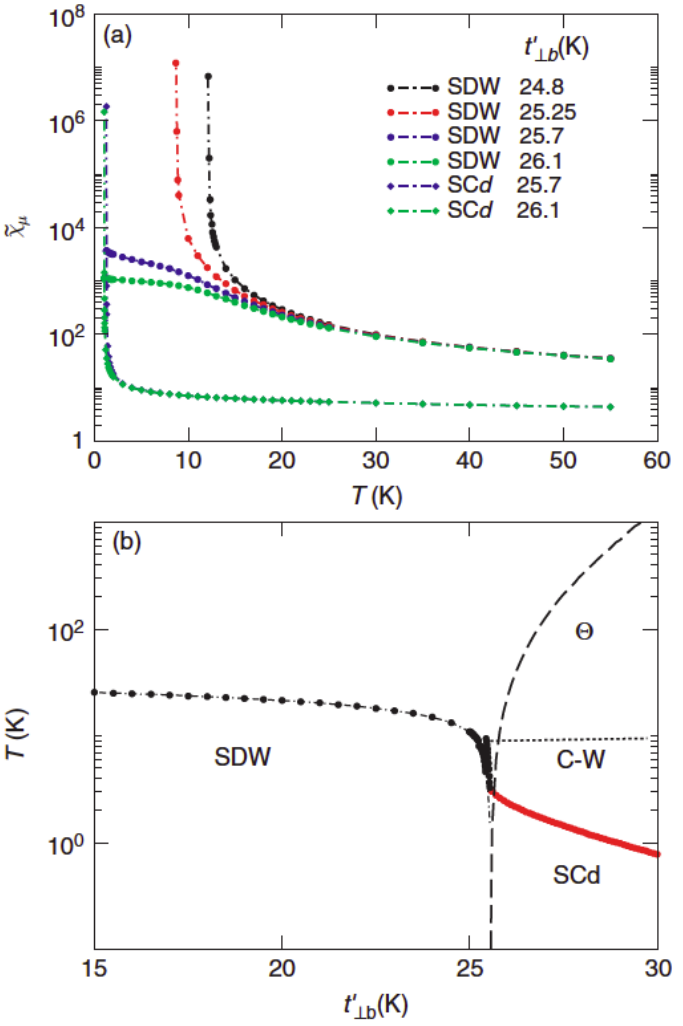

Figure 105. Renormalization group results of the Q1D electron gas model. (a) Temperature dependence of the normalized static susceptibility χ_μ of the μ = SDW and μ = SCd channels at various transverse coupling t'_b on either side of the threshold value $t'^{\star}_b \simeq 25.4$ K. (b) Phase diagram. Source: [363, Fig. 1 p. 4].

be correlated with T_c, as both scattering and pairing are caused by the same antiferromagnetic correlations.

The observation of a T-linear law for the resistivity up to 8 K in $(TMTSF)_2PF_6$ under a pressure of 11.8 kbar as displayed in Fig. 99 is therefore consistent with the value of $\theta = 8$ K determined from NMR relaxation at 11kbar displayed in Fig. 98.

More recently, Bakrim et al. [381] studied the effects of electron-phonon interactions on the SC and SDW channels. Interestingly, it is revealed that intermolecular electron-phonon coupling, though much weaker in amplitude than the Coulomb terms, enhances spin fluctuations, leading to unusual phenomena such as the prediction of a positive isotope effect. "Unpublished experiments at Orsay on deuterated $(TMTSF)_2ClO_4$ have shown a tendency to increase T_c. This is op-

posite to the usual isotope effect in superconductors but it may be due to an expansion of the deuterated volume cell unit."

We add one comment that, in $(TMTSF)_2X$, the boundary between the SDW and SC phases very close to P_c is observed to be weakly first-order [382, 383], indicating that the quantum - second order - critical point within the pressure-temperature phase diagram is actually unstable to first-order effects and the emergence of the superconducting dome. However, it has been recently revealed that other typical "quantum critical" materials such as iron pnictides [384] indeed exhibit a first-order-like-behavior in the vicinity of the quantum critical point, evidenced by phase separation between magnetically ordered and paramagnetic phases detected by μSR studies [385]. Thus, it is now getting clearer that the quantum criticality near a first-order transition observed in $(TMTSF)_2X$ probably shares general and important physics with a broader class of materials.

A complete presentation of the theory related to all these experimental findings will be published in a forthcoming issue of *Comptes Rendus Physique*.

4.6. *A very brief overlook at the two dimensional organic superconductors*

The presentation of the $(TM)_2X$ superconductors given in the previous sections has emphasized the role of the parent state, a "mother" insulating state neighbouring superconductivity. As an itinerant antiferromagnet (Slater-Overhauser phase), its stability is very sensitive to the intensity of the interchain coupling. The low temperature situation is quite different in two-dimensional organic solids.

The 2D compounds have provided not only higher values of T_c and a textbook example for the two dimensional fermiology but also a playground for the study of the 2D Mott transition as well as the metallic phase in its vicinity. A vast variety of quantum phenomena can be studied with these materials, based on the celebrated BEDT – TTF electron donating molecule and a variety of polymerized anions, leading to strong coupling compounds in which the mother state is a Mott insulating state. The wealth of quantum phenomena exhibited by these 2D materials has been recently reviewed by Dressel and Tomic [386].

To complete this presentation it is useful to have a brief look at the 2D family of organic superconductors whose physical properties are particularly interesting to compare with those of one-dimensional compounds.

At the beginning of the 80's, a new organic cation radical of the fulvalene molecule has been proposed by G. Saito et al. [387], which paved the way for the synthesis of new families of organic superconductors. This molecule is (BEDT-TTF)(bis(ethylenedithiolo)tetrathiafulvalene), an elongated version of TTF also called ET, Fig. 106. When complexed to the ClO_4^- anion, the material exhibits a metallic character down to 1.4 K with pronounced 2D features (*albeit* without traces of superconductivity) [387].

This molecule has been the first to give a radical cation salt with ReO_4 which becomes superconducting under pressure at a temperature of 2 K, slightly higher temperature than the T_c of $(TM)_2X$ [388]. However, the crystal structure of $(BEDT-TTF)_2ReO_4$ revealed a pronounced 1D character with a molecular packing bearing much similarity with the $(TM)_2X$ series. Notice that the metal-insulator transition observed around 80 K under ambient pressure in this compound is very likely due to an anion ordering transition similar to what has been encountered in $(TMTSF)_2ReO_4$ and commented in Sec. 4.3.

Furthermore, one year later, the same ET molecule contributed to the elaboration of half-filled band organic conductors with quite novel structures namely, materials displaying a two dimensional (2D) conducting (or layer) structure. The first representatives of this 2D class of

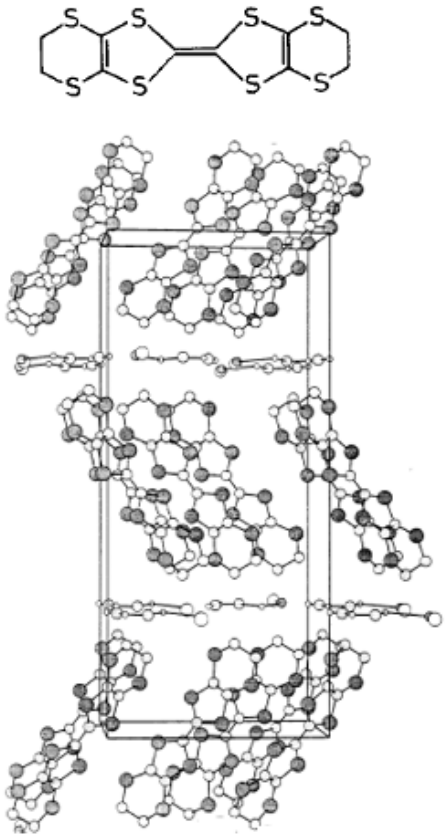

Figure 106. The unit cell of the $\kappa-(ET)_2Cu(N(CN)_2)Br$ containing four ET dimers arranged in a 2D structure separated by the polymeric anion layer. The ET molecule is displayed at the top without their ethylene end groups.

organic materials have been the $\beta-(ET)_2X$ compounds where X is a linear triatomic anion such as I_3, IBr_2, AuI_2 etc.

The salt with X= I_3 is of a particular interest since the so-called β_H-phase, which can be stabilized at low temperature after a special pressure-temperature cycling, has provided a large increase of the superconducting T_c for organic superconductors from 1-2 K in the $(TMTSF)_2X$ series up to 8 K [389–391].

When $\beta-(ET)_2I_3$ is cooled rapidly without any pressure treatment, random disorder of the ethylene groups of the ET molecules remains in the β_L-phase and strongly reduces the stability of the superconducting state with a T_c dropping down to 1.4 K [392] in line with the role of non magnetic defects on the superconductivity of 1D organics [332] and discussed in Sec. 4.4.4.

Besides, β_H-$(ET)_2I_3$ has provided a textbook example for Shubnikov–de Haas oscillations in a 2D conductor with extraordinarily large oscillations of the magnetoresistance [393]. Such a study has also enabled the determination of the overlap integral between conducting planes of 0.5 meV, a clear-cut illustration for the pronounced 2D character and the existence of angular magnetoresistance oscillations due to the c-axis warping of the Fermi surface in these ET conductors [394, 395].

A further increase in the T_c above 10 K has been accomplished in the 90's with the discovery of the κ-phase salts namely $\kappa-(ET)_2X$ with polymeric anions, X =$Cu(NCS)_2$ at T_c = 10.4 K [396], in

$Cu(N(CN)_2)Br$ (κ-Br) at 11.6 K [397], and even up to 12.5 K in $Cu(N(CN)_2)Cl$ (κ-Cl) under a modest pressure of 0.3 kbar [398].

Most κ-phase salts show an isostructural face to face molecular dimers packing forming a 2D checker-board pattern. Very much like the compounds belonging to the $(TM)_2X$ family, most κ-phase systems can be gathered together in the generic Temperature-Pressure and Chemistry phase diagram displayed on Fig. 107.

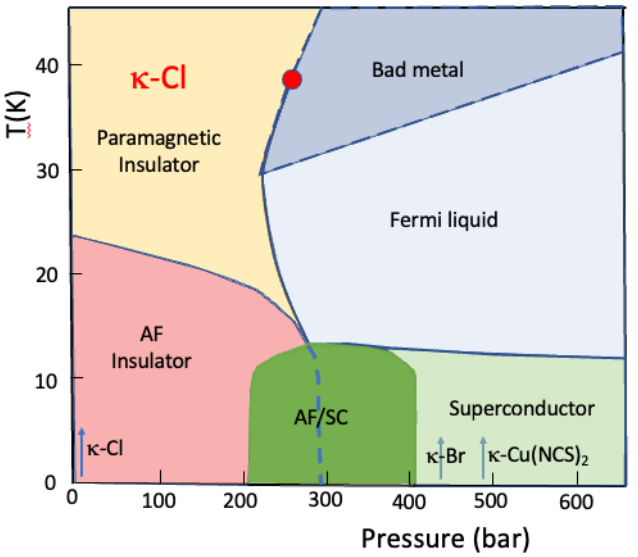

Figure 107. T-P phase diagram of $Cu(N(CN)_2)Cl$ (κ-Cl). Sources: [399, Fig. 1 p. 5421] and [400, Fig. 1 p. 1]. The arrows a and b are the respective locations of compounds $\kappa-Br$ and $\kappa-Cu(NCS)_2$ under ambient pressure. The dark green area AS/SC defines a region of coexistence between AFI and SC orders which implies that the transition between the AF and SC phases (dashed blue line) is first order with a finite hysteresis under pressure, not shown on the figure. The first order transition between a paramagnetic Mott insulator and a Fermi liquid ends at the Mott critical point (red dot) above which the transition becomes second order. Under high pressures the material is crossing-over at the temperature T^* (dashed line) from a low temperature Fermi liquid with a quadratic temperature dependence of the resistivity to a still metallic regime ($d\rho/dT < 0$) although exceeding the Mott–Ioffe–Regel criterion by several orders of magnitude, this regime is commonly called the bad metal regime [400, 401].

The compound X=$Cu(N(CN)_2)Br$ is thus of particular interest since superconductivity at T_c = 11.6 K occurs at ambient pressure making NMR studies in the superconducting state easily measurable over one decade in temperature.

^{13}C Knight shift and relaxation studies, *see* Fig. 108, in a κ-$(ET)_2Cu(N(CN)_2)Br$ single crystal have shown conclusively that the pairing in 2D organic superconductors must be spin singlet with the existence of nodes in the gap [402, 403] in line with what has been observed in $(TM)_2X$ superconductors, Sec. 4.4.2.

Although the law $1/T_1 \propto T^3$ which has been reported by several experimentalists is very suggestive of a d-wave gap situation, it is still questionable to conclude for the existence of zeros on the Fermi surface of these 2D superconductors since it is not so easy to differentiate

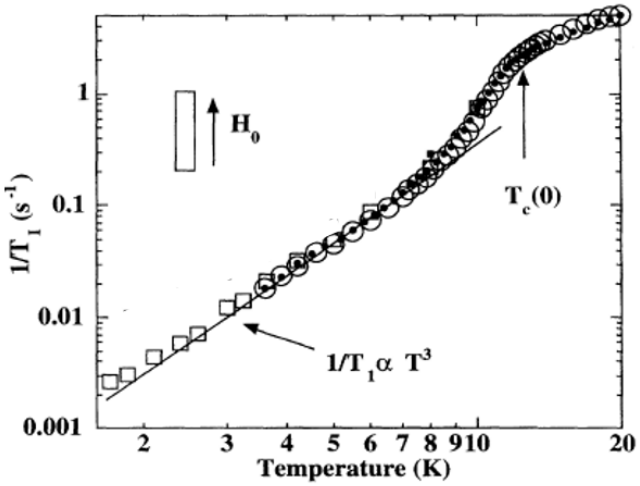

Figure 108. $^{13}C(1/T_1)$ in the superconducting phase of κ-Cu(N(CN)$_2$)Br in a parallel magnetic field showing the T^3 law and the absence of any Hebel-Slichter peak at the transition as expected for d-wave superconductivity [306]. Source: [402, Fig. 5 p. 4124].

between a very anisotropic node-less gap and a gap with nodes on the Fermi surface [402]. Investigations of anion alloying performed in $\kappa-(ET)_2Cu(N(CN)_2)Br_xCl_{1-x}$ failed to report any significant effect of disorder on $T_c \approx 12$ K [404, 405] at variance with the findings in the β-type ET salts for the mixed anion I_3-IBr_2 system [406].

Among all compounds, κ-Cl is also particularly interesting as it is the prototype in the series showing under increasing pressure the complete sequence of states, namely, paramagnetic Mott insulating, antiferromagnetic, metallic and superconducting states within a few hundred bars which have been studied with the helium-gas pressure technique [399]. Magnetic [399], acoustic [407] and transport experiments [400, 408] have shown with κ-Cl the existence of a first order transition line in the T-P plane with a phase coexistence regime ending at a Mott critical point, *see* Fig. 107.

The recent reinvestigation of κ-Br suggests that the critical regime around the critical end point does not appear to obey the 2D Ising model universality class [411] *at variance* with a similar study of the 3D Mott transition performed in the vanadium sesquioxide [412].

A single crystal NMR relaxation study of the κ-Br compound [409] reveals a large enhancement of the relaxation rate $1/T_1T$ above the Korringa law ($1/T_1T \propto K^2$), Fig. 109. The data on this figure have also been confirmed on a powder sample by Kawamoto et al. [413].

In close relation with these 2D organic compounds, it is illuminating to go back to the work of the 1970's particularly on vanadium sesquioxides [414, 415], after Neville Mott, Fig. 111, suggested in 1961 [416, 417] that by reducing the U/W ratio between the Coulombic repulsion and the electron kinetic energy, a material naturally insulating due to strong inter-electron correlations could undergo a metal to insulator transition.

NMR data displayed on Fig. 109 show that for $(V_{0.99}Cr_{0.01})_2O_3$ the relaxation rate is temperature independent in the high temperature Mott insulator regime. A similar behaviour is also observed for κ-(ET)$_2$Cu(N(CN)$_2$)Br in the low pressure domain, *see* Fig. 109 (top) whereas a more common (Korringa) metallic behaviour is recovered at higher pressures.

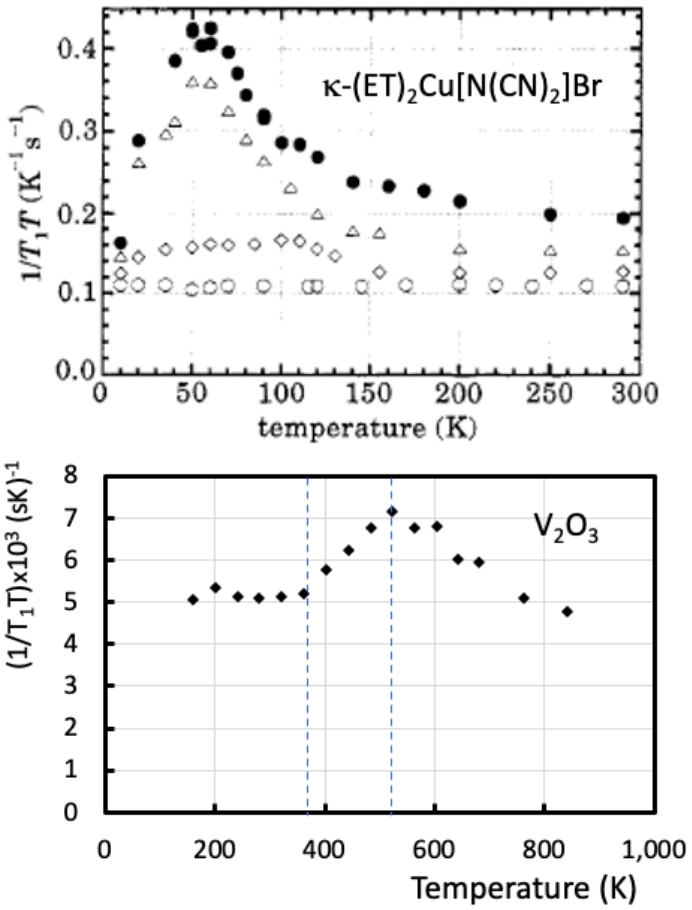

Figure 109. (Top) ^{13}C($1/T_1T$) variation with temperature at various pressures from 1 bar up to 4 kbar. Source: [409, Fig. 4 p. 208] 1 bar (•), 1.5 kbar (△), 3 kbar (◇), 4 kbar (○). (Bottom) ^{51} V($1/T_1T$) variation with temperature in V_2O_3 at ambient pressure, derived from Ref. [410].

The large decrease of $1/T_1T$ observed below 50 K for κ-(ET)$_2$Cu(N(CN)$_2$)Br is the signature of a magnetic pseudogap also visible in Knight shifts data [409, 413] that disappears above 3 kbar or so.

As far as V_2O_3 is concerned, the decrease of $1/T_1T$ between the two blue dotted lines as shown on Fig. 109 is the signature of a phase coexistence regime with a progressive evolution between a high temperature Mott insulating regime with $1/T_1$= const and the low temperature paramagnetic metal where $1/T_1 \propto T$, *see* also Fig. 110.

In conclusion, the comparative presentation of organics and oxides has shown that in addition to being textbook models for one-dimensional physics, organic (2D) conductors are remarkable prototype compounds for studying the physics of the Mott transition.

Eventhough the stability of the low temperature antiferromagnetic state is known to be depressed by introduction of charge carriers in $(V_{1-x}Cr_x)_2O_3$ alloys [400], an attempt to look for possible superconductivity in the alloy x = 0.01 managed to remove the AF insulating state at helium temperature but failed to stabilize superconductivity[3] [400].

[3] High pressure investigation of V_2O_3 performed in the thesis work of G. Lesino at Orsay in 1972, unpublished.

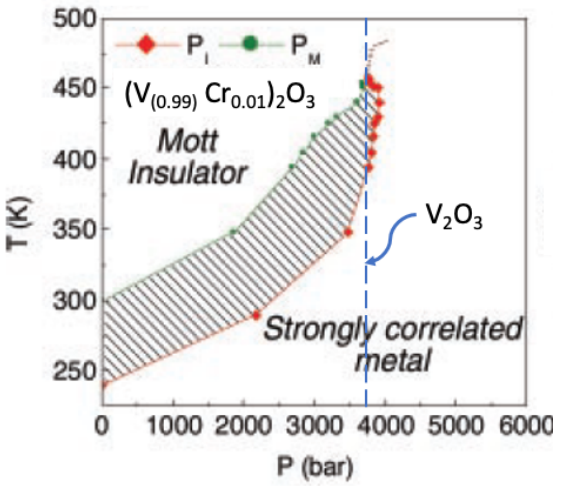

Figure 110. Limited phase diagram of $(V_{0.99}Cr_{0.01})_2O_3$ as a function of temperature and pressure. Source: [412, Fig. 1B p. 89]. ©2003 Science Magazine. All rights reserved. The shaded phase coexistence region is delimited by two spinodals and terminates at the critical point 3.7 kbar, 457 K. Above the critical point, the Mott insulator is crossing over under pressure to a strongly correlated metal. The dotted blue line shows the location of V_2O_3 in this phase diagram.

An other aspect of the 2D organics is the experimental realization of the Jaccarino–Peter mechanism for superconductivity in systems comprising magnetic ions [418]. This mechanism is probably the one which allows the stabilization of superconductivity in $(BETS)_2FeCl_4$ (where BETS is the selenide parent molecule of ET) under intense magnetic field [419,420] compensating the exchange field of aligned Fe^{3+} ions.

A review on organic conductors with much emphasis on 2D compounds has been recently published in Ref. [421].

4.7. *Charge density wave and superconductivity in 1D conductors*

It is now important to dedicate a section of this overview to organic conductors that were among the first to be discovered and that have been studied exhaustively by several research teams in Portugal in cooperation with others, not only because these materials are interesting in their own right, but also for the contrast between their properties and those of Bechgaard superconductors.

In the search of highly conductive charge-transfer compounds of one-dimensional (1D) character, perylene was one of the first donors used with bromine as anion exhibiting high conductivity but of non metallic character [16]. Then, in 1974, Alcacer reported electrically conducting metal dithiolate-perylene complexes in with the metal-maleonitriledithiolate ($M(mnt)^2$) anion, (D_2A-type salt) [423] giving a conductivity of $50(\Omega.cm)^{-1}$ at room temperature but still behaving as semiconductors at lower temperature where M is a transition metal atom. A major progress has been accomplished with the synthesis of the 2 : 1 salts $(Per)_2Pt(mnt)_2$. The single crystals conductivity of the M = Pt salt is large and metallic down to a metal insulator transition at 15 K [424], *see* structure on Fig. 112.

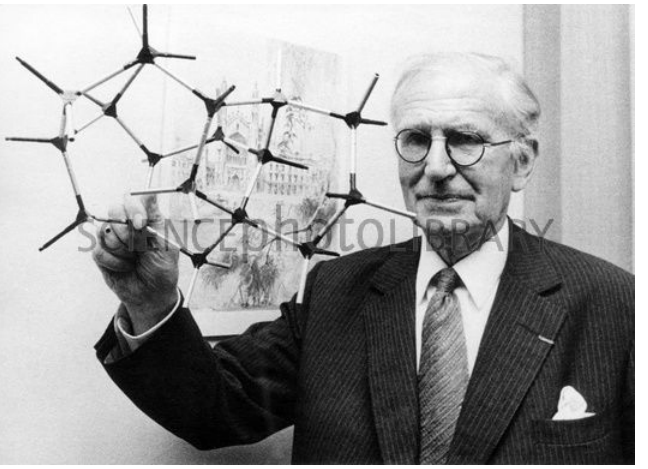

Figure 111. Sir Neville Mott (1905-1996), 1977 Nobel laureate in Physics. Sir Neville has been a pioneer in the physics of electrons in metals. The ideas presented in his textbook "Metal Insulator Transitions" have influenced the research on a large number of current materials [422]. We thank Jean Friedel for the communication of this photograph.

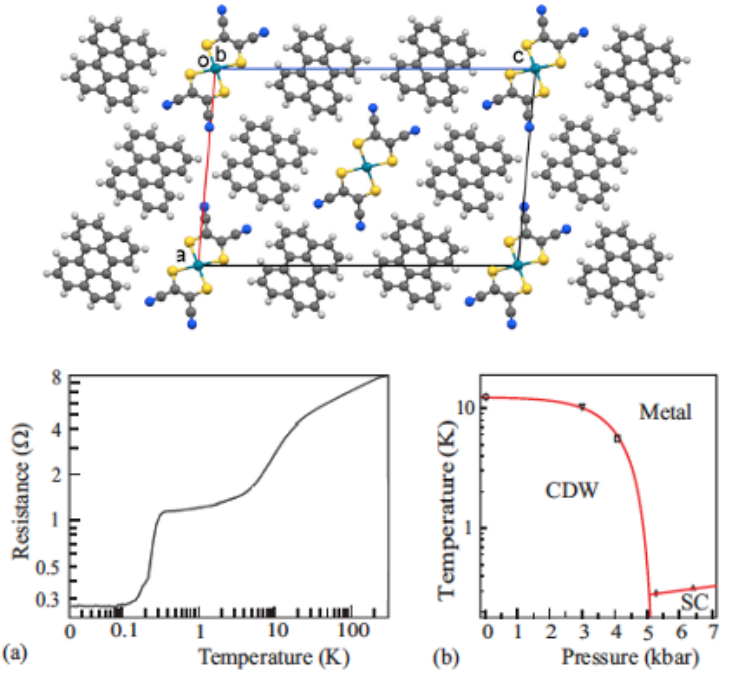

Figure 112. (Top) Room-temperature crystal structure of $(Per)_2Pt(mnt)_2$ projected along the packing axis *b*. (Bottom) (a) Temperature dependence of the resistance of $(Per)_2Au(mnt)_2$ under 5.3 kbar with $T_c = 0.35$ K. (b) $T-P$ phase diagram. Adapted from [424, Fig. 1 p. 946] (top), [425, Figs. 1, 5 p. 2, 4] (bottom).

The metallic properties are related to the existence of stacks along the b axis of cation molecules Per_2^+ parallel to anions $M(mnt)_2^-$. The anion stacks do not contribute to the electrical conductivity but play a key role in the magnetic properties. Whereas for M= Au the anion is diamagnetic and the metal insulator transition at 12 K is of the Peierls nature, for M = Pt the anions which are half filled bands carry a magnetic moment ($S = 1/2$) and give rise to a Mott insulator leading in turn to a spin-Peierls transition for $(Per)_2Pt(mnt)_2$ accompanied by a dimerization of the $Pt(mnt)_2$ molecules and a concomitant tetramerization of the interstack coupled perylene chain around 7.5 K [424, 426].

A ^{1}H-NMR investigation conducted on $(Per)_2Pt(mnt)_2$ has confirmed the existence of localized spins on the $Pt(mnt)_2$ chains and their dominant influence on the relaxation through an interstack dipolar coupling [427]. A scaling relation of the form $T_1^{-1} \propto T\chi_s(T)$ is found to exist in the entire temperature domain, including the regime of one dimensional spin-Peierls $Pt(mnt)_2$ lattice fluctuations observed by x-ray experiments below 30 K [428]. Contrasting with the previous compound, $Au(mnt)_2$ there are no localized spins on the the dithiolate chains and the perylene proton relaxation is due to the fluctuating field provided by the mobile electrons of perylene chains.

Once the Peierls transition of $Au(mnt)_2$ at 12 K is suppressed by a moderate pressure of 5 kbar, a metallic state is stable at low temperature and the compound becomes superconducting below 0.3 K [425], *see* Fig. 112. We may note that this metallic phase presents under magnetic field a phenomenon somewhat similar to what will be detailed in Sec. 4.9 about $(TM)_2X$ compounds namely, magnetoresistance oscillations due to quantum interferences between two open trajectories on open Fermi surfaces [429]. These oscillations are periodic in $1/B$ with a frequency of 19.5T which is determined by the area enclosed by the two open trajectories in k space, *see* Fig. 113. They can be related to the peculiar Fermi surface of $(Per)_2M(mnt)_2$ proposed by Canadell [430] after the calculation of the electronic structure of these molecular conductors.

The unit cell containing four perylene units and two anions together with a pronounced 1D character resulting from a weak interstack coupling leads to the double sheet Fermi surface displayed on Fig. 113. As this area is proportional to the magnitude of the transverse coupling, it is quite reasonable to find for the very 1D conductor $(Per)_2Au(mnt)_2$ a value for the frequency much smaller than what is observed in the more 2D coupled $(TMTSF)_2X$ conductors, *vide infra*.

Two additional points on Fig. 112 are worth noticing. First, the resistance, which is weakly dependent on temperature below 10 K, *see* Fig. 112, is contrasting with the behaviour of the $(TMTSF)_2X$ superconductors, Sec. 4.5, for which the single particle scattering is dominated by magnetism close to a quantum critical point.

Second, the $P-T$ phase diagram of $(Per)_2Au(mnt)_2$ reveals a tendency for T_c to increase under pressure which is also *at variance* with the behaviour of T_c in the $(TM)_2X$ family. Such a behaviour could be understood following the model developed by Bakrim and Bourbonnais [431] predicting a power law increase of the superconducting $T_c \approx \omega_D^{0.7}$ with the Debye frequency, from a quantum a quantum critical point of CDW order triggered by nesting alterations under pressure.

There exists an other series of charge transfer conductors based on transition metal (M=Ni, Pd, Pt) complexes of dmit (dmit = 1,3-dithia-2-thione-4,5-dithiolato) [432] which have attracted a great deal of attention after the discovery of superconductivity in $TTF[Ni(dmit)_2]_2$ at 1.6 K under a pressure of 7 kbar [433]. Two other compounds of this family have also been found superconduting later, $(CH_3)_4N[Ni(dmit)_2]_2$ (T_c = 5 K at 7 kbar) [434] and $\alpha' - TTF[Pd(dmit)_2]_2$ (T_c = 6.5 K at 20 kbar) [435].

Moreover, an interesting feature of $TTF[M(dmit)_2]_2$ (M = Ni, Pd) is the occurrence of charge density wave (CDW) instabilities observed in X-ray diffuse scattering studies at ambient pressure [436]. Thus, these materials provide also an interesting example of competition between CDW and superconductivity in molecular metals. Unlike most molecular conductors presented

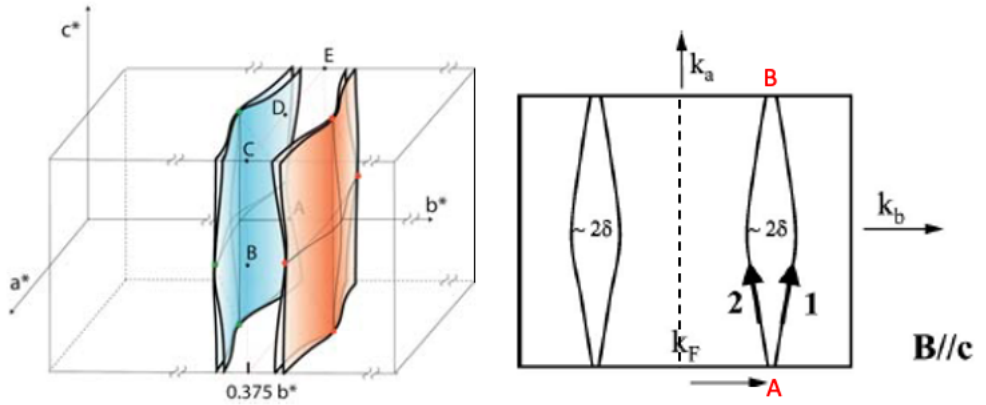

Figure 113. Schematic Fermi surface of $(Per)_2M(mnt)_2$ according to [430] showing one pair of the double-sheet surface intersecting the b^* (stacking axis in reciprocal space) at $+\frac{3}{8}b^*$. The enlarged picture (after [429]) shows the open electron trajectories on the double sheet surface leading to quantum interferences under magnetic field at A and B.

up to now, the $TTF[M(dmit)_2]_2$ (M = Ni, Pd) family is characterized by a small energy difference between the $M(dmit)_2$ highest occupied molecular orbital and lowest unoccupied molecular orbitals energy difference (HOMO-LUMO) which leads to a contribution at the Fermi level of both LUMO and HOMO orbitals of the acceptor as evidenced by early band structure calculations [437]. A recent the band structure and Fermi surface as a function of temperature has been carried out on the basis of the centered unit cell containing four TTF and eight $Ni(dmit)_2$ molecules using a numerical atomic orbital density functional theory (DFT) approach [438] which was developed for efficient calculations in large systems and implemented in the SIESTA code [439].

As revealed in the 1986 experiments [433] $TTF[Ni(dmit)_2]_2$ remains metallic under ambient pressure at low temperature with a conductivity of the order of $1.5\times10^5(\Omega.cm)^{-1}$ at 4 K, but becomes a superconductor at 1.62 K under 7 kbar. A subsequent investigation of this phase diagram under pressure revealed an unexpected complexity suggesting that superconductivity is coexisting with CDW instabilities at higher temperature [440] as hinted by X-ray studies at ambient pressure [436].

This phase diagram re-investigated 14 years later using transport properties under pressure has led to a better knowledge of this complex system [438]. The most recent determination of the T-P phase diagram is displayed on Fig. 115. This diagram is confirming previous experimental results in particular, ^{13}C NMR Knight shift data showing that even the 3D ordered CDW below 60 K does not open a gap throughout the entire Fermi surface and instead decreases the density of states at Fermi level [441].

As a result of the complex situation of this multiband system a superconducting state can be stabilized at low temperature even in the presence of several CDW instabilities but when the consequence of distortions on the density of states is reduced under pressure, $N(E_F)$ increases and T_c is favored. The situation where a competition arises between superconductivity and CDW is reminiscent of what has been revealed long ago in the study of transition-metal dichalcogenides [200], *see* Fig. 116.

According to a simple argument proposed by Friedel in 1975 [202], as far as 2D chalcogenides are concerned the creation of a superlattice lowers T_c because of a concomitant

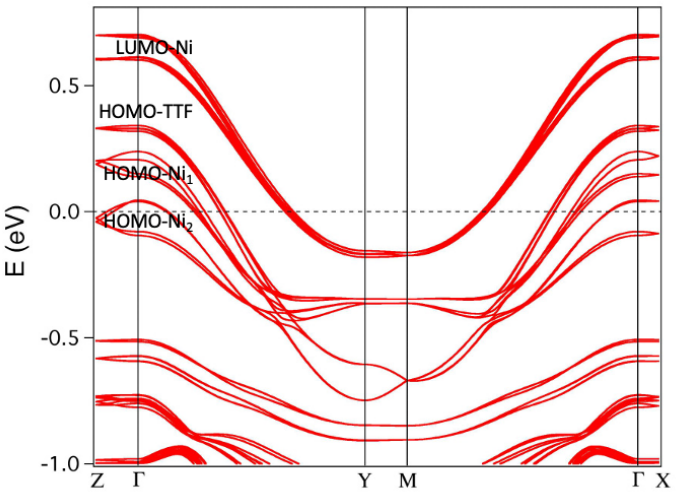

Figure 114. Most recent calculation of the band structure of TTF[Ni(dmit)$_2$]$_2$ at 150 K. Source: [438, Fig. 7 p. 4]. The Fermi level at zero energy is crossing the TTF HOMO band, the Ni(dmit)$_2$ LUMO band and two low lying Ni(dmit)$_2$ HOMO bands. ©American Physical Society and the authors. All rights reserved.

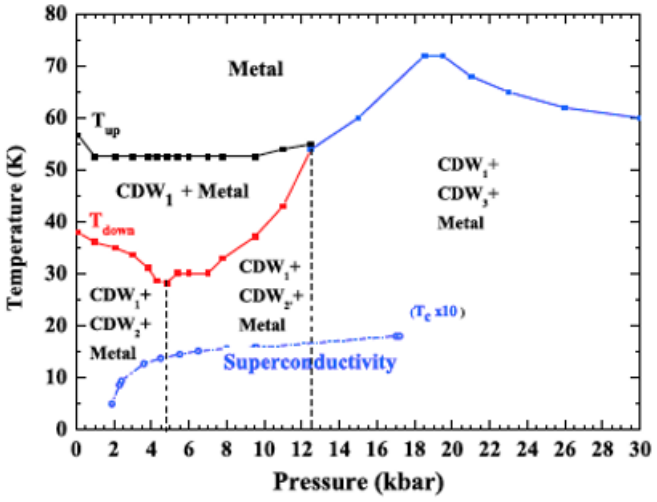

Figure 115. A recent determination of the phase diagram of TTF[Ni(dmit)$_2$]$_2$ from transport properties under pressure. Source: [438, Fig. 10 p. 6]. Onset of CDW orderings have been detected by small anomalies in susceptibility and sharp anomalies on transverse transport (only). The superconducting T_c is multiplied by ten on this diagram. ©American Physical Society and the authors. All rights reserved.

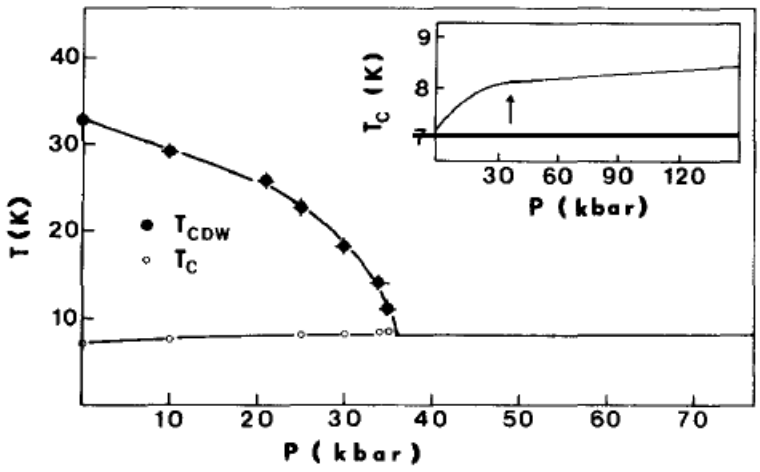

Figure 116. T-P phase diagram of 2H-$NbSe_2$ determined on the same sample batch by transport and NMR [442]. Source: [443, Fig. 2 p. 1394]. *see also* Fig. 117.

Figure 117. Claude Berthier (1946-2018) after a PhD in NMR in solids at Grenoble University, did a postdoctoral stay at Orsay in 1975. He has been the first to carry out very smart NMR studies on small single crystals of transition metal dichgalcogenides and organic conductors. Back to Grenoble, he became a leading scientist at the High Magnetic Fields Laboratory and contributed to major advances in the physics of one and two dimensional compounds.

lowering of $N(E_F)$. Consequently, suppressing the distortion under pressure results in an enhancement of T_c. If the same argument is applied to TTF[Ni(dmit)$_2$]$_2$ it must be applied with caution since unlike di-chalcogenides the temperature-pressure phase diagram on Fig. 115 does not provide a complete suppression of the distortions. However this interpretation may be more

relevant for the superconducting phase of TTF[Pd(dmit)$_2$]$_2$ which is stabilized at 5.5 K under a pressure of 24 kbar instead of an insulating phase at lower pressure [435].

4.8. *Single-component molecular superconductors*

Until now, all the molecular conductors mentioned in this review have two components, either charge transfer compounds such as TTF-TCNQ, or organic cationic salts like Bechgaard–Fabre salts, (TMTSF)$_2X$. We have presented in Sec. 4.7 the case of different molecular metals in which some highest occupied molecular orbitals (HOMO) belonging to the acceptor molecule being only slightly depressed in energy below the lowest unoccupied orbitals (LUMO) contribute both to the density of states at the Fermi level (together with HOMO levels from the TTF donor molecule) as shown on Fig. 114.

These compounds are based on transition metal complex molecules such as Ni(dmit)$_2$ which have been at the origin of the development of new molecular conductors and superconductors composed of only one chemical specie at Nihon University Tokyo [444].

The design of a single-component molecular metal is difficult because most molecules have an even number of electrons and their HOMO is usually doubly occupied with a HOMO-LUMO gap larger than the intermolecular interaction leading to a finite bandwidth in the solid state. Therefore, in order to achieve metallicity with partially filled bands, the energy separation between HOMO and the lowest unoccupied molecular LUMO orbitals should be small enough to make the HOMO and LUMO bands overlap each other as a result of two-dimensional or three-dimensional intermolecular interactions in order to form.

To obtain a molecule with a very small HOMO-LUMO gap, metal complexes with extended-TTF dithiolate ligands were adopted because on the one hand the HOMO of the metal dithiolate complex can be roughly expressed as a bonding combination of left and right ligand orbitals while the LUMO is roughly the anti-bonding combination of them, including very small d_{xz} orbital of the central metal atom with appropriate symmetry to mix in the LUMO leading to a relatively weak interaction between left and right ligands through sulfur atoms [445], *see* Fig. 118.

These HOMO and LUMO orbitals suggest the possibility of a small HOMO-LUMO gap due to the relatively weak interaction between left and right ligands through ligand sulfur atoms.

Furthermore, strong intermolecular interactions through S-S atoms in extended-TTF ligands play a very important role in the enlargement of the bandwidth. Consequently, as sketched on Fig. 118, the small HOMO-LUMO gap and strong intermolecular interaction through S-S atoms produce HOMO band and LUMO band overlaps around E_F, and electron and hole Fermi surfaces are produced.

A lot of transition metal single-component compounds have been synthesized by the Nihon group and their physical properties studied in temperature and very high pressure [445, 449]. Among them, let us mention [Ni(tmdt)$_2$] (tmdt = trimethylenetetrathiafulvalenedithiolate), which reveals a metallic resistivity behaviour down to 0.6 K and a semi-metallic electronic structure consistent with extended Hückel band calculations of a 3D crystal and a HOMO-LUMO gap of the order of 0.1 eV [447].

The compound [Ni(hfdt)$_2$] (hfdt = bis(trifluoromethyl -tetrathiafulvalenedithiolate) is a semiconductor under ambient pressure with an activated resistivity, ($E_a \sim 0.14$ eV), in fair agreement with the LDA band structure calculation [446]. According to the band structure performed with lattice parameters under pressure derived by first principle calculation, the band gap disappears around 6 GPa in agreement with the observed stabilization of a two dimensional metallic state leading to superconductivity below $\sim$ 5.5 K in a very narrow pressure range (7.5-8.6) GPa [448]. However, what is remarkable about the stabilization of superconductivity in this single-component molecular conductor is the absence of lattice or magnetic precursors in the

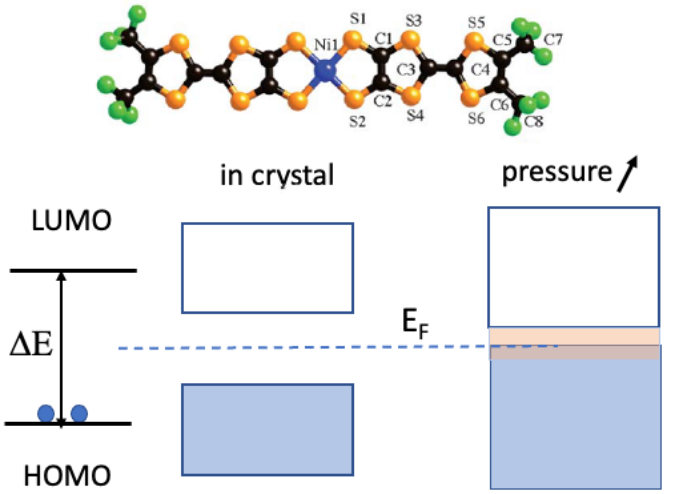

Figure 118. Molecular structure of the transition metal complex [Ni(hfdt)$_2$] which is the unique ingredient in the single component molecular superconductor. Source: [446]. Notice the bulky fluorinated terminal groups which enhance the coupling between the $a-b$ layers *at variance* with other transition metal single-component molecular conductors. Schematic diagram showing how a single component molecular semi-metal such as [Ni(hfdt)$_2$] can form if the HOMO-LUMO gap ΔE is not too large compared to individual bandwidths in the solid. The compound is a classical band insulator under ambient and low pressure. In the case of [Ni(tmdt)$_2$] the overlap between valence and conduction bands exists already under ambient pressure leading in turn to a metallic behaviour [447]. However, for [Ni(hfdt)$_2$] it is the high pressure increasing the intermolecular interaction which makes both bands overlapping, giving rise to a semi-metallic band structure with a superconducting phase [448].

high temperature metal phase. It can thus be concluded that the physics of this one-component superconductor is likely to be closer to that of classical band semiconductors than to that of low-dimensional conductors presented above.

4.9. *Magnetic field-induced SDW phases in 1D conductors and magnetoresistance oscillations*

Quasi one-dimensional conductors pertaining to the (TM)$_2X$ family exhibit under magnetic field properties that are unique in solid state physics. These properties are the magnetic Field Induced Spin Density Wave (FISDW) phases on the brink of superconductivity, which have contributed to another success story mixing theory and experiments (with the quantized nesting model and a nice application of the magnetic breakdown theory). Even if the link between FISDW and superconductivity is not conclusively established, it would be a shame to conclude this overview without mentioning even very briefly these phenomena under magnetic field.

It is remarkable to note that this research domain was developed very actively at the beginning of 1983 simultaneously by two groups on both sides of the Atlantic and at the Landau Institute of Moscow. While we tend to focus on the historical development of the field, the interested reader can find more details in several articles published in the textbook edited by A. Lebed [450].

The new physics concerning the conductive phase of (TM)$_2X$ compounds under magnetic field began with the experimental observation that in magnetic fields of a few Tesla applied

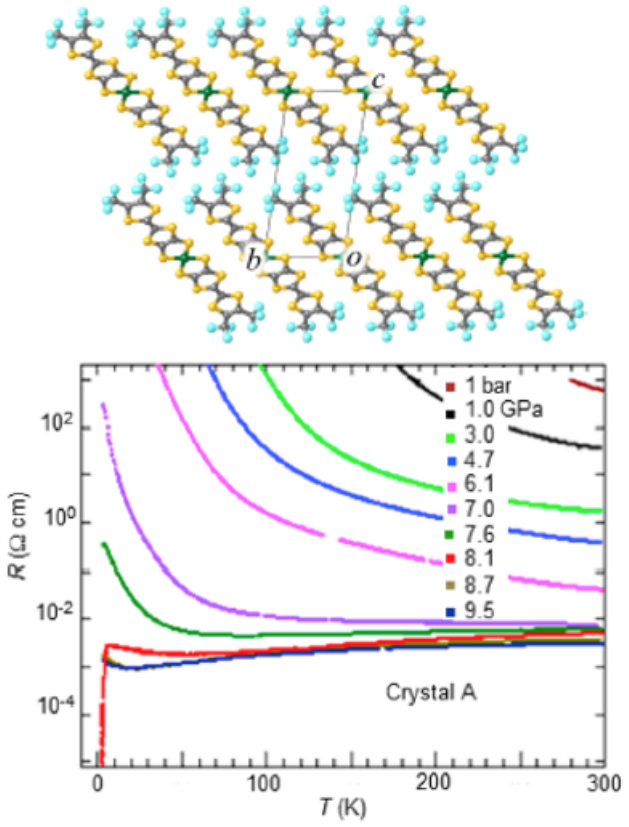

Figure 119. Molecular packing of $[Ni(hfdt)_2]$. Temperature dependence of the resistivity up to the pressure of 9.5 Gpa showing the superconducting transition at ~ 5.5 K in a narrow pressure window around 8 Gpa. Source: [448, Fig. 3a p. 7620]. ©2004, American Chemical Society. All rights reserved.

along the lowest conductivity axis, novel phases appear in $(TMTSF)_2ClO_4$, of semi-metallic nature [288], characterized by a magnetic order of the SDW nature [280] and an unexpected step-like behaviour of the Hall voltage [451], *see* Fig. 120. Subsequent investigations revealed other unexpected phenomena such as the existence of Hall plateaus alternating in sign at increasing magnetic field the so-called "Ribault anomaly" [457]. Negative plateaus have been also observed and extensively studied in $(TMTSF)_2PF_6$ under pressure [454, 458, 459].

Shortly after publications of these experiments, Gorkov and Lebed proposed a model [291] in which the orbital effect of a magnetic field aligned perpendicular to the $a-b$ plane of the Q1D conductor with a finite transverse coupling along b tends to restrict the excursion along the b direction for an electron moving along the a axis. The effect of the magnetic field amounts to increasing the one dimensionality as in the case of open orbits the transverse excursion along b is inversely proportional to the magnetic field [312]. Hence, going to low temperature, the Q1D electron gas is likely to undergo an instability towards a semi-metallic SDW phase with a wave vector $\mathbf{Q} = (2k_F, \pi/b^*, \pi/c^*)$. The Gorkov and Lebed's argument on the effect of a magnetic field on nesting has been improved by the Orsay group, Héritier, Montambaux and Lederer [460]. G. Montambaux using Gorkov–Lebed's formalism in his PhD thesis work, derived the staggered

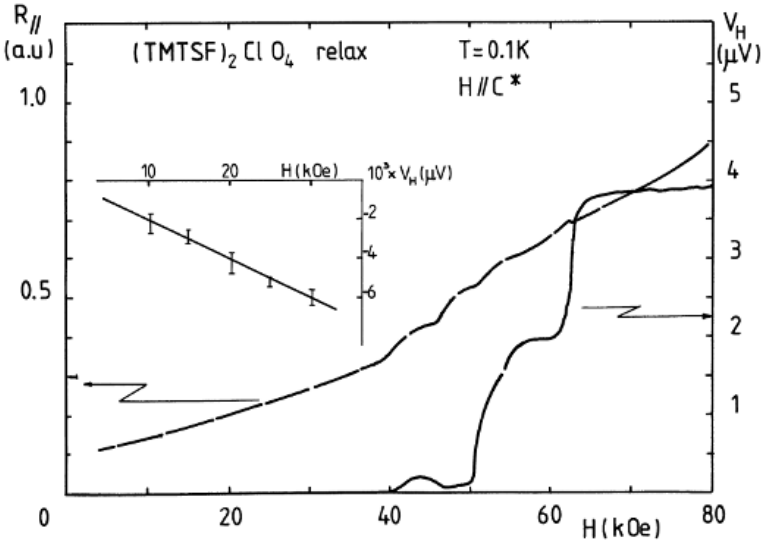

Figure 120. Magnetic field dependence of the Hall voltage in slowly-cooled $(TMTSF)_2ClO_4$ at 0.1 K. The inset shows the low field regular hole-like part before the onset of the FISDW phases. Source: [451, Fig. 2b p. 956]. ©EDP sciences. All rights reserved.

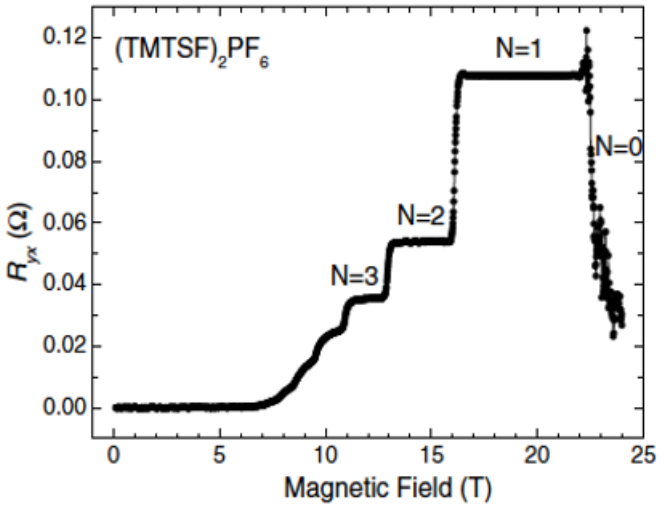

Figure 121. Magnetic field dependence of the transverse resistance of $(TMTSF)_2PF_6$ under 10 kbar. Source: [452, Fig. 3b p. 265]. These results have been chosen among many others for their high quality. They even enable a quantum measurement of the sample thickness namely, 0.29 mm. ©(2003) Elsevier. All rights reserved.

static 2D spin susceptibility $\chi_0(\mathbf{Q}, H, T)$ of the noninteracting electron gas with open Fermi surface [461, 462]. Starting from the condition of minimum diamagnetic energy, allowing the wave vector $\mathbf{Q}(H)$ to adapt to the field so that the nesting becomes quantized, it was predicted that the field induces a succession of SDW phases with $\mathbf{Q}(H)$ varying linearly, separated by first

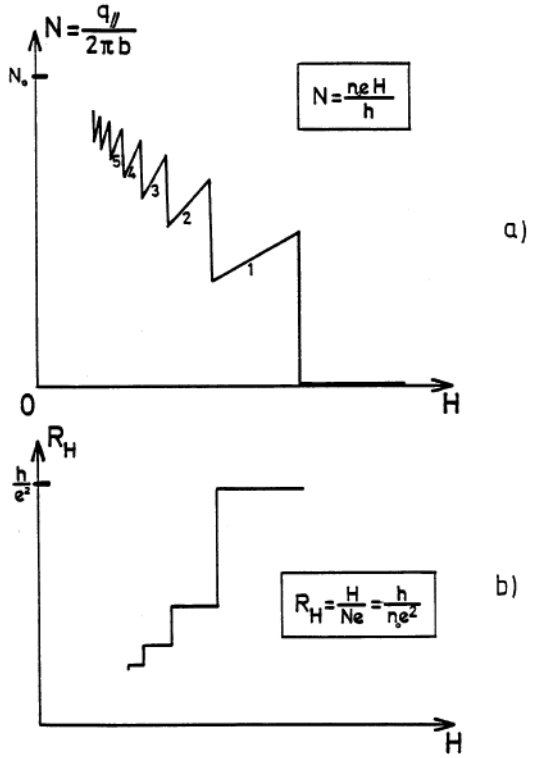

Figure 122. a) N is the number of unpaired carriers in the pocket formed by the Fermi surface and the translated surface by $\mathbf{Q}(H)$. This vector varies with the field so as to maintain in the pocket an integer number n of completely full Landau levels, a condition for the minimum of diamagnetic energy. b) The Hall resistance (without spin degeneracy) $R_H = \frac{H}{Ne}$ is quantized within each phases with n filled Landau levels since $N = \frac{neH}{h}$ according to a). This is in perfect agreement with the experimental data displayed on Fig. 123. This figure is borrowed from the thesis of G. Montambaux [453].

order transitions with $\mathbf{Q}(H)$ discontinuities and Hall voltage plateaus within each phases. This theory is known as the Quantized Nesting Model, *see* Fig. 122.

The model was even improved taking into account slight modifications of the dispersion relation in the metallic phase [463] to explain the existence of negative Hall voltage plateaus as displayed on Fig. 123 for $(TMTSF)_2PF_6$ although first evidenced in $(TMTSF)_2ClO_4$ [457].

The sequence of negative plateaus appearing in $(TMTSF)_2PF_6$ [454, 459] below 9 kbar with even quantum numbers have been understood by a slight modification of the strongly pressure sensitive dispersion relation of the metallic phase [464], *see* Fig. 124. As far as $(TMTSF)_2ClO_4$ is concerned the existence of the negative plateaus is very dependent on the ordering of the ClO_4^- anions [457] which is closely related to the peculiar granular structure likely to develop upon fast cooling, *see* Sec. 4.4.5. Taking into account the third direction along c, Montambaux [462] noticed that *at variance* with 2D case given by $T_{c2D}(H)$, there exists at $T = 0$ K in the 3D situation a finite threshold field H_t for the stability of the SDW phase such as, $T_{c2D}(H_t) = t_c'$ where t_c' is the measure of the deviation from perfect nesting along the third direction.

Furthermore, a wealth of fascinating phenomena have been observed regarding the magnetoresistance of these model materials, either at fixed orientations of the field with respect to crystals axes or rotating a fixed field in well defined planes. This area of research has

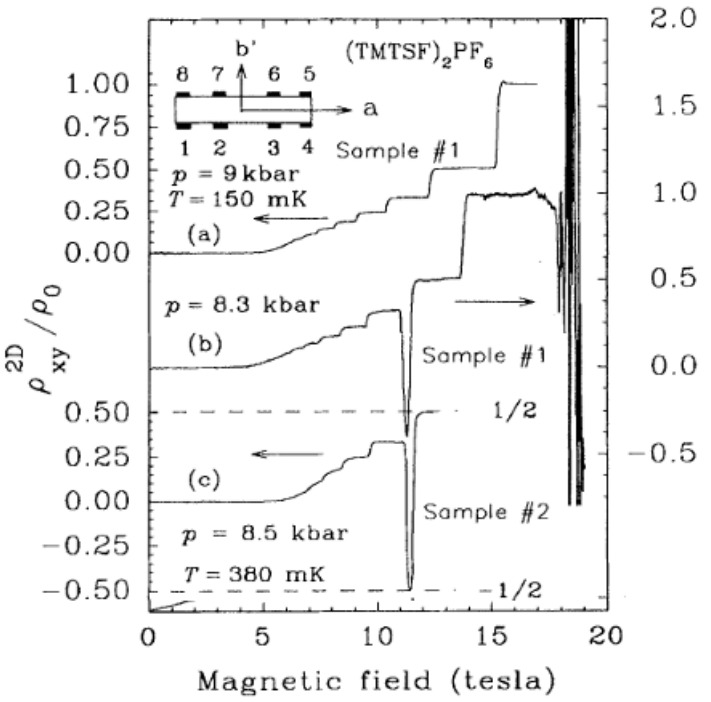

Figure 123. Transverse resistance ρ_{xy}^{2D} for two samples at pressures less than 10 kbar, multiplied by the number of conducting layers to obtain the single layer resistance and normalized to the resistance quantum ρ_0 which amounts to 12906 Ω including spin. Negative Hall conductivity becomes visible in the pressure range $p \leq 8.5$ kbar, (N = −2 signal in sample #1 at 8.5 kbar for instance). Source: [454, Fig. 1 p. 2001]. These data corroborate previously published results, [455, 456] but they are displayed here because of their higher quality.

been very productive and has given rise to many publications. In the present article we give only a short overview and refer the interested reader to the various contributions published in textbooks [293, 450]. A recent account for part of these questions has been published in *Comptes Rendus Physique* [465].

First, it is well established in low dimensional organic conductors that the Landau quantization of closed electronic orbits originating from pockets of unpaired carriers left after density waves instabilities of the 1D electron gas (CDW or SDW) give rise to magnetic oscillations of transport properties. The quantization of the electronic motion along these closed pockets leads to Shubnikov–de Haas (SdH) oscillations (periodic in $1/B$) the period of which is proportional to the size of the pocket. The typical field B_f characteristic of the oscillations is proportional to the area $\mathscr{A}$ of the closed orbits in reciprocal space. The characteristic energy of deviation from perfect nesting, named t'_b in Eq. (27), is usually of order of 10-30 K, so that

$$\mathscr{A} \propto \frac{t'_b}{\hbar v_F b} \quad \text{and the typical field} \quad B_f \propto \frac{t'_b}{e v_F b}$$

is of order of a few dozen Tesla. In Bechgaard salts, the competition between Spin Density Wave (SDW) ordering and the quantization due the magnetic field leads to the cascade of SDW subphases in which the Hall effect is quantized as presented above.

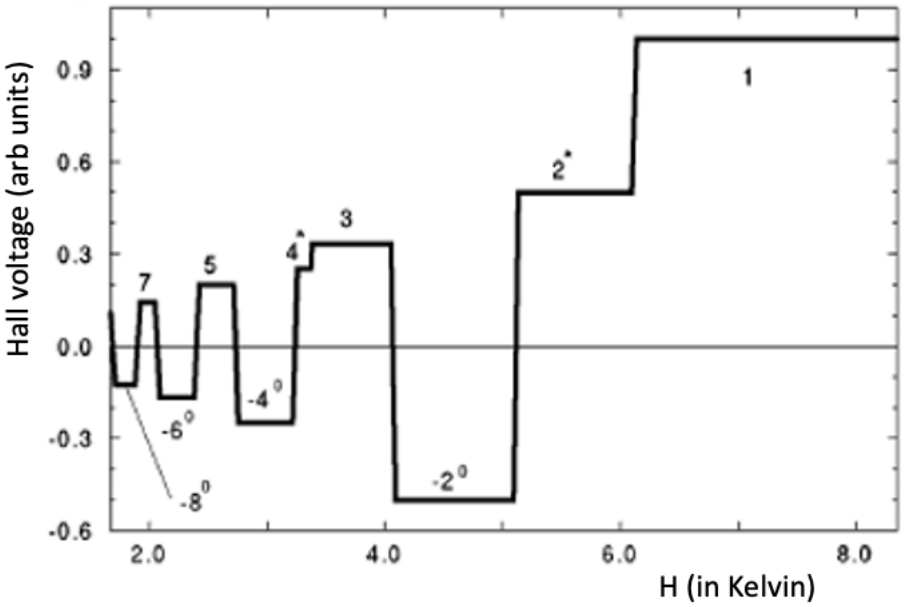

Figure 124. Theory of the Hall voltage versus magnetic field (1 K=0.5 T). Source: [464, Fig. 3b p. 369]. ©American Physical Society and the authors. All rights reserved.

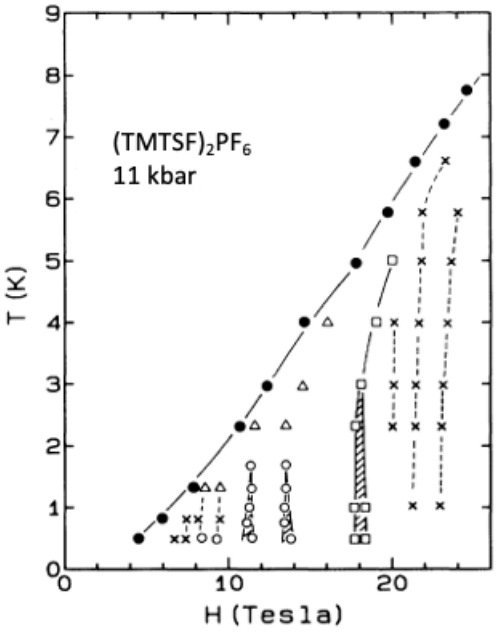

Figure 125. T-H phase diagram of $(TMTSF)_2PF_6$ under pressure displaying the FISDW phases. Shaded areas denote hysteresis between Hall plateaus. The high field state arises above 18T and the crosses represent peaks in ρ_{xx}. Source: [455, Fig. 4 p. 1986]. ©American Physical Society and the authors. All rights reserved.

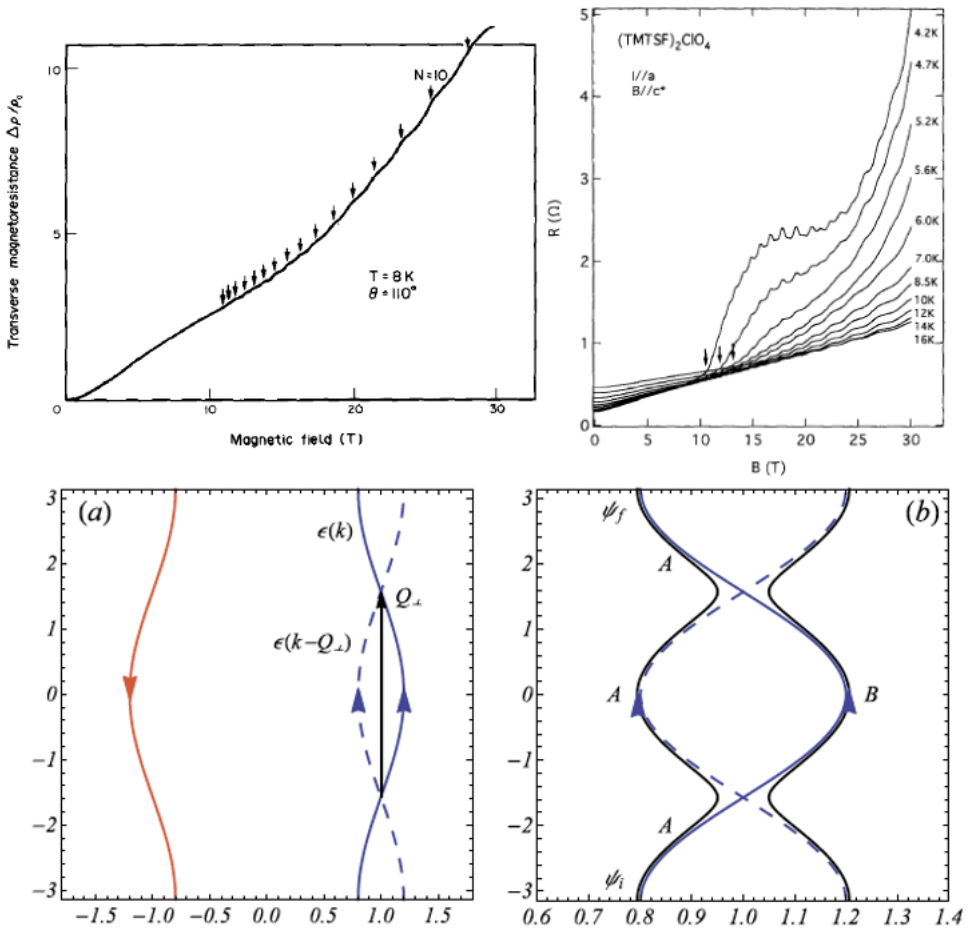

Figure 126. (Top left) Observation of rapid oscillations in the metallic phase of R-$(TMTSF)_2ClO_4$ (a axis magnetoresistance with the field perpendicular to a but 20 degrees off $c*$ axis, T = 8 K). (Top right) Magnetoresistance in the metallic phase of R-$(TMTSF)_2ClO_4$ from T = 16 K down to the FISDW phase. (Bottom) (a) A schematic picture of the $(TMTSF)_2ClO_4$ Fermi surface in the presence of a modulation with transverse wave vector $\mathbf{Q}_\perp = (0, \pi/b)$ which couples states on the same side of the Fermi surface. The dashed blue electron trajectory under magnetic field $\|c*$ is the result of the FS folding at $\pm\pi/2b$ due to the anionic external potential creating two open warped sheets AAA and BBB on (b). An electron starting on sheet A may travel either along two interfering paths either AAA or ABA trajectories through a magnetic breakdown, leading in turn to magnetic oscillations in the conductance with the frequency $\propto t_b$, according to sources: [466, Fig. 3 p. 548] (Top left), [467, Fig. 2 p. 389] (Top right), [465, Fig. 1 p. 377] (Bottom).

What is more intriguing are the so-called rapid oscillations of the magnetoresistance, characterized by a much larger characteristic field of the order of a few hundred Tesla [467]. These rapid oscillations have been observed in the FISDW phases of $(TMTSF)_2PF_6$ under pressure (11 kbar at room temperature) measuring ρ_{xx} above 18T with a period of 286T [455], *see* Fig. 125, and reexamined in more details by Kornilov *et al.* [468] 18 years later. As noticed in Refs. [455] and [468],

the amplitude of the "fast" oscillations periodic in 1/H with the frequency of 286T do not follow the classical temperature dependence of Shubnikov oscillations. Instead their amplitude progressively diminishes below 2 K.

Rapid oscillations had also been observed in the metallic phase at temperatures larger than those of the FISDW instabilities. This is for instance the case for the slowly-cooled phase of $(TMTSF)_2ClO_4$ (R-$(TMTSF)_2ClO_4$) [467] or also in $(TMTSF)_2ReO_4$under pressure [469].

Rapid oscillations are observed as well in the fast-cooled phase of $(TMTSF)_2ClO_4$ (Q-$(TMTSF)_2ClO_4$), but only in the presence of a FISDW instability [470]. At *variance* with the slow oscillations, the frequency of these rapid oscillations is related to interchain coupling t_b, that is to the warping of the open Fermi surface much larger than the unnesting contribution t_b' in Eq. (27).

Since an overview of all situations where rapid oscillations arise in these materials with an unified theoretical model based on the experimental results has been published recently in Ref. [465] we only wish to illustrate here the concept of open orbits, magnetic breakdown and Stark interference with the simple situation of the anion-ordered $(TMTSF)_2ClO_4$.

As displayed on Fig. 126, under a magnetic field perpendicular to the $a-b$ plane, the electrons travel on both FS sheets along the same direction, and may experience a tunneling through magnetic breakdown from one sheet to the other. Hence, the two different paths AAA and ABA on Fig. 126 may interfere and lead to Stückelberg oscillations of the conductivity [471], which are proportional to $\cos(2\pi\frac{B_f}{B})$ where the frequency becomes now $B_f \propto \frac{t_b}{ev_F b}$ i.e. a much larger frequency (≈ 260 T) compare to the slow oscillations (≈ 30 T). A detailed review covering all cases of rapid oscillations in 1D conductors is proposed in the reference [465] on open access.

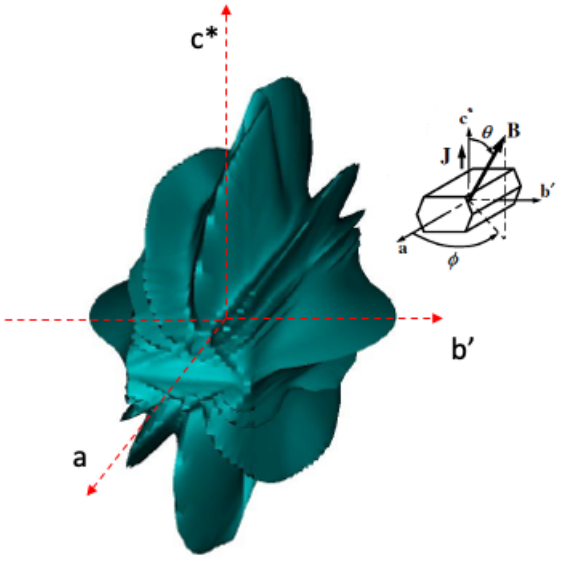

Figure 127. A 3-D representation of the measured interlayer conductivity σ_{zz} in polar coordinates of $(TMTSF)_2PF_6$ at high pressure under a magnetic field of fixed amplitude with respect to the field orientation defined in an orthogonal frame by angles θ and ϕ. The radial distance from the origin is proportional to $\log\sigma_{zz}(\theta,\phi)$. Source: [472, Fig. 1 p. 1]. We thank Wuon Kang for allowing us to use the figure for an adaptation.

In addition, a wealth of phenomena have emerged from the magnetoresistance measured when a constant magnetic field is rotated in a frame characterized by angles θ and ϕ (the angles between H and a' in the $a-b'$ plane and between H and c' in the c^*-b' planes respectively).

In 2007 W. Kang and his colleagues [472] "The nice view presented in this figure is a result which has been made possible thanks to the construction of a two-axis rotator for the pressurized sample under high magnetic field". have revisited this topic and summarized all previous experimental works providing a 3-D representation of the angular dependence of transport over 4π steradian in the case of the simplest 1D conductor namely, $(TMTSF)_2PF_6$ under pressure, *see* Fig. 127. The figure shows that the interlayer conductivity ($\sigma_{zz} \approx 1/\rho_{zz}$) behaves in a way far from the smooth expectation of the Boltzmann transport theory applied to an anisotropic conductor, peaks and dips of magneto-conductivity at well established angles are superimposed to the semiclassical Boltzmann transport.

The field of angular magnetoresistance in Q1D conductors began after Lebed [473] predicted that tilting the field away from the $c*$ direction in the c^*-b' plane should decrease the threshold field H_t requested for the stabilization of the FISDW phase at $T = 0$ K *see*, Sec. 4.9 recovering the 2D limit. For these special orientations of the field the electron motion would become commensurate along the c and b directions, i.e frequencies to cross the Brillouin zone along b and c directions become commensurate. Subsequently Lebed and Bak [474] dealing with transport in the metallic phase, derived from the calculation of the scattering rate of carriers moving along the 1D axis the existence of anomalies of the magnetoresistance (peaks) departing from the Boltzmann calculation, at well identified orientation (so-called magic angles) when the magnetic field is rotated in the b^*-c^* plane. Crudely speaking these magic angles are given for an orthorhombic approximation by,

$$\tan\phi = \frac{m}{n}\frac{b}{c} \tag{28}$$

where ϕ is the angle for H in the b^*-c^* plane from the c^* axis and n and m integers. Under magnetic field in general, the 3D electron motion along the 1D axis follows a complex trajectory winding around the 1D axis with incommensurate periods along b and c unless the field is tilted from the c^* by an angle satisfying Eq. (28). When the two trajectories become commensurate, anomalies of magnetoresistance are expected at magic angles according to Eq. (28) for example at 29.6° and 48.7° for $m/n = 1$ or 2 respectively with the $(TMTSF)_2ClO_4$ lattice parameters at low temperature [475].

The first experimental confirmation of these angular resonances came in 1991 with the observation of fine structures superimposed on the angular dependence of magnetoresistance in the metallic phase of $(TMTSF)_2ClO_4$ [476,477]. Weak dip structures are clearly observed around ± 48° and ± 65° in $(TMTSF)_2ClO_4$ [476] with similar results in Ref. [477] at magnetic fields lower than any threshold field for the stabilization of the FISDW phase [476]. This hypothesis is consistent with the fact that the unit cell of $(TMTSF)_2ClO_4$ is doubled along b at low temperature after the ordering of the ClO_4^- anions. More recent results have been published by W. Kang and colleagues, see Fig. 128 where the difference between the position of the oscillations in $(TMTSF)_2ClO_4$ and $(TMTSF)_2PF_6$ is made clear.

Although the position of the angular anomalies agrees with the theory [474], there is still a contradiction with their sign since the experiments show a suppression of the resistivity instead of the enhancement predicted by Lebed's theory [473] although dips derived from Osada's theory [478].

Until now the Lebed's angular oscillations depend only on the geometry of the Q1D lattice and do not provide any information about the band structure of the materials. However, the band structure parameters become relevant for an other kind of oscillations, when the magnetic field is rotated from a to c^* in the plane parallel to $a-c^*$ as shown in Fig. 129.

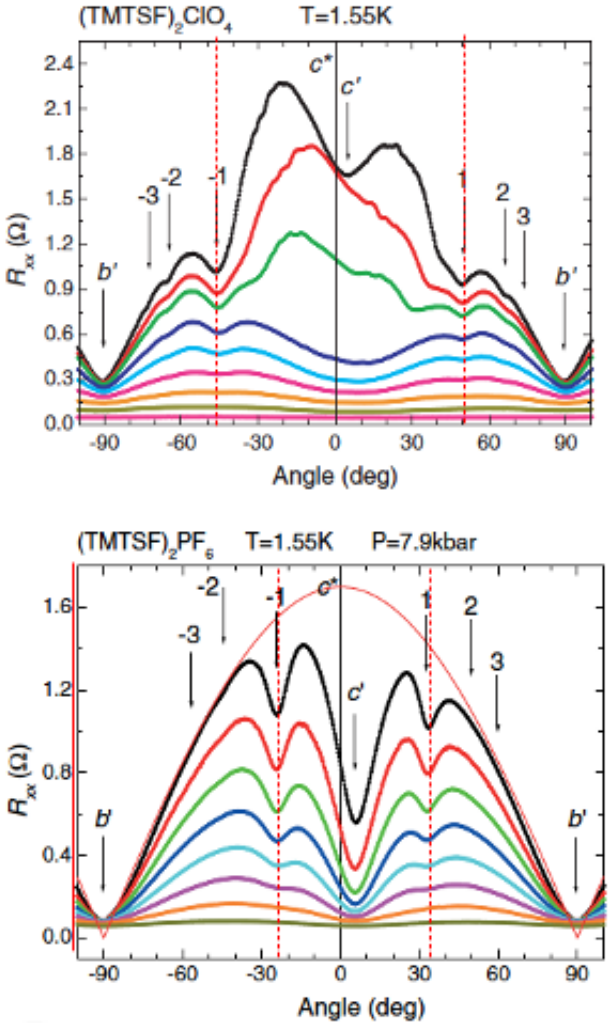

Figure 128. Angular magnetoresistance ρ_{xx} of $(TMTSF)_2ClO_4$ (top) and $(TMTSF)_2PF_6$ under 7.9 kbar(bottom). Source: [452]. Arrows indicate the position of magic angles proposed by Lebed for the respective compounds. Source: [312]. Magnetic fields start from 1T and increase by steps of 1T. ©(2003) Elsevier. All rights reserved.

In such a situation, the resistance presents a major peak when the field is slightly tilted off the a axis. This is known as the Danner–Kang–Chaikin (DKC) oscillation (DKC) [479] as shown on Fig. 129.

Using the equation of motion for an electron in a uniform magnetic field, Danner et al. [479] managed to derive the time dependence of the velocity component $v_z(t)$ along z. Depending on the orientation of the magnetic field with respect to the quasi planar Fermi surface, the averaging of $v_z(t)$ over time is more or less efficient. When the field is parallel to the a axis, orbits traversing the Fermi surface along c average $v_z(t)$ to zero (such as orbits 1 on Fig. 129) and therefore do not contribute to the magneto-resistivity. When the magnetic field is tilted by a small angle θ the orbits follow a restricted path along c but move to infinity along the b direction (orbit 2 on Fig. 129). However, the averaging of $v_z(t)$ to zero is still particularly

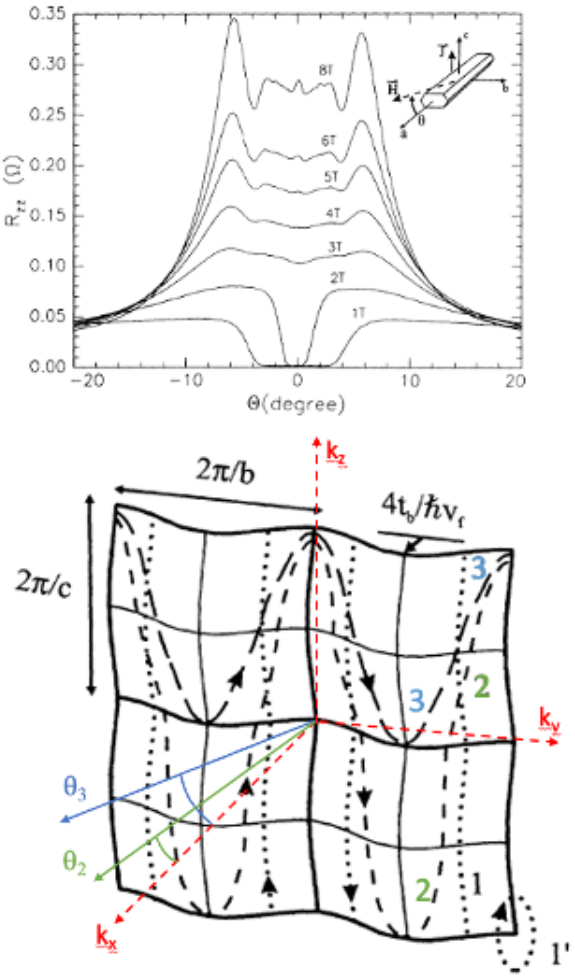

Figure 129. (Top) Angular dependence of the c axis resistance for a rotation in the $a-c^*$ plane at a temperature of 0.5 K. Above 4 T the angular dependence is no longer influenced by superconductivity according to the data in Fig. 78. Superimposed to the semi-classical Boltzmann angular dependence, a primary spike of resistance is observed at $\pm$ 6° which, is related to the transverse coupling t_b and possibly a secondary spike around $\pm$ 2° developing at 8T. The small spike visible at $\theta = \pm 0°$ enables the measurement of the tunneling coupling t_c between $a-b$ planes. (Bottom) Some possible orbits according to the field orientation in the $a-c^*$ plane, *see* text for details. Sources: [479, Figs. 1, 2 p. 3715].

efficient when the orbit sweeps periodically an integral number of lattice points along c as shown by the path 3 on Fig. 129 which sweeps one Brillouin zone leading in turn to a strong spike of angular magnetoresistance at an angle corresponding to θ_3 in the figure. Path 3 can be approximated by the cross section of the Fermi surface by a plane tilted θ_3 degrees from the normal. Therefore, $\tan\theta_3$ amounts to $\approx (4t_b/\hbar v_F)/(2\pi/c)$ and provides information about t_b/v_F. Given the existence of a magnetoresistance peak around $\pm$ 6°, a value of $t_b = 12$ meV is then derived (with $v_F = 1.8 \times 10^5$ m/s). A much weaker peak is also visible around $\pm$ 2° under the

highest field. This result is in agreement with the more quantitative treatment according to which anomalies are given by Bessel function zeros [479]. In addition the small peak observed at $\theta = 0°$ has been taken as an evidence for a coherent transport along the least conductive direction in line with similar findings in 2D organic compounds when a magnetic field is aligned parallel to the 2D layers [480].

The DKC oscillations can therefore provide informations on the parameters of the electronic structure namely t_b = 12 meV and t_c = 0.8 meV for $(TMTSF)_2ClO_4$ [479] and t_b = 32.5 meV for $(TMTSF)_2PF_6$ [481]. The difference by a factor of about 2 between b axis couplings of $(TMTSF)_2ClO_4$ and $(TMTSF)_2PF_6$ has to be considered in the context of the ClO_4^- ordering reducing the coupling $\sim 1/2$ from its room temperature value. Similar magnetoresistance studies along the $a-c^*$ plane on $(TMTSF)_2PF_6$ under pressure adding a small field along the b direction have suggested that this compound, unlike $(TMTSF)_2ClO_4$, could be a marginal Fermi liquid [481].

The section about angular magnetoresistance cannot be concluded without mentioning the anomaly of magnetoresistance when the magnetic field is rotated in the most conducting $a-b$ plane (the so-called third angular oscillation) [482]. Under such conditions, ρ_{zz} reveals a single kink behaviour at an angle measured from the a axis in the vicinity of 15°. This phenomenon has been related to the vanishing above a critical tilt angle of the closed orbits existing on the sides of the Q1D surface with an incomplete cancellation of the v_z carrier velocity when the field is weakly tilted from the normal axis, *see* top of Fig. 130. The value of the critical angle being a measure of the ratio t_b/t_a is shown in Fig. 130 to increase under pressure as the conductor becomes more 2D coupled. A similar behaviour has been reported in $(TMTSF)_2PF_6$ [483] and in other Q1D conductors [484].

These studies of transport as a function of a controlled orientation of the magnetic field have provided an overview of the generality of the method and its usefulness in gaining knowledge of the band parameters.

5. General Conclusion

This short retrospective for the search of superconductivity in organic matter has been based on an historical approach since we feel it is instructive to see how the whole story has developed from novel, stimulating and sometime provocative theoretical statements leading finally to the discovery of the first organic superconductor thanks to a very productive work between Chemistry and Physics communities over the past 50 years. The results described in this review which have enabled a comparison with theoretical models could not have been obtained without a sustained effort in the synthesis and growth of single crystals of very good quality.

Thanks to the determining role of high pressure governing their physical properties, organic conductors (and superconductors) have shown their interest compared to high T_c cuprates in terms of purity and variety of phenomena which can be studied in a single system keeping both structure and chemical purity constant.

It has been claimed in 2000 that the physics of organics including superconductivity could be reproduced without the burden of chemistry and high pressure techniques by simply tuning the carrier concentration using a field effect technique. We all wished that this could be true, but it turned out one year later that the claims were fraudulent. However, when the storm calmed down, more fruitful research began a few years later trying to fabricate organic electronic devices. Some of them will be reported shortly in the next section of this overview.

As early as 1974 Aviram and Ratner had considered the use of molecules as components of electronic circuitry and suggested according to a calculation the feasibility of such molecular devices [53]. It is not the goal of the present article to cover the vast domain of organics electronics which is exhaustively presented in the recent texbook by Alcacer [486]. However, we wish to

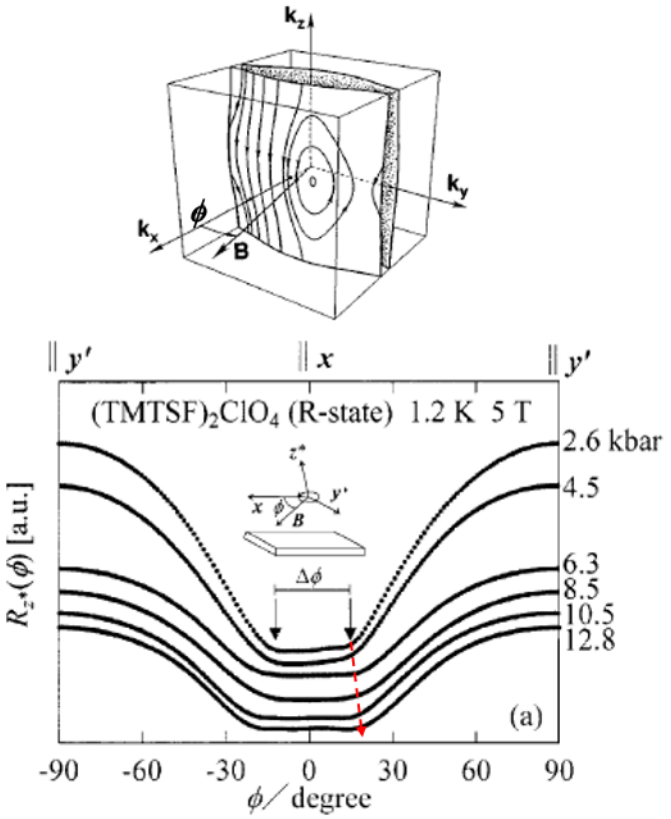

Figure 130. (Top) Semiclassical electron orbits on the warped Fermi surface under magnetic field tilted by an angle ϕ from the normal to the surface. (Bottom) Angular dependence of ρ_{zz} in slowly cooled $(TMTSF)_2ClO_4$ at 1.2 K. The dashed red line shows how the ratio t_b/t_a is increasing under pressure. Sources: (Top) [482, Fig. 2 p. 5263], [485, (Bottom) Fig. 1a p. 56]. ©(2003) Elsevier. All rights reserved. ©American Physical Society and the authors. All rights reserved.

emphasize only in a few words in this conclusion about the fabrication of prototype organic field effect transistors because they are directly inspired by the diversified physical properties of the 2D organics presented in Sec. 4.6.

Taking advantage of the proximity between insulating and superconducting phases which is evidenced by the phase diagram of $\kappa-(ET)_2X$ compounds [399], the control of the ground state of organic materials via the application of a gate voltage turned out to be successful [487, 488].

The low temperature state of the device depends on both chemical nature of the bulk and substrate (in addition to cooling rate) since what matters is the differential contraction between bulk and substrate [489, 490], *see* Fig. 107. The use of the various physical properties of these organic conductors appears therefore very promising for the fabrication of future devices.

A perfect illustration for the scientific interest of organic conductors is provided by the amount of knowledge and new physical concepts which came out of the studies of organic superconductors.

To summmarize, both experimental and theoretical results point to the contribution of electron correlations to the SC pairing problem. The extensive experimental evidence in favour of the emergence of superconductivity in the $(TM)_2X$ family next to the stability pressure threshold for the Slater-Overhauser antiferromagnetism has shown the need for a unified description of all

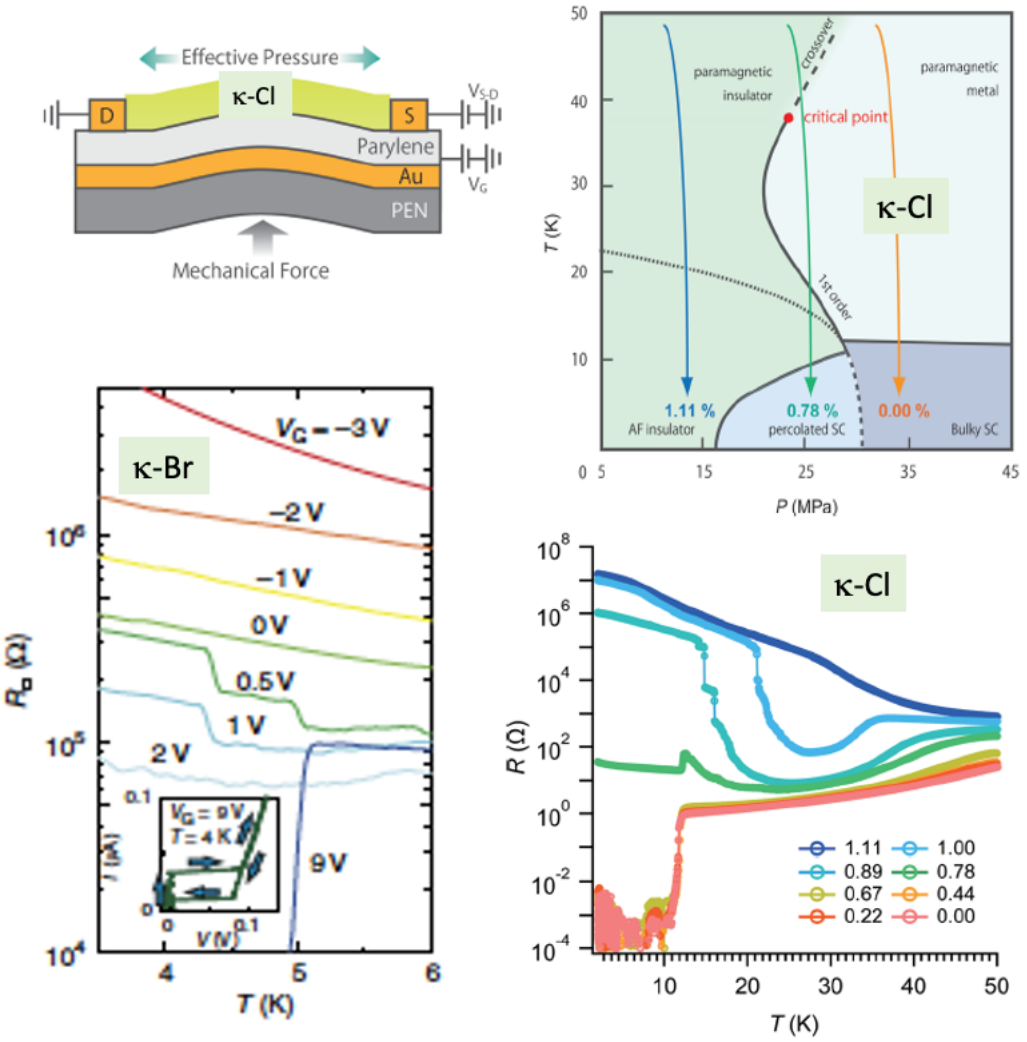

Figure 131. Organic FET devices based on κ-$(ET)_2X$. (Top, left) A thin layer of $\kappa-(ET)_2Cl$ is deposited on a substrate of polyethylene naphtalate sheet with thermally evaporated Au-gate electrodes and parylene gate-dielectric. Given the differential thermal contraction between the bulk sample and the substrate, cooling the device without any strain (0.00%), drives it into the SC state at low temperature (Bottom, right), while the bulk sample SC phase is stable only above 30 Mpa (= 300 bar) [399]. Increasing the strain (up to 1.11%) at high temperature and cooling down (Top, right), moves the device towards the AF insulating state. Sources: [487, Figs. 1a, 3ac]. An other FET device using κ-$(ET)_2Br$ on top of a metallic Nb-doped $SrTiO_3$ substrate covered with a 28 nm of Al_2O_3 dielectric layer grown by atomic deposition showing the stabilization of the SC state under a gate voltage of 9V and switching to an insulating behaviour at negative gate voltages (Bottom, left). Source: [488, Fig. 2 p. 4].

electronic excitations that lies at the core of both density-wave and SC correlations. In this matter, the recent progresses of the renormalization group method for the 1D-2D electron gas model have resulted in predictions about the possible symmetries of the SC order parameter when a purely electronic mechanism is involved, predictions that often differ from phenomenologically based approaches to superconductivity but are in fair agreement with recent experimental findings.

Firstly, the SC order parameter is displaying lines of nodes that are governing the stability against impurity and the thermodynamics of the SC phase. Important constraints on the nodal position have been obtained by the field angular dependence of the specific heat.

Secondly, electron scattering in the metallic phase above T_c suggests the existence of strong antiferromagnetic fluctuations leading to the possibility of a spin-mediated pairing in the SC phase. The pairing mechanism behind organic superconductivity is likely different from the proposal made by Little, but it is nevertheless a phonon-less mechanism, at least in $(TM)_2X$ superconductors.

What is also emerging from the work on these prototype 1D organic superconductors is their very simple electronic structure with only a single band at the Fermi level, no prominent spin orbit coupling and an extremely high chemical purity and stability.

They should be considered in several respects as very simple model systems to inspire the physics of the more complex high T_c superconductors, especially for pnictides and electron-doped cuprates.

Most concepts discovered in these simple low-dimensional conductors may also become of interest for the study of other 1D or Q1D systems such as carbon nanotubes, artificial 1D structures, the black bronze superconductor $Li_{0.9}Mo_6O_{17}$ with Mo-O chains [491], the newly-discovered telluride superconductor $Ta_4Pd_3Te_{16}$ with Ta-Pd chains [492], and the recently discovered $A_2Cr_3As_3$ (A = K, Rb, Cs) materials comprising $[(Cr_3As_3)^{-2}]_\infty$ chains [493]. It should be noted that the electronic anisotropy of the latter two classes of compounds seems to be weaker than originally expected and much weaker than those of the Bechgaard superconductors. Nevertheless, unconventional behaviours, such as possible nodal superconductivity in $Ta_4Pd_3Te_{16}$ [494] and unusually large H_{c2} in $Li_{0.9}Mo_6O_{17}$ [495] and $A_2Cr_3As_3$ [493, 496, 497], resemble those observed in $(TM)_2X$ and thus it is interesting to explore the common nature of Q1D superconductivity amongst a wide class of materials.

In addition, it might be profitable to reconsider the properties of copper-free superconducting perovskites such as the Sr_2RuO_4 type [498] in the light of the properties of quasi-1D organic superconductors presented in this overview. Although the electronic structure of these compounds are two dimensional with three bands crossing the Fermi level instead of a single band in organics, many of their electronic properties [325] are very similar to those observed in the far more simple Q1D conductors, e.g. temperature dependence of transport along the stacking axis, specific heat in the superconducting state, the sensitivity of T_c to impurities [499] or the behaviour of T_c under pressure [500], the existence of a FFLO state [501], not to mention recent NMR results which are favoring singlet over triplet superconducting pairing [502–504]. A new visit to Sr_2RuO_4 taking into account experimental results on Q1D superconductors and the theories that explain them successfully, would now be very valuable.

Two dimensional organic superconductors although not extensively reviewed in the present article have been very popular due to the possibility to stabilize superconductivity up to 10 K even under ambient pressure and also to the great diversity of stable phases which can be achieved depending on the chemical components. It has been shown that the optimized location for the superconducting T_c is the with a Mott localization resulting from a compromise between the interchain coupling and the strength of the correlations. They also revealed the likeliness of an unconventional pairing mechanism which makes them model materials for 2D superconductors.

And last but not least, the lesson to be learned from these 1D and 2D organic superconductors is that the term unconventional superconductivity currently used should be taken with a grain of salt and possibly no longer be used. The proper denomination should be more in line with the results of research in 1D and 2D organics as well as in cuprates, etc. and qualify superconducting materials according to their Cooper pairs binding mechanism carried out either via phonons or via an exchange of magnetic fluctuations.

Concluding this retrospective overview, it seems appropriate to quote the words of V. L. Ginzburg in 1989 [505]. Talking about organic superconductors and intercalated layered superconductors, he wrote: "I believe that it was undoubtedly the discussion of the possible exciton mechanism of superconductivity that stimulated the search for such superconductors and studies of them". In addition, the other statement of Ginzburg: "the organic superconductors (produced for the first time in 1980) are clearly interesting by themselves or, to be more precise, irrespective of the high T_c problem" cannot be more appropriate.

The reader may realize that a lot has been accomplished since 1991 when P. W. Anderson declared in a conversation with R. Schrieffer reported by *Physics Today* [506] "Organic superconductors are still almost a complete mystery".

It is also a pleasure to agree with Paul Chaikin and cite his presentation celebrating the fiftieth anniversary of the BCS theory in 2007 at University of Illinois "Quasi 1D organic $(TMTSF)_2PF_6$ superconductor is the most interesting material ever discovered".

Declaration of interests

The authors do not work for, advise, own shares in, or receive funds from any organization that could benefit from this article, and have declared no affiliations other than their research organizations.

Acknowledgments

The research activity on low dimensional conductors has involved researchers from all continents over a period of more than 50 years. Within the framework of this worldwide cooperation, the Laboratoire de Physique des Solides de l'Université de Paris-Sud à Orsay and the HC Øersted Institute at Copenhagen together with the Département de Physique de l'Université de Sherbrooke have played a major role that we wish to underline and acknowledge.

CNRS, French Ministry of Research, Université Paris-Sud and the European Commission are acknowledged for the support of this research.

The particular characteristic of the Orsay laboratory, of which Jacques Friedel was one of the co-founders in 1959, was its multidisciplinary character, bringing together physical measurements (electronic and structural properties of solids, condensed matter theory and chemistry of materials with an efficient internal cooperation. As the partnerships of the Orsay laboratory have been so numerous, we will rather mention countries and institutions involved.

To be noticed is the openness of the Orsay laboratory to numerous national cooperations (Montpellier, Rennes, Nantes and Angers for chemistry, Marseilles for tunnel junctions measurements, Grenoble and Toulouse for high magnetic fields physics), as well as international cooperations (Great Britain with the Cavendish laboratory at Cambridge, Switzerland with the Institut de Physique at Geneva and Ecole Polytechnique Fédérale at Lausanne, Germany with the University at Stuttgart and the Max Planck Institut at Heidelberg, Croatia with the Institute of Physics at Zagreb, Tunisia with the University at Tunis, Japan with the Universities of Kyoto, Tsukuba Research Centers and Osaka and Gakushuin University at Tokyo, Russia with the Landau Institute at Moscow, Korea with the Ewha Women University at Seoul, Israel with the Hebrew University,

the United States with the University of California at Los Angeles and the National High Magnetic Fields Laboratory at Tallahassee, Canada with Mc Master University at Hamilton, Portugal with the Department of Chemistry at Sacavem and Instituto Superior Tecnico at Lisbon, Spain with the University at Barcelona). These cooperations have enabled to welcome a large number of brilliant thesis students and international post-doctoral visitors who, once back in their countries, have successfully pursued their activities in the field.

We wish to make a special mention to our colleagues who have contributed in a decisive way to the progress of the field and who sadly passed away much too soon; Gen Soda who died accidentally at the Institute for Molecular Science, Okazaki in 1987, Klaus Bechgaard (1945-2017) without whom this field would not have been able to develop and Heinz Schulz (1954-1998) one of the major contributors to theoretical low dimensional physics and François Creuzet (1957-2020) whose NMR contribution is fundamental to the understanding of these materials and recently Robert Comés (1937-2022) who has been the first with his collaborators to use diffuse X-ray scattering techniques to reveal charge density wave fluctuations in the one-dimensional compound, platinum chains, KCP. It is this result obtained in 1973 at Orsay which triggered the beginning of the study of one-dimensional conductors, rapidly extended to organic conductors.

Supplementary data

Supporting information for this article is available on the journal's website under https://doi.org/10.5802/crphys.164 or from the author.

References

[1] H. K. Onnes, "Further experiments with Liquid Helium. On the change of Electrical Resistance of Pure Metals at very low Temperatures, etc. The Disappearance of the resistance of mercury", in *KNAW Proceedings*, vol. 14 I, KNAW; Johannes Müller, Amsterdam, 1911, online at https://dwc.knaw.nl/DL/publications/PU00013124.pdf, p. 113-115.

[2] H. K. Onnes, "Further experiments with Liquid Helium. On the electrical resistance of Pure Metals etc. On the Sudden Change in the Rate at which the Resistance of Mercury Disappears", in *KNAW Proceedings*, vol. 14 II, KNAW; Johannes Müller, Amsterdam, 1911-1912, online at https://dwc.knaw.nl/DL/publications/PU00013242.pdf, p. 818-821.

[3] P. H. E. Meijer, "Kamerlingh Onnes and the discovery of superconductivity", *Am. J. Phys.* **62** (1994), p. 1105-1108.

[4] J. Bardeen, L. N. Cooper, J. R. Schrieffer, "Microscopic Theory of Superconductivity", *Phys. Rev.* **106** (1957), p. 162-164.

[5] J. Bardeen, L. N. Cooper, J. R. Schrieffer, "Theory of Superconductivity", *Phys. Rev.* **108** (1957), p. 1175-1204.

[6] H. N. McCoy, W. C. Moore, "Organic amalgams: substances with metallic properties composed in part of non-metallic elements", *J. Am. Chem. Soc.* **33** (1911), p. 273-292.

[7] F. London, H. London, "Supraleitung und Diamagnetismus", *Physica* **2** (1935), p. 341-354.

[8] L. Pauling, "The diamagnetic anisotropy of aromatic molecules", *J. Chem. Phys.* **4** (1936), p. 673-677.

[9] F. London, "Théorie quantique des courants interatomiques dans les combinaisons aromatiques", *J. Phys. Radium* **8** (1937), no. 10, p. 397-409.

[10] F. London, "Supraconductivity in Aromatic Compounds", *J. Chem. Phys.* **5** (1937), p. 837-838.

[11] H. Bouchiat, G. Montambaux, "Persistent currents in mesoscopic rings : ensemble averages and half-flux-quantum periodicity", *J. Phys. I France* **50** (1989), p. 2695-2707.

[12] H. J. Keller (ed.), *Low-Dimensional Cooperative Phenomena and the Possibility of High Temperature Superconductivity*, NATO Advanced Study Institutes Series. Series B : Physics, vol. 7, Plenum Press, 1975, Lectures presented at the 1974 Nato Advanced Study Institute, held in Starnberg, Germany, September 3-15, 1974.

[13] D. D. Eley, G. D. Parfitt, M. J. Perry, D. H. Taysum, "The Semiconductivity of Organic Substances", *Trans. Faraday Soc.* **49** (1953), p. 79-86.

[14] H. Akamatu, H. Inokuchi, "On the Electrical Conductivity of Violanthrene, Iso-Violanthrene, and Pyranthrene", *J. Chem. Phys.* **18** (1950), no. 6, p. 810-811.

[15] H. Inokuchi, "The Effect of Pressure on the Semi-conductivity of Isoviolanthrone", *Bull. Chem. Soc. Jpn.* **28** (1955), no. 8, p. 570-572.

[16] H. Akamatu, H. Inokuchi, Y. Matsunaga, "Electrical Conductivity of the Perylene-Bromine Complex", *Nature* **173** (1954), p. 168-169.

[17] D. S. Acker, R. J. Harder, W. R. Hertler, W. Mahler, L. R. Melby, R. E. Benson, W. E. Mochel, "7,7,8,8-Tetracyanoquinodimethane and its electrically conducting Anion-Radical Derivatives", *J. Am. Chem. Soc.* **82** (1960), p. 6408-6409.

[18] J. J. André, A. Bieber, F. Gautier, "Physical properties of highly anisotropic systems: Radical-Ion salts and charge transfer complexes", *Ann. Phys.* **1** (1976), p. 145-256.

[19] L. R. Melby, R. J. Harder, W. R. Hertler, W. Mahler, R. E. Benson, W. E. Mochel, "Substituted Quinodimethans. Anion-radical Derivatives and Complexes of 7,7,8,8-Tetracyanoquinodimethan", *J. Am. Chem. Soc.* **84** (1962), p. 3374-3387.

[20] I. F. Shchegolev, L. I. Burarov, A. V. Zvarykina, R. B. Lyubovskii, "Conduction mechanism of highly-conducting organic complexes based on TTF-TCNQ", *JETP Lett.-USSR* **8** (1968), p. 218-+.

[21] I. F. Shchegolev, "Electric and Magnetic Properties of Linear Conducting Chains", *Phys. stat. sol. (a)* **12** (1972), p. 9-45.

[22] V. L. Ginzburg, "The Problem of High Temperature Superconductivity", *Contemp. Phys.* **9** (1968), no. 4, p. 355-374.

[23] L. R. Melby, "Salts derived from the 7,7,8,8-Tetracyanoquinodimethans. Anion-radical and Benzologues of Quaternary Pyrazinium Cations", *Can. J. Chem.* **43** (1965), p. 1448-1453.

[24] A. J. Epstein, A. F. Garito, S. D. Etemad, A. J. Heeger, "Metal–Insulator Transition in an organic Solid: Experimental Realization of the one-dimensional Hubbard Model", *Solid State Comm.* **9** (1971), p. 1803-1808.

[25] F. Devreux, M. Nechtchein, "Nuclear relaxation in 1D conductors", in *Proc. of the International Conference of Quasi-One-Dimensional Conductors I* (S. Barišić, A. Bjeliś, J. R. Cooper, B. Leontić, eds.), Lectures Notes in Physics, vol. 95, Springer, 1978, p. 145-152.

[26] S. Flandrois, D. Chasseau, "Longueurs de Liaison et Transfert de Charge dans les Sels du Tetracyanoquinodiméthane", *Acta Cryst. B* **B33** (1977), p. 2744-2750.

[27] R. Comès, M. Lambert, H. Launois, H. R. Zeller, "Evidence for a Peierls Distortion or a Kohn Anomaly in One-Dimensional Conductors of the Type $K_2Pt(CN)_4Br_{0.30}xH_2O$", *Phys. Rev. B* **8** (1973), p. 571-575.

[28] F. Denoyer, R. Comès, A. F. Garito, A. J. Heeger, "X-ray diffuse sattering evidence for a phase transition in TTF-TCNQ", *Phys. Rev. Lett.* **35** (1975), p. 445-449.

[29] J.-P. Pouget, R. Comès, A. J. Epstein, J. S. Miller, "X-ray observation of cross over of $2k_F$ to $4k_F$ scattering in $(NMP)_xPhen_{1-x}(TCNQ)0.5 \leq 1 \leq 1$", *Mol. Cryst. Liq. Cryst.* **85** (1982), no. 1–4, p. 203-213.

[30] G. Hardy, J. K. Hulm, "Superconducting Silicides and Germanides", *Phys. Rev.* **87** (1953), p. 884.

[31] B. T. Matthias, T. H. Geballe, S. Geller, E. Corenwitz, "Superconductivity of Nb_3Sn", *Phys. Rev* **95** (1954), p. 1435.

[32] J. R. Gavaler, "Superconductivity in Nb-Ge films above 22 K", *Appl. Phys. Lett* **23** (1973), p. 480-482.

[33] B. T. Matthias, "The search for high-temperature superconductors", *Physics Today* **24** (1971), p. 23-28.

[34] M. Weger, "The Electronic Band Structure of V_3Si and V_3Ga", *Reviews of Modern Physics* **36** (1964), p. 175-177.

[35] J. Labbé, J. Friedel, "Instabilité électronique et changement de phase cristalline des composés du type V_3Si à basse température", *J. Phys. I France* **27** (1966), p. 153-165.

[36] J. Labbé, S. Barišić, J. Friedel, "Strong-coupling superconductivity in V_3X type of Compounds", *Physical Review Letters* **19** (1967), no. 18, p. 1039-1041.

[37] G. M. Eliashberg, "Interactions between Electrons and Lattice vibrations in a Superconductor", *Sov. Phys. JETP* **11** (1960), no. 3, p. 696-702.

[38] W. Kohn, J. M. Luttinger, "New Mechanism for Superconductivity", *Phys. Rev. Lett.* **15** (1965), p. 524-526.

[39] J. Friedel, "Metallic alloys", *Nuovo Cim.* **7** (1958), no. 2, p. 287-311.

[40] W. A. Little, "Possibility of Synthesizing an Organic Superconductor", *Phys. Rev. A* **134** (1964), p. A1416-A1424.

[41] D. Jerome, "Historical Approach to Organic Superconductivity", in *The Physics of Organic Superconductors and Conductors* (A. G. Lebed, ed.), Springer Series in Materials Science, vol. 110, Springer, 2008.

[42] W. A. Little, "Superconductivity at Room Temperature", *Scientific American* **212** (1965), no. 2, p. 21-27.

[43] V. L. Ginzburg, "High Temperature Superconductivity", *J. Polymer. Sci. C.* **29** (1970), p. 3-16.

[44] J. Ladik, G. Biczó, J. Redly, "Possibility of Superconductive-Type Enhanced Conductivity in DNA at Room Temperature", *Phys. Rev.* **188** (1969), p. 710-715.

[45] W. A. Little, *International symposium on the physical and chemical problems of possible organic superconductors*, Physics Department, Stanford University, 1969.

[46] W. A. Little, "The exciton mechanism in superconductivity", *J. polym. sci., Polym. symp.* **9** (1970), p. 17-26.

[47] Y. A. Byschkov, L. P. Gorkov, I. E. Dzyaloshinskii, "Possibility of Superconductivity type phenomena in a one-dimensional system", *Sov. Phys. JETP* **23** (1966), p. 489-501.

[48] L. D. Landau, E. M. Lifshitz, *Statistical Physics*, Pergamon Press, London, 1959, 482 pages.

[49] N. D. Mermin, H. Wagner, "Absence of ferromagnetism or antiferromagnetism in one or two-dimensional isotropic Heisenberg models", *Phys. Rev. Lett.* **17** (1966), p. 1133-1136.

[50] F. Wudl, G. M. Smith, E. J. Hufnagel, "Bis−1,3 =dithiolium Chloride: an Unusually Stable Organic Radical Cation", *Chem. Comm.* (1970), p. 1453-1454.

[51] F. Wudl, D. Wobschall, E. J. Hufnagel, "Electrical Conductivity by the Bis-l,3-dithiole-Bis-1,3-dithiolium System", *J. Am. Chem. Soc.* (1972), p. 670-672.
[52] M. R. Bryce, "Tetrathiafulvalenes as pi-Electron Donors for Intramolecular Charge-Transfer Materials", *Adv. Mater.* **1** (199), p. 11-23.
[53] A. Aviram, M. A. Ratner, "Molecular rectifiers", *Chem. Phys. Lett.* **29** (1974), p. 277-283.
[54] M. Bendikov, F. Wudl, D. M. Perepichka, "Tetrathiafulvalenes, Oligoacenenes, and Their Buckminsterfullerene Derivatives: The Brick and Mortar of Organic Electronics", *Chem. Rev.* **104** (2004), p. 4891-4945.
[55] S. J. La Placa, P. W. R. Corfield, R. Thomas, B. A. Scott, "Non-integral charge transfer in an organic metal: The structure and stability range of (TTF)Br_x", *Solid State Comm.* **17** (1975), p. 635-638.
[56] P. M. Chaikin, R. A. Craven, S. D. Etemad *et al.*, "Commensurate Peierls transition in a quasi-one-dimensional compound: The bromide salt of tetrathiafulvalene (TTF)", *Phys. Rev. B* **22** (1980), p. 5599-5605.
[57] L. B. Coleman, M. J. Cohen, D. J. Sandman, F. G. Yamagishi, A. F. Garito, A. J. Heeger, "Superconducting Fluctuations and the Peierls instability in an organic solid", *Solid State Comm.* **12** (1973), p. 1125-1132.
[58] J. Ferraris, D. O. Cowan, W. Walatka, J. H. Perlstein, "Electron Transfer in a New Highly Conducting Donor-Acceptor Complex", *J. Am. Chem. Soc* **95** (1973), p. 948-949.
[59] A. A. Bright, A. F. Garito, A. J. Heeger, "Optical properties of TTF-TCNQ in the visible and infrared", *Solid State Comm.* **13** (1973), p. 943-948.
[60] T. J. Kistenmacher, T. E. Phillips, D. O. Cowan, "The Crystal Structure of the 1:1 radical cation-radical anion salt of 2,2′-bis-*l*,3-dithiole (TTF) and 7,7,8,8-tetracyanoquinodimethane (TCNQ)", *Acta Cryst. B* **30** (1974), p. 763-768.
[61] K. Bechgaard, C. S. Jacobsen, K. Mortensen, H. J. Pedersen, N. Thorup, "The properties of five highly conducting salts derived from TMTSF", *Solid State Comm.* **33** (1980), p. 1119-1125.
[62] R. P. Van Duyne, T. W. Cape, M. R. Suchanski, A. R. Seidle, "Determination of the Extent of Charge Transfer in Partially Oxidized Derivatives of Tetrathiafulvalene and Tetracyanoquinodimethan by Resonance Raman Spectroscopy", *J. Phys. Chem.* **90** (1986), p. 739-743.
[63] H. Anzai, "Growth of Large-Crystals of Charge-Transfer complex, Tetrathiofulvalene-Tetracyanoquinodimethane (TTF-TCNQ)", *J. Cryst. Growth.* **33** (1976), p. 185-187.
[64] "Molecular Conductors", in *Chem. Rev.* (P. Batail, ed.), vol. 104, 2004, p. 4887-5782.
[65] R. L. Greene, J. J. Mayerle, R. Schumaker, G. Castro, P. M. Chaikin, S. D. Etemad, S. J. La Placa, "The Structure, Conductivity, and Thermopower of HMTTF-TCNQ", *Solid State Comm.* **20** (1976), p. 943-946.
[66] A. A. Bright, A. F. Garito, A. J. Heeger, "Optical conductivity studies in a one-dimensional organic metal: Tetrathiofulvalene tetracyanoquinodimethan (TTF-TCNQ)", *Phys. Rev. B* **10** (1974), p. 1328-1342.
[67] P. Calas, J.-M. Fabre, E. Toreilles, L. Giral, "Synthèse de dérivés du tétrathiofulvalène", *C. R. Hebd. Seances Acad. Sci. C* **280** (1975), p. 901-903, online at https://gallica.bnf.fr/ark:/12148/bpt6k6224856m/f51.item.
[68] G. Brun, S. Peytavin, B. Liautard, M. Maurin, E. Toreilles, J.-M. Fabre, L. Giral, "Sur quelques nouveaux complexes organiques à propriétés anisotropes", *C. R. Hebd. Seances Acad. Sci. C* **284** (1977), no. 5, p. 211-213, online at https://gallica.bnf.fr/ark:/12148/bpt6k62367869/f223.item.
[69] J. C. Scott, A. F. Garito, A. J. Heeger, "Magnetic susceptibility studies of tetrathiofulvalene-tetracyanoquinodimethan TTF-TCNQ and related organic metals", *Phys. Rev. B* **10** (1974), p. 3131-3139.
[70] K. Bechgaard, D. O. Cowan, A. N. Bloch, "Synthesis of the Organic Conductor Tetramethyltetraselenofulvalenium, 7,7,8,8-tetracyano-p-quinodimethanide (TMTSF–TCNQ)[4,4′,5,5′-tetramethyl-Δ2,2′-bis-1,3-diselenolium 3,6-bis-(dicyanomethylene)cyclohexadienide]", *J. Chem. Soc., Chem. Commun.* (1974), p. 937-938.
[71] E. M. Engler, V. M. Patel, "Structure Control in Organic Metals. Synthesis of Tetraselenofulvalene and Its Charge Transfer Salt with Tetracyano-p -quinodimethane", *J. Am. Chem. Soc* **96** (1974), p. 7376-7378.
[72] K. Bechgaard, D. O. Cowan, A. N. Bloch, "Stabilization of the organic metallic state: The Properties of Two Substituted Tetraselenafulvalenes and Their TCNQ Salts", *Mol. Cryst. Liq. Cryst.* **49** (1976), no. 32, p. 227-230.
[73] F. Wudl, D. E. Schafer, W. M. Walsh *et al.*, "A systematic study of an isomorphous series of organic solid state conductors based on tetrathiafulvalene", *J. Chem. Phys.* **66** (1977), p. 377-385.
[74] H. Strzelecka, L. Giral, J.-M. Fabre, E. Torreilles, G. Brun, "Nouvelle voie d'accès à des conducteurs organiques: Action du Thiocyanogene sur le Tetrathiofulvalene et le Tetramethyltetrathiofulvalene", *C. R. Hebd. Seances Acad. Sci. C* **284** (1977), no. 12, p. 463-465, online at https://gallica.bnf.fr/ark:/12148/bpt6k6216790n/f35.item.
[75] P. Delhaes, C. Coulon, J. Amiell, S. Flandrois, E. Toreilles, J.-M. Fabre, L. Giral, "Physical Properties of One Dimensional Conductors", *Mol. Cryst. Liq. Cryst.* **50** (1979), p. 43-58.
[76] A. A. Edelsack, D. U. Gubser, S. A. Wolf, "The rocky road to high temperature superconductivity", in *Novel Supercondcutivity* (S. A. Wolf, V. Z. Kresin, eds.), vol. 12, Plenum Press, New York, 1987, p. 1-8.
[77] J. G. Bednorz, K. A. Müller, "Possible High Tc Superconductivity in the BaLaCu0 System", *Z. Phys. B - Condensed Matter* **64** (1986), p. 189-193.
[78] K. Bechgaard, *Wikipedia*, https://en.wikipedia.org/wiki/Klaus_Bechgaard.
[79] C. S. Jacobsen, K. Mortensen, J. R. Andersen, K. Bechgaard, "Transport properties of some derivatives of tetrathiafulvalene-tetracyano-p-quinodimethane (TTF-TCNQ)", *Phys. Rev. B* **18** (1978), p. 905-921.

[80] V. N. Laukhin, A. I. Kotov, M. L. Khidekel, I. F. Shchegolev, E. B. Yagubskiĭ, "Metallic high pressure phase in tetraselenotetracene chloride $(TSeT)_2Cl$", *JETP Lett.* **28** (1978), no. 5, p. 284-287.
[81] K. Bechgaard, "$(TMTSF)_2X$ Salts: Preparation, Structure and Effect of the Anions", *Mol. Cryst. Liq. Cryst.* **79** (1982), p. 357-369, Proc International Conference on Low-Dimensional Conductors.
[82] P. Batail, K. Boubekeur, M. Fourmigué, J. C. P. Gabriel, "Electrocrystallization, an Invaluable Tool for the Construction of Ordered, Electroactive Molecular Solids", *Chem. Mater.* **10** (1998), p. 3005-3015.
[83] K. Bechgaard, D. Jerome, A. Moradpour, "Electrocrystallisation of organic superconductors", 2023, Video, Zenodo, online at https://doi.org/10.5281/zenodo.8064104.
[84] A. F. Garito, A. J. Heeger, "The Design and Synthesis of Organic Metals", *Acc. Chem. Res.* **7** (1974), p. 232-240.
[85] A. J. Berlinsky, J. F. Carolan, L. Weiler, "Band structure parameters for SolidTTF-TCNQ", *Solid State Comm.* **15** (1974), p. 795-801.
[86] D. Jerome, H. J. Schulz, "Organic conductors and superconductors", *Adv. Phys.* **31** (1982), p. 299-490.
[87] S. Shitzkovsky, M. Weger, H. Gutfreund, "Band Structure of TTF-TCNQ", *J. Phys. I France* **39** (1978), p. 711-717.
[88] D. Jerome, M. Weger, "Electronic properties of organic conductors: pressure effects", in *Chemistry and Physics of One-Dimensional Metals* (H. J. Keller, ed.), Plenum Press (New York), 1977, p. 341-367.
[89] G. Soda, D. Jerome, M. Weger, K. Bechgaard, E. Pedersen, "Spin relaxation and Magnetic susceptibility studies of HMTSF-TCNQ", *Solid State Comm.* **20** (1976), p. 107-113.
[90] R. E. Peierls, *Quantum Theory of Solids*, Oxford University Press, London, 1955.
[91] G. Lubkin, "Superconducting fluctuations at 60K?", *Physics Today* **May** (1973), p. 17.
[92] B. R. Patton, "Fluctuation Theory of the Superconducting Transition in Restricted Dimensionality", *Phys. Rev. Lett.* **27** (1971), no. 19, p. 1273-1276.
[93] S. D. Etemad, T. Penney, E. M. Engler, B. A. Scott, P. E. Seiden, "DC Conductivity in an Isostructural Family of Organic Metals", *Phys. Rev. Lett.* **34** (1975), p. 741-744.
[94] S. Barišić, "Rigid-Atom Electron-Phonon Coupling in the Tight-Binding Approximation", *Phys. Rev. B* **5** (1972), no. 3, p. 932-941.
[95] D. E. Schafer, F. Wudl, G. A. Thomas, J. P. Ferraris, D. O. Cowan, "Apparent Giant Conductivity peaks in an anisotropic medium TTF-TCNQ", *Solid State Comm.* **14** (1974), p. 347-351.
[96] G. A. Thomas, D. E. Schafer, F. Wudl *et al.*, "Electrical conductivity of tetrathiofulvalenium-tetracyanoquinodimethanide (TTF-TCNQ)", *Phys. Rev. B* **13** (1976), no. 11, p. 5105-5110.
[97] J. R. Cooper, J. Lukatela, M. Miljak, J.-M. Fabre, L. Giral, E. Aharon-Shalom, "Isotope Effect in the Peierls transition temperature of TTF-TCNQ", *Solid State Comm.* **25** (1978), p. 699-704.
[98] R. H. Friend, M. Miljak, D. Jerome, "Pressure dependence of the phase transitions in tetrathiafulvalene-tetracyanoquinodimethane: Evidence for a longitudinal lockin at 20 kbar", *Phys. Rev. Lett.* **40** (1978), p. 1048-1051.
[99] G. Soda, D. Jerome, M. Weger, J. Alizon, J. Gallice, H. Robert, J.-M. Fabre, L. Giral, "Electronic Properties of TTF-TCNQ: an NMR Approach", *J. Phys. I France* **38** (1977), p. 931-948.
[100] J. R. Cooper, D. Jerome, S. D. D. Etemad, E. M. Engler, "On the behaviour of TSF-TCNQ under pressure", *Solid State Comm.* **22** (1977), p. 257-263.
[101] P. M. Grant, R. L. Greene, G. C. Wrighton, G. Castro, "Temperature Dependence of the Near-Infrared Optical Properties of Tetrathiofulvalinium Tetracyanoquinodimethane TTF-TCNQ", *Phys. Rev. Lett.* **31** (1973), p. 1311-1314.
[102] N. P. Ong, A. M. Portis, "Microwave Hall effect in a quasi-one-dimensional system: Tetrathiafulvalenium-tetracyanoquinodimethanide TTF-TCNQ", *Phys. Rev. B* **15** (1977), p. 1782.
[103] M. J. Cohen, L. B. Coleman, A. F. Garito, A. J. Heeger, "Electrical conductivity of tetrathiofulvalinium tetracyanoquinodimethan TTF-TCNQ", *Phys. Rev. B* **10** (1974), no. 4, p. 1298-1307.
[104] D. Jerome, "Fluctuating collective conductivity and single particle conductivity in 1-D organic conductors", in *The Physics and Chemistry of Low Dimensional Solids* (L. Alcacer, ed.), D. Reidel, 1980, p. 123-142.
[105] J. Bardeen, "Superconducting Fluctuations in one-dimensional Organic Solids", *Solid State Comm.* **13** (1973), p. 357-359.
[106] D. Allender, J. W. Bray, J. Bardeen, "Theory of fluctuation superconductivity from electron-phonon interactions in pseudo-one-dimensional systems", *Phys. Rev. B* **9** (1974), no. 1, p. 119-129.
[107] H. Fröhlich, "On the theory of superconductivity: the one-dimensional case", *Proc. R. Soc. Lond. A* **223** (1954), p. 296-305.
[108] B. R. Patton, L. J. Sham, "Fluctuation conductivity in the incommensurate Peierls system", *Phys. Rev. Lett.* **35** (1974), no. 11, p. 638-641.
[109] S. Kagoshima, H. Anzai, K. Kajimura, T. Ishiguro, "Observation of the Kohn anomaly and the Peierls transition in TTF-TCNQ by X-ray scattering", *J. Phys. Soc. Jpn.* **39** (1975), no. 4, p. 1143-1144.
[110] R. Comès, S. M. Shapiro, G. Shirane, A. F. Garito, A. J. Heeger, "Neutron-Scattering Study of the 38 and 54K Phase Transitions in Deuterated Tetrathiafulvalene-Tetracyanoquinodimethane TTF-TCNQ", *Phys. Rev. Lett.*. **35** (1975), no. 22, p. 1518-1521.

[111] T. Takahashi, D. Jerome, F. Masin, J.-M. Fabre, L. Giral, "^{13}C NMR studies of TTF(^{13}C)-TCNQ", *J. Phys. C: Solid State Phys.* **17** (1984), p. 3777-3792.

[112] E. F. Rybaczewski, S. Smith, A. F. Garito, A. J. Heeger, B. G. Silbernagel, "^{13}C Knight shift in TTF-TCNQ ^{13}C: Determination of the local susceptibility", *Phys. Rev. B* **14** (1976), no. 7, p. 2746-2756.

[113] Y. Tomkiewicz, A. R. Taranko, J. B. Torrance, "Spin susceptibility of tetrathiafulvalene tetracyanofluinodimethane, TTF-TCNQ in the semiconducting regime: Comparison with conductivity", *Phys. Rev. B* **15** (1977), no. 2, p. 1017-1023.

[114] P. Bak, V. J. Emery, "Theory of the Structural Phase Transformations in Tetrathiafulvalene-Tetracyanoquinodimethane TTF-TCNQ", *Phys. Rev. Lett.* **36** (1976), p. 978-982.

[115] T. Nishiguchi, M. Kageshima, N. Ara-Kato, A. Kawazu, "Behavior of Charge Density Waves in a One-Dimensional Organic Conductor Visualized by Scanning Tunneling Microscopy", *Phys. Rev. Lett.* **81** (1998), no. 15, p. 3187-3190.

[116] Z. Z. Wang, J. C. Girard, C. Pasquier, D. Jerome, K. Bechgaard, "Scanning tunneling microscopy in TTF-TCNQ: Phase and amplitude modulated charge density waves", *Phys. Rev. B* **67** (2003), article no. 121401.

[117] N. A. Kato, M. Hara, H. Sasabe, W. Knoll, "An interpretation for the STM imaging of an organic molecule, tetrathiafulvalene–tetracyanoquinodimethane (TTF-TCNQ)", *Nanotechnology* **7** (1996), p. 122-127.

[118] E. Abrahams, J. Solyom, F. Woynarovich, "The Landau theory of phase transitions in TTF-TCNQ", *Phys. Rev. B* **16** (1977), p. 5238-5249.

[119] A. Bjelić, S. Barišić, "Commensurate Ordering in Tetrathiafulvalene-Tetracyanoquinodimethane", *Phys. Rev. Lett.* **37** (1976), p. 1517.

[120] R. Comès, G. Shirane, "X-ray scattering and Neuron scattering from one-dimensional conductors", in *Highly Conducting One-Dimensional Solids* (J. T. Devreese, ed.), Plenum Press, New York, 1979, p. 17-67.

[121] J.-P. Pouget, S. K. Khanna, F. Denoyer, R. Comès, A. F. Garito, A. J. Heeger, "X Ray Observation of $2k_F$ and $4k_F$ Scatterings in Tetrathiafulvalene-Tetracyanoquinodimethane (TTF-TCNQ)", *Phys. Rev. Lett.* **37** (1976), p. 437-440.

[122] J.-P. Pouget, "The Peierls instability and charge density wave in one-dimensional electronic conductors", *Comptes Rendus Physique* **17** (2016), p. 332-356.

[123] S. K. Khanna, J.-P. Pouget, R. Comes, A. F. Garito, A. J. Heeger, "X-ray studies of $2k_F$ and $4k_F$ anomalies in tetrathiafulvalene-tetracyanoquinodimethane (TTF-TCNQ)", *Phys. Rev. B* **16** (1977), no. 4, p. 1468-1479.

[124] V. J. Emery, "New Mechanism for a Phonon Anomaly and Lattice Distortion in Quasi One-Dimensional Conductors", *Phys. Rev. Lett.* **37** (1976), p. 107-110.

[125] J. Voit, H. J. Schulz, "Electron-phonon interaction and phonon dynamics in one-dimensional conductors", *Phys. Rev. B* **37** (1988), p. 10068-10085.

[126] H. Basista, D. A. Bonn, T. Timusk, J. Voit, D. Jerome, K. Bechgaard, "Far-infrared optical properties of tetrathiofulvalene-tetracyanoquinodimethane (TTF-TCNQ)", *Phys. Rev. B* **42** (1990), p. 4088-4099.

[127] J.-P. Pouget, "Chapter 3 Structural Instabilities" (E. Conwell, ed.), Semiconductors and Semimetals, vol. 27, Elsevier, 1988, p. 87-214.

[128] J. Bernasconi, M. J. Rice, W. R. Schneider, S. Strässeler, "Peierls transition in the strong-coupling Hubbard chain", *Phys. Rev. B* **12** (1975), p. 1090-1092.

[129] G. Malfait, D. Jerome, "Techniques de hautes pressions à trés basses températures", *Revue de Physique Appliquée* **4** (1969), p. 467-470.

[130] G. Delplanque, G. Malfait, M. Rieux, D. Jérome, "Appareil de pression hysdrostatique pour mesures éléctriques jusqu'à 17 kbar à très basse température", *Rev. Phys. Appl. (Paris)* **5** (1970), p. 731-736.

[131] A. Andrieux, H. J. Schulz, D. Jerome, K. Bechgaard, "Conductivity of the One-Dimensional Conductor Tetrathiafulvalene-Tetracyanoquinodimethane (TTF-TCNQ) near Commensurability", *Phys. Rev. Lett.* **43** (1979), no. 3, p. 227-230.

[132] A. Andrieux, H. J. Schulz, D. Jerome, K. Bechgaard, "Fluctuation conductivity in $1-D$ conductor tetrathiafulvalene-tetracyanoquinodimethane (TTF-TCNQ)", *J. Physique Lett.* **40** (1979), p. 385-389.

[133] S. Megtert, R. Comès, C. Vettier, R. Pynn, A. F. Garito, "Structural evidence of $2k_F$ commensurablity in TTF-TCNQ under pressure", *Solid State Comm.* **37** (1981), p. 875-877.

[134] D. Jerome, H. J. Schulz, "Quasi-One-Dimensional conductors:The Peierls instability, Pressure and Fluctuations effects", in *Extended Linear Chain Compounds* (J. S. Miller, ed.), vol. 2, Plenum Press, New York, 1982, p. 159.

[135] B. Welber, P. E. Seiden, P. M. Grant, "Pressure dependence of the Drude optical edge of tetrathiafulvalenium (TTF) and tetraselenafulvalenium (TSF) tetracyanoquinodimethanide (TCNQ)", *Phys. Rev. B* **118** (1978), p. 2692-2700.

[136] S. Bouffard, R. Chipaux, D. Jerome, K. Bechgaard, "Pinning of charge density waves in irradiated TTF-TCNQ", *Solid State Comm.* **37** (1981), p. 405-408.

[137] D. B. Tanner, K. D. Cummings, C. S. Jacobsen, "Far-Infrared Study of the Charge Density Wave in Tetrathiafulvalene Tetracyanoquinodimethane (TTF-TCNQ)", *Phys. Rev. Lett.* **47** (1981), p. 597-600.

[138] R. H. Friend, M. Miljak, D. Jérome, D. L. Decker, D. Debray, "Linear Temperature Dependence of the constant Volume Resistivity of TTF-TCNQ", *J. Physique Lett.* **39** (1978), p. 134-138.

[139] F. Herman, "Scattered Wave Calculations of Monomers and Dimers of Tetraselenafulvalene (mathrmTSeF)", *Phys. Scr.* **16** (1977), p. 303-306.
[140] F. Herman, D. R. Salahub, R. P. Messmer, "Xa scattered-wave calculations for dimers and trimers of tetrathiafulvalene (TTF) and tetracyanoquinodimethane (TCNQ)", *Phys. Rev. B* **16** (1977), p. 2453-2465.
[141] G. Grüner, P. Monceau, "Dynamical properties of charge density waves", in *Charge Density Waves in Solids* (L. V. Gorkov, G. Grüner, eds.), North Holland, Amsterdam, 1989, p. 137-190.
[142] L. Forro, R. C. Lacoe, S. Bouffard, D. Jerome, "Defect-concentration dependence of the charge-density-wave transport in tetrathiafulvalene tetracyanoquinodimethane", *Phys. Rev. B* **35** (1987), p. 5884-5886.
[143] R. C. Lacoe, H. J. Schulz, D. Jerome, K. Bechgaard, I. Johannsen, "Observation of Nonlinear Electrical Transport at the Onset of a Peierls Transition in an Organic Conductor", *Phys. Rev. Lett.* **55** (1985), no. 21, p. 2351-2354.
[144] R. C. Lacoe, J. R. Cooper, D. Jerome, F. Creuzet, K. Bechgaard, I. Johannsen, "Nonlinear Electrical Transport Effects in Tetrathiafulvalene-Tetracyanoquinodimethane as Driven through Charge-Density-Wave Commensurability", *Phys. Rev. Lett.* **58** (1987), no. 3, p. 262-265.
[145] G. Grüner, P. Monceau, "Dynamical Properties of charge density waves", in *Charge Density Waves in Solids* (L. V. Gorkov, G. Grüner, eds.), Modern Problems in Condensed Matter Sciences, vol. 25, North-Holland, 1989, p. 137-189.
[146] S. Yasuzuka, K. Murata, T. Arimoto, R. Kato, "Temperature-Pressure Phase Diagram in TTF-TCNQ: Strong Suppression of Charge-Density-Wave State under Extremely High Pressure", *J. Phys. Soc. Jpn.* **76** (2007), no. 3, article no. 033701.
[147] B. Horovitz, H. Gutfreund, M. Weger, "Interchain coupling and the Peierls transition in linear-chain systems", *Phys. Rev. B* **12** (1975), p. 3174-3185.
[148] E. M. Engler, B. A. Scott, S. D. Etemad, T. Penney, V. V. Patel, "Organic Alloys: Synthesis and Properties of Solid Solutions of Tetraselenafulvalene- Tetracyano-p-quinodimethane (TSF-TCNQ) and Tetrathiafulvalene-Tetracyano-p-quinodimethane (TTF-TCNQ)", *J. Am. Chem. Soc.* **99** (1977), p. 5909-5916.
[149] J.-P. Pouget, S. Megtert, R. Comès, "X ray diffuse scattering study of 1D organic conductors: TTF-TCNQ and its family", in *Proceeding of the International Conference Dubrovnik, SR Croatia, SFR Yugoslavia*, Lecture Notes in Physics, vol. 95, Springer, Berlin, Heidelberg, 1979, p. 14-27.
[150] P. M. Chaikin, R. L. Greene, S. D. Etemad, E. M. Engler, "Thermopower of an isostructural series of organic conductors", *Phys. Rev. B* **13** (1976), p. 1627-1632.
[151] C. Weyl, E. M. Engler, K. Bechgaard, G. Jehanno, S. D. Etemad, "Diffuse X-ray scattering in the metallic state of TSF-TCNQ and HMTSF-TCNQ", *Solid State Comm.* **19** (1976), p. 925-930.
[152] S. D. Etemad, "Systematic study of the transitions in tetrathiafulvalene-tetracyanoquinodimethane (TTF-TCNQ) and its selenium analogs", *Phys. Rev. B* **13** (1976), no. 6, p. 2254-2261.
[153] J. C. Scott, S. D. Etemad, E. M. Engler, "Magnetic susceptibility of TSF-TCNQ (tetraselenafulvalene-tetracyanoquinodimethane) and its alloys with TTF-TCNQ", *Phys. Rev. B* **17** (1978), p. 2269-2275.
[154] F. E. Bates, J. E. Eldridge, M. R. Bryce, "High-resolution polarized far-infrared vibrational spectra of semiconducting TTF-TCNQ and TSF-TCNQ", *Can. J. Phys* **59** (1981), p. 339-362.
[155] S. Kagoshima, T. Ishiguro, T. D. Schultz, Y. Tomkiewicz, "Peierls transition and short range order of charge-density waves in TSeF-TCNQ - an X ray study", in *Quasi One-Dimensional Conductors I* (S. Barišić, A. Bjeliš, J. R. Cooper, B. A. Leontić, eds.), Lecture Notes in Physics, vol. 95, Springer, 1979, p. 28-30.
[156] J. F. Thomas, "Fluctuating and single particles conductivity channels in TSF – TCNQ", *Solid State Comm.* **42** (1982), p. 587-589.
[157] S. Megtert, J.-P. Pouget, R. Comès, "Structural Investigations of the Peierls Transitions in TTF-TCNQ and Related Compounds (TSEF-TCNQ, HMTTF-TCNQ, NMP-TCNQ)", in *Molecular Metals* (W. E. Hatfield, ed.), Plenum Press, New York, 1979, p. 87-103.
[158] J. F. Thomas, D. Jerome, "Commensurability and fluctuating conductivity in the organic conductor TSF-TCNQ", *Solid State Comm.* **36** (1980), p. 813-816.
[159] G. Beni, "Peierls transition in a quasi—one dimensional system", *Solid State Comm.* **15** (1974), p. 269-272.
[160] A. N. Bloch, D. O. Cowan, K. Bechgaard, R. E. Pyle, R. H. Banks, T. O. Poehler, "Low-Temperature Metallic Behavior and Resistance Minimum in a New Quasi One-Dimensional Organic Conductor", *Phys. Rev. Lett.* **34** (1975), p. 1561-1564.
[161] R. H. Friend *et al.*, "Stabilisation of the metallic state at low temperatures in HMTTF-TCNQ under pressure", *J. Phys. C: Solid State Phys.* **11** (1978), p. 263.
[162] T. E. Phillips, T. J. Kistenmacher, A. N. Bloch, D. O. Cowan, "X-Ray Crystal Structure of the Organic Conductor from 2,2′ - Bi - (2,4 - diselenabicyclo[3.3.0]octylidene) and 7,7,8,8-Tetracyano - p -quinodimethane (HMTSF-TCNQ)", *J. Chem. Soc., Chem. Commun.* (1976), p. 334-335.
[163] B. Korin, J. R. Cooper, M. Miljak, A. Hamzic, K. Bechgaard, "Magnetoresistance studies of HMTSF – TCNQ", *Chem. Scr.* **17** (1981), no. 1-5, p. 45-46.

[164] R. J. Cooper, M. Weger, D. Jerome, D. Lefur, K. Bechgaard, A. N. Bloch, D. O. Cowan, "Semi-Metallic Behaviour of HMTSF-TCNQ at low temperatures under pressure", *Solid State Comm.* **19** (1976), p. 749-754.
[165] M. Weger, "A model for the electronic band structure of HMTSeF-TCNQ", *Solid State Comm.* **19** (1976), p. 1149-1155.
[166] J. R. Cooper, M. Weger, G. Delplanque, D. Jerome, K. Bechgaard, "The Hall effect in HMTSF-TCNQ", *J. Physique Lett.* **37** (1976), p. 349-353.
[167] M. Miljak, A. Andrieux, R. H. Friend, G. Malfait, D. Jerome, K. Bechgaard, "Observation of de Haas-Shubnikov oscillations in an organic metal, HMTSF-TCNQ", *Solid State Comm.* **26** (1978), p. 969-971.
[168] K. Murata, Y. Fukumoto, K. Yokogawa, R. Takaoka, W. Kang, J. S. Brooks, D. Graf, H. Yoshino, T. Sasaki, R. Kato, "Magnetic-field-induced phase transitions in the quasi-one-dimensional organic conductor HMTSF–TCNQ", *Low Temp. Phys.* **40** (2014), no. 4, p. 371-376, a Memorial Issue for the 60th Year Anniversary of Lifschitz-Kosevich theory.
[169] A. G. Lebed, *The Physics of Organic Superconductors and Conductors*, Springer: Berlin, Heidelberg, 2008.
[170] K. Murata, Y. Fukumoto, K. Yokogawa *et al.*, "Magnetic-Field-Induced Phase Transition and a Possible Quantum Hall Effect in the Quasi-One-Dimensional CDW Organic Conductor HMTSF-TCNQ", *J. Mod. Phys.* **5** (2014), article no. 46453.
[171] Y. Tomkiewicz, J. R. Andersen, A. R. Taranko, "Relative stability of donor and acceptor stacks against Peierls distortion in the tetrathia- and tetraselenafulvalene-tetracyanoquinodimethane family of organic metals", *Phys. Rev. B* **17** (1978), p. 1579-1591.
[172] J.-P. Pouget, "Diffuse X-ray scattering studies of one-dimensional organic metals", *Chem. Scr.* **55** (1981), no. 1-5, p. 85-91.
[173] A. Andrieux, P. M. Chaikin, C. Duroure, D. Jerome, C. Weyl, K. Bechgaard, J. R. Andersen, "Transport properties of the metallic state of TMTSF-DMTCNQ", *J. Phys. I France* **40** (1979), p. 1199-1206.
[174] S. Bouffard, M. Ribault, D. Jerome, K. Bechgaard, "Shubnikov–de Haas oscillations in an organic conductor, tetramethyltetraselenafulvalene-2,5-dimethyl-7,7′,8,8′ tetracyanoquinodimethane TMTSF-DMTCNQ", *J. Physique Lett.* **44** (1983), p. 285-293.
[175] L. M. Roth, P. N. Argyres, "Magnetic Quantum Effects", in *Semiconductors and Semimetals. Vol. 1* (R. K. Willardson, A. C. Beer, eds.), vol. 1, Academic Press Inc.: New York and London, 1966, p. 159-202.
[176] U. Hardebusch *et al.*, "The magnetic susceptibility of TMTSF-DMTCNQ under pressure", *Solid State Comm.* **32** (1979), p. 1151-1154.
[177] H. J. Schulz, D. Jerome, A. Mazaud, M. Ribault, K. Bechgaard, "Possibility of superconducting precursor effects in quasi-one-dimensional organic conductors : theory and experiments", *J. Phys. France* **42** (1981), p. 991-1002.
[178] J. Friedel, D. Jerome, "Organic superconductors: the $(TMTSF)_2X$ family", *Contemp. Phys.* **23** (1982), no. 6, p. 583-624.
[179] J. L. Galigné, B. Liautard, S. Peytavin, G. Brun, J.-M. Fabre, E. Torreilles, L. Giral, "Étude structurale du bromure de tétraméthyltétrathiafulvalène $(TMTTF)_2Br$", *Acta Cryst. B* **34** (1978), p. 620-624.
[180] A. P. Drozdov, M. I. Eremets, I. A. Troyan, V. Ksenofontov, S. I. Shylin, "Conventional superconductivity at 203 Kelvin at high pressures in the sulfur hydride system", *Nature* **525** (2015), p. 73-76.
[181] D. Jerome, "Organic Superconductivity: A Mouse may be of Service to a Lion", in *Superconductivity in New Materials* (Z. Fisk, H. R. Ott, eds.), Contemporary Concepts of Condensed Matter Science, vol. 4, Elsevier, 2011, p. 149-216.
[182] J. R. Andersen, K. Bechgaard, C. S. Jacobsen, G. Rindorf, H. Soling, N. Thorup, "The Crystal and Molecular Structure of the Organic Conductor 2,3,6,7-Tetramethyl 1,4,5,8-tetraselenafulvalenium 2,5- Dimethyl- 7,7,8,8-tetracyano-p-quinodimethanide (TMTSF-DMTCNQ)", *Acta Cryst. B.* **34** (1978), p. 1901-1905.
[183] A. Andrieux, C. Duroure, D. Jerome, K. Bechgaard, "The metallic state of the organic conductor TMTSF-DMTCNQ at low temperature under pressure", *J. Physique Lett.* **40** (1979), p. 381-383.
[184] I. F. Schegolev, R. B. Lubovskii, "Properties of the quasi-one-dimensional organic metal $(TSeT)_2Cl$", in *Quasi One-Dimensional Conductors I*, vol. 95, Springer-Verlag, 1979, p. 39.
[185] V. N. Laukhin, I. F. Schegolev, "Study of phase transitions in $(TSeT)_2Cl$ under pressure at low temperatures", *Sov. Phys. JETP* **47** (1978), no. 6, p. 1170-1173.
[186] K. Bechgaard, J. R. Andersen, "Molecular Properties of the Molecules used in Conducting Organic Solids", in *The Physics and Chemistry of Low Dimensional Solids* (L. Alcácer, ed.), Springer Netherlands: Dordrecht, 1980, p. 247-263.
[187] D. Jerome, A. Mazaud, M. Ribault, K. Bechgaard, "Superconductivity in a synthetic organic conductor $(TMTSF)_2PF_6$", *J. Physique Lett.* **41** (1980), p. 95-98.
[188] D. Jerome, A. Mazaud, M. Ribault, K. Bechgaard, "Supraconductibilité dans un conducteur synthétique organique $(TMTSF)_2PF_6$", *C. R. Hebd. Seances Acad. Sci. B* **290** (1980), no. 2, p. 27-30, online at https://gallica.bnf.fr/ark:/12148/bpt6k54905962/f103.item.
[189] J.-P. Pouget, S. Ravy, "X-ray evidence of charge density wave modulations in the magnetic phases of $(TMTSF)_2PF_6$ and $(TMTTF)_2Br$", *Synth. Met.* **85** (1997), p. 1523-1528.
[190] M. Ribault, G. Benedek, D. Jerome, K. Bechgaard, "Diamagnetic AC susceptibility in the quasi-one dimensional organic conductor : $(TMTSF)_2PF_6$", *J. Physique Lett. Paris* **41** (1980), p. 397-399, https://hal.archives-ouvertes.fr/jpa-00231806.

[191] K. Andres, F. Wudl, D. B. McWhan, G. A. Thomas, D. Nalewajek, A. L. Stevens, "Observation of the Meissener effect in an Organic Superconductor", *Phys. Rev. Lett.* **45** (1980), p. 1449-1452.
[192] J. C. Scott, H. J. Pedersen, K. Bechgaard, "Magnetic properties of the organic conductor $(TMTSF)_2PF_6$: a new phase transition", *Phys. Rev. Lett.* **45** (1980), p. 2125-2128.
[193] W. M. Walsh, F. Wudl, G. A. Thomas, D. Nalewajek, J. J. Hauser, P. A. Lee, T. Poehler, "Restoration of Metallic Behavior in organic Conductors by Small Electric Fields", *Phys. Rev. Lett.* **45** (1980), p. 829-832.
[194] A. Andrieux, D. Jerome, K. Bechgaard, "Spin-density wave ground state in the one-dimensional conductor $(TMTSF)_2PF_6$: microscopic evidence from ^{77}Se and ^{1}H NMR experiments", *J. Physique Lett.* **42** (1981), p. 87-90.
[195] K. Mortensen, Y. Tomkiewicz, T. D. Schultz, E. M. Engler, "Antiferromagnetic Ordering in the Organic Conductor bis-Tetramethyltetraselenafulvalene-Hexafluorophosphate $(TMTSF)_2PF_6$", *Phys. Rev. Lett.* **46** (1981), no. 18, p. 1234–1237.
[196] J. C. Slater, "Magnetic Effects and the Hartree–Fock Equation", *Phys. Rev.* **82** (1951), p. 538-541.
[197] W. M. Lomer, "Electronic Structure of Chromium Group Metals", *Proc. Phys. Soc.A* **80** (1962), p. 489.
[198] A. W. Overhauser, "Spin Density Waves in an Electron Gas", *Phys. Rev.* **128** (1962), p. 1437-1452.
[199] R. H. Friend, D. Jerome, "Periodic lattice distortions and charge density waves in one-and two-dimensional metals", *J. Phys. C: Solid State Phys.* **12** (1979), p. 1441.
[200] P. Molinié, D. Jerome, A. J. Grant, "Pressure enhanced superconductivity and superlattice structures in transition metal dichalcogenide layer crystals", *Phil. Mag* **30** (1974), p. 1091-1103.
[201] J. A. Wilson, F. J. Di Salvo, S. Mahajan, "Charge-density waves and superlattices in the metallic layered transition metal dichalcogenides", *Adv. Phys.* **24** (1975), p. 117-201.
[202] J. Friedel, "On the pressure Dependence of Superconductivity in transition metal Dichalcogenide layer Crystals", *J. Phys. Lett.* **36** (1975), p. 279-280.
[203] R. L. Greene, E. M. Engler, "Pressure dependence of superconductivity in a organic superconductor $(TMTSF)_2PF_6$", *Phys. Rev. Lett.* **45** (1980), p. 1587-1590.
[204] D. Jerome, "The physics of organic superconductors", *Science* **252** (1991), p. 1509-1514.
[205] H. J. Schulz, D. Jerome, M. Ribault, A. Mazaud, K. Bechgaard, "Pressure dependence of the organic superconductivity in $(TMTSF)_2PF_6$", *J. Physique. Lett* **42** (1981), p. 51-54.
[206] R. Brusetti, M. Ribault, D. Jerome, "Insulating, conducting and superconducting states of (TMTSF)2AsF6 under pressure and magnetic field", *J. Phys. I France* **43** (1982), p. 801-808.
[207] D. Jerome, "Organic Superconductors: a survey of low dimensional phenomena", *Mol. Cryst. Liq. Cryst.* **79** (1982), p. 511-538.
[208] D. Jaccard, H. Wilhelm, D. Jerome, J. Moser, C. Carcel, J.-M. Fabre, "From spin-Peierls to superconductivity: $(TMTTF)_2PF_6$ under high pressure", *J. Phys. Cond. Matter* **13** (2001), article no. L89.
[209] M. Itoi, M. Kano, N. Kurita, M. Hedo, Y. Uwatoko, T. Nakamura, "Pressure-Induced Superconductivity in the Quasi-One-Dimensional Organic Conductor $(TMTTF)_2AsF_6$", *J. Phys. Soc. Jpn.* **76** (2007), no. 5, article no. 053703.
[210] M. Itoi, C. Araki, M. Hedo, Y. Uwatoko, T. Nakamura, "Anomalously Wide Superconducting Phase of One-Dimensional Organic Conductor $(TMTTF)_2SbF_6$", *J. Phys. Soc. Jpn.* **77** (2008), no. 2, article no. 023701.
[211] S. S. P. Parkin, M. Ribault, D. Jerome, K. Bechgaard, "Superconductivity in the family of organic salts based on the tetramethyltetraselenafulvalene (TMTSF) molecule: $(TMTSF)_2X(X = ClO_4, PF_6, AsF_6, SbF_6, TaF_6)$", *J. Phys. C: Solid State Phys.* **14** (1981), p. 5305.
[212] S. S. P. Parkin, F. Creuzet, M. Ribault, D. Jérome, K. Bechgaard, J.-M. Fabre, "Superconductivity in the Organic Charge Transfer Salts: $(TMTTF)_2X$ and $(TMTSF)_2X$", *Mol. Cryst. Liq. Cryst.* **79** (1982), p. 605-615.
[213] L. Balicas, K. Behnia, W. Kang, E. Canadell, P.-S. Auban, D. Jerome, M. Ribault, J.-M. Fabre, "Superconductivity and magnetic field induced spin density waves in the $(TMTTF)_2X$ family", *J. Phys. I France* **4** (1994), p. 1539-1549.
[214] S. Tomić, D. Jerome, "A hidden low-temperature phase in the organic conductor $(TMTSF)_2ReO_4$", *J. Phys.: Condens. Matter* **1** (1989), p. 4451.
[215] H. Wilhelm *et al.*, "The case for universality of the phase diagram of the Fabre and Bechgaard salts", *Eur. Phys. Jour. B* **21** (2001), p. 175-183.
[216] T. Adachi, E. Ojima, K. Kato, H. Kobayashi, "Superconducting Transition of $(TMTTF)_2PF_6$ above 50 kbar", *J. Am. Chem. Soc.* **122** (2000), p. 3238-3239.
[217] V. J. Emery, "Theory of the One-Dimensional Electron Gas", in *Highly Conducting One-Dimensional Solids* (J. T. Devreese, R. E. Evrard, V. E. van Doren, eds.), Physics of Solids and Liquids, Plenum Press, New York, 1979, p. 247-303.
[218] J. Solyom, "The Fermi Gas model of one-dimensional conductors", *Adv. Phys.* **28** (1979), p. 201-303.
[219] H. J. Schulz, "Fermi liquids and non-Fermi liquids", in *Proceedings of Les Houches Summer School LXI* (E. Akkermans, G. Montambaux, J. Pichard, J. Zinn-Justin, eds.), Elsevier, Amsterdam, 1995, p. 533.
[220] J. Voit, "One-dimensional Fermi liquids", *Rep. Prog. Phys.* **58** (1995), p. 977.
[221] T. Giamarchi, *Quantum Physics in One-Dimension*, Clarendon Press, Oxford, 2003.

[222] V. J. Emery, R. Bruinsma, S. Barišić, "Electron-Electron Umklapp Scattering in Organic Superconductors", *Phys. Rev. Lett.* **48** (1982), p. 1039-1043.
[223] S. Barišić, S. Brazovskii, in *Recent Developments in Condensed Matter Physics* (J. T. Devreese, ed.), vol. 1, Plenum Press: New York, 1981.
[224] K. Penc, F. Mila, "Charge gap in the one-dimensional dimerized Hubbard model at quarter-filling", *Phys. Rev. B* **50** (1994), p. 11429-11445.
[225] P. M. Grant, "Band-structure parameters of a series of tetramethyltetraselenafulvalene $(TMTSF)_2X$ compounds", *Phys. Rev. B* **26** (1982), p. 6888-6895.
[226] C. Coulon, P. Delhaes, S. Flandrois, R. Lagnier, E. Bonjour, J.-M. Fabre, "Effect of doping $(TMTSF)_2ClO_4$ with TMTTF I. Ambient pressure results: a competition between the different possible ground states", *J. Phys. I France* **43** (1982), p. 1721-1729.
[227] L. G. Caron, C. Bourbonnais, "Importance of one-dimensional correlations in the phase diagram of the $(TMTTF)_2X-(TMTSF)_2X$ salts", *Physica B+C* **143** (1986), p. 453-455.
[228] S. Brazovskii, Y. Yakovenko, "On the theory of organic superconducting materials", *Sov. Phys. JETP* **62** (1985), p. 1340-1352.
[229] T. Giamarchi, "Umklapp process and resistivity in one-dimensional fermion systems", *Phys. Rev. B* **44** (1991), p. 2905-2913.
[230] M. Shahbazi, C. Bourbonnais, "Electrical transport near quantum criticality in low dimensional organic superconductors", *Phys. Rev. B* **92** (2015), article no. 195141.
[231] T. Giamarchi, "Mott transition in one dimension", *Phys. B: Condens. Matter* **230-232** (1997), p. 975-980.
[232] F. Mila, X. Zotos, "Phase Diagram of the One-Dimensional Extended Hubbard Model at Quarter-Filling", *Europhys. Lett.* **24** (1993), p. 133.
[233] M. Tsuchiizu, H. Yoshika, Y. Suzumura, "Crossover from Quarter-Filling to Half-Filling in a One-Dimensional Electron System with a Dimerized and Quarter-Filled Band", *J. Phys. Soc. Jpn.* **70** (2001), p. 1460–1463.
[234] T. Giamarchi, "Theoretical Framework for Quasi-One Dimensional Systems", *Chem. Rev.* **104** (2004), p. 5037-5056.
[235] A. S. Rüetschi, D. Jaccard, "High pressure study of the organic compound $(TMTTF)_2BF_4$", *Eur. Phys. J. B* **67** (2009), p. 43-49.
[236] C. Bourbonnais, D. Jerome, "Electronic Confinement in Organic Metals", *Science* **281** (1998), p. 1155-1156.
[237] L. Ducasse, A. Abderraba, J. Hoarau, M. Pesquer, B. Gallois, J. Gaultier, "Temperature dependence of the transfer integrals in the $(TMTSF)_2X$ and $(TMTTF)_2X$ families", *J. Phys. C: Solid State Phys.* **19** (1986), article no. 3805.
[238] J.-M. Fabre, "Synthesis Strategies and Chemistry of Nonsymmetrically Substituted Tetrachalcogenafulvalenes", *Chem. Rev.* **104** (2004), p. 5133-5150.
[239] F. Creuzet, C. Bourbonnais, L. G. Caron, D. Jerome, K. Bechgaard, "A ^{13}C NMR in study of the interplay between the Spin–Peierls and antiferromagnetic ground states of $(TMTTF)_2PF_6$ under pressure", *Synth. Met.* **19** (1987), p. 289-294.
[240] C. Bourbonnais, P. Wzietek, F. Creuzet, D. Jerome, K. Bechgaard, P. Batail, "Scaling Relation between Nuclear Relaxation and Magnetic Susceptibility in Organic Conductors: Evidence for 1D Paramagnon Effects", *Phys. Rev. Lett.* **62** (1989), p. 1532.
[241] P. Wzietek, F. Creuzet, C. Bourbonnais, D. Jerome, K. Bechgaard, P. Batail, "Nuclear relaxation and electronic correlations in quasi-one-dimensional organic conductors. II. Experiments", *J. Phys. I France* **3** (1993), p. 171-201.
[242] J.-P. Pouget, R. Moret, R. Comès, K. Bechgaard, J.-M. Fabre, L. Giral, "X-Ray Diffuse Scattering Study of Some $(TMTSF)_2X$ and $(TMTTF)_2X$Salts", *Mol. Cryst. Liq. Cryst.* **79** (1982), p. 129.
[243] P. Auban-Senzier, D. Jerome, C. Carcel, J.-M. Fabre, "Longitudinal and transverse transport of the quasi-one dimensional organic conductor $(TMTTF)_2PF_6$ studied under high pressure", *J. Phy. IV France* **114** (2004), p. 41-44.
[244] C. Bourbonnais, L. G. Caron, "New Mechanisms for Phase Transitions in Quasi-One-Dimensional Conductors", *Europhys. Lett.* **5** (1988), p. 209.
[245] P. M. Grant, "Electronic Structure of the 2 : 1 Charge Transfer Salts of TMTCF", *J. Phys. Colloques* **44** (1983), p. 847-857.
[246] D. Jerome, "Organic Conductors: From Charge Density Wave TTF-TCNQ to Superconducting $(TMTSF)_2PF_6$", *Chem. Rev.* **104** (2004), p. 5565-5592.
[247] A. Schwartz, M. Dressel, G. Grüner, V. Vescoli, L. Degiorgi, T. Giamarchi, "On-chain electrodynamics of metallic $(TM)_2X$ salts: Observation of Tomonaga–Luttinger liquid response", *Phys. Rev. B* **58** (1998), p. 1261-1271.
[248] V. Vescoli, L. Degiorgi, W. Henderson, G. Grüner, K. P. Starkey, L. K. Montgomery, "Dimensionality-Driven Insulator-to-Metal Transition in the Bechgaard salts", *Science* **281** (1998), p. 1181-1184.
[249] L. Degiorgi, D. Jerome, "Transport and Optics in Quasi-One-Dimensional Organic Conductors", *J. Phys. Soc. Jpn.* **75** (2006), article no. 051004.
[250] S. Biermann, A. Georges, A. Lichtenstein, T. Giamarchi, "Deconfinement Transition and Luttinger to Fermi Liquid Crossover in Quasi-One-Dimensional Systems", *Phys. Rev. Lett.* **87** (2001), article no. 276405.

[251] J. Moser, M. Gabay, P.-S. Auban, D. Jerome, K. Bechgaard, J.-M. Fabre, "Transverse transport in $(TM)_2X$ organic conductors: possible evidence for a Luttinger liquid", *Eur. Phys. Jour. B* **1** (1998), p. 39-46.

[252] F. Creuzet, C. Bourbonnais, L. G. Caron, D. Jerome, A. Moradpour, "^{77}Se NMR Spin-Lattice relaxation rate properties in the $(TMTSF)_2X$ series under pressure: cooperative phenomena and SDW Transition", *Synth. Met.* **19** (1987), p. 277-282.

[253] B. Gallois, J. Gaultier, T. Lamcharfi, F. Bechtel, A. Filhol, L. Ducasse, M. Abderrabba, "Cristallographic structures of $(TMTSF)_2PF_6$ under constraints: evidence of a change in the electronic structure", *Synth. Met.* **19** (1987), p. 321-326.

[254] C. Bourbonnais, D. Jerome, "The normal phase of quasi-one-dimensional organic superconductors", in *Advances in Synthetic Metals: Twenty Years of Progress in Science and Technology* (P. Bernier, S. Lefrant, G. Bidan, eds.), Elsevier, 1999, p. 206-261.

[255] P. Auban-Senzier, D. Jerome, J. Moser, "Non Fermi-Liquid features in $(TM)_2X$ 1-D Conductors from transport properties", in *Proceedings of the Physical Phenomena at High Magnetic Fields-III* (Z. Fisk, L. Gorkov, R. Schrieffer, eds.), World Scientific: Singapore, 1999, p. 211-+.

[256] D. S. Chow, F. Zamborsky, B. Alavi, D. J. Tantillo, A. Baur, C. A. Merlić, S. E. Brown, "Charge Ordering in the TMTTF Family of Molecular Conductors", *Phys. Rev. Lett.* **85** (2000), p. 1698-1701.

[257] F. Nad, P. Monceau, C. Carcel, J.-M. Fabre, "Dielectric response of the charge-induced correlated state in the quasi-one-dimensional conductor", *Phys. Rev. B* **62** (2000), p. 1753-1756.

[258] P. Monceau, F. Nad, S. Brazovskii, "Ferroelectric Mott–Hubbard Phase of Organic $(TMTTF)_2X$ Conductors", *Phys. Rev. Lett.* **86** (2001), p. 4080-4083.

[259] C. Bourbonnais, F. Creuzet, D. Jerome, K. Bechgaard, A. Moradpour, "Cooperative phenomena in $(TMTSF)_2ClO_4$: an NMR evidence", *J. Physique Lett.* **45** (1984), p. 755-765.

[260] S. Tomić, J. R. Cooper, W. Kang, D. Jerome, K. Maki, "The influence of chemical impurities and X-ray induced defects on the single-particle and spin-density wave conductivity in the Bechgaard salts", *J. Phys. I France* **1** (1991), p. 1603-1625.

[261] N. Cao, T. Timusk, K. Bechgaard, "Unconventional Electrodynamic Response of the Quasi One Dimensional Organic Conductor $(TMTSF)_2ClO_4$", *J. Phys. I France* **6** (1996), p. 1719-1726.

[262] W. Henderson, V. Vescoli, P. Tran, L. Degiorgi, G. Grüner, "Anisotropic electrodynamics of low dimensional metals: Optical studies of $(TMTSF)_2ClO_4$", *Eur. Phys. J. B* **11** (1999), p. 365-368.

[263] D. G. Clarke, S. P. Strong, P. W. Anderson, "Conductivity between Luttinger Liquids in the Confinement Regime and c-Axis Conductivity in the Cuprate Superconductors", *Phys. Rev. Lett.* **74** (1995), p. 4499-4502.

[264] M. Dressel, A. Schwartz, G. Grüner, Giorgi, L. De, "Deviations from Drude Response in Low-Dimensional Metals: Electrodynamics of the Metallic State of $(TMTSF)_2PF_6$", *Phys. Rev. Lett.* **77** (1996), p. 398-401.

[265] C. S. Jacobsen, D. B. Tanner, K. Bechgaard, "Dimensionality Crossover in the Organic Superconductor Tetramethyltetraselenafulvalene Hexafluorophosphate $(TMTSF)_2PF_6$", *Phys. Rev. Lett.* **46** (1981), p. 1142-1145.

[266] M. Dressel, "Electrodynamics of Bechgaard Salts: Optical Properties of One-Dimensional Metals", *ISRN Condensed Matter Physics* **2012** (2012), article no. 732973.

[267] A. Georges, T. Giamarchi, N. Sandler, "Interchain conductivity of coupled Luttinger liquids and organic conductors", *Phys. Rev. B* **61** (2000), p. 16393-16396.

[268] K. Heuzé, M. Fourmigué, P. Batail, C. Coulon, R. Clérac, E. Canadell, P. Auban-Senzier, R. Ravy, D. Jerome, "A genuine quarter-filled band Mott insulator, $(EDT-TTF-CONMe_2)_2AsF_6$: where the chemistry and Physics of weak intermolecular interactions act in unison", *Adv. Mater.* **15** (2003), p. 1251-1254.

[269] D. S. Chow, P. Wzietek, D. Fogliatti, B. Alavi, D. J. Tantillo, C. A. Merlic, S. E. Brown, "Singular Behavior in the Pressure-Tuned Competition between Spin–Peierls and Antiferromagnetic Ground States of $(TMTTF)_2PF_6$", *Phys. Rev. Lett.* **81** (1998), p. 3984-3987.

[270] L. Zorina, S. Simonov, C. Mézière, E. Canadell, S. Suh, S. E. Brown, P. Foury-Leylekian, P. Fertey, J.-P. Pouget, P. Batail, "Charge ordering, symmetry and electronic structure issues and Wigner crystal structure of the quarter-filled band Mott insulators and high pressure metals $(EDT-TTF-CONMe_2)_2X$, X = Br and AsF_6^-", *Journal of Materials Chemistry* **19** (2009), p. 6980-6994.

[271] P. Auban-Senzier, C. R. Pasquier, D. Jerome, S. Suh, S. E. Brown, C. Meziere, P. Batail, "Phase Diagram of Quarter-Filled Band Organic Salts $(EDT-TTF-CONMe_2)_2X$, X= AsF_6^- and Br", *Phys. Rev. Lett.* **102** (2009), article no. 255001.

[272] K. Bechgaard, M. Carneiro, M. Olsen, F. B. Rasmussen, C. S. Jacobsen, "Zero-Pressure Organic Superconductor $(TMTSF)_2ClO_4$", *Phys. Rev. Lett.* **46** (1981), p. 852-855.

[273] K. Bechgaard, K. Carneiro, M. Olsen, F. B. Rasmussen, M. Olsen, "Superconductivity in an Organic Solid. Synthesis, Structure, and Conductivity of Bis(tetramethyltetraselenafulva1enium) Perchlorate, $(TMTSF)_2ClO_4$", *J. Am. Chem. Soc* **103** (1981), p. 2440-2442.

[274] N. Thorup, G. Rindorf, H. Soling, K. Bechgaard, "The Structure of $(TMTSF)_2PF_6$ the First Superconducting Organic Solid", *Acta Cryst. B* **37** (1981), p. 1236-1240.

[275] H. Kowada, R. Kondo, S. Kagoshima, "Development of Uniaxial Elongation Method and Its Application to Low Dimensional Conductors", *J. Phys. Soc. Jpn.* **76** (2007), article no. 114710.

[276] L. Ducasse, M. Abderrabba, B. Gallois, "Temperature dependence of the Fermi surface topography in the $(TMTSF)_2X$ and $(TMTTF)_2X$ families", *J. Phys. C: Solid State Phys.* **18** (1985), article no. L947.
[277] R. Bruinsma, V. J. Emery, "Theory of Anion ordering in TMTSF Compounds", *J. Phys. Colloques* **44** (1983), no. C3, p. 1115-1120.
[278] V. J. Emery, "Some basic Questions in organic Superconductivity", *J. Phys. Colloques* **44** (1983), p. 977-982.
[279] J.-P. Pouget, G. Shirane, K. Bechgaard, J.-M. Fabre, "X-ray evidence of a structural transition in $(TMTSF)_2ClO_4$ pristine and slightly doped", *Phys. Rev. B* **27** (1983), p. 5203-5206.
[280] T. Takahashi, K. Bechgaard, D. Jerome, "Observation of a magnetic state in the organic superconductor $(TMTSF)_2ClO_4$: influence of the cooling rate", *J. Physique Lett.* **43** (1982), p. 565-573.
[281] L. Pasteur, "Talk at the University of Lille", 1854, https://innovationetserendipite.files.wordpress.com/2011/01/discours-de-louis-pasteur.pdf.
[282] R. Moret, S. Ravy, J.-P. Pouget, R. Comes, K. Bechgaard, "Anion-Ordering Phase Diagram of Di(tetramethyltetraselenafulvalenium) Perrhenate, $(TMTSF)_2ReO_4$", *Phys. Rev. Lett.* **57** (1986), p. 1915-1918.
[283] S. S. P. Parkin, D. Jerome, K. Bechgaard, "Pressure dependence of the metal-insulator and superconducting phase transitions in $(TMTSF)_2ReO_4$", *Mol. Cryst. Liq. Cryst.* **79** (1982), p. 569-580.
[284] D. U. Gubser, W. W. Fuller, T. O. Poehler, D. O. Cowan, M. Lee, R. S. Potemberg, L. Y. Chiang, A. N. Bloch, "Magnetic susceptibility and resistive transitions of superconducting $(TMTSF)_2ClO_4$: critical fields", *Phys.Rev.B* **24** (1981), p. 478-480.
[285] H. Schwenk, K. Andres, F. Wudl, "Resistivity of the organic superconductor $(TMTSF)_2ClO_4$ in its relaxed, quenched, and intermediate state", *Phys. Rev. B* **29** (1984), p. 500-502.
[286] D. U. Gubser, W. W. Fuller, T. O. Poehler, J. Stokes, D. O. Cowan, M. Lee, A. N. Bloch, "Resistive and Magnetic Susceptibility Transitions in Superconducting $(TMTSF)_2ClO_4$", *Mol. Cryst. Liq. Cryst.* **79** (1982), p. 581-590.
[287] J. I. Oh, M. J. Naughton, "Magnetic Determination of Hc2 under Accurate Alignment in $(TMTSF)_2ClO_4$", *Phys. Rev. Lett.* **92** (2004), article no. 067001.
[288] P. Garoche, R. Brusetti, D. Jerome, K. Bechgaard, "Specific heat measurements of organic superconductivity in $(TMTSF)_2ClO_4$", *J. Physique Lett.* **43** (1982), p. 147-152.
[289] D. Mailly, M. Ribault, K. Bechgaard, J.-M. Fabre, L. Giral, "Anisotropy of the Meissner effect and the diamagnetic shielding in $(TMTSF)_2ClO_4$", *J. Physique Lett.* **43** (1982), p. 711-717.
[290] S. Yonezawa, Y. Maeno, K. Bechgaard, D. Jerome, "Nodal superconducting order parameter and thermodynamic phase diagram of $(TMTSF)_2ClO_4$", *Phys. Rev. B* **85** (2012), article no. 140502R.
[291] L. P. Gorkov, D. Jerome, "Back to the problem of the upper critical fields in organic superconductors", *J. Physique Lett.* **46** (1985), p. 643-646.
[292] S. Yonezawa, C. A. Marrache-Kikuchi, K. Bechgaard, D. Jerome, "Crossover from impurity-controlled to granular superconductivity in $(TMTSF)_2ClO_4$", *Phys. Rev. B* **97** (2018), article no. 014521.
[293] T. Ishiguro, K. Yamaji, G. Saito, *Organic Superconductors*, Springer Series in Solid-State Sciences, vol. 88, Springer, Heidelberg, 1998.
[294] K. Murata, M. Tokumoto, H. Anzai, K. Kajimura, T. Ishiguro, "Upper critical field of the anisotropic organic superconductors, $(TMTSF)_2ClO_4$", *Jpn. J. Appl. Phys.* **26** (1987), no. S3-2, p. 1367-1368.
[295] I. J. Lee, M. J. Naughton, G. M. Danner, P. M. Chaikin, "Anisotropy of the Upper Critical Field in $(TMTSF)_2PF_6$", *Phys. Rev. Lett.* **78** (1997), p. 3555-3558.
[296] I. J. Lee, P. M. Chaikin, M. J. Naughton, "Exceeding the Pauli paramagnetic limit in the critical field of $(TMTSF)_2PF_6$", *Phys. Rev. B* **62** (2000), p. R14669-R14672.
[297] I. J. Lee, A. P. Hope, M. J. Leone, M. J. Naughton, "Revisiting the Superconducting Phase Diagram of $(TMTSF)_2ClO_4$", *Synthetic Metals* **70** (1995), p. 747-750.
[298] S. Yonezawa, S. Kusaba, Y. Maeno, P.-S. Auban, C. Pasquier, D. Jerome, "Magnetic-Field Variations of the Pair-Breaking Effects of Superconductivity in $(TMTSF)_2ClO_4$", *J. Phys. Soc. Jpn.* **77** (2008), article no. 054712.
[299] S. Yonezawa, S. Kusaba, Y. Maeno, P.-S. Auban, C. Pasquier, K. Bechgaard, D. Jerome, "Anomalous In-Plane Anisotropy of the Onset of Superconductivity in $(TMTSF)_2ClO_4$", *Phys. Rev. Lett.* **100** (2008), article no. 117002.
[300] A. M. Clogston, "Upper limit for the critical field in hard superconductors", *Phys. Rev. Lett.* **9** (1962), p. 266-267.
[301] P. J. Hirschfeld, P. Wolfe, D. Einzel, "Consequences of resonant impurity scattering in anisotropic superconductors: Thermal and spin relaxation properties", *Phys. Rev. B* **37** (1988), p. 83-97.
[302] D. Jerome, S. Yonezawa, "Novel superconducting phenomena in quasi-one-dimensional Bechgaard salts", *C. R. Physique* **17** (2016), p. 357-375.
[303] J. Shinagawa, Y. Kurosaki, F. Zhang, C. Parker, S. E. Brown, D. Jerome, "Superconducting State of the Organic Conductor $(TMTSF)_2ClO_4$", *Phys. Rev. Lett.* **98** (2007), article no. 147002.
[304] D. Aoki, K. Ishida, J. Flouquet, "Review of U-based ferromagnetic superconductors: comparaison betwen UGe_2, URhGe and UCoGe", *J. Phys. Soc. Jpn.* **88** (2018), article no. 022001.
[305] M. Takigawa, H. Yasuoka, G. Saito, "Proton spin lattice relaxation in the superconducting state of $(TMTSF)_2ClO_4$", *J. Phys. Soc. Jpn.* **56** (1987), p. 873-876.

[306] Y. Hasegawa, H. Fukuyama, "NMR rexation time of anisotropic superconding state in quasi-one dimensional systems", *J. Phys. Soc. Jpn.* **56** (1987), p. 877-880.
[307] I. J. Lee, M. J. Naughton, P. M. Chaikin, "Triplet Superconductivity in an Organic Superconductor Probed by NMR Knight Shift", *Phys. Rev. Lett.* **88** (2002), article no. 017004.
[308] P. Fulde, R. A. Ferrell, "Superconductivity in a Strong Spin-Exchange Field", *Phys. Rev.* **135** (1964), p. A550-A563.
[309] A. I. Larkin, Y. N. Ovchinnikov, "Nonuniform State of Superconductors", *Sov. Phys. JETP* **20** (1965), no. 3, p. 762-+.
[310] S. P. Strong, D. G. Clarke, P. W. Anderson, "Magnetic Field Induced Confinement in Strongly Correlated Anisotropic Materials", *Phys. Rev. Lett.* **73** (1994), p. 1007-1010.
[311] N. Joo, P.-S. Auban, C. R. Pasquier, S. Yonezawa, R. Higashinaka, Y. Maeno, S. Haddad, S. Charfi-Kaddour, M. Héritier, D. Jerome, "Field-induced confinement in $(TMTSF)_2ClO_4$ under accurately aligned magnetic fields", *Eur. Phys. B* **52** (2006), p. 337-343.
[312] A. G. Lebed, "Reversible nature of the orbital mechanism for the suppression of superconductivity", *JETP Lett.* **44** (1986), no. 2, p. 114-117.
[313] Y. Fuseya, C. Bourbonnais, K. Miyake, "On the Origin of the Anomalous Upper Critical Field in Quasi-One-Dimensional Superconductors", *Eur. Phys. Lett.* **100** (2012), article no. 57008.
[314] N. Miyawaki, S. Shimahara, "Dimensional Crossover of the Fulde–Ferrell–Larkin–Ovchinnikov State in Strongly Pauli-Limited Quasi-One-Dimensional Superconductor", *J. Phys. Soc. Jpn.* **83** (2014), article no. 024703.
[315] Y. Matsuda, H. Shimahara, "Fulde–Ferrell–Larkin–Ovchinnikov State in Heavy Fermion Superconductors", *J. Phys. Soc. Jpn.* **76** (2007), article no. 051005.
[316] H. Mayaffre, P. Auban-Senzier, M. Nardone, D. Jerome, D. Poilblanc, C. Bourbonnais, U. Ammerrahl, G. Dhalenne, A. Revcolevschi, "Absence of a Spin Gap in the Superconducting Ladder Compound $Sr_2Ca_{12}Cu_{24}O_{41}$", *Science* **279** (1998), p. 345-348.
[317] D. Braithwaite *et al.*, "Upper critical field of the spin ladder system $Sr_2Ca_{12}Cu_{24}O_{41}$", *Solid State Comm.* **114** (2000), p. 533-536.
[318] T. Nakanishi, N. Motoyama, H. Mitamura, N. Takeshita, H. Takahashi, H. Eisaki, S. Uchida, N. Môri, "Magnetic field effect on the pressure-induced superconducting state in the hole-doped two-leg ladder compound $Sr_2Ca_{12}Cu_{24}O_{41}$", *Phys. Rev. B* **72** (2005), article no. 054520.
[319] G. Roux, S. R. White, S. Capponi, D. Poilblanc, "Zeeman Effect in Superconducting Two-Leg Ladders: Irrational Magnetization Plateaus and Exceeding the Pauli Limit", *Phys. Rev. Lett.* **97** (2006), article no. 087207.
[320] D. F. Agterberg, K. Yang, "The effect of impurities on Fulde–Ferrell–Larkin–Ovchinnikov superconductors", *J. Phys.: Condens. Matter* **13** (2001), p. 9259-9270.
[321] M. Shahbazi, Y. Fuseya, H. Bakrim, A. Sedeki, C. Bourbonnais, "Superconducting and density-wave instabilities of low-dimensional conductors with a Zeeman coupling to a magnetic field", *Phys. Rev. B* **95** (2017), no. 16, article no. 165111.
[322] P. W. Anderson, "Theory of dirty Superconductors", *J. Phys. Chem. Solids* **11** (1959), p. 26-30.
[323] A. A. Abrikosov, L. P. Gorkov, "Contribution to the theory of superconducting alloys with paramagnetic impurities", *Sov. Phys. JETP* **12** (1961), no. 6, p. 1243-1253.
[324] K. Maki, H. Won, S. Haas, "Quasiparticle spectrum of the hybrid s+g-wave superconductors YNi_2B_2C and $LuNi_2B_2C$", *Phys. Rev. B* **69** (2004), article no. 012502.
[325] A. P. MacKenzie, Y. Maeno, "The superconductivity of Sr_2RuO_4 and the physics of spin-triplet pairing", *Reviews of Modern Physics* **75** (2003), p. 657-712.
[326] Y. Maeno, S. Kittaka, T. Nomura, S. Yonezawa, K. Ishida, "Evaluation of Spin-Triplet Superconductivity in Sr_2RuO_4", *J. Phys. Soc. Jpn.* **81** (2012), article no. 011009.
[327] S. Bouffard, M. Ribault, R. Brusetti, D. Jerome, K. Bechgaard, "Low-temperature metallic state and superconductivity in quasi-one-dimensional organic conductors: pressure and irradiation investigations", *J. Phys. C: Solid State Phys.* **15** (1982), p. 2951-2964.
[328] M. Y. Choi, P. M. Chaikin, S. Z. Huang, P. Haen, E. M. Engler, R. L. Greene, "Effect of radiation damage on the metal-insulator transition and low temperature transport in the $(TMTSF)_2PF_6$ salt", *Phys. Rev. B* **25** (1982), p. 6208-6217.
[329] A. A. Abrikosov, "Superconductivity in a quasi-one-dimensional metal with impurities", *J. Low Temp. Phys.* **53** (1983), p. 359-374.
[330] M. Miljak, B. Korin, J. R. Cooper, K. Holczer, A. Jánossy, "Low temperature magnetic susceptibility of quasi one-dimensional conductors", *J. Physique* **41** (1980), p. 639-646.
[331] O. Traetteberg, *The spin density wave collective mode in* $(TMTSF)_2AsF_{6(1-x)}SbF_{6x}$, PhD Thesis, Université Paris-Sud – Paris XI, Orsay (France), 1993.
[332] N. Joo, P. Auban-Senzier, C. Pasquier, D. Jerome, K. Bechgaard, "Impurity-controlled superconductivity spin density wave interplay in the organic superconductor: $(TMTSF)_2ClO_4$", *Eur. Phys. Lett.* **72** (2005), p. 645-651.
[333] N. Joo, P. Auban-Senzier, C. R. Pasquier, P. Monod, D. Jerome, K. Bechgaard, "Suppression of superconductivity by non-magnetic disorder in the organic superconductor $(TMTSF)_2(ClO_4)_{(1-x)}(ReO_4)_x$", *Eur. Phys. J. B* **40** (2004), p. 43-48.

[334] N. Doiron-Leyraud, P. Auban-Senzier, S. René de Cotret, C. Bourbonnais, D. Jerome, K. Bechgaard, L. Taillefer, "Linear-T scattering and pairing from antiferromagnetic fluctuations in the $(TM)_2X$ organic superconductors", *Eur. Phys. Jour. B* **78** (2010), p. 23-36.

[335] P. Auban-Senzier, C. R. Pasquier, D. Jérome, S. Suh, S. E. Brown, C. Mézière, P. Batail, "Fluctuating spin density wave conduction in $(TMTSF)_2(ClO_4)_{(1-x)}(ReO_4)_x$ organic superconductors", *Eur. Phys. Lett.* **94** (2011), article no. 17002.

[336] Y. Sun, K. Maki, "Impurity effects in d-wave superconductors", *Phys. Rev. B* **51** (1995), p. 6059-6063.

[337] N. Matsunaga *et al.*, "Anion disorder and two-dimensionality in the superconducting and SDW states of $(TMTSF)_2ClO_4$", *J. Low Temp. Phys.* **117** (1999), p. 1735-1739.

[338] S. Kagoshima, T. Yasunaga, T. Ishiguro, H. Anzai, G. Saito, "Quenching Effect on the Anion Ordering in the Organic Superconductor $(TMTSF)_2ClO_4$: An X-ray study", *Solid State Comm.* **46** (1983), p. 867-870.

[339] R. Moret, J.-P. Pouget, R. Comès, K. Bechgaard, "X-ray study of the anion ordering transition in $(TMTSF)_2ClO_4$: quenching and irradiation effects", *J. Phys. I France* **46** (1985), p. 1521-1532.

[340] J.-P. Pouget, S. Kagoshima, T. Tamegai, Y. Nogami, K. Kubo, T. Nakajima, K. Bechgaard, "High resolution x-ray scattering study of the anion ordering phase transition of $(TMTSF)_2ClO_4$", *J. Phys. Soc. Jpn.* **59** (1990), no. 6, p. 2036-2053.

[341] P. G. De Gennes, *Superconductivity of metals and alloys*, CRC Press: Boca Raton, 2019.

[342] G. Deutscher, O. Entin-Wohlman, S. Fishman, Y. Shapira, "Percolation description of granular superconductors", *Phys. Rev. B* **21** (1980), p. 5041-5047.

[343] E. Puchkaryov, K. Maki, "Impurity scattering in d-wave superconductivity. Unitarity limit versus Born limit", *Eur. Phys. J. B* **4** (1998), p. 191-194.

[344] Y. Suzumura, H. J. Schulz, "Thermodynamic properties of impure anisotropic quasi-one-dimensional superconductors", *Phys. Rev. B* **39** (1989), p. 11398-11405.

[345] G. Preosti, H. Kim, P. Muskar, "Density of states in unconventional superconductors: Impurity-scattering effects", *Phys. Rev. B* **50** (1994), p. 1259-1263.

[346] J. C. Nickel, R. Duprat, C. Bourbonnais, N. Dupuis, "Triplet Superconducting Pairing and Density-Wave Instabilities in Organic Conductors", *Phys. Rev. Lett.* **95** (2005), article no. 247001.

[347] T. Sakakibara, A. Yamada, J. Custers, K. Yano, T. Tayama, H. Aoki, K. Machida, "Nodal Structures of Heavy Fermion Superconductors Probed by the Specific-Heat Measurements in Magnetic Fields", *J. Phys. Soc. Jpn.* **76** (2007), article no. 051004.

[348] K. An, T. Sakakibara, R. Settai, Y. Onuki, M. Hiragi, M. Ichioka, K. Machida, "Sign Reversal of Field-Angle Resolved Heat Capacity Oscillations in a Heavy Fermion Superconductor $CeCoIn_5$ and $d(x2-y2)$ Pairing Symmetry", *Phys. Rev. Lett.* **104** (2010), article no. 037002.

[349] K. Izawa, H. Yamaguchi, T. Sasaki, Y. Matsuda, "Superconducting Gap Structure of $\kappa-(BEDT-TTF)_2Cu(NCS)_2$ Probed by Thermal Conductivity Tensor", *Phys. Rev. Lett.* **88** (2002), article no. 027002.

[350] K. Izawa, A. Shibata, Y. Matsuda, Y. Kato, H. Takeya, K. Hirata, C. J. van der Beek, M. Konczykowski, "Low Energy Quasiparticle Excitation in the Vortex State of Borocarbide Superconductor YNi_2B_2C", *Phys. Rev. Lett.* **86** (2001), p. 1327-1330.

[351] K. Deguchi, Z. Q. Mao, H. Yaguchi, Y. Maeno, "Gap structure of the spin-triplet superconductor Sr_2RuO_4 determined from the field orientation dependence of the specific heat", *Phys. Rev. Lett.* **92** (2004), article no. 047002.

[352] G. E. Volovik, "Superconductivity with lines of gap nodes:density of states in the vortex", *JETP Lett.* **58** (1993), no. 6, p. 457-461.

[353] G. E. Volovik, "Fermionic entropy of the vortex state in d-wave superconductors", *JETP Lett.* **65** (1997), p. 491-496.

[354] I. Vekhter, P. J. Hirschfeld, J. P. Carbotte, E. J. Nicol, "Anisotropic thermodynamics of d-wave superconductors in the vortex state", *Phys. Rev. B* **59** (1999), p. R9023-R9026.

[355] S. Yonezawa, Y. Maeno, D. Jerome, "Extended analysis of the field-angle-dependent heat capacity of $(TMTSF)_2ClO_4$ toward identification of the superconducting gap structure", *J. Phys. Conf. Ser.* **449** (2013), article no. 012032.

[356] D. Le Pevelen, J. Gaultier, Y. Barrans, D. Chasseau, F. Castet, L. Ducasse, "Temperature and pressure dependencies of the crystal structure of the organic superconductor $(TMTSF)_2ClO_4$", *Eur. Phys. J. B* **19** (2001), p. 363-373.

[357] Y. Nagai, H. Nakamura, M. Machida, "Superconducting Gap Function in an Organic Superconductor $(TMTSF)_2ClO_4$ with Anion Ordering; First-principles Calculations and Quasi-classical Analyses for Angle-resolved Heat Capacity", *Phys. Rev. B* **83** (2011), article no. 104523.

[358] F. Creuzet, C. Bourbonnais, D. Jerome, K. Bechgaard, "Cooperative phenommena in $(TMTSF)_2ClO_4$ NMR relaxation", *Mol. Cryst. Liq. Cryst.* **119** (1985), p. 45-51.

[359] C. Bourbonnais, A. Sedeki, "Superconductivity and antiferromagnetism as interfering orders in organic conductors", *Comptes Rendus Physique* **12** (2011), p. 532-541.

[360] W. Wu, P. M. Chaikin, W. Kang, J. Shinagawa, W. Yu, S. E. Brown, "^{77}Se NMR probe of magnetic excitations of the magic angle effect in $(TMTSF)_2PF_6$", *Phys. Rev. Lett.* **94** (2005), article no. 097004.

[361] S. E. Brown, P. M. Chaikin, M. J. Naughton, "La tour des sels de Bechgaard", in *The Physics of Organic Superconductors and Conductors* (A. G. Lebed, ed.), Springer, Heidelberg, 2008, p. 49-87.

[362] T. Moryia, K. Ueda, "Spin fluctuations and high temperature superconductivity", *Adv. Phys.* **49** (2000), p. 555-606.
[363] C. Bourbonnais, A. Sedeki, "Link between antiferromagnetism and superconductivity probed by nuclear spin relaxation in organic conductors", *Phys. Rev. B* **80** (2009), article no. 085105.
[364] Y. Kimura, M. Misawa, A. Kawamoto, "Correlation between non-Fermi-liquid behavior and antiferromagnetic fluctuations in $(TMTSF)_2PF_6$ observed using ^{13}C NMR spectroscopy", *Phys. Rev. B* **84** (2011), article no. 045123.
[365] N. Doiron-Leyraud, P. Auban-Senzier, S. René de Cotret, C. Bourbonnais, D. Jerome, K. Bechgaard, L. Taillefer, "Correlation between linear resistivity and T_c in the Bechgaard salts and the pnictide superconductor $Ba(Fe_{1-x}Co_x)_2As_2$", *Phys. Rev. B* **80** (2009), article no. 214531.
[366] P. Auban-Senzier, D. Jérome, N. Doiron-Leyraud, S. René de Cotret, A. Sedeki, C. Bourbonnais, L. Taillefer, P. Alemany, E. Canadell, K. Bechgaard, "The metallic transport of $(TM)_2X$ organic conductors close to the superconducting phase", *J. Phys.: Condens. Matter* **23** (2011), article no. 345702.
[367] L. G. Azlamazov, A. I. Larkin, "Effect of Fluctuations on the properties of a Superconductor above the critical Temperature", *Sov. Phys. Solid State* **10** (1968), p. 875-898.
[368] P. A. Lee, T. M. Rice, P. W. Anderson, "Conductivity from charge or spin density waves", *Solid State Comm.* **14** (1974), p. 703-709.
[369] E. Barthel, G. Quirion, P. Wzietek, D. Jérome, J. B. Christensen, M. Jørgensen, K. Bechgaard, "NMR incommensurate and incommesurate spin density waves", *Europhys. Lett* **21** (1993), p. 87-92.
[370] G. Grüner, "The dynamics of spin density waves", *Rev. Mod. Phys.* **66** (1994), p. 1-24.
[371] C. Bourbonnais, "Nuclear relaxation and electronic correlations in quasi-one dimensional organic conductors. I. Scaling theory", *J. Phys. I France* **3** (1993), p. 143-169.
[372] L. Fang, H. Luo, P. Cheng, Z. Wang, Y. Jia, G. Mu, B. Shen, I. I. Mazin, L. Shan, C. Ren, H.-H. Wen, "Roles of multiband effects and electron hole asymmetry in the superconductivity and normal properties of $Ba(Fe_{1-x}Co_x)_2As_2$", *Phys. Rev. B* **80** (2009), article no. 140508.
[373] K. Jin, N. P. Butch, K. Kirshenbaum, J. Paglione, R. L. Greene, "Link between spin fluctuations and electron pairing in copper oxide superconductors", *Nature* **476** (2011), p. 73-75.
[374] J. C. Nickel, R. Duprat, C. Bourbonnais, N. Dupuis, "Superconducting pairing and density-wave instabilities in quasi-one-dimensional conductors", *Phys. Rev. B* **73** (2006), article no. 165126.
[375] R. Duprat, C. Bourbonnais, "Interplay between spin-density-wave and superconducting states in quasi-one-dimensional conductors", *Eur. Phys. J. B* **21** (2001), p. 219-228.
[376] V. J. Emery, "The Mechanisms of Organic Superconductivity", *Synth. Met.* **13** (1986), p. 21.
[377] M. T. Béal-Monod, C. Bourbonnais, V. J. Emery, "Possible superconductivity in nearly antiferromagnetic itinerant fermion systems", *Phys. Rev. B* **34** (1986), p. 7716-7720.
[378] D. J. Scalapino, E. Loh, J. E. Hirsch, "d-wave pairing near a spin-density-wave instability", *Phys. Rev. B* **34** (1986), p. 8190-8192.
[379] A. Sedeki, D. Bergeron, C. Bourbonnais, "Interfering antiferromagnetism and superconductivity in quasi-one-dimensional organic conductors", *Physica B* **405** (2009), p. S89-S91.
[380] A. Sedeki, D. Bergeron, C. Bourbonnais, "Extended quantum criticality of low-dimensional superconductors near a spin-density-wave instability", *Phys. Rev. B* **85** (2012), article no. 165129.
[381] H. Bakrim, C. Bourbonnais, "Role of electron-phonon interaction in a magnetically driven mechanism for superconductivity", *Phys. Rev. B* **90** (2014), article no. 125119.
[382] T. Vuletić, P. Auban-Senzier, C. Pasquier, S. Tomic, D. Jerome, M. Héritier, K. Bechgaard, "Coexistence of superconductivity and spin density wave orderings in the organic superconductor $(TMTSF)_2PF_6$", *Eur. Phys. J. B* **25** (2002), p. 319-331.
[383] I. J. Lee, P. M. Chaikin, M. J. Naughton, "Critical Field Enhancement near a Superconductor-Insulator Transition", *Phys. Rev. Lett.* **88** (2002), article no. 207002.
[384] T. Goko, A. A. Aczel, E. Baggio-Saitovitch, S. L. Bud'ko, P. C. Canfield, J. P. Carlo, G. F. Chen, P. Dai, A. C. Hamann, W. Z. Hu, H. Kageyama, G. M. Luke, J. L. Luo, B. Nachumi, N. Ni, D. Reznik, D. R. Sanchez-Candela, A. T. Savici, K. J. Sikes, N. L. Wang, C. R. Wiebe, T. J. Williams, T. Yamamoto, W. Yu, Y. J. Uemura, "Superconductivity coexisting with phase-separated static magnetic order in $(Ba,K)Fe_2As_2$, $(Sr,Na)Fe_2As_2$ and $CaFe_2As_2$", *Phys. Rev. B* **80** (2009), article no. 024508.
[385] Y. J. Uemura, "Muon spin relaxation studies of unconventional superconductors: first-order behavior and comparable spin-charge energy scales", Springer Series in Solid-State Sciences, vol. 180, p. 237-267, Springer Series in Solid-State Sciences, Springer, 2015.
[386] M. Dressel, S. Tomic, "Molecular quantum materials: electronic phases and charge dynamics in two-dimensional organic solids", *Adv. Phys.* **69** (2020), p. 1-120.
[387] G. Saito, T. Enoki, K. Toriumi, H. Inokuchi, "Two-dimensionality and suppression of metal-semiconductor transition in a new organic metal with Alkylthio substituted TTF and perchlorate", *Solid State Comm.* **42** (1982), no. 8, p. 557-560.

[388] S. S. P. Parkin, E. M. Engler, R. R. Schumaker, R. Lagier, V. Y. Lee, J. C. Scott, R. L. Greene, "Superconductivity in a New Family of Organic Conductors", *Phys. Rev. Lett.* **50** (1983), no. 4, p. 270-273.

[389] V. N. Laukhin, E. E. Kostyuchenko, Y. Sushko, I. F. Shchegolev, E. B. Yagubskii, "Effect of pressure on the superconductivity of $\beta-(ET)_2I_3$", *JETP Lett.* **41** (1985), no. 2, p. 81-84.

[390] K. Murata, M. Tokumoto, H. Anzai, H. Bando, G. Saito, K. Kajimura, T. Ishiguro, "Pressure phase diagram of the organic superconductor $\beta-(BEDT-TTF)_2I_3$", *J. Phys. Soc. Jpn.* **54** (1985), p. 2084-2087.

[391] F. Creuzet, G. Creuzet, D. Jerome, D. Schweitzer, H. J. Keller, "Homogeneous superconducting state at 8.1 K under ambient pressure ion the organic conductor $\beta-(BEDT-TTF)_2I_3$", *J. Physique Lett.* **46** (1988), p. 1079-1085.

[392] E. Yagubskii, I. Shchegolev, S. Pesotskii, V. Laukhin, P. Kononovich, M. Kartsovnik, A. Zvarykina, "Superconducting Properties of the Orthorhombic Phase of Bis-(ethylenedithiolo)tetrathiofulvalene Triiodide", *JETP Lett.* **39** (1984), no. 6, p. 328-332.

[393] W. Kang, G. Montambaux, J. R. Cooper, D. Jerome, P. Batail, C. Lenoir, "Observation of Giant Magnetoresistance Oscillations in the High-T_c Phase of the Two-Dimensional Organic Conductor β-(BEDT-TTF)$_2$I$_3$", *Phys. Rev. Lett.* **62** (1989), p. 2559-2562.

[394] M. Kartsovnik, P. Kononovich, V. Laukhin, I. Shchegolev, "Anisotropy of Magnetoresistance and Shubnikov–De Haas oscillations in the Organic Metal Beta-$(ET)_2IBr_2$", *JETP Lett.* **48** (1988), no. 9, p. 541-544.

[395] K. Yamaji, "On the angle dependence of the magnetoresistance in quasi-two-dimensional organic superconductors", *J. Phys. Soc. Jpn.* **58** (1989), p. 1520-1523.

[396] H. Urayama, H. Yamochi, G. Saito, K. Nozawa, T. Sugano, M. Kinoshita, S. Sato, K. Oshima, A. Kawamoto, J. Tanaka, "A New Ambient Pressure Organic Superconductor Based on BEDT-TTF with T_c Higher than 10K (T_c = 10.4K)", *Chem. Lett.* **17** (1988), p. 55-58.

[397] A. M. Kini, U. Geiser, H. H. Wang, K. D. Carlson, J. M. Williams, W. K. Kwok, K. G. Vandervoort, J. E. Thompson, D. L. Stupka, "A New Ambient-Pressure Organic Superconductor, $\kappa-(ET)_2Cu(N(CN)_2)Br$, with the Highest Transition Temperature Yet Observed (Inductive Onset T_c = 11.6 K, Resistive Onset=12. K", *Inorg. Chem.* **29** (1990), p. 2555-2557.

[398] J. M. Williams, A. M. Kini, H. H. Wang, K. D. Carlson, U. Geiser, L. K. Montgomery, G. J. Pyrka, D. M. Watkins, J. M. Kommers, "From Semiconductor-Semiconductor Transition (42 K) to the Highest-T_c Organic Superconductor, κcl($T_c = 12.5K$)", *Inorg. Chem.* **29** (1990), p. 3272-3274.

[399] S. Lefebvre, P. Wzietek, S. E. Brown, C. Bourbonnais, D. Jerome, C. Mézière, M. Fourmigué, P. Batail, "Mott Transition, Antiferromagnetism, and Unconventional Superconductivity in Layered Organic Superconductors", *Phys. Rev. Lett.* **85** (2000), no. 25, p. 5420-5423.

[400] P. Limelette, P. Wzietek, S. Florens, A. Georges, T. A. Costi, P. Pasquier, D. Jerome, C. Mézière, P. Batail, "Mott Transition and Transport Crossovers in the Organic Compound $\kappa-(ET)_2Cu[N(CN)_2]Cl$", *Phys. Rev. Lett.* **91** (2003), article no. 016401.

[401] A. Georges, G. Kotliar, W. Krauth, M. Rosenberg, "Dynamical mean-field theory of strongly correlated fermion systems and the limit of infinite dimensions", *Rev. Mod. Phys.* **68** (1996), p. 13-125.

[402] H. Mayaffre, P. Wzietek, D. Jerome, C. Lenoir, P. Batail, "Superconducting state of $\kappa-(ET)_2Cu(N(CN)_2)Br$ studied by 13C NMR: Evidence for vortex-core-induced nuclear relaxation and unconventional pairing", *Phys. Rev. Lett.* **75** (1995), p. 4122-4125.

[403] K. Kanoda, K. Miyagawa, A. Kawamoto, Y. Nakazawa, "NMR relaxation rate in the superconducting state of the organic conductor NMR relaxation rate in the superconducting state of the organic conductor $\kappa-(ET)_2Cu(N(CN)_2)Br$", *Phys. Rev. B* **54** (1996), p. 76-79.

[404] S. Yasin, M. Dumm, B. Salameh, P. Batail, C. Meźière, M. Dressel, "Transport studies at the Mott transition of the two-dimensional organic metal $\kappa-(BEDT)_2Cu(N(CN)_2)Br_xCl_{1-x}$", *Eur. Phys. J. B* **79** (2011), p. 383-390.

[405] V. A. Bondarenko, R. A. Petrosov, M. A. Tanatar, V. S. Yefanov, N. D. Kushch, "Transport Properties of $\kappa-(ET)_2Cu(N(CN)_2)Br_xCl_{1-x}(0 \le x \le 1)$ Organic Superconductors", *Physica C Supercond.* **235** (1994), p. 2467-2468.

[406] M. Tokumoto, H. Anzai, K. Kajimura, T. Ishiguro, "High T_c superconducting states in organic metals $\beta-(ET)_2X$", *Jpn. J. Appl. Phys.* **26-3** (1987), p. 1977-1982.

[407] D. Fournier, M. Poirier, M. Castonguay, M. Truong, "Mott Transition, Compressibility Divergence and the P-T Phase Diagram of Layered Organic Superconductors: An Ultrasonic Investigation", *Phys. Rev. Lett.* **90** (2003), article no. 127002.

[408] F. Kagawa, T. Itou, K. Miyagawa, K. Kanoda, "Transport criticality of the first-order Mott transition in the quasi-two-dimensional organic conductor $\kappa-(ET)_2Cu[N(CN)_2]Cl$", *Phys. Rev. B* **69** (2004), article no. 064511.

[409] H. Mayaffre, P. Wzietek, C. Lenoir, D. Jerome, P. Batail, "^{13}C NMR Study of a Quasi-Two Dimensional Organic Superconductor $\kappa-(ET)_2Cu(N(CN)_2)Br$", *Eur. Phys. Lett.* **28** (1994), p. 205-210.

[410] A. L. Kerlin, H. Nagasawa, D. Jerome, "Metal-Insulator transition investigation in V_2O_3 by nuclear magnetic resonance and relaxation", *Solid State Comm.* **13** (1973), p. 1125-1129.

[411] F. Kagawa, K. Miyagawa, K. Kanoda, "Unconventional critical behaviour in a quasi-twodimensional organic conductor", *Nature* **436** (2005), p. 534-537.

[412] P. Limelette, A. Georges, D. Jerome, P. Wzietek, P. Metcalf, J. M. Honig, "Universality and Critical Behavior at the Mott Transition", *Science* **302** (2003), p. 89-92.
[413] A. Kamawamoto *et al.*, "^{13}C NMR study of layered organic superconductors based on BEDT-TTF molecules", *Physical Review Letters* **74** (1995), p. 3455-3458.
[414] D. B. McWhan, J. P. Remeika, "Metal-Insulator Transition in $(V_{1-x}Cr_x)_2O_3$", *Phys. Rev. B* **2** (1970), no. 9, p. 3734-3750.
[415] A. Jayaraman, D. B. McWhan, J. P. Remeika, P. D. Dernier, "Critical Behavior of the Mott Transition in Cr-Doped V_2O_3", *Phys. Rev. B* **2** (1970), no. 9, p. 3751-3756.
[416] N. F. Mott, "The transition to the metallic state", *Phil. Mag* **6** (1961), p. 287-309.
[417] N. F. Mott, "The Metal-non-Metal Transition", *J. Phys. Colloques* **32** (1971), no. C1, p. 11-14.
[418] V. Jaccarino, M. Peter, "Ultra-High-Field Superconductivity", *Phys. Rev. Lett.* **9** (1962), p. 290-292.
[419] S. Uji, H. Shinagawa, C. Terakura, T. Terashima, T. Yakabe, Y. Terai, M. Tokumoto, A. Kobayashi, H. Tanaka, H. Kobayashi, "Magnetic-field-induced superconductivity in a two-dimensional organic conductor", *Nature* **410** (2001), p. 908-910.
[420] L. Balicas, J. S. Brooks, K. Storr, S. Uji, M. Tokumoto, K. Kobayashi, A. Kobayashi, H. Tanaka, V. Barzykin, L. P. Gorkov, "Superconductivity in an Organic Insulator at Very High Magnetic Fields", *Phys. Rev. Lett.* **87** (2001), article no. 067002.
[421] T. Naito, "Modern History of Organic Conductors: An Overview", *Crystals* **11** (2021), article no. 838.
[422] N. F. Mott, *Metal-Insulator Transitions*, Taylor and Francis, London, 1974.
[423] L. Alcacer, A. H. Maki, "Electrically Conducting Metal Dithiolate-Perylene Complexes", *J. Phys. Chem.* **78** (1974), no. 3, p. 215-217.
[424] L. Alcacer *et al.*, "Synthesis, structure and preliminary results on electrical and magnetic properties of $(Perylene)_2[Pt(mnt)_2]$", *Solid State Comm.* **35** (1980), p. 945-949.
[425] D. Graf, J. S. Brooks, M. Almeida, J. C. Dias, S. Uji, T. Terashima, M. Kimata, "Evolution of superconductivity from a charge-density-wave ground state in pressurized $(Per)_2Au(mnt)_2$", *Eur. Phys. Lett.* **85** (2009), article no. 27009.
[426] G. Bonfait, E. B. Lopes, M. J. Matos, R. T. Henriques, M. Almeida, "Magnetic field dependence of the metal-insulator transition in $(Per)_2Pt(mnt)_2$ and $(Per)_2Au(mnt)_2$", *Solid State Comm.* **6** (1991), p. 391-394.
[427] C. Bourbonnais, R. T. Henriques, P. Wzietek, D. Köngeter, J. Voiron, D. Jérome, "Nuclear and electronic resonance approaches to magnetic and lattice fluctuations in the two-chain family of organic compounds $(Per)_2M(mnt)_2$ (M = Pt,Au)", *Phys. Rev. B* **44** (1991), p. 641-651.
[428] R. T. Henriques, L. Alcacer, J.-P. Pouget, D. Jerome, "Electrical conductivity and x-ray diffuse scattering study of the family of organic conductors $(Per)_2M(mnt)_2$, M = Pt, Pd, Au)", *J. Phys. C: Solid State Phys.* **17** (1984), article no. 5197.
[429] D. Graf, J. S. Brooks, E. S. Choi, M. Almeida, R. T. Henriques, J. C. Dias, S. Uji, "Quantum interference in the quasi-one-dimensional organic conductor $(Per)_2Pt(mnt)_2$", *Phys. Rev. B* **75** (1997), article no. 255101.
[430] E. Canadell, M. Almeida, J. S. Brooks, "Electronic band structure of $\alpha - (Per)_2M(mnt)_2$ compounds", *Eur. Phys. J. B* **42** (2004), p. 453-456.
[431] H. Bakrim, C. Bourbonnais, "Superconductivity close to the charge-density-wave instability", *Eur. Phys. J. B* **90** (2010), p. 27001.
[432] M. Bousseau, L. Valade, J.-P. Legros, P. Cassoux, M. Garbauskas, L. V. Interrante, "Highly Conducting Charge-Transfer Compounds of Tetrathiafulvalene and Transition Metal-dmit-Complexes", *J. Am. Chem. Soc* **108** (1986), p. 1908-1916.
[433] L. Brossard, M. Ribault, M. Bousseau, L. Valade, P. Cassoux, "Un nouveau type de supraconducteur moléculaire: $TTF[Ni(dmit)_2]_2$", *C. R. Acad. Sci. II* **302** (1986), no. 5, p. 205-210, online at https://gallica.bnf.fr/ark:/12148/bpt6k6296984t/f219.item.
[434] A. Kobayashi, R. Kato, H. Kobayashi, S. Moriyama, Y. Nishino, K. Kajita, W. Sasaki, "Anion arrangement in a new molecular superconductor, $\Theta - (BEDT-TTF)_2(I3)_{1-x}(AuI2)_x$, $(x < 0.02)$", *Chem. Lett.* **15** (1986), p. 2017-2020.
[435] L. Brossard, M. Ribault, L. Valade, P. Cassoux, "Pressure induced superconductivity in molecular $TTF[Pd(dmit)_2]_2$", *J. Phys. I France* **50** (1989), p. 1521-1534.
[436] S. Ravy, J.-P. Pouget, L. Valade, J.-P. Legros, "Structural Evidence of Charge Density Waves in the Series of Molecular Conductors and Superconductors: $TTF[M(dmit)_2]_2$ (M = Pd, Ni)", *Eur. Phys. Lett.* **9** (1989), p. 391-396.
[437] E. Canadell, I. E.-I. Rachidi, S. Ravy, J.-P. Pouget, L. Brossard, J.-P. Legros, "On the band electronic structure of $X[M(dmit)_2]_2$(X = TTF, $(CH_3)_4N$; M = Ni, Pd) molecular conductors and superconductors", *J. Phys. I France* **50** (1989), p. 2967-2981.
[438] W. Kaddour, P. Auban-Senzier, H. Raffy, M. Monteverde, J.-P. Pouget, C. R. Pasquier, P. Alemany, E. Canadell, L. Valade, "Charge density wave and metallic state coexistence in the multiband conductor $TTF[Ni(dmit)_2]2$", *Phys. Rev. B* **90** (2014), article no. 205132.
[439] "SIESTA code", For more information on the SIESTA code visit: http://Sicmab.cat/leem/siesta.
[440] L. Brossard, M. Ribault, L. Valade, P. Cassoux, "Simultaneous competition and coexistence between charge density waves and reentrant superconductivity in the pressure-temperature phase diagram of the molecular conductor $TTF[Ni(dmit)_2]_2$", *Phys. Rev. B* **42** (1990), p. 3935-3943.

[441] A. Vainrub, D. Jerome, M. F. Bruniquel, P. Cassoux, "Coexistence of Metallic Character and Charge Density Wave on $Ni(dmit)_2$ Stacks in $TTF[Ni(dmit)_2]_2$", *Eur. Phys. Lett.* **12** (1990), p. 267.
[442] C. Berthier, D. Jerome, P. Molinié, J. Rouxel, "Charge density waves in layer structures: A NMR study on a 2H-$NbSe_2$ single Crystal", *Solid State Comm.* **19** (1976), p. 131-135.
[443] C. Berthier, P. Molinié, D. Jerome, "Evidence for a connection between charge density Waves and the pressure enhancement of superconductivity in 2H—$NbSe_2$", *Solid State Comm.* **18** (1976), p. 1393-1395.
[444] A. Kobayashi, E. Fujiwara, H. Kobayashi, "Single-Component Molecular Metals with Extended-TTF Dithiolate Ligands", *Chem. Rev.* **104** (2004), p. 5243-5264.
[445] A. Kobayashi, B. Zhou, R. Takagi, K. Miyagawa, S. Ishibashi, A. Kobayashi, T. Kawamura, E. Nishibori, K. Kanoda, "Single-Component Molecular Conductors — Multi-Orbital Correlated $\Pi - d$ Electron Systems", *Bull. Chem. Soc. Jpn* **94** (2021), p. 2540-2562.
[446] M. Sasa, A. Yamada, J. Custers, K. Yano, T. Tayama, H. Aoki, K. Machida, "Crystal structures and physical properties of single-component molecular conductors consisting of nickel and gold complexes with bis(trifluoromethyl) tetrathiafulvalenedithiolate ligands", *J. Mater. Chem* **15** (2005), p. 155-163.
[447] H. Tanaka, Y. Okano, H. Kobayashi, W. Suzuki, A. Kobayashi, "A Three-Dimensional Synthetic Metallic Crystal Composed of Single-Component Molecules", *Science* **291** (2001), p. 285-287.
[448] H. Cui, H. Kobayashi, S. Ishibashi, M. Sasa, F. Iwase, R. Kato, A. Kobayashi, "A Single-Component Molecular Superconductor", *J. Am. Chem. Soc* **136** (2014), p. 7619-7622.
[449] A. Kobayashi, H. Tanaka, H. Kobayashi, "Molecular design and development of single-component molecular metals", *J. Mater. Chem* **11** (2001), p. 2078-2088.
[450] A. Lebed, *The Physics of Organic Superconductors and Conductors*, Springer Series in Materials Science, vol. 110, Springer-Verlag, Berlin, 2008.
[451] M. Ribault, D. Jerome, J. Tuchendler, C. Weyl, K. Bechgaard, "Low-field and anomalous high-field Hall effect in $(TMTSF)_2ClO_4$", *J. Physique Lett.* **44** (1982), p. 953-961.
[452] W. Kang, "Magnetoresistance study of low-dimensional electrons in the Bechgaard salts", *Curr Appl Phys.* **4** (2004), p. 263-266.
[453] G. Montambaux, *Contribution à l'étude des conducteurs quasi-unidimensionnels sous champ magnétique*, PhD Thesis, Université Paris-Sud, Orsay (France), 1985.
[454] L. Balicas, G. Kriza, F. I. B. Williams, "Sign Reversal of the Quantum Hall Number in $(TMTSF)_2PF_6$", *Phys. Rev. Lett.* **75** (1995), no. 10, p. 2000-2003.
[455] J. R. Cooper, W. Kang, P. Auban, G. Montambaux, D. Jerome, K. Bechgaard, "Quantized Hall effect and a New Field-Induced Phase Transition in the Organic Superconductor $(TMTSF)_2PF_6$", *Phys. Rev. Lett.* **65** (1989), p. 1984-1987.
[456] S. T. Hannahs, J. S. Brooks, W. Kang, L. Y. Chiang, P. M. Chaikin, "Quantum Hall effect in a bulk crysal", *Phys. Rev. Lett.* **63** (1989), p. 1988-1991.
[457] M. Ribault, "Electronic States below 5K IN $(TMTSF)_2ClO_4$", *Mol. Cryst. Liq. Cryst.* **119** (1985), p. 91-95.
[458] B. Piveteau *et al.*, "Hall effect study of the field-induced instabilities in $(TMTSF)_2PF_6$ under pressure", *J. Phys. C: Solid State Phys* **19** (1986), p. 4483.
[459] H. Cho, W. Kang, "Negative Hall plateaus and quantum Hall effect in $(TMTSF)_2PF_6$", *Phys. Rev. B* **59** (1999), p. 9814-9817.
[460] M. Héritier, G. Montambaux, P. Lederer, "Stability of the spin density wave phases in $(TMTSF)_2ClO_4$: quantized nesting effect", *J. Physique Lett.* **45** (1984), p. 943-952.
[461] G. Montambaux, M. Héritier, P. Lederer, "Spin Susceptibility of the Two-Dimensional Electron Gas with Open Fermi Surface under Magnetic Field", *Phys. Rev. Lett.* **55** (1985), p. 2078-2081.
[462] G. Montambaux, "Susceptibility and instability of the Q1D electron gas under magnetic field", in *Low dimensional Conductors and Superconductors* (D. Jerome, L. G. Caron, eds.), Plenum Press: New York, 1986, p. 233-242.
[463] G. Montambaux, D. Zanchi, "The quantum Hall effect in Q1D conductors", *Synthetic Metals* **86** (1997), p. 2235-2240.
[464] D. Zanchi, G. Montambaux, "Sign Reversals of the Quantum Hall Effect in Quasi-1D Conductors", *Phys. Rev. Lett.* **77** (1996), p. 366-369.
[465] G. Montambaux, D. Jerome, "Rapid magnetic oscillations and magnetic breakdown in quasi-1D conductors", *Comptes Rendus Physique* **17** (2016), p. 376-388.
[466] S. Uji, J. S. Brooks, S. Takasaki, J. Yamada, H. Anzai, "Origin of rapid oscillations in the metallic phase for the organic conductor $(TMTSF)_2ClO_4$", *Solid State Comm.* **103** (1997), p. 387-392.
[467] J. P. Ulmet, P. Auban, S. Askenazy, "High-Field Shubnikov–de-Haas effect and magnetoresistance in the organic metal $(TMTSF)_2ClO_4$", *Solid State Comm.* **52** (1984), p. 547-549.
[468] A. V. Kornilov *et al.*, "Origin of rapid oscillations in low-dimensional $(TMTSF)_2PF_6$", *Phys. Rev. B* **76** (2007), article no. 045109.
[469] W. Kang, J. R. Cooper, D. Jerome, "Quantized Hall effect in the organic superconductor $(TMTSF)_2ReO_4$", *Phys. Rev. B* **43** (1991), p. 11467-11470.
[470] J. S. Brooks, J. O'Brien, R. P. Starrett, R. G. Clark, R. H. McKenzie, S.-Y. Han, J. S. Qualls, S. Takasaki, J. Yamada,

H. Anzai, C. H. Mielke, L. K. Montgomery, "Quantum oscillations in quasi-one-dimensional metals with spin-density-wave ground states", *Phys. Rev. B* **59** (1999), p. 2604-2608.

[471] E. C. G. Stuckelberg, "Theory of Inelastic Collisions between Atoms", *Helv. Phys. Acta* **5** (1932), p. 369-422.

[472] W. Kang, T. Osada, Y. J. Jo, H. Kang, "Interlayer Magnetoresistance of Quasi-One-Dimensional Layered Organic Conductors", *Phys. Rev. Lett.* **99** (2007), article no. 017002.

[473] A. G. Lebed, "Anisotropy of an instability for a spin density wave induced by a magnetic field in a Q1D conductor", *JETP Lett.* **43** (1986), no. 3, p. 174-177.

[474] A. G. Lebed, P. Bak, "Theory of Unusual Anisotropy of Magnetoresistance in Organic Superconductors", *Phys. Rev. Lett.* **63** (1989), p. 1315-1317.

[475] B. Gallois, D. Chasseau, J. Gaultier, C. Hauw, A. Filhol, K. Bechgaard, "$(TMTSF)_2ClO_4$: Meanstructure at 7K comparative studt with 300K and 125K data", *J. Phys. Colloques* **44** (1983), no. C3, p. 1071-1074.

[476] T. Osada, A. Kawasumi, S. Kagoshima, N. Miura, G. Saito, "Commensurability Effect of Magnetoresistance Anisotropy in the Quasi-One-Dimensional Conductor Tetramethyltetraselenafulvalenium Perchlorate, $(TMTSF)_2ClO_4$", *Phys. Rev. Lett.* **66** (1991), p. 1525-1528.

[477] M. J. Naughton, O. H. Chung, M. Chaparala, X. Bu, P. Coppens, "Commensurate Fine Structure in Angular-Dependent Studies of $(TMTSF)_2ClO_4$", *Phys. Rev.. Letters* **67** (1991), p. 3712-3715.

[478] T. Osada, S. Kagoshima, N. Miura, "Resonance effect in magnetotransport anisotropy of quasi-one-dimensional conductors", *Phys. Rev. B* **46** (1992), p. 1812-1815.

[479] G. M. Danner, W. Kang, P. M. Chaikin, "Measuring the Fermi surface of quasi-one-dimensional metals", *Phys. Rev. Lett.* **72** (1994), p. 3714-3717.

[480] J. Singleton *et al.*, "Test for Interlayer Coherence in a Quasi-Two-Dimensional Superconductor", *Phys. Rev. Lett.* **88** (2002), article no. 037001.

[481] G. M. Danner, P. M. Chaikin, "Non Fermi liquid Transport in $(TMTSF)_2PF_6$", *Phys. Rev. Lett.* **75** (1995), p. 4690-4693.

[482] T. Osada, S. Kagoshima, N. Miura, "Third Angular Effect of Magnetoresistance in Quasi-One-Dimensional Conductors", *Phys. Rev. Lett.* **77** (1996), p. 5261-5264.

[483] H. Yoshino, A. Oda, K. Murata, H. Nishikawa, K. Kikuchi, I. Ikemoto, "Direct evidence of dimensionality enhancement of Q1D TMTSF and DMET salts", *Synth. Met.* **120** (2001), p. 885-886.

[484] H. Yoshino *et al.*, "Anomalous Angular Dependence of Magnetoresistance of an Organic Superconductor, $(DMET)_2I_3$", *J. Phys. Soc. Jpn.* **64** (1995), p. 2307-2310.

[485] H. Yoshino, S. Shodai, K. Murata, "Third angular effect of $(TMTSF)_2ClO_4$ in R- and Q-states under pressure", *Synth. Met.* **133-134** (2003), p. 55-56.

[486] L. Alcacer, *The Physics of organic electronics. From molecules to crystals and polymers*, IOP Publishing, 2023.

[487] M. Suda, Y. Kawasugi, T. Minari, K. Tsukagoshi, R. Kato, H. M. Yamamoto, "Strain-Tunable Superconducting Field-Effect Transistor with an Organic Strongly-Correlated Electron System", *Adv. Mater.* **26** (2014), p. 3490-3495.

[488] H. M. Yamamoto, M. Nakano, M. Suda, Y. Iwasa, M. Kawasaki, R. Kato, "A strained organic field-effect transistor with a gate-tunable superconducting channel", *Nature Comm.* **4** (2013), article no. 2379.

[489] Y. Kawasugi, H. M. Yamamoto, N. Tajima, T. Fukunaga, K. Tsukagoshi, R. Kato, "Electric-field-induced Mott transition in an organic molecular crystal", *Phys. Rev. B* **84** (2011), article no. 125129.

[490] G. Kawaguchi, H. M. Yamamoto, "Control of Organic Superconducting Field effect Transistor by Cooling Rate", *Crystals* **9** (2019), article no. 605.

[491] M. Greenblatt, W. H. McCarroll, R. Neifeld, M. Croft, J. V. Waszczak, "Quasi two-dinensional electronic Properties of the Lithium Molybdenum Bronze, $Li_{0.9}Mo_6O_{17}$", *Solid State Comm.* **51** (1984), p. 671-674.

[492] W. H. Jiao, Z.-T. Tang, Y.-L. Sun, Y. Liu, Q. Tao, C.-M. Feng, Y.-W. Zeng, Z.-A. Xu, G.-H. Cao, "Superconductivity in a Layered $Ta_4Pd_3Te_{16}$ with $PdTe_2$ Chains", *J. Am. Chem. Soc* **136** (2014), p. 1284-1287.

[493] Z.-T. Tang, J.-K. Bao, Y. Liu, Y.-L. Sun, A. Ablimit, H.-F. Zhai, H. Jiang, C.-M. Feng, Z.-A. Xu, G.-H. Cao, "Unconventional superconductivity in quasi-one-dimensional $A_2Cr_3As_3$", *Phys. Rev. B* **91** (2015), article no. 020506.

[494] J. Pan, W. H. Jiao, X. C. Hong, Z. Zhang, L. P. He, P. L. Cai, J. Zhang, G.-H. Cao, S. Y. Li, "Nodal superconductivity and superconducting dome in new layered superconductor $Ta_4Pd_3Te_{16}$", *Phys. Rev. B* **92** (2015), article no. 180505.

[495] J. F. Mercure, A. F. Bangura, X. Xu, N. Wakeham, A. Carrington, P. Walmsley, M. Greenblatt, N. E. Hussey, "Upper Critical Magnetic Field far above the Paramagnetic Pair-Breaking Limit of Superconducting One-Dimensional $Li_{0.9}Mo_6O_{17}$ Single Crystals", *Phys. Rev. Lett.* **108** (2012), article no. 187003.

[496] J.-K. Bao, J.-Y. Liu, C.-W. Ma, Z.-H. Meng, Z.-T. Tang, Y.-L. Sun, H.-F. Zhai, H. Jiang, H. Bai, C.-M. Feng, Z.-A. Xu, G.-H. Cao, "Superconductivity in Quasi-One-Dimensional $K_2Cr_3As_3$ with Significant Electron Correlations", *Phys. Rev. X* **5** (2015), article no. 011013.

[497] T. Kong, S. L. Bud'ko, P. C. Canfield, "Anisotropic H_{c2}, thermodynamic and transport measurements, and pressure dependence of T_c in $K_2Cr_3As_3$ single crystals", *Phys. Rev. B* **91** (2015), article no. 020507.

[498] Y. Maeno, H. Hashimoto, K. Yoshida, S. Nishizaki, T. Fujita, J. G. Bednorz, F. Lichtenberg, "Superconducvity in a layered perovskite whitout copper", *Nature* **372** (1994), p. 532-534.

[499] A. P. Mackenzie, "A Personal Perspective on the Unconventional Superconductivity of Sr_2RuO_4", *J. Supercond. Nov. Magn.* **33** (2019), p. 177-182.

[500] N. Shirakawa *et al.*, "Pressure dependence of superconducting critical temperature of Sr_2RuO_4", *Phys. Rev. B* **56** (1997), no. 13, p. 7890-7893.

[501] K. Kinjo, M. Manago, S. Kitagawa, Z. Q. Mao, S. Yonezawa, Y. Maeno, K. Ishida, "Superconducting spin smecticity evidencing the Fulde–Ferrell–Larkin–Ovchinnikov state in Sr_2RuO_4", *Science* **376** (2022), no. 6591, p. 397-400.

[502] A. Pustogow, Y. Luo, A. Chronister, Y.-S. Su, D. A. Sokolov, F. Jerzembeck, A. P. Mackenzie, C. W. Hicks, N. Kikugawa, S. Raghu, E. D. Bauer, S. E. Brown, "Constraints on the superconducting order parameter in Sr_2RuO_4 from oxygen-17 nuclear magnetic resonance", *Nature* **574** (2019), p. 72-75.

[503] K. Ishida, M. Manago, K. Kinjo, Y. Maeno, "Reduction of the ^{17} O Knight Shift in the Superconducting State and the Heat-up Effect by NMR Pulses on Sr_2RuO_4", *J. Phys. Soc. Jpn.* **89** (2020), article no. 034712.

[504] A. Chronister, A. Pustogow, N. Kikugawa, D. A. Sokolov, F. Jerzembeck, C. W. Hicks, A. P. Mackenzie, E. D. Bauer, S. E. Brown, "Evidence for even parity unconventional superconductivity in Sr_2RuO_4", *Proc. Natl. Acad. Sci. U. S. A.* **118** (2020), no. 25, article no. e2025313118.

[505] V. L. Ginzburg, "High-Temperature Superconductivity: some remarks", Progress in Low Temperature Physics, vol. 12, Elsevier, 1989, p. 1-44.

[506] P. W. Anderson, J. R. Schrieffer, "A dialogue on the theory of High T_c", *Physics Today* **44** (1991), p. 54-61.